Intramedullary Spinal Cord Tumors

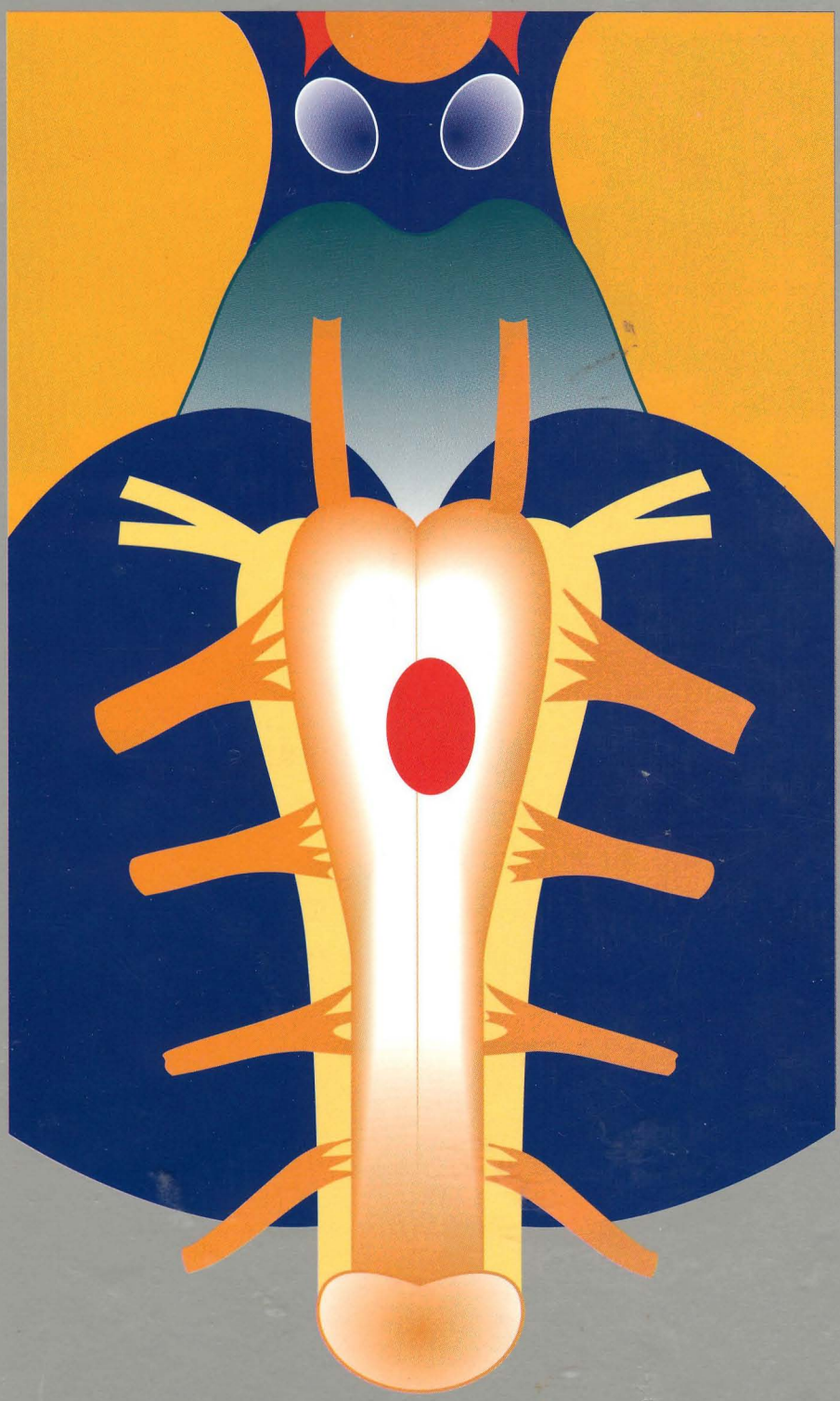

Georges Fischer
Jacques Brotchi

Thieme

Library of Congress Cataloging-in-Publication Data

Fischer, Georges, 1936 –
Intramedullary spinal cord tumors / Georges Fischer and Jacques Brotchi ; contributors, D. Baleriaux ... [et al.] ; foreword by Leonard I. Malis ; preface by Paul R. Cooper.
p. cm.
Includes bibliographical references and index.
ISBN 3-13-101871-2 (GTV). – ISBN 0-86577-593-1 (TMP)
1. Spinal cord – Tumors. I. Brotchi, Jacques. II. Baleriaux, D.
[DNLM: 1. Spinal Cord Neoplasms. WL 400 F52881 1995.
RC280.S7F56 1995
616,99'282 – dc20
DNLM/DLC
for Library of Congress 95-49531
CIP

Cover drawing by Renate Stockinger

Important Note: Medicine is an ever-changing science undergoing continual development. Research and clinical experience are continually expanding our knowledge, in particular our knowledge of proper treatment and drug therapy. Insofar as this book mentions any dosage or application, readers may rest assured that the authors, editors and publishers have made every effort to ensure that such references are in accordance **with the state of knowledge at the time of production of the book**.

Nevertheless this does not involve, imply, or express any guarantee or responsibility on the part of the publishers in respect of any dosage instructions and forms of application stated in the book. **Every user is requested** to examine carefully the manufacturers' leaflets accompanying each drug and to check, if necessary in consultation with a physician or specialist, whether the dosage schedules mentioned therein or the contraindications stated by the manufacturers differ from the statements made in the present book. Such examination is particularly important with drugs that are either rarely used or have been newly released on the market. **Every dosage schedule or every form of application used is entirely at the user's own risk and responsibility**. The authors and publishers request every user to report to the publishers any discrepancies or inaccuracies noticed.

This book is an authorized, updated, and adapted translation of the French edition published and copyrighted 1994 by Masson, Paris, France.

Title of the French edition: Les tumeurs intramédullaires in Neurochirurgie. 1994; 40 : 1-108

Rüdigerstraße 14, D-70469 Stuttgart, Germany
Thieme Medical Publishers, Inc., 381 Park Avenue South, New York, NY 10016

Typesettings by Fotosatz-Service Köhler OHG,
D-97084 Würzburg, Germany
Apple Macintosh/Belichter Linotype SQ 230

Printed in Germany by Gulde-Druck,
D-72070 Tübingen

ISBN 3-13-101871-2 (GTV, Stuttgart)
ISBN 0-86577-593-1 (TMP, New York)

1 2 3 4 5 6

Foreword

It has been a very great pleasure for me to read the present volume, which makes such an impression and contributes so much to its field. Dr. Fischer and Dr. Brotchi have assembled the largest personal series of intramedullary spinal cord tumors yet published (171 patients), and have reviewed a total of 1117 cases. The additional cases were provided by their colleagues in the Société de Neuro-Chirurgie de Langue Française. This is a phenomenal number in a field that is mostly confined to case reports of a few cases at most.

Intramedullary spinal cord tumors are relatively rare, with perhaps 200 per year occurring in the United States. The revolutionary changes that have been brought about by new neurosurgical techniques in the last 25 years, including microsurgical techniques, bipolar coagulation, and ultrasonic aspiration, have made the majority of these tumors curable rather than usually hopeless. Diagnosis has now become simple and noninvasive, with enhanced MRI making the answer obvious.

Nevertheless, in my personal series of ependymomas – the most common lesion – most patients have been referred to me after an unsuccessful surgical approach, usually resulting in damage and scarring. Failure to suspect or recognize the neurologic problem and seek the appropriate study leads to damaging delay, and intervention by surgeons inexperienced in the special problems of these lesions compounds the danger.

The documentation and scholarship in the present book are of the highest order, as is the surgical planning, understanding, and microsurgical expertise. This is the only major neurosurgical manuscript I have read in a great many years for which I had not a single criticism or disagreement. This text is required reading for everyone who deals with spinal cord patients, and it has the potential to produce a major improvement in outcomes. Reading the book is an effort that is amply repaid by the satisfaction it provides.

New York *Leonard I. Malis*

Preface

Intramedullary spinal cord tumors present the neurosurgeon with unique challenges. These lesions are rare, and with a few notable exceptions, the experience of most neurosurgeons is limited to a very occasional case. This limited familiarity, in turn, has led to suboptimal results: incomplete removal of potentially resectable tumors; surgical timidity, and consequent failure to locate tumors or provide the neuropathologist with sufficient material to arrive at a diagnosis; and unsatisfactory neurological outcomes due to intraoperative misjudgments.

In 1925, Elsberg published his now classic work on tumors of the spinal cord. Since that time, there has been no shortage of case reports and series documenting the management of intramedullary spinal cord tumors. However, until now there has been no comprehensive work dealing with the tremendous conceptual and technical advances that have occurred since the appearance of Elsberg's book, over 70 years ago. This monograph by Dr. Fischer and Dr. Brotchi admirably fills this gap.

I became aware of the authors' intention to produce a book on this subject when they were planning the work and were soliciting the opinions of colleagues who had experience in dealing with these difficult tumors. I first read the monograph in French when it appeared as a supplement to the journal *Neurochirurgie*. It was clear that it was a superlative piece of scholarship based on the extensive experience that Dr. Fischer and Dr. Brotchi have collected, and which they have examined in a critical and dispassionate fashion. The book is authoritative and comprehensive without being dogmatic and is filled with insights that will enlighten both the novice and the expert alike.

The text discusses the extraordinary advances that have taken place in the management of spinal cord tumors during the last few decades, in a variety of fields: neuroanatomy, electrophysiology, neuroimaging, operative technique, and neuropathology. The authors synthesize these developments for the reader, and provide a modus operandi for the treatment of spinal cord tumors that is based on logic and common sense. It is likely that this book will become the classic on this topic for contemporary neurosurgeons that Elsberg's monograph was for the neurosurgeons of his era.

New York *Paul R. Cooper*

Authors' Preface

The improvements that have been made over the past 30 years in the diagnosis and treatment of intramedullary spinal cord tumors have prompted us to report our own experience in a book entirely devoted to this subject. In doing this, we are following the example set in 1964 by Guidetti, Fortuna, Moscatelli, and Riccio; and, in the same year, by Slooff, Kernohan, and MacCarty. Since then, there have been very few reports dealing with intramedullary spinal cord tumors, with the exception of the odd chapter in general treatises on spinal cord tumors. The Société de Neuro-Chirurgie de Langue Française devoted two of its annual reports to intraspinal tumoral pathology: *Hemangioblastomas* (M. Hurth, 1975) and *Ependymomas* (G. Fischer, 1977).

The present report deals exclusively with intramedullary spinal cord tumors. In the first part, we discuss the intramedullary spinal cord tumor in general, i.e., diagnostic and therapeutic problems that are common to all intramedullary spinal cord tumors. Next, we describe the particular aspects of intramedullary spinal cord tumors according to their individual histological type. Finally, we report our results with a series of 171 patients who underwent surgery, and express our opinion with regard to radiotherapy.

Throughout this work, we have focused our attention on presenting a study of cases that is thoroughly consistent with our real experience. For this reason, both in the text, legends, and tables, patients are referred to by the reference numbers assigned to them in Table **2** (the table summarizing the clinical data). Patient reference numbers appear in italics between square brackets: *[12]*, to distinguish them from bibliographical references, which appear in round brackets in normal type: (12).

Georges Fischer
Jacques Brotchi

Introduction

Magnetic resonance imaging (MRI) has revolutionized the diagnosis of intramedullary spinal cord tumors (IMTs). The lesion within the cord, whether solid or cystic, or both, and whether isolated or multiple, can now be directly visualized, and the precise cause of the enlarged spinal cord can often be determined. With nonglial tumors, MRI has a high degree of accuracy; but for glial tumors, accurate distinction between astrocytomas and ependymomas may often require histological examination.

All IMTs raise problems in terms of surgical technique that may be specific to each type of tumor, or common to all tumors. For this reason, the present monograph includes a chapter on features common to all IMTs, and a further chapter dealing with the particular aspects of each IMT.

On the strength of our shared experience, we feel justified in publishing this study of 171 patients, which may be regarded as a homogeneous series. The two of us compiled the results obtained with our Lyons and Brussels patients during a follow-up period ranging from one to 29 years. Above all, it seemed important to us to emphasize this long-term follow-up and its advantages, as this is rarely found in the literature.

The controversy over the efficacy of radiotherapy has led us to extensively review everything that has been published on the subject, including both benign and malignant tumors, and the very different problems these pose in pediatric and adult patients.

Our investigation in collaboration with members of the Société de Neuro-Chirurgie de Langue Française (SNCLF) has allowed us to assess the relative frequency of the different types of IMTs. The fundamental value of this assessment is, therefore, epidemiological. We wish to thank the following colleagues who agreed to fill out our questionnaire: J. Auque and H. Hepner (Nancy, France), J.D. Born (Liège, Belgium), G. Broggi (Milan, Italy), J. Brunon (St-Etienne, France), S. Cambria (Messina, Italy), J.P. Castel and A. Rougier (Bordeaux, France), J. Chabannes and B. Irthum (Clermont-Ferrand, France), J.P. Chirossel (Grenoble, France), M. Choux and G. Léna (Marseilles, France), J.L. Christiaens and R. Assaker (Lille, France), P.R. Cooper (New York, USA), A. Czorny (Besançon, France), P. Delhemmes (Lille, France), B. Demierre and J. Berney (Geneva, Switzerland), J. D'Haens (Brussels, Belgium), E. de Divitiis (Naples, Italy), M. Djindjian and Y. Kéravel (Créteil, France), A. Dubuisson and A. Stevenaert (Liège, Belgium), J.M. Fuentès and J. Bénezech (Montpellier, France), C. Gilliard (Yvoir, Belgium), Y. Guégan and G. Brassier (Rennes, France), M. Gueye (Dakar, Senegal), J.P. Houtteville (Caen, France), M. Jan (Tours, France), P. Jourdan (Toulon, France), K. Kalangu (Harare, Zimbabwe), J. Lagarrigue (Toulouse, France), F. Lapierre (Poitiers, France), D. Le Gars (Amiens, France), P. Mercier and G. Guy (Angers, France), K.L. Mourier, J. Cophignon and B. George (Paris, France), A. Pansini (Florence, Italy), W. Pellet (Marseilles, France), R. Ravon and J.J. Moreau (Limoges, France), J.J. Santini (Tours, France), P. Selosse (Antwerp, Belgium), J. Trémoulet (Toulouse, France), A.F. Vincentelli (Marseilles, France), D. Woscoboïnik (San Luis, Argentina). Our special acknowledgments go to Fred Epstein and Paul Cooper, whose personal experience is considerable, and whom we visited in their respective hospital departments in New York; they kindly answered all our questions. We also wish to thank François Resche (Nantes, France) for checking the section on hemangioblastomas.

Neither the present study of IMTs nor its bibliography makes any claim to being exhaustive. Our main concerns have been to mention the most useful references for further study of IMTs and to emphasize the most recent work done in each particular field. We are fully aware we have not solved the manifold problems related with IMTs. Some areas of knowledge, such as the pathophysiology of intramedullary cysts, the genetics of hemangioblastomas, and the pathogenesis of lipomas, have been intentionally omitted, since our purpose first and foremost was to present our opinion on the practical problems confronting the neurosurgeon when diagnosing and treating intramedullary spinal cord lesions.

We are very grateful to Paul Cooper, M.D., Professor of Neurosurgery at New York University, to whom we express our most sincere and friendly thanks for his advice and his great help in revising our English.

Finally, we would like to thank our secretaries, Catherine Bardin and Sylvie Marécaux, for their considerable help and endless patience throughout the drafting of this work.

List of Contributors

Danielle Balériaux
Professeur, Clinique de Neuroradiologie
Hôpital Erasme, Université Libre de Bruxelles
808, route de Lennik
1070 Brussels
Belgium

Gilles Brassier
Professeur, Service de Neuro-Chirurgie
Hôpital Pontchaillou, Centre Hospitalier Universitaire de Rennes
1, rue Le Guillou
35033 Rennes
France

Jacques Brotchi
Professeur, Service de Neuro-Chirurgie
Hôpital Erasme, Université Libre de Bruxelles
808, route de Lennik
1070 Brussels
Belgium

Georges Chignier
Service de Neuro-Chirurgie
Hôpital Pierre Wertheimer, Centre Hospitalier Universitaire de Lyon
59, boulevard Pinel
69394 Lyon
France

Philippe David
Clinique de Neuroradiologie
Hôpital Erasme, Université Libre de Bruxelles
808, route de Lennik
1070 Brussels
Belgium

Christophe Destrieux
Service de Neuro-Chirurgie
Hôpital Bretonneau, Centre Hospitalier Universitaire de Tours
2, boulevard Tonnellé
37044 Tours
France

Olivier De Witte
Service de Neuro-Chirurgie
Hôpital Erasme, Université Libre de Bruxelles
808, route de Lennik
1070 Brussels
Belgium

Georges Fischer
Professeur, Service de Neuro-Chirurgie
Hôpital Pierre Wertheimer, Centre Hospitalier Universitaire de Lyon
59, boulevard Pinel
69394 Lyon
France

Jean-Claude Froment
Professeur, Service de Radiologie
Hôpital Pierre Wertheimer, Centre Hospitalier Universitaire de Lyon
59, boulevard Pinel
69394 Lyon
France

Paul Garassus
Service de Neurologie Fonctionnelle et d'Epileptologie
Hôpital Pierre Wertheimer, Centre Hospitalier Universitaire de Lyon
59, boulevard Pinel
69394 Lyon
France

Paul Hallacq
Service de Neuro-Chirurgie
Hôpital Pierre Wertheimer, Centre Hospitalier Universitaire de Lyon
59, boulevard Pinel
69394 Lyon
France

Vicente Ibáñez
Service de Neurologie Fonctionnelle et d'Epileptologie
Hôpital Pierre Wertheimer, Centre Hospitalier Universitaire de Lyon
59, boulevard Pinel
69394 Lyon
France

Anne Jouvet
Laboratoire d'Anatomie Pathologique
Hôpital Pierre Wertheimer, Centre Hospitalier Universitaire de Lyon
59, boulevard Pinel
69394 Lyon
France

Anne Liard
Service de Neurologie
Hôpital Erasme, Université Libre de Bruxelles
808, route de Lennik
1070 Brussels
Belgium

Celso Matos
Clinique de Neuroradiologie
Hôpital Erasme, Université Libre de Bruxelles
808, route de Lennik
1070 Brussels
Belgium

François Mauguière
Professeur, Service de Neurologie Fonctionnelle et d'Epileptologie
Hôpital Pierre Wertheimer, Centre Hospitalier Universitaire de Lyon
59, boulevard Pinel
69394 Lyon
France

Philippe Menei
Service de Neuro-Chirurgie
Centre Hospitalier Universitaire d'Angers
4, rue Larrey
49033 Angers
France

Philippe Mercier
Professeur, Laboratoire d'Anatomie et Service de Neuro-Chirurgie
Hôpital de la Haute Chaline, Centre Hospitalier Universitaire d'Angers
4, rue Larrey
49033 Angers
France

Jacques Noterman
Professeur, Service de Neuro-Chirurgie
Hôpital Erasme, Université Libre de Bruxelles
808, route de Lennik
1070 Brussels
Belgium

Zoltan Patay
Clinique de Neuroradiologie
Hôpital Erasme, Université Libre de Bruxelles
808, route de Lennik
1070 Brussels
Belgium

Joël Rémond
Service de Neuro-Chirurgie
Hôpital Pierre Wertheimer, Centre Hospitalier Universitaire de Lyon
59, boulevard Pinel
69394 Lyon
France

Fatima Rio
Clinique de Neuroradiologie
Hôpital Erasme, Université Libre de Bruxelles
808, route de Lennik
1070 Brussels
Belgium

Tony Rizk
Service de Neuro-Chirurgie
Hôpital Pierre Wertheimer, Centre Hospitalier Universitaire de Lyon
59, boulevard Pinel
69394 Lyon
France

Marie-Christine Rousselet
Laboratoire d'Anatomie Pathologique
Centre Hospitalier Universitaire d'Angers
4, rue Larrey
49033 Angers
France

Ghislaine Saint-Pierre
Laboratoire d'Anatomie Pathologique
Hôpital Pierre Wertheimer, Centre Hospitalier Universitaire de Lyon
59, boulevard Pinel
69394 Lyon
France

Isabelle Salmon
Laboratoire d'Anatomie Pathologique
Hôpital Erasme, Université Libre de Bruxelles
808, route de Lennik
1070 Brussels
Belgium

Michel Tommasi
Professeur, Laboratoire d'Anatomie Pathologique
Hôpital Pierre Wertheimer, Centre Hospitalier Universitaire de Lyon
59, boulevard Pinel
69394 Lyon
France

Philippe Tournut
Service de Radiologie
Hôpital Pierre Wertheimer, Centre Hospitalier Universitaire de Lyon
59, boulevard Pinel
69394 Lyon
France

Gabriella Turano
Service de Neurologie Fonctionnelle et d'Epileptologie
Hôpital Pierre Wertheimer, Centre Hospitalier Universitaire de Lyon
59, boulevard Pinel
69394 Lyon
France

Francis Turjman
Service de Radiologie
Hôpital Pierre Wertheimer, Centre Hospitalier Universitaire de Lyon
59, boulevard Pinel
69394 Lyon
France

Stéphane Velut
Professeur, Service de Neuro-Chirurgie
Hôpital Bretonneau, Centre Hospitalier Universitaire de Tours
2, boulevard Tonnellé
37044 Tours
France

Gustavo Zomosa
Service de Neuro-Chirurgie
Hôpital Erasme, Université Libre de Bruxelles
808, route de Lennik
1070 Brussels
Belgium; *also* Hôpital Fach, Santiago, Chile

Contents

Abbreviations

AIDS	Acquired immunodeficiency syndrome
CT	Computed tomography
CUSA	Cavitron ultrasonic surgical aspirator
EMA + or –	Epithelial membrane antigen (positive or negative)
FC	Fasciculus cuneatus
FG	Fasciculus gracilis
GFAP + or –	Glial fibrillary acid protein (positive or negative)
HPS	Hemalum, phloxine, and saffron
IMT	Intramedullary spinal cord tumor
MBP + or –	Myelin basic protein (positive or negative)
MEP	Motor evoked potentials
MRI	Magnetic resonance imaging
PS 100 + or –	Protein S 100 (positive or negative)
SAS	Subarachnoid space
SEP	Somatosensory evoked potentials
SNCLF	Societé de Neuro-Chirurgie de Langue Française
WHO	World Health Organization

1 Intramedullary Spinal Cord Tumors

Intramedullary spinal cord tumors (IMTs) are tumors that affect the spinal cord proper. They have to be distinguished from tumors involving the medulla and cauda equina, which are not truly intramedullary. It is now well established that tumors of the filum terminale that invaginate into the conus medullaris are not IMTs (77). In this study, we have therefore not included cauda equina ependymomas, and we have focused our discussion solely on tumors that occur and develop in the conus medullaris. The distinction is all the more relevant in that IMTs are exophytic only in exceptional cases. The boundary between the spinal cord and the medulla oblongata is somewhat less clear. Numerous tumors may develop on either side of the border between these two structures. We have excluded tumors of the medulla that do not extend beyond the anatomic limit marked by the middle of the anterior arch of the atlas, but we have included IMTs that develop as far rostrally as the obex of the fourth ventricle. Some slowly developing IMTs may involve the entire spinal cord, and these are termed holocord tumors (79); we have studied nine of our own cases *[4, 8, 27, 37, 50, 52, 79, 137, 167]*. IMTs usually involve only the spinal cord; exophytic IMTs are a fairly rare phenomenon, which we have encountered in only five cases *[50, 69, 97, 100, 109]*. There are also IMTs that grow in a multifocal fashion (4), and infiltrating tumors that involve the entire neuraxis. Both of these types initially manifest by spinal cord signs, as in our two cases of malignant glioma *[105]* and lymphoma *[123]* formerly referred to as reticulum-cell sarcoma (27). Independent of their histology, IMTs have a number of clinical, laboratory, and therapeutic features in common. For this reason, the present chapter will discuss the intramedullary spinal cord tumor in general terms.

1.1 General Considerations

Anatomy of the Spinal Cord

G. Brassier, C. Destrieux, P. Mercier, S. Velut

Descriptive Anatomy

General Features

The spinal cord is the part of the central nervous system that is located within the spinal canal. The spinal cord has the shape of a roughly cylindrical stem, is of whitish color, and is slightly flattened ventrally and dorsally. It has two enlargements or bulges, one in the cervical region and another in the thoracolumbar region. It is 45 cm long in males, 42 cm in females, and is 1 cm wide. It has a mean weight of 30 grams (109, 268). The cervical enlargement is 10 cm long, extending from the C4 to the T1 vertebral levels; the widening in this region is due to the extensive innervation of the upper extremities and diaphragm. The lumbar enlargement is 8 cm long, extending from T9 to T12, and supplies the innervation of the lower extremities. It is located above and is continuous with the conus medullaris, which tapers off (202) at the level of the L1–L2 disk space into the filum terminale, an atrophic remnant of the caudal segment of the embryonic spinal cord, at the caudal end of the dural tube.

The rostral end of the spinal cord is continuous with the caudal portion of the medulla, marked by the pyramidal decussation located under the foramen magnum, in front of the middle of the anterior arch of the atlas. This limit corresponds to the upper border of the C1 nerve root, the first of the 31 spinal nerves. However, De Oliveira et al. (48) have emphasized the difficulty of identifying this limit dorsally (as only ventral roots are constantly present). The first cervical nerve runs below the foramen magnum and emerges from the dura immediately behind the vertebral artery. The spinal accessory nerve (XI) often provides a branch to the first cervical nerve when the latter has no dorsal root emerging from the dorsolateral sulcus, and always provides one when this dorsal root is missing (48).

External Aspect

The spinal cord has four surfaces: ventral (anterior), dorsal (posterior), and two lateral ones.

The ventral surface is marked by a ventral median fissure that runs the entire length of the spinal cord (Figs. **1–4**); the depth of the fissure is 2–3 mm, and its edges can be separated to reveal the white ventral commissure. This longitudinal fissure, or *anterior median sulcus*, splits the ventral aspect of the

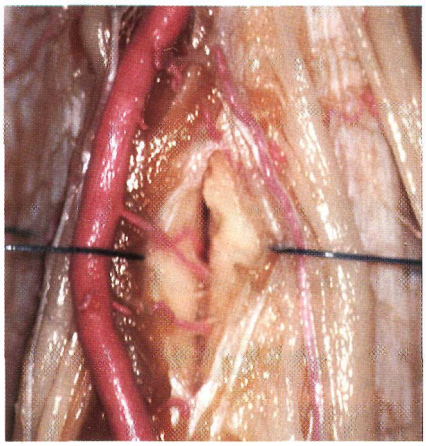

Fig. 1 **Anterior view of the cervical spinal cord,** with the anterior fissure edges separated to visualize the central arteries (sulco-commissural arteries)

Fig. 2 **Anterior view of the thoracic spinal cord;** the anterior spinal artery does not lie in the anterior median fissure

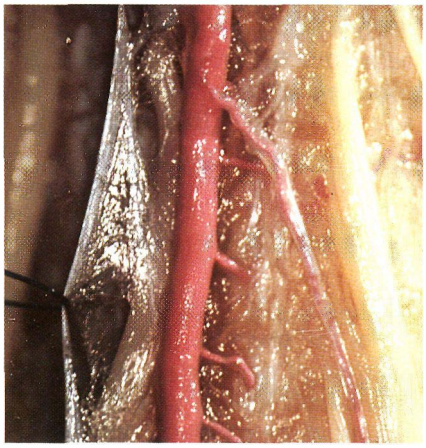

Fig. 3 **Anterior view of the cervical spinal cord,** with the anterior fissure edges separated to visualize the central arteries

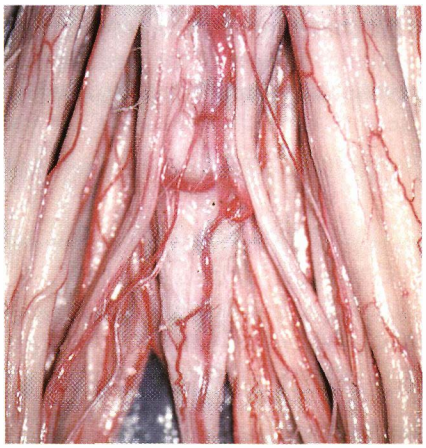

Fig. 4 **Anterior view of the lumbar spinal cord;** the anterior spinal artery does not lie in the anterior median fissure

spinal cord into two symmetrical ventral columns 2–3 mm wide, the lateral borders of which give rise to the ventral roots.

On the **dorsal surface** there is also a *dorsal medial sulcus.* Although it is not a fissure, it is also possible to separate its edges. On either side of this sulcus, at a distance of about 3 mm, the dorsal roots assume the shape of a vertical fan before entering the spinal cord at the level of the corresponding *dorsal collateral sulcus.* The dorsal median sulcus and the two dorsal collateral sulci form the borders of the two dorsal columns.

The lateral surface of the cord contains a lateral column located between the entrance of the dorsal roots and the exit of the ventral roots. In addition, from C1 to C5 or C6, the rootlets of the spinal accessory nerve (XI) arise from the lateral aspect of the spinal cord and merge into a common trunk that ascends along the lateral surface of the spinal cord before entering the foramen magnum. The 31 pairs of spinal nerves assume increasing obliquity in a rostrocaudal direction. Each of the ventral and dorsal roots of these nerves arise from six to eight rootlets.

Internal Configuration

Gray matter. The spinal cord gray matter consists of nerve cells, and has a typical H shape in cross-section. In fact, it closely resembles a butterfly shape, and is characterized by a *central* or *ependymal canal.* The spinal cord is arranged symmetrically about this central axis, forming two lateral masses joined by a

transverse layer (central intermediate substance). Each lateral mass of gray matter consists of two horns.

The *ventral horn* is massive and bulging, and consists of motor neurons divided into three groups of cells (medial, central, and lateral); the central group is present only in the cervical region. The neurons of the ventral horn are arranged in a somatotopic fashion: those innervating the axial musculature lie medially, those which supply the muscles of the extremities lie laterally; the neurons providing innervation to the extensors lie ventrally to those innervating the flexors.

The *dorsal horn* is oblong, and consists of cells arranged, according to Rexed (219), in laminae or layers, numbered from I to VI. The thin, tapering dorsal end consists of the substantia gelatinosa (laminae II and III), covered by the substantia spongiosa (lamina I). Behind this lies the dorsolateral bundle, or marginal zone of Lissauer, separating the dorsal horn from the spinal cord surface. The components of the dorsal horn are arranged axially, and show a glomerular organization (97). The first synapse of the contralateral neospinothalamic tract is located in lamina I. The fibers reaching this area are poorly-myelinated type A delta fibers and, mainly, unmyelinated type C fibers. In laminae V and VI, the long dendritic arborization reaches laminae II and III and joins the afferent A delta fibers. Axons arising there constitute the contralateral paleospinothalamic tract. Other structures complete this basic configuration, consisting of interneurons, segmental (A beta myelinated fibers) and suprasegmental afferent fibers (crossing and reticular pyramidal fibers of the lateral cord). The intermediolateral region is located laterally where the dorsal and ventral horns join; in the thoracic spinal cord, this region is more prominent (lateral horn), and is the site of the reticular formation.

White matter. The white matter contains the ascending and descending pathways of the spinal cord.

The *descending pathways* consist, for the most part, of the *pyramidal or corticospinal tracts.* The crossing pyramidal tract is the most important, and occupies the posterior region of the lateral funiculus, where its fibers are arranged somatotopically (medial fibers innervating the cervical region, lateral fibers supplying the sacral roots). At each spinal level, fibers leave the pyramidal tract to reach the ventral gray horn medioventrally (lamina VII) where they join the second-order neurons (motoneurons) that form the ventral nerve root. The uncrossed pyramidal tract (less than 20% of pyramidal fibers) runs in the ventral column, close to the anterior median fissure; its destination is the cervical muscles, and its distribution is bilateral. The *extrapyramidal bundles,* which belong to the descending pathways, arise from the suprasegmental centers of the brain stem, and consist of two parts. One is the *anteromedial* column (vestibulospinal, medial reticulospinal, olivospinal, tectospinal, and interstitiospinal tracts), whose fibers are located in the ventral cord and terminate bilaterally in the gray horn (lamina VII). This has a facilitatory action on postural tone (extensor and antigravity muscles). The other is the *posterolateral bundle,* located deep within the lateral column (rubrospinal, bulbar reticulospinal tracts), whose fibers terminate ipsilaterally or contralaterally in lamina VII of the ventral horn. This has a facilitatory action on the distal flexor muscles.

Ascending pathways are formed where the posterior roots enter the spinal cord. The *dorsal root junction* (246) comprises the central part of the dorsal roots, Lissauer's tract, and layers I to V of the gray horn (area of synapse with the extralemniscal ascending pathway). Where they enter the dorsal collateral sulcus, their fibers lie in a specific fashion: small fibers lie laterally, large fibers lie dorsomedially. In Lissauer's tract, two areas can be distinguished: a medial area composed of small diameter fibers, and a lateral one consisting of large, longitudinal proprioceptive fibers connected to the substantia gelatinosa at several levels. This tract functions as an intersegmental moderator for nociceptive afferent signals. Its medial region transmits excitatory impulses from each dorsal root to adjacent segments. Its lateral region has inhibitory effects, from the substantia gelatinosa and to the adjacent spinal segments. Most nociceptive fibers travel through the medial region of Lissauer's tract, cross the dorsal region, and enter the dorsal horn. The recurrent collaterals arising from the large lemniscal fibers reach the dorsal horn via the ventral region of the substantia gelatinosa. The latter has a role in modulating the nociceptive influx at each segment due to the presence of synaptic connections between the dendrites of the spinoreticulothalamic bundle and the primary afferent fibers. The *dorsal columns* contain the large-diameter A beta fibers that transmit epicritical and proprioceptive sensation. Their distribution is strictly ipsilateral, and their arrangement is somatotopic: the medial fibers arise in the lumbosacral region and constitute the *fasciculus gracilis* (Goll's column); the fibers from the cervical region are located laterally inside the *fasciculus cuneatus* (Burdach's column). These ascending fibers give off short descending collateral branches before entering the homolateral dorsal gray horn; they travel to the nucleus gracilis and nucleus cuneatus where the medial lemniscal pathway begins, and to the accessory cuneate nucleus, which projects into the cerebellum (190). The *anterolateral column* contains several bundles whose nerve cells are located in the dorsal horns. After decussation, the *neospinothalamic tract,* a second-order neuron of

nociceptive pain and temperature sensation, reaches the anterolateral bundle anterior to the ventral horn. The arrangement of its fibers is somatotopic: the sacral fibers lie superficially, the cervical fibers lie deeply. The *paleospinothalamic and spinoreticular tracts* consist of fibers derived from the contralateral V, VI, and VII laminae. The latter fibers lie more medially than the former in the anterolateral bundle, travel to the pontine reticular formation, and participate in the genesis of somatovegetative response to pain and in the activation of the descending serotoninergic and noradrenergic analgesic systems. The spinocerebellar pathways consist of two tracts: the *dorsal spinocerebellar tract* (Flechsig's direct tract), arising from cells located in the ipsilateral thoracic column, carries proprioceptive information to the cerebellum; the *ventral spinocerebellar tract* (Gowers' tract) consists of fibers arising from the contralateral ventral horn (lamina VII) and coursing through the ventral part of the lateral column after decussating at the level of the ventral spinal commissure. The bundle crosses the midline a second time to enter the superior cerebellar peduncle. It transmits already integrated information from proprioceptive afferent neurons to the interneurons of the ventral horn (97).

Central or ependymal canal. This vestigial canal, which runs the entire length of the spinal cord, is a remnant of the large embryonic central canal. Its diameter ranges from 0.1 to 0.2 mm at birth. In the adult, the persistence of this canal is a rare phenomenon; it is nearly always completely obliterated by ependymal cells or neuroglial clusters (187). It may persist over a few millimeters in length, but lies indistinctly in the central substantia gelatinosa, and is lined with ependymal cells.

Meningeal Relationships

The spinal meninges differ from those of the brain due to the presence of a thicker pia mater attached to the inner dural surface by the dentate ligaments, and the presence of an intermediate leptomeningeal layer and a fatty extradural space. The meninges are thus adapted to a mobile vertebral column, with the spinal cord suspended and centered within the subarachnoid space (SAS). The SAS is contained, in turn, within a nonelastic dural sac that adapts perfectly to movements of the spinal column.

Pia Mater

The spinal pia mater is mechanically stronger than the pia mater of the brain. According to Maillot (152), it consists of loose connective tissue made of elastic collagen fibers and reticulin-containing mesothelial cells. It is fused with the surface of the spinal cord, and consists of circular fibers in two layers: a deep one, or pia intima, and a superficial one, or epipia. The pia lines the ventral median fissure, forms the dorsal median septum, and terminates at the junction of the spinal cord and nerve roots. Only the superficial layer, consisting of longitudinal fibers, surrounds the roots, giving them a white hue. Fissures between these two layers allow communication with the SAS. The ventral longitudinal vessels course between the two layers, and are covered with a pial condensation, the linea splendens, a structure 1 mm thick (185) that has no attachment to the dura or arachnoid. The pial sheath covers the vessels as far as the capillaries, and separates the SAS from the perivascular spaces. Cloyd and Low (37) have described fenestrations in the pia mater, around the conus medullaris. According to Nicholas and Weller (189), the pia mater is a single continuous layer of cells, separated from the nervous tissue by a thick subpial collagenous layer extending laterally to the dentate ligament.

Dentate Ligaments (Fig. **5**)

Thick at their rostral ends, the dentate ligaments attach the lateral surface of the spinal cord to the dura transversely. The medial border of each, thinner than the lateral border, is adherent to the lateral column anterior to the border between the dorsolateral column (corticospinal tract) and the ventrolateral column (anterolateral tract). The lateral border of each ligament is free, with the exception of the areas adjacent to the roots. These are thick serrations whose apices are attached to the dura between the overlying and underlying root sheaths, although they are closer to the latter. This arrangement results in a pattern of arcades located in front of the emerging nerve roots. At the cervical level, the ligament is located anterior to the spinal accessory nerve. The

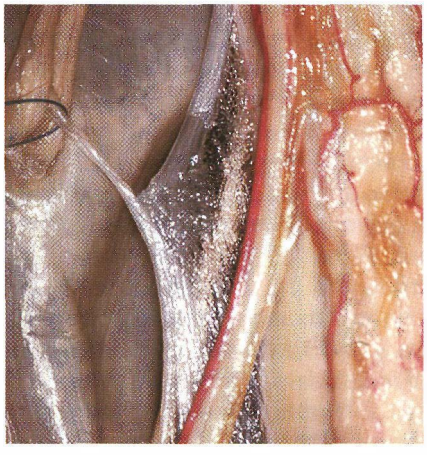

Fig. **5** **Posterior view of the thoracic spinal cord.** A nerve root artery can be seen behind the dentate ligament

cervical serrations are horizontal, the thoracic serrations are vertical. The first serration has an ascending direction, surrounding the dural bulge of the vertebral artery, and is attached immediately above and behind its dural penetration, under and behind the foramen of nerve XII, at the edge of the foramen magnum. The most caudal serration is thin and filiform, and its point of insertion is above the exit of the first lumbar nerve. Its medial border extends into the filum terminale. When there is one arcade per spinal nerve, the total number of serrations is 21, but there may be one arcade for two nerves, or two arcades for one nerve. Thus, the number of serrations may vary from 18 to 22. According to Rabischong et al. (211), the dentate ligament is composed of the pia medially and the dura laterally. According to Nauta et al. (185), it is a part of the pia that traverses the superficial layer of the arachnoid and is attached to the dura. Nicholas and Weller (189) believe that this ligament consists of fibrous tissue emerging from the subpial layer and covered with leptomeningeal cells that are continuous with the arachnoid.

Arachnoid

The older descriptions of the arachnoid by Key and Retzius (128) remain valid today. These authors described dorsal and dorsolateral arachnoidal septa, but did not observe any in the area anterior to the dentate ligaments, in agreement with the embryologic study by Osaka et al. (194). The latter investigators showed that the SAS, which will later contain the cerebrospinal fluid, initially develops on the ventral aspect of the spinal cord, and then on its dorsal aspect. Consisting of a dense, impermeable, superficial layer adherent to the dura, the arachnoid may contain calcifications. It has processes by which it is attached to the pial surface of the spinal cord and to the inner layer of the dura, from which it may easily be detached, however.

Laterally, the pia and arachnoid taper off at the point of contact between the spinal nerves and the dura, the latter becoming continuous with the epineurium (152). At this level, the arachnoid has intradural and transdural processes (220), as well as transvenous processes, similar to the pacchionian granulations found intracranially (285), which may be involved in cerebrospinal fluid resorption. In the SAS, several types of septa have been described (185). The *median dorsal septum* is fenestrated, and runs from the superficial layer of the arachnoid to the dorsal aspect of the spinal cord along the dorsal median vein, whose winding course determines the shape of the septum. This septum, of which there are sometimes two, extends from the middle part of the cervical cord to the upper part of the lumbar cord, rarely as far as the filum terminale. Several fenestrated *dorsolateral septa* extend from the area of penetration of the dorsal roots, which they connect dorsolaterally, to the superficial layer of the arachnoid. Laterally, these septa merge and extend to the area where the dorsal and ventral roots meet. No septum sheathes the ventral roots. The dorsolateral septa are more conspicuous in the lower cervical and thoracic areas. A dorsolateral septum may arise from the median septum (especially if the latter is winding) to form a rostrocaudal partition. According to Nicholas and Weller (189), there is a distinct intermediate leptomeningeal layer, lining the deep aspect of the superficial leaflet of the arachnoid, which constitutes the dorsal septum, and is attached to the pial surface of the spinal cord, which it covers, along with nerve roots, blood vessels, and dentate ligaments. In summary, the spinal cord is protected and strengthened by three structures: the subpial connective tissue, the pia mater, and the arachnoid.

Dura Mater

The spinal dura encloses the caudal end of the medulla, the spinal roots of the spinal accessory nerves, the spinal cord, the filum terminale, and the cauda equina, and extends from the foramen magnum to the sacrum. The dura, which forms a cylindrical sheath, is separated from the spinal canal by the epidural space, and contains fat and the epidural venous plexuses.

The **thick rostral end of the dural sheath** is adherent to the margin of the foramen magnum, to the dorsal aspect of the process of the axis, from which it is separated by the tectorial membrane (an extension of the common dorsal vertebral ligament) and to the dorsal craniospinal ligaments. This adhesion disappears below the axis. Laterally, each vertebral artery pierces the dura immediately below the foramen magnum, flanked posteriorly by the first spinal nerve and surrounded by a 4–5-mm dural sleeve that merges with the adventitia. Where it penetrates the dura, it gives rise to the posterior spinal artery (48), which is the vascular supply to the posterior part of the spinal cord.

The **caudal end of the dural sac** terminates abruptly at the bottom of the dural "cul-de-sac" at the lower border of the second sacral vertebra, or, in children, at the upper border of the third sacral vertebra. Below, the dura mater surrounds the filum terminale and provides its coccygeal attachment.

The diameter of the dural tube is smaller than that of the spinal canal, but much larger than that of the spinal cord. The epidural space is narrower anteriorly. Although the dura mater has no connection with the dorsal osteoligamentous plane, it adheres to the dorsal vertebral ligament by means of fibrous bands. In the intervertebral foramen, the dura is adherent to the periosteum, before it becomes continuous with the epineurium. The blood supply to the dura is

provided by the radicular, spinoradicular, and radiculopial arteries (156).

Vascularization

For this monograph, spinal cords from 20 adults were dissected, and arterial or venous injections, or both, with red or blue latex were carried out.

Arterial Blood Supply

The spinal cord is vascularized by a pial anastomotic network supplied by the radiculospinal and radiculopial arteries, which give rise to the intrinsic spinal cord arteries.

The **pial arterial network** includes longitudinal arteries and transverse branches that form a vague grid-like pattern, in which a predominantly longitudinal blood flow can be perceived. The *anterior spinal artery* arises from the vertebral arteries in the upper cervical region. It runs down the ventral aspect of the cord, in front of the ventral median fissure, which it does not penetrate. A single anterior spinal artery, which is continuous from the cervical region down to the conus, is usually present (Fig. **6**). In the upper thoracic region, the anterior spinal artery may be discontinuous (Fig. **7**), and in the cervical region (Figs. **2**, **4**), it may split into a paired anterior spinal artery (272). The diameter of the anterior spinal artery (200–500 μm) is at its maximum at the level of the lumbar and cervical enlargements (141). The *posterior blood supply* is provided by discontinuous arteries of smaller size (100–200 μm), consisting of predominantly longitudinal anastomotic vessels within the pial network. Usually, there is no arterial trunk in front of the dorsal median fissure, but there are two dorsal arteries that run just behind the dorsal roots

Fig. **6** **Anterior view of the conus medullaris.** The anterior spinal artery and the posterolateral longitudinal trunks can be seen converging

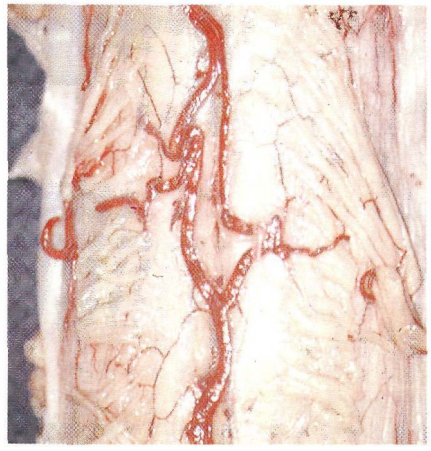

Fig. **7** **Anterior view of the cervical spinal cord.** Duplication of the anterior spinal artery

Fig. **8** **Posterior view of the thoracic spinal cord.** The two posterolongitudinal arteries are shown

Fig. **9** **Posterior view of the conus medullaris.** Between the two posterolongitudinal arteries, the posterior longitudinal venous trunk can be seen

Fig. **10** **Posterior view of the conus medullaris.** Between the two postero-longitudinal arteries, the posterior longitudinal venous trunk can be seen

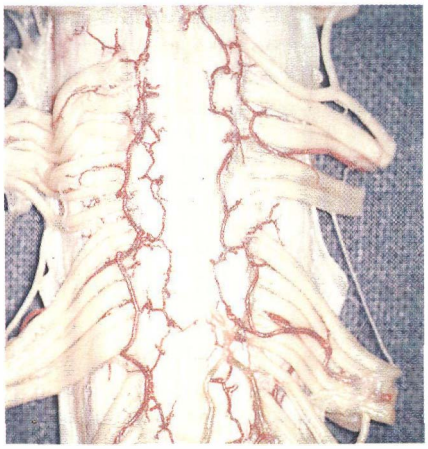

Fig. **11** **Posterior view of the thoracic spinal cord.** The two posterolongitudinal arteries are shown

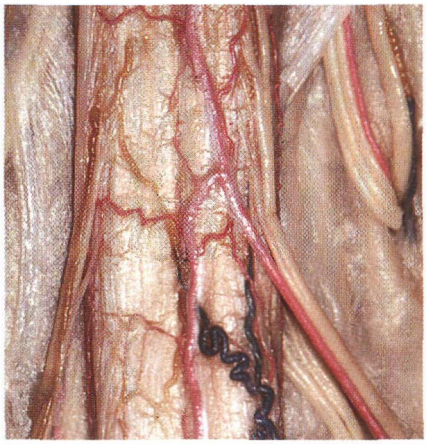

Fig. **12** **Anterior view of the thoracolumbar spinal cord.** A large lumbar radiculomedullary artery can be seen joining the anterior spinal artery

(Figs. **5**, **8–11**). In the upper cervical region, two additional lateral blood vessels (the lateral spinal arteries) may run between the dorsal roots and the dentate ligament (141, 142).

The **radiculospinal and radiculopial arteries** supply blood mainly to the white matter of the spinal cord, and they run with the spinal nerves (Figs. **5**, **12**). The radiculopial arteries run to the transverse anastomoses, while the radiculomedullary arteries terminate in the longitudinal vessels with a typical, inferiorly concave hairpin course. Although the radiculospinal arteries provide most of the spinal cord blood supply, they are few in number, and their arrangement lacks consistency. Where the cord enlarges, they are more numerous in the dorsal aspect of the cord (11–16 of them) than in the ventral aspect (2–14), and they are more frequently seen on the right ventral aspect of the spinal cord than on the left (143, 272), and at the level of the cervical and lumbar enlargements. However, there is no difference in the arterial distribution of the dorsal aspect of the cord. Because of their size, a number of ventral radiculospinal arteries have been named. The artery of the lumbar enlargement (Adamkiewicz) (Fig. **12**) runs with a spinal nerve on the left side in 75–85% of cases, and between T9 and T12 in 75% of cases (143). When this artery arises above T8 or below L2, there is an additional artery that supplies the lumbar enlargement (56, 141, 143). The artery of the cervical enlargement follows the course of a nerve root between C4 and C8.

The **intrinsic medullary arteries** supply blood to the gray matter. The *central or sulcocommissural arteries* arise from the anterior spinal artery, run in the median ventral fissure, and give rise to terminal branches that run horizontally and vertically (143, 272). In the horizontal plane, there is a central artery that supplies only one half of the spinal cord; its branches have a comb-like pattern, with a long vertical axial stem. In the vertical plane, the complexity of the arborizations varies according to the spinal cord level. Arterial arborization is particularly rich in the thoracic region, compensating for the relative paucity of central arteries in this area. The 170–210 central arteries of the spinal cord are unevenly distributed: 7–12 per centimeter in the lumbar and cervical enlargement, versus only 2–3 per centimeter in the thoracic region (143, 272). Arising from the pial network, the perforating arteries penetrate the spinal cord in a radial fashion. The perforating and pial networks (272) give rise to the *vasa coronae.*

Anastomoses and arterial territories. At the *surface of the spinal cord,* the pial network forms multiple anastomoses between dorsal and ventral longitudinal vessels, connected around the conus medullaris by the anastomotic loop of Lazorthes (143). In the thoracic region, several central arteries are linked by anastomoses located in the ventral median fissure (141, 272). *Within the spinal cord parenchyma,* the ascending and descending branches of two contiguous central arteries join. In the thoracic region, *transmedullary anastomoses* between central arteries and the pial network occur rarely; indeed, their very existence is a matter of dispute (141, 143, 183, 272). The lack of anastomoses partially justifies the reputation of the mid-thoracic spinal cord as being "surgically fragile." The *central arteries* supply the gray matter, and the radially penetrating arteries supply the white matter. The *territory of the anterior spinal artery* includes the anterior two-thirds of the cord, while the remaining posterior third is supplied by dorsal vessels.

Venous Drainage

Venous drainage takes place first via the intrinsic vessels, which drain in turn into the pial veins (91).

The **intrinsic veins** are of two types: central and radially penetrating. The *central veins* drain part of the blood from one side of the spinal cord, and are arranged in a comb-like pattern, with a long vertical axial stem. In the ventral median fissure, several central veins merge before draining into the anterior spinal vein via a single trunk. These veins are more numerous, but smaller, than the corresponding arteries. The *radially penetrating veins* play a much more important role than their arterial counterparts. The radially penetrating veins of the dorsal sulcus (44, 272) arise from the adjacent gray matter, and drain into the pial network. As in the case of the arteries, intraspinal cord anastomoses between central and radially penetrating veins seem to exist in the thoracic region, and the role of these is unknown (141, 272).

The **pial venous network** consists of *longitudinal vessels* with transverse anastomoses. This network drains the cord via the ventral and radially penetrating veins, and the nerve roots via radicular veins (178). *The anterior spinal vein* lies dorsal to the artery (Fig. **12**). Unlike the course followed by the artery, that of the vein sometimes penetrates deeply into the ventral median spinal fissure over several centimeters. It continues rostrally as the median ventral medullary vein, and caudally as the vein of the filum terminale. The central veins, a few anterior radially penetrating veins, and the anterior radicular veins drain into it (178). The *posterior spinal vein,* which is often very large (Figs. **9**, **10**, **13**), is sometimes replaced by two or three smaller longitudinal veins. Their diameter (400–1000 μm) is larger than that of their arterial counterparts. This venous system has a winding pattern, particularly in the thoracic region, and zigzags from one posterior column to the other over the posterior median sulcus. *Anastomoses* are longitudinal and lateral, limited to a few centimeters in length, or transverse, linking the longitudinal veins.

The whole system forms a pial network of anastomoses between the anterior and posterior spinal veins around the conus medullaris, in the form of *venous rami cruciantes,* a pattern that occurs less consistently than is the case with the corresponding arterial network (272).

The **radicular veins** arise from the pial network and, laterally, anastomose on a ventral or dorsal nerve root. Several veins may join along this subdural course before draining into the internal longitudinal vertebral venous plexuses outside the dural sheath. According to Tadié et al. (265, 266), the size of the veins changes as they penetrate the dura through a baffle, which may function as a valve to prevent any backflow of blood. The relative paucity of the pial venous network is offset by the large number of radicular veins (30–70) and the homogeneity of their distribution. In 90% of cases, an anterior vein is present in the lumbar enlargement, coursing along a ventral nerve root between T12 and L3; in 40–90% of cases, there is also a posterior vein in the lumbar enlargement, running with one of the first lumbar nerve roots.

Conclusion

The surgical approach to the ventral *fissure* is blocked by the anterior spinal artery and the branches arising from it. The posterior approach is not blocked by arteries and veins, but there is no fissure on this side of the spinal cord. In order to remove an IMT, it is also possible to open the dorsal medial *sulcus,* by separating its edges without damaging the dorsal columns and their vessels.

Fig. **13** **Posterior view of the thoracic spinal cord.** The dura mater has been opened, and the posterior longitudinal venous trunk can be seen

Epidemiology

IMTs of the spinal cord account for two to four percent of central nervous system tumors in adults (41, 61, 98, 153, 165, 249). In children, the proportion is more or less the same (54, 68, 135), though it is higher (12%) during the first year of life (53, 200). Most IMTs are of glial origin.

The proportion of astrocytomas and ependymomas varies in different series. In adult series, the incidence of ependymomas has been reported to be higher (77, 153, 249), equal (254) or slightly less (24) than the incidence of astrocytomas. In pediatric series, the incidence of astrocytomas has been reported to be higher (67, 214) or equal to (68) the incidence of ependymomas, but a predominance of

Table 1 **Epidemiology:** survey of SNCLF members

	SNCLF	Lyons/ Brussels	*Total*
Ependymoma	322	64	386
Astrocytoma	298	41	339
Other gliomas	28	5	33
Metastases from CNS tumors	11	7	18
Metastatic visceral cancer	43	2	45
Melanoma	6	2	8
Lymphoma	1	2	3
Hemangioblastoma	61	19	80
Lipoma	71	11	82
Schwannoma	17	2	19
Meningioma	4	1	5
Cavernoma	22	5	27
Dermoid and epidermoid cysts	28	4	32
Neuroglial cyst	12	2	14
Sarcoidosis	2	3	5
Other IMTs	20	1	21
Total	946	171	1117

CNS: central nervous system.

ependymomas has not been observed. The investigation we conducted in collaboration with the members of the Société de Neuro-Chirurgie de Langue Française enabled us to document 946 cases of IMT on the basis of histological criteria. In the entire series, including our own patients (bringing the total to 1117 cases), there is a slight prevalence of ependymomas (386 cases) over astrocytomas of all grades (339 cases) (Table **1**).

Clinical Material (Table 2)

G. Fischer, J. Brotchi, G. Chignier, A. Liard, G. Zomosa, P. Menei, P. Hallacq

In our personal series of 171 patients, 41 presented with astrocytomas (24%) and 64 with ependymomas (37%). There were only a few children (13 cases, 7.6%), and two of these were infants with intramedullary spinal cord lipomas *[149, 151]*. The mean age was 37 ± 16 years (range four months to 73 years). There were ninety males (52.6%) and 81 females (47.4%). The ages of the patients at the time of surgery (Fig. **14a**; the date of the first operation is given if the patient underwent several) and sex (Fig. **14b**) are reported in detail in Table **2** for each of the 171 patients.

Location

Figure **14c** indicates the respective percentages of tumors occurring in the various locations: holocord in nine cases (5.3%), cervicomedullary in 19 cases (11.1%), cervical in 40 cases (23.4%), cervicothoracic in 42 cases (24.6%), thoracic in 38 cases (22.2%), and thoracolumbar in 23 cases (13.5%) (including 13 tumors – 7.6% – located in the conus medullaris).

Clinical Presentation

Intramedullary spinal cord tumors have no typical clinical presentation (77). Most commonly, adult patients complain of back or radicular pain, or paresthesias; children present with scoliosis or neurological complaints. The clinical course may be insidious, abrupt in onset, or may progress episodically. The clinical symptoms of our 171 patients are summarized in Table **2**.

A **variety of sensory symptoms** may be present. Sciatica related to dorsal column compression or paresthesias, or both, was seen in 54 patients (31.6%), back pain in 46 (27%), and radicular pain or paresthesias, or both, in 29 (17%) – affecting either the trunk (15 cases) or an extremity (14 cases). Nocturnal increases in pain, a characteristic element of the clinical presentation, were present in 15 cases (8.7%); 48 patients (28%) had no pain.

The **initial presentation** consisted of subjective or objective sensory disorders, or both, in 101 patients (59%), eight of whom presented with torticollis, motor disorders (n = 63, 36.8%) and urinary dysfunction (n = 4) *[52, 88, 144, 153]*. In one patient *[79]*, the presenting finding was scoliosis without other symptoms; in one case *[171]*, it was myoclonus of the big toe; and in one *[151]*, it was a subcutaneous mass noted at birth. The mean duration of symptoms prior to presentation was 3.8 years (range 15 days to 24 years).

The state of the patients' **clinical functioning** at the time of operation was graded using the McCormick classification, taking into account both sensory and motor deficits (Table **3**).

The **clinical presentation** is related to the level of the lesion. However, it is not unusual to see IMT patients with cervical involvement who have no sensory or motor deficit in the upper extremities. In addition, in patients with IMT involving the conus (24 cases), the expected sphincter dysfunction may be absent, as was observed in 12 of these cases (50%). Finally, in our series of 171 patients, we observed only four cases of papilledema *[12, 47, 113, 149]*, and no cases of subarachnoid hemorrhage. Hydrocephalus with intracranial hypertension was seen in two patients *[24, 110]*, and only at the time of extensive malignant tumor recurrence.

Table 2 **Clinical data**

Key to abbreviations, listed by column

PN°	Patient number		
n/O	Number of the operation		
S	Sex F Female M Male		
Histo	Histology, with the grade of severity, if evaluated Cavern Cavernoma C-Met Cancer metastasis dA Dysplastic astrocytoma derm-C Dermoid cyst E Ependymoma Epid-C Epidermoid cyst Gg ganglioglioma gr Graft Hb Hemangioblastoma im Intramedullary Lymph Lymphoma Med-gr Medulloblastoma graft Melano Melanoma Mening Meningioma Meta-gr Metastasis graft M-Met Melanoma metastasis Ngl-C Neuroglial cyst oA Ordinary astrocytoma Odg Oligodendroglioma pA Pilocytic astrocytoma Sarcoid Sarcoidosis Schwa Schwannoma sE Subependymoma		
Level	Level of the intramedullary tumor site B°- Medulla oblongata- conus-m Conus medullaris pan-m Panmedullary (holocord) whole sc Whole spinal cord		
Prev O	Previous operations. The time between the current operation and the previous operation (sometimes at another center), expressed in days (d), months (m), or years (y) AC Another center B Biopsy C Complete removal CEE Cauda equina ependymoma CPS Cystoperitoneal shunt Cut Mel Cutaneous melanoma I Incomplete removal NF2 Neurofibromatosis 2 P Partial removal PC Met Pulmonary cancer metastasis S Subtotal removal 2nd IMT Second intramedullary tumor 4 VE Fourth ventricle ependymoma 4 VMed Fourth ventricle medulloblastoma		
YO	Year of the operation		
Aop	Age of the patient at the time of operation		
poP	Preoperative tumor progression time in days (d), months (m), and years (y)		
ES	Early symptom b Bilateral bt Myo Big toe myoclonus Cerv p Cervical pain dc Dorsal column Dors p Dorsal pain hb Half-body h/pd Heat/pain deficit 4Ls Four limbs L Left side LL Lower limb Lumb p Lumbar pain Md Motor deficit N Nocturnally enhanced symptom p Pain Parapl Paraplegia pE Paresthesia R Right side rp Radicular pain Sc Sciatica sC Lip Sub-cutaneous lipoma sD Sensory deficit Tetrapl Tetraplegia Tortic Torticollis Tripl Triplegia UL Upper limb Urd Urinary disorders		
N	Nocturnally enhanced symptom		
F	Fundus of the eye N Normal P Papillary edema		
LP	Lumbar puncture: cerebrospinal fluid albumin (g/L); 0 = no LP		
M°	Myelography * Performed np Not performed		
T°	CT scan * Performed np Not performed		
I	MRI * Performed np Not performed		
A°	Spinal cord angiography * Performed np Not performed		

Table 2 **Clinical data** (continued)

Key to abbreviations, listed by column

g1	First (preoperative) evaluation of gait	
	g1	Patient can walk
	0	Patient cannot walk
M1	First (preoperative) evaluation of functional condition, according to the McCormick classification (grades I to IV)	
SDef (preop)	Preoperative sensory deficit, with the exact level specified	
	anesth	Anesthesia
	astereo	Astereognosis
	b	Bilateral
	BS	BrownSequard
	dcd	Dorsal column deficit
	hb	Half body
	HºE tam	Hypesthesia to all modes
	h/pd	Heat/pain deficit
	hypE	Hyperesthesia
	L	Left side
	LL	Lower limb
	perin	perineal
	sD	Sensory deficit
	R	Right side
	UL	Upper limb
U	Preoperative urinary disorders	
	C	Requiring catheterization
	d	Dysuria
	0	None
SpD1	Preoperative spinal deformity	
	abnC	Abnormal curvature
	C	Cervical
	CT	Cervicothoracic
	impC	Impaired curvature
	K	Kyphosis
	L	Lumbar
	S	Scoliosis
	T	Thoracic
	TL	Thoracolumbar
R	Extent of surgical resection	
	B	Biopsy
	C	Complete
	D	Decompression
	I	Incomplete
	P	Partial
	S	Subtotal
Lamin	Level of laminectomy, or (**bold** type) level of laminotomy; associated occipital craniectomy (+O)	
P	Quality of the cleavage plane between the tumor and healthy spinal cord	
	w	Well-defined
	i	Ill-defined
	?	Uncertain
	0	No cleavage plane
Cy	Associated cyst or cysts	
	0	None
	1C	One cyst
	2C	Two cysts
	xC	Xanthochromic cyst
H	Associated hematoma (H); 0 = no hematoma	
C	Use of Cavitron: C yes, 0 no	
s	Pial or arachnoid suture (s); 0 = no suture	
D	Duroplasty	
	0	No plasty
	Ap	Aponeurosis
	Ly	Lyophilized dura mater
	nlp	Non-leakproof dural suture
	Tc	Tissucol
1 > 2	Progression of functional condition between the first (i.e., preoperative) evaluation and the second evaluation (i.e., postoperative, at hospital discharge)	
	0	Lostto follow-up
	†	Death
	ag	Worsening (or Aggravation)
	d	days
	>HC	Use of hyperbaric chamber
	imp	Improvement
	uc	Unchanged
g2	Second evaluation of gait (i.e., postoperative, at hospital discharge)	
	g2	Patient can walk
	0	patient cannot walk
M2	Second evaluation (postoperative, on hospital discharge) of functional condition according to the McCormick classification (grades I to IV)	
RºT	Postoperative radiotherapy (total doses)	
2 > 3	Progression of functional condition between the second evaluation (i.e., postoperative, at hospital discharge) and the third evaluation (three months after surgery). Abbreviations as in column "1 > 2"	
g3	Third evaluation of gait (three months after surgery)	
	g3	Patient can walk
	0	Patient cannot walk

Table 2 **Clinical data** (continued)

Key to abbreviations, listed by column

M3 Third evaluation of functional condition (three months after surgery) according to the McCormick classification (grades I to IV)

SDef Postoperative sensory deficit. Abbreviations (postop) as in column "Sdef preop": slight deficit (–), marked deficit (+)

pS Progression of objective sensory disorders between preoperative and postoperative conditions (three months after surgery). Abbreviations as in column "1 > 2"

LT p Long-term postoperative pain (at least one year). Abbreviations as in column "ES"

*	Reoperated patients
◊	Lost to follow-up
†	Death

SPA Postoperative spasticity (at least one year after surgery)

*	Slight
**	Moderate
***	Severe
0	None
◊	Lost to follow-up
†	Death

U+Sx Postoperative urinary and sexual disorders. Other abbreviations as in column "U"

+Sx	Marked sexual disorders
*	Reoperated patients
◊	Lost to follow-up
†	Death

SpD2 Postoperative spinal deformity. Other abbreviations as in column "SpD1"

lor	Lordosis
*	Reoperated patients
◊	Lost to follow-up
†	Death

3 > 4 Progression of functional condition between the third evaluation (i.e., three months after surgery) and the fourth (i.e., the final evaluation, at least one year after surgery). Abbreviations as in columns "1 > 2" and "U + Sx"

g4 Fourth evaluation of gait (long-term, at least one year after surgery)

m4	Patient can walk
0	Patient cannot walk
*	Reoperated patients
◊	Lost to follow-up
†	Death

M4 Fourth evaluation (long-term, at least one year after surgery) of functional condition according to the McCormick classification (grades I to IV)

F-UP Postoperative follow-up. The duration is given in days (d), months (m), and years (y). The period between the first and second operations is given

*	Reoperated patients
◊	Lost to follow-up
†	Death

Recur? Postoperative recurrence

2 op	Patients undergoing two operations
2nd op AC	Subsequent operation at another center
2 st op	Two-stage operation
AC	Operation at another center
>>metast	Metastasis
ml recur	Malignant recurrence
MRI recur	Recurrence on MRI
mult loc	Multiple localizations
pr op AC	Previous operation at another center
rec>>reop	True recurrence requiring reoperation
reop/res T	Reoperation on residual tumor
Trm	Postoperative tumor remnants

Table 2 **Clinical data** (continued)

Pt n°	n/O	S	HISTO	LEVEL	Prev O	YO	Aop	poP	ES	N	F	LP	M°	T°	I	A°	g1	M1	SDef (preop)	U	SpD1	R	LAMIN	P	Cy	H	C	a	D
1	1	M	E-II	T9-L2	0	73	20	7y	RLL dcp	0	N	5	*	np	np	np	g1	II	b h/pd T12-L1	0	TS	C	T9-L2	w	xC	0	0	0	0
2	2	F	E-II	C2-T1	0	83	53	5m	LL Md	0	N	7,4	*	np	np	np	g1	II	b H°E tam/T12	0	0	P	C2-T1	w	xC	0	0	0	Ly
	3		E-II	T1-T8	15d-P	83	53			0	N	np	np	np	np	np	0	III	b H°E tam/T12	0	0	C	T1-T9	w	0	0	0	s	0
3	4	F	E-II	C2-C7	0 (NF2)	80	19	3m	Cerv p	0	N	15	*	*	np	*	0	III	R perin H°E	0	CTS	C	C1-C7	w	2C	0	0	s	0
4	5	M	E-II	whole sc	0	73	25	2y	LL Md	0	N	2,1	*	np	np	np	g1	II	b H°E tam/T6	0	TLKS	C	C7-L1	w	2C	0	0	0	Ly
5	6	F	E-II	C4-T6	0	92	40	8m	Rhb dcpE	0	N	0,3	np	np	*	np	g1	I	R LL dcd	0	0	C	C4-T6	w	1C	0	C	0	0
6	7	F	E-II	B°-C4	0	81	40	6y	Rhb Md	0	N	0,5	*	*	np	np	g1	II	R hb anesth/C2	0	0	C	C1-3+O	w	0	0	0	s	0
7	8	M	E-II	C2-T2	0	73	51	15y	LL Md	0	N	np	*	np	np	np	g1	I	b h/pd C2-T2	0	CK	C	C2-T2	w	xC	H	0	0	0
8	9	F	E-II	whole sc	0	71	27	3y	4Ls dcpE	0	N	0,5	*	np	np	np	0	IV	L dcd/C2	C	TLKS	C	C1-T11	w	1C	0	0	0	0
9	10	F	E-II	B°-T3	0	87	27	7y	4Ls dcpE	0	N	7	*	*	*	np	g1	I	0	0	CTKS	C	C1T7+O	w	0	0	C	0	Ly
10	11	F	E-II	C1-T4	0	88	47	8y	Cerv p	0	N	np	np	*	*	np	g1	II	R BS/C2	0	0	I	C1-T4	?	1C	0	C	0	0
	12		E-II	C1-T4	3m-I	88	47			0	N	np	np	np	*	np	g1	II	b H°E tam/C7	0	0	C	C1T4+O	w	1C	0	C	0	0
11	13	M	E-II	T12-L2	0	70	50	1y	R dc Sc	0	N	2,2	*	np	np	*	np	g1	II	b perin anesth	0	0	C	T12-L2	w	0	0	0	0	Ly
12	14	M	E-II	C4-T7	0	89	42	3y	LL Md	0	P	np	np	np	*	np	g1	II	b dcd/T5	0	0	C	T1-T5	w	2C	0	C	0	0
13	15	F	E-II	C1-C3	0	93	37	8y	LL dcpE	0	N	0,6	np	np	*	np	g1	II	0	0	0	C	C1C3+O	w	1C	0	C	0	0
14	16	M	E-II	C2-T4	0	90	36	3y	RUL Md	0	N	np	np	np	*	np	g1	II	b dcd/C4	d	impC	C	C2-T4	w	0	0	0	0	0
15	17	M	E-II	C1-C7	0	88	24	4y	UL sD	0	N	3,9	np	np	*	np	g1	II	b h/pd C4-T1	0	0	C	C1-C7	w	1C	0	C	s	0
16	18	M	E-II	T10-L2	0	84	73	6y	LLL Md	0	N	0,1	*	*	np	np	0	IV	b dcd/T6	C	0	C	T10-12	w	1C	0	0	0	0
17	19	M	E-II	C1-C7	0	81	52	19m	RUL Md	0	N	np	*	np	np	np	g1	I	R h/pd C5-C7	0	0	C	C2-C7	w	xC	0	0	s	0
18	20	M	E-II	T6-T9	0	83	51	7m	LL Md	0	N	np	*	np	np	np	0	IV	b h/pd T6-T9	C	0	C	T6-T9	w	1C	H	0	0	0
19	21	M	E-II	C2-C6	0	66	26	6y	UL dcpE	N	N	6	*	np	np	np	g1	II	0	0	0	C	C2-C5	w	1C	0	0	0	0
20	22	M	E-II	T7-T12	0	77	28	20m	LL Md	0	N	1,3	*	np	np	np	g1	II	b H°E tam/T6 b	0	0	C	T7-T12	w	0	0	0	s	Ly
21	23	F	E-II	C3-C7	0	68	43	6y	Tripl	0	N	np	*	np	np	np	g1	I	b UL h/pd	0	0	I	C3-C7	i	1C	H	0	0	0
22	24	M	E-II	T2-T5	0	84	52	6y	RLL dcpE	0	N	np	*	*	*	*	g1	II	b H°E tam/T7	0	0	C	T2-T5	w	0	H	C	0	0
23	25	F	E-II	C2-T1	0	91	44	6m	LL Md	0	N	np	*	*	*	np	g1	II	b h/pd C6-T1	0	0	C	C1-T2	w	0	0	C	s	0
24	26	M	E-II	T11-L2	0	73	31	3m	LL dcp	0	N	7	*	np	np	np	0	III	Feet anesth	C	0	I	T11-L1	0	0	0	0	0	Ly
	27		E-II	V4-C1	3m-I	73	31			0	N	np	np	np	np	np	0	IV	Feet anesth	C	0	I	C1+O	0	0	0	0	0	Ly
25	28	M	E-II	C5-C7	0	86	52	6y	LL Md	0	N	0,2	*	*	*	np	g1	II	L UL anesth	0	0	P	C2-T1	w	1C	0	C	0	0
	29		E-II	C5-C7	1m-P	86	52			0	N	np	np	np	np	np	0	III	L UL anesth	0	0	C		w	0	0	0	0	0
26	30	M	E-II	C2-T1	0	85	43	2y	LL Md	0	N	2,3	*	np	np	np	g1	III	L UL anesth	0	0	C	C2-T1	w	2C	0	0	0	0
27	31	F	E-II	whole sc	0	87	45	3y	LL Md	0	N	np	*	*	*	np	0	III	b H°E tam/T4	C	0	C	C6-T4	w	2C	0	C	0	0
28	32	M	E-II	C2-T2	0	90	36	8m	Tortic	0	N	np	np	np	*	np	g1	I	0	0	0	C	C1-C3	w	2C	0	C	s	0
29	33	M	E-II	C3-C7	0	83	40	6y	UL dcpE	0	N	0,6	*	np	np	*	g1	II	b h/pd/T4	0	0	C	C1-T1	w	1C	0	0	0	0
30	34	F	E-II	B°-T1	0	89	57	6m	UL rp	0	N	np	np	*	*	np	g1	I	b dcd/C4	0	impC	C	C1T1+O	w	1C	0	C	0	0
31	35	F	E-II	B°-C4	0	84	37	9y	Cerv p	0	N	0,5	*	*	*	*	g1	I	L hb H°E tam	0	0	C	C1-4+O	w	1C	H	0	0	0
32	36	F	E-II	C3-C7	0	70	45	4y	LUL rp	0	N	1	*	np	np	np	g1	II	b UL h/pd	0	0	C	C3-C7	w	0	0	0	0	0
	37		E-II	C3-C7	18y-C	88	63			0	N	np	np	np	*	np	g1	I	b UL h/pd	0	0	C		w	0	0	C	0	0
33	38	M	E-II	C4-C7	0	69	41	13m	LUL rp	0	N	2,2	*	np	np	np	g1	I	b H°E tam/C4	0	0	C	C4-C7	w	0	0	0	0	0
34	39	F	E-II	C2-C7	0	88	35	3y	UL dcpE	0	N	np	np	np	*	np	g1	I	R hand H°E	0	0	C	C3-C6	w	1C	0	C	0	0
35	40	F	E-II	C2-T5	0	87	54	2m	LL Md	0	N	1,9	*	*	*	np	g1	II	L h/pd C3-T4	0	0	S	C2-T7	w	2C	0	C	0	Ly
36	41	M	E-II	T11-L2	0	66	58	3m	LL Md	0	N	1,2	*	np	np	np	0	IV	b anesth/T11	C	0	S	T11-L1	w	0	0	0	0	0
37	42	M	E-II	whole sc	0	90	36	5y	RUL Md	0	N	np	np	*	*	np	g1	I	b H°E tam/C2	0	0	C	T9-L1	w	2C	0	C	0	0
38	43	M	E-II	C2-C6	0	93	49	1y	LUL dcpE	0	N	np	np	*	*	np	g1	I	L UL+LLs H°E	0	0	C	C3-C6	w	2C	0	C	s	0
39	44	M	E-II	C2-T7	0	87	41	5y	Cerv p	0	N	0,3	*	*	*	*	g1	I	b H°E tam/C4	0	0	C	C2-T7	w	1C	0	C	0	0
40	45	M	E-II	T10-L2	0	90	62	10y	Lumb p	0	N	np	np	np	*	np	g1	I	0	0	0	I	T10-L2	?	0	0	0	0	0
	46		E-II	T10-L2	18m-I	92	64			0	N	np	np	np	*	np	g1	II	b H°E tam/L5	0	0	C		w	1C	0	0	0	0
41	47	M	E-II	B°-C6	0	92	39	3y	Tortic	0	N	np	np	np	np	np	g1	II	L BS/C2	0	0	I	C1-C6	i	1C	H	0	0	0
42	48	M	E-II	C7-T2	0	90	44	5y	RUL dcpE	N	N	np	np	np	*	np	g1	I	b h/pd T1-T3	0	0	C	C6-T3	w	0	H	C	0	0
43	49	F	E-II	C6-T10	0	88	42	14y	RUL sD	0	N	0,5	np	np	*	np	g1	I	L BS/C2	0	0	S	C6-T10	w	2C	0	C	0	0
44	50	M	E-II	C4-T3	0	81	37	10y	LLL Md	0	N	0,2	*	*	np	np	g1	I	R hand anesth	0	0	C	C3-T3	w	0	0	0	0	0
45	51	F	E-II	C6-T1	0	82	46	5y	LL sD	0	N	0,8	*	*	np	*	g1	II	R H°E tam/T4	0	0	B	C6-T1	?	2C	0	0	0	Ly
	52		E-II	C6-T1	2y-B	84	48			0	N	0,7	*	*	np	np	0	III	R H°E tam/T4	C	0	C		w	1C	0	0	0	Ly
46	53	F	E-II	C5-T8	0	75	47	5y	LLL dcpE	0	N	0,7	*	np	np	*	g1	II	L LL h/pd	d	0	C	C2-T9	w	0	0	0	0	Ly
47	54	M	E-II	T8-T10	1y AC-B	88	38	13m	LLL dcpE	0	P	np	np	np	*	np	0	III	b dcd/T8	C	0	C	T8-T10	w	0	0	0	0	0
48	55	F	E-II	C4	0	87	49	13m	RUL dcpE	0	N	0,6	np	np	*	np	0	III	L H°E tam/C5	C	0	C	C3-C6	w	0	0	C	0	Tc
49	56	M	E-II	C2-C7	0	89	32	2y	Cerv p	N	N	np	np	np	*	np	g1	I	b UL H°E tam	0	0	C	C2-T1	w	2C	0	C	0	0
50	57	M	E-II	whole sc	0	89	36	5y	Cerv p	0	N	np	np	np	*	np	g1	II	b H°E tam/C5	0	0	I	C1-C6	?	0	0	C	0	Ly
	58		E-II	pan-m	1m-I	89	36			0	N	np	np	np	*	np	g1	II	b H°E tam/C5	0	0	C	C7-T10	w	0	0	C	0	Ly
51	59	M	E-II	C1-T5	0	90	57	3y	UL rpE	0	N	np	*	np	*	np	g1	II	R H°E tam/C8	C	0	C	C2-C7	w	2C	0	C	s	0
52	60	F	E-II	whole sc	0	84	32	15m	Ur d	0	N	11	*	*	np	np	g1	I	0	C	TS	I	C5-L3	w	2C	0	0	0	Ly
	61		E-II	pan-m	2m-I	84	32			0	N	np	np	np	np	np	0	III	b H°E tam/C5	C	TS	C		w	1C	0	0	0	Ap
53	62	F	E-II	T8-T12	0	86	56	2y	LL Md	0	N	9,2	*	np	np	np	g1	II	b LL anesth	0	0	C	T8-T12	w	2C	H	0	0	0
54	63	M	E-II	B°-C2	0	83	32	5y	Cerv p	0	N	0,5	*	*	*	np	g1	I	0	0	0	C	C1-2+O	w	2C	0	0	0	0
55	64	F	E-II	C2-T10	0	85	20	16m	LUL dcpE	0	N	0,8	*	*	*	*	g1	I	b h/pd T2-T6	0	0	I	C3-T4	w	2C	0	0	0	Ly
	65		E-II	C2-T10	13d-I	85	20			0	N	np	np	np	np	np	g1	I	b h/pd T2-T6	0	0	C		w	1C	0	C	0	Ly
56	66	F	E-II	C3-C7	0	84	59	1y	LL Md	0	N	1,6	*	np	*	np	g1	II	b h/pd C8-T5	0	0	C	C3-C7	w	1C	0	C	0	0
57	67	F	E-II	C3-C7	0	82	38	1y	LL Md	N	N	3	*	*	np	np	g1	I	L hb H°E/C5	0	0	D	C3-C7	0	1C	0	0	0	0
	68		E-II	C7-T8	1y-CPS	83	39			0	N	np	np	*	*	np	0	III	L hb H°E/C5	0	0	C	T1-T8	w	1C	0	0	0	Ly
58	69	F	E-II	T5-10	0	88	40	16m	Dors p	N	N	np	np	np	*	np	g1	I	R h/pd T8-T10	0	0	C	T5-10	w	0	0	C	s	0
59	70	F	E-II	C6-T1	0	92	68	2y	LL dcpE	0	N	0,5	np	np	*	np	g1	II	b LL dcd	0	0	C	C5-T1	w	0	N	C	s	0

Table 2 **Clinical data** (continued)

PN°	1>2	g2	M2	R°T	2>3	g3	M3	SDef (postop)	pS	LT p	SPA	U+Sx	SpD2	3>4	g4	M4	F-UP	Recur?
1	uc	g2	II	0	uc	g3	II	b H°E tam/T12	*ag*	0	*	0	TS	Imp	m4	I	20y	0
2	*ag>H*	0	III	0	reop	*15d	*15d	b H°E tam/T12	uc	*15d	15d-reop	*15d	*15d	*15d	*15d	*15d	15d*	op 2 st
	uc	0	III	0	uc	0	III	b H°E tam/T12	uc	0	0	C	0	uc	0	III	10y	0
3	Imp	g2	II	0	Imp	g3	I	b dcd/T1	*ag*	b dcp	0	0	TKS	*ag*	0	III	13y	2nd lmt?
4	*ag*	0	III	0	Imp	g3	II	b H°E tam/T3	*ag*	0	*	0	TLKS	*ag*	0	III	20y	0
5	*ag*	g2	II	0	Imp	g3	I	b H°E tam/T2	*ag*	0	0	0	0	uc	m4	I	1y	0
6	†22d	†22d	†22d	†22d	†22d	†22d	†22d	†22d	†22	†22d	†22d	†22d	†22d	†22d	†22d	†22d	†22d	†22d
7	*ag*	g2	II	0	Imp	g3	I	b h/pd C2-T2	uc	0	0	0	CK	uc	m4	I	20y	0
8	uc	0	IV	0	Imp	0	III	b H°E tam/C2	*ag*	b dcp	* * *	0	TLKS	uc	0	III	22y	0
9	*ag*	g2	II	0	uc	g3	II	R hand astereo	*ag*	0	* *	0	TLKS	uc	m4	II	6y	0
10	uc	g2	II	0	uc	g3	II	R BS/C2	uc	*3m	3m-reop	*3m	*3m	reop	*3m	*3m	3m*	op 2 st
	ag	0	III	0	uc	g3	II	b H°E tam/C7	uc	Cerv p	*	0	0	uc	m4	II	5y	0
11	*ag*	0	III	0	uc	0	III	b anesth/T12	*ag*	0	0	d+Sx	0	Imp	m4	II	23y	0
12	*ag*	0	III	0	uc	0	III	b H°E tam/T4	*ag*	0	* *	C	0	Imp	m4	II	4y	MRI recur
13	uc	g2	II	0	Imp	g3	I	0	uc	0	0	0	0	uc	m4	I	1y	0
14	uc	g2	II	0	uc	g3	II	R BS/C4	Imp	0	0	d	0	Imp	m4	I	3y	0
15	uc	g2	II	0	uc	g3	II	2 hands astereo	*ag*	0	0	0	0	*ag*	m4	III	5y	0
16	uc	0	IV	0	uc	0	IV	b H°E tam/T6	*ag*	0	0	d	0	uc	0	IV	9y	0
17	*ag*	g2	II	0	uc	g3	II	2 hands astereo	*ag*	RULrp	* *	0	CK	*ag*	m4	III	12y	0
18	uc	?	IV	0	uc	0	IV	b anesth/T6	*ag*	b dcp	* *	C	0	uc	0	IV	10y	0
19	*ag*	g2	III	0	Imp	g3	II	b anesth/C6	*ag*	0	0	0	0	Imp	m4	I	27y	0
20	uc>H	g2	II	0	Imp	g3	I	b LL h/pd	Imp	b dcp	0	0	0	uc	m4	I	17y	0
21	*ag*	g2	II	60 Gy	Imp	g3	I	b H°E tam/C4	*ag*	0	* *	d	TK	uc	m4	I	20y†	0
22	uc	g2	II	0	Imp	g3	I	b anesth/C4	*ag*	0	0	d	0	uc	m4	I	10y	0
23	uc	g2	II	0	uc	g3	II	b H°E tam/C5	*ag*	LULrp	* *	d	0	uc	m4	II	2y	0
24	*ag*	0	IV	45 Gy	uc	0	IV	b H°E tam/T4	*ag*	*3m	3m-reop	*3m	*3m	reop	*3m	*3m	3m*	reop/res T
	†10d	†10d	†10d	†10d	†10d	†10d	†10d	†10d	†	†10d	†10d	†10d	†10d	†10d	†10d	†10d	10d†	mi recur
25	*ag*	0	III	0	reop	*1m	*1m	L UL anesth	uc	*1m	1m-reop	*1m	*1m	*1m	*1m	*1m	1m*	op 2 st
	Imp	g2	II	0	uc	g3	II	L UL anesth	uc	Lumb p	0	0	0	uc	m4	II	5y†	0
26	*ag>H*	g2	III	0	uc	g3	III	b UL anesth	*ag*	0	*	d	impC	uc	m4	III	8y	0
27	uc	0	III	0	uc	0	III	b H°E tam/T4	uc	LULrp	* * *	0	0	uc	0	III	6y◊	0
28	uc	g2	I	0	uc	g3	I	0	uc	Cerv p	0	0	CK	uc	m4	I	3y	0
29	*ag>H*	0	III	0	Imp	g3	II	b H°E tam/C5	*ag*	b dcp	* *	d+Sx	0	uc	m4	II	10y	0
30	uc	g2	I	0	uc	g3	I	b dcd/C4	uc	LULrp	0	0	CK	uc	m4	I	5y	0
31	uc	g2	I	0	uc	g3	I	L hb H°E tam(-)	Imp	Cerv p	0	0	0	uc	m4	I	9y	0
32	uc	g2	II	0	Imp	g3	I	b UL h/pd	uc	0	0	0	0	uc	m4	I	18y*	rec >> reop
	uc	g2	I	0	uc	g3	I	b UL h/pd	uc	0	0	0	0	uc	m4	I	5y	0
33	*ag*	g2	II	0	Imp	g3	I	b H°E tam/C4(-)	Imp	0	0	0	0	uc	m4	I	24y	0
34	*ag*	0	III	0	Imp	g3	II	R hand H°E	uc	R dcp	0	0	ImpC	uc	m4	II	5y	0
35	*ag*	0	III	0	uc	0	III	b H°E tam/C4	*ag*	b UL rp	* *	0	TK	Imp	m4	II	6y	0
36	uc	0	IV	0	uc	0	IV	b anesth/T11	uc	0	0	C	0	uc	0	IV	4y†	0
37	*ag*	g2	II	0	Imp	g3	I	b h/pd T3-T9	Imp	R dcp	0	0	0	uc	m4	I	3y	0
38	*ag*	0	III	0	Imp	g3	II	L UL+LLs H°E	uc	0	0	0	0	uc	m4	II	1y	0
39	uc	g2	I	0	uc	g3	I	anesth/C2 b	uc	0	0	0	0	uc	m4	I	7y	0
40	*ag*	g2	II	0	uc	g3	II	b H°E tam/T12	*ag*	0	0	0	0	uc	m4	II	18m*	reop/res T
	ag	0	III	0	Imp	g3	II	b H°E tam/L2	uc	0	* *	0	TK	uc	m4	II	2y	0
41	*ag*	g2	III	0	uc	0	III	b H°E tam/C2	*ag*	0	* * *	0	0	uc	0	III	18m	po Trm
42	*ag*	g2	II	0	Imp	g3	I	b h/pd T1-T3	uc	Dors p	*	d	0	uc	m4	I	3y	0
43	*ag*	g2	II	0	Imp	g3	I	b H°E tam/C4	*ag*	0	* *	d	0	uc	m4	I	5y	0
44	*ag*	g2	II	0	uc	g3	I	b H°E tam/C5	*ag*	0	*	0	TK	uc	m4	I	12y	0
45	*ag*	0	III	75 Gy	uc	0	III	R H°E tam/T4	uc	b dcp	*	C	0	uc	0	III	18m*	reop/res T
	uc	0	III	0	uc	0	III	R H°E tam/T4	uc	b T rp	*	C	0	uc	0	III	1y◊	0
46	uc	g2	II	0	uc	g3	II	L h/pd C4-L2	*ag*	b dcp	* *	0	CTK	uc	m4	II	18y	0
47	*ag*	0	IV	0	Imp	0	III	b H°E tam/T8	uc	R dcp	* * *	d	0	Imp	m4	II	5y	1 pr op AC
48	uc	0	III	0	Imp	g3	II	L H°E tam/C5	uc	0	* *	0	0	uc	m4	II	6y	0
49	uc	g2	I	0	uc	g3	I	b UL H°E tam	uc	0	0	0	0	uc	m4	I	4y	0
50	*ag*	0	III	0	reop	*1m	*1m	b H°E tam/C5	uc	*1m	1m-reop	*1m	*1m	*1m	*1m	*1m	1m*	op 2 st
	uc	g2	II	0	Imp	g3	I	b H°E tam/C5	uc	0	0	0	0	uc	m4	I	5y	0
51	*ag*	0	III	0	Imp	g3	II	R H°E tam/C8	uc	0	0	0	0	Imp	m4	I	3y	0
52	uc	g2	I	0	reop	*2m	*2m	b H°E tam/C5	*ag*	*2m	2m-reop	*2m	*2m	*2m	*2m	*2m	2m*	op 2 st
	ag	0	IV	0	Imp	g3	II	L H°E tam/C5	uc	0	* *	C	TS	uc	m4	II	9y	0
53	*ag*	0	IV	0	Imp	0	III	b LL anesth	*ag*	R dcp	* *	C	0	uc	0	III	7y	0
54	uc	g2	I	0	uc	g3	I	b dcd/C2	*ag*	0	0	0	0	uc	m4	I	10y	0
55	uc	g2	I	0	reop	*13d	*13d	b h/pd T2-T6	uc	*13d	13d-reop	*13d	*13d	*13d	*13d	*13d	13d*	op 2 st
	uc	g2	I	0	uc	g3	I	0	Imp	R dcp	0	0	0	uc	m4	I	8y	0
56	uc	g2	II	0	uc	g3	II	b h/pd C8-T5	uc	◊3m	◊3m	◊3m	◊3m	pdv	◊3m	◊3m	3m◊	0
57	*ag*	0	III	0	uc	0	III	L hb H°E/C5	uc	0	* *	d	C lor	Imp	m4	II	1y*	op 2 st
	uc	0	III	0	Imp	g3	II	L hb H°E/C5	uc	0	* *	0	0	uc	m4	II	10y	0
58	*ag*	g2	II	0	Imp	g3	I	b H°E tam/T5	*ag*	b dcp	0	0	CTK	uc	m4	I	5y	0
59	uc	0	II	0	uc	g3	II	b LL dcd	*ag*	0	* *	C	ImpC	uc	m4	II	1y	0

Table 2 **Clinical data** (continued)

PN°	n/O	S	HISTO	LEVEL	Prev O	YO	Aop	poP	ES	N	F	LP	M°	T°	I	A°	g1	M1	SDef (preop)	U	SpD1	R	LAMIN	P	Cy	H	C	s	D
60	71	M	E-II	C3-T1	0	90	45	5y	RUL Md	0	N	np	np	np	*	np	g1	II	b h/pd C6-T12	C	0	I	C2-T2	?	2C	H	C	0	0
	72		E-II	C3-T1	18m-I	92	47	2m		0	N	np	np	np	*	np	g1	II	b h/pd C5-T12	0	0	C		w	0	0	C	s	0
61	73	M	E-II	C2-T2	0	66	18	12y	LL dcpE	0	N	32	*	np	np	np	0	IV	b H°E tam/C3	C	0	P	T2-L2	0	xC	H	0	0	nlp
62	74	F	E-II	T1-T6	0	77	32	1y	LLL Md	0	N	0,6	*	np	np	np	g1	II	b dcd/T4	0	TS	C	C7-T7	w	0	0	0	0	0
63	75	F	/sE-I	C2-C6	0	89	32	6m	Dors p	0	N	0,3	np	*	*	np	g1	II	L UL H°E tam	0	0	C	C2-C6	w	0	0	C	0	0
64	76	M	/sE-I	C2-T1	0	88	43	4y	Rhb dcp	0	N	np	np	np	*	np	g1	I	0	0	0	C	C2-T1	i	0	0	C	0	Tc
65	77	M	dA-I	C1-C4	0	66	29	2y	LUL dcp	0	N	0,8	*	np	np	np	g1	II	L hb anesth/C2	0	0	C	C1-C5	w	0	0	0	0	0
66	78	M	dA-I	T6-L1	0	68	6	1y	LL Md	0	N	0,7	*	np	np	np	g1	II	b h/pd T6-T12	0	0	C	T6-L1	w	0	0	0	0	0
67	79	M	dA-I	T3-T8	0	87	18	4y	RLL Md	0	N	np	np	np	*	np	g1	II	0	0	TS	C	T1-T10	w	0	0	C	s	Ly
68	80	M	dA-I	C1-T1	0	89	29	10y	C h/pd	0	N	np	np	*	*	np	g1	II	b H°E tam/C2	0	0	S	C1T1+O	i	1C	H	0	0	0
69	81	M	dA-I	T3-T11	0	87	29	1y	L dc Sc	0	N	np	np	*	*	np	g1	I	L BS/T10	0	0	S	T3-L11	P	0	0	0	0	Ly
70	82	M	dA-I	C2-C7	0	87	38	3y	R hb dcp	0	N	0,9	*	np	*	*	g1	II	b H°E tam/C8	0	0	I	C2-C6	i	2C	0	C	0	0
	83		dA-I	C7-T1	10m-I	88	39			0	N	np	np	np	*	np	g1	II	b anesth/C7	0	0	S	C7-T1	I	2C	0	C	0	0
71	84	M	pA-I	T5-T9	0	86	40	7y	RLL Md	0	N	0,3	*	np	*	np	g1	I	L BS/T5	0	0	I	T5-T10	0	0	0	C	0	Ly
72	85	F	pA I	T4-T7	0	68	20	4m	bT rp	0	N	0,6	*	np	np	np	g1	I	b dcd/T9	0	TS	S	T4-T7	P	0	0	0	0	0
73	86	F	pA-I	C5-C6	0	65	34	4y	UL dcp	0	N	0,5	*	np	np	np	0	IV	b UL h/pd	C	0	B	C5-C6	i	0	0	0	0	0
74	87	M	pA-I	T8-T11	0	87	34	6m	RLL dcpE	0	N	np	np	np	*	np	g1	II	b H°E tam/T5	0	0	C	T8-T11	w	1C	0	C	0	0
75	88	F	pA-I	conus-m	0	86	28	6m	LLL Md	0	N	np	*	np	*	np	g1	I	0	0	TLK	B	T11-L2	0	0	0	C	0	0
76	89	F	pA-I	T7-L1	0	59	2	2m	LL Md	0	N	11	*	np	np	np	0	III	0	C	0	B	T10-L1	i	1C	0	0	0	0
	90		pA-I	T7-L1	5y-B	64	7			0	N	np	*	np	np	np	g1	II	L BS/T7	0	TLKS	S	T7-L2	i	2C	0	0	0	0
77	91	M	pA-I	C1-T6	0	90	9	2y	Tortic	0	N	np	np	np	*	np	g1	II	R UL H°E tam	C	0	I	C6-T6	i	2C	0	C	s	0
78	92	M	pA-I	C3-C5	0	67	29	7m	Tetrapl	0	N	13	*	np	np	np	0	IV	b anesth/C2	C	0	B	C3-C5	0	0	N	0	0	0
79	93	F	pA-I	whole sc	0	87	16	2y	S	0	N	30	*	*	*	np	g1	II	0	d	TLKS	C	T5-L3	w	2C	0	C	0	0
80	94	M	oA-II	TIO-T12	0	86	68	1y	L dc Sc	0	N	0,4	*	*	np	np	0	III	b h/pd T10-T12	0	0	C	TIO-12	w	0	0	C	0	0
81	95	F	oA-II	B°-C6	0	86	24	14y	Rhb Md	0	N	0,7	*	np	*	np	g1	I	b UL h/pd	0	CKS	P	C1-7+O	0	2C	0	C	0	Ly
82	96	M	oA-II	B°-C5	0	79	30	2y	RUL rp	0	N	0,6	*	np	np	np	g1	II	b H°E tam/C4	C	0	I	C1-7+O	0	0	0	0	0	Ap
83	97	F	oA-II	C2-T9	0	87	48	4y	RT rp	0	N	1,5	*	*	*	np	g1	I	R hypE/T5	0	0	C	C7-T8	0	2C	0	C	0	0
84	98	M	oA-II	B°-C2	0	67	41	24y	L hb sD	0	N	0,1	*	np	np	np	0	III	L dcd/C2	C	CTS	B	C1-2+O	0	0	0	0	0	nlp
85	99	F	oA-II	T2-T9	0	83	36	6m	LL sD	0	N	0,2	*	*	*	np	g1	II	b H°E tam/T11	0	0	B	T2-T9	i	1C	0	0	0	0
	100		oA-II	T2-T9	18m-I	84	37	6m		0	N	np	np	np	*	np	0	IV	b anesth/T6	C	0	S		i	1C	0	C	0	0
86	101	M	oA-II	C6-T2	0	82	44	3y	LUL dcpE	0	N	0,3	*	*	*	np	g1	I	L h/pd C8-T2	0	0	C	C6-T2	w	1C	0	0	0	0
87	102	F	oA-II	C4-T4	0	90	58	18y	Rhb Md	0	N	0,3	np	*	*	*	0	III	R BS/C5	C	0	C	C4-T4	w	0	0	C	0	0
88	103	F	oA-II	C2-T9	1y AC-B	84	31	18m	Ur d	0	N	1,1	*	*	np	np	0	III	b h/pd T5-T9	d	0	C	C2-T9	w	1C	0	C	0	Ly
89	104	M	oA-II	conus-m	1y AC-P	88	60	3y	Parapl	0	N	np	np	np	*	np	0	III	0	0	CTS	S	T11-L2	i	0	H	C	0	0
90	105	M	oA-II	T1-T9	0	90	60	11y	Lumb p	0	N	0,5	*	*	*	np	g1	I	R H°E tam/T8	0	0	C	T1-T9	w	0	0	C	s	0
91	106	F	oA-II	C1-T3	0	90	16	10y	Tortic	0	N	np	np	np	*	np	g1	II	0	C	CTKS	I	C3-C7	i	1C	0	C	0	0
92	107	M	oA-II	T10-L2	0	69	11	18m	LL Md	N	N	1,3	*	np	np	np	g1	II	0	0	0	I	T10-L1	i	0	0	0	0	0
	108		oA-II	T10-L1	5m-I	69	12		LL Md	0	N	np	np	np	np	np	g1	II	b H°E tam/T10	0	0	C		i	1C	0	0	0	0
93	109	M	oA-II	T12-L2	2y AC-I	87	31	6y	LLL Md	0	N	1,3	*	np	*	np	g1	II	L dcd/T12	0	0	C	T10-L1	w	0	0	C	0	0
94	110	F	oA-II	C1-T1	0	76	9	1y	Tortic	0	N	0,6	*	np	np	np	g1	I	0	0	impC	C	C1-T1	w	1C	0	0	s	Ly
95	111	F	oA-II	C4-C7	0	90	40	15m	RUL dcp	0	N	np	np	*	*	np	g1	II	L H°E tam/C4	0	0	B	C4-C7	0	0	0	0	s	0
96	112	F	oA-II	B°-C2	0	90	31	9m	UL dcpE	N	N	np	np	np	*	np	g1	II	b UL H°E tam	0	0	C	C1-3+O	w	2C	0	C	s	Ly
97	113	M	oA-II	C1-C6	R°T AC	86	22	8m	Cerv p	0	N	np	np	np	*	np	0	III	b H°E tam/C2	C	0	S	C1-C6	I	0	0	C	0	Ly
98	114	M	oA-II	B°-C2	0	91	49	2m	4Ls sD	0	N	np	np	*	*	np	0	IV	b dcd/C2	C	0	B	C1-2+O	0	0	0	0	0	0
99	115	M	oA-III	T4-T8	0	68	20	3m	LL Md	0	N	0,2	*	np	np	np	0	IV	b dcd/T4	C	0	S	T4-T8	P	0	0	0	0	0
100	116	F	oA-III	conus-m	0	92	27	10m	LLL Md	0	N	0,2	np	np	*	np	g1	II	0	0	0	B	T11-L2	i	0	0	0	0	0
	117		oA-III	conus-m	8m-B	92	27			0	N	np	np	np	*	np	0	III	L LL H°E tam	C	0	I		i	0	0	C	0	0
101	118	M	oA-III	C2-T1	0	85	10	6m	Cerv p	0	N	2,9	*	*	*	np	g1	II	b h/pd T6-T12	0	CK	P	C3-C7	P	0	0	0	0	Ly
102	119	M	oA-III	T7-T11	0	89	42	6m	LLL Md	0	N	3,2	*	*	*	np	0	IV	b H°E tam/T10	0	0	B	T7-T11	0	0	0	0	0	Ly
	120		oA-III	T7-T11	1m-B	89	42			0	N	np	np	np	*	np	0	IV	b anesth/T10	C	0	I		0	0	0	C	0	nlp
103	121	M	oA-III	T7-T9	0	70	10	9m	Parapl	0	N	1,2	*	np	np	np	0	III	b anesth/T8	C	0	C	T7-T9	w	0	0	0	0	0
	122		oA-III	T7-T9	18m-C	71	11			0	N	1,5	*	np	np	np	0	IV	b anesth/T8	C	0	S	T5-T11	0	0	0	0	0	0
104	123	F	oA-IV	T2-T7	0	84	20	20m	Parapl	0	N	0,4	*	*	np	np	0	IV	b dcd/T5	C	0	S	T2-T7	P	0	0	0	0	0
105	124	M	oA-IV	T7-T11	0	66	13	6m	LL Md	0	N	2,5	*	np	np	np	0	IV	b dcd/T12	C	0	S	T7-T11	0	0	0	0	0	0
106	125	M	Gg-I	B°-C2	0	66	24	9y	RUL rp	0	N	1,4	*	np	np	np	g1	II	L BS/C2	0	0	P	C1-2+O	i	0	0	0	0	0
107	126	M	Gg-I	C6-T2	0	86	66	15m	LL Md	N	N	1,5	*	np	*	*	g1	II	R H°E tam/T4	0	0	S	C6-T3	w	2C	0	C	0	0
108	127	M	Gg-II	C1-C3	0	85	22	10m	Cerv p	N	N	1	*	*	np	*	g1	I	b H°E tam/C2	0	0	C	C1-C6	0	0	0	0	0	0
	128		Gg-III	B°-C4	2m-I	85	22			N	N	1,5	*	np	np	np	0	III	b H°E tam/C2	C	0	P		0	0	0	0	0	Ly
109	129	F	Gg-II	B°-C2	0	88	12	3m	Cerv p	0	N	np	np	*	*	np	g1	II	L UL dcd	0	impC	B	C1-C2	0	0	0	0	0	Ap
110	130	F	Odg-III	B°-C2	0	65	18	1y	Rhb Md	0	N	np	np	np	np	np	g1	II	R hand astereo	C	0	B	C1-2+O	i	1C	0	0	0	nlp
	131		Odg-III	B°-C2	1y-B	66	19	1y		0	N	np	np	np	np	np	0	III	R hand astereo	C	0	P		i	1C	0	0	0	nlp
111	132	F	E-II gr	T8-T9	0	84	19	14m	Lumb p	0	N	2	*	np	np	*	g1	I	b h/pd T6-T9	d	0	S	T8-L5	i	0	0	0	0	Ly
	133		E-II gr	C4-C5	5y-S	89	23			0	N	2,5	*	np	*	np	g1	II	b H°E tam/T12	C	TLKS	C	C4-C5	i	0	0	0	0	0
112	134	M	E-II gr	T9-12	CEE-1y	90	21	1y	LL Md	0	N	1,8	*	*	*	np	g1	I	R LL H°E tam	d	0	S	T9-T12	i	0	0	0	0	0
113	135	F	E-II gr	T4-L2	CEE-1y	79	15	6y	LL Md	0	P	0,8	*	np	np	np	0	III	b H°E tam/T4	C	0	S	T4-L5	i	1C	H	0	0	Ap
114	136	F	E-II gr	conus-m	CEE-2y	85	39	1y	Lumb p	0	N	3,4	*	*	np	np	g1	I	b dcd/T11	d	0	S	T12-L3	i	0	0	0	0	0
115	137	F	E-III gr	B°-C3	4VE-3y	86	27	6y	Tortic	0	N	20	*	np	np	np	g1	II	L UL h/pd	0	0	I	C2-C7	0	0	0	C	0	Ly
116	138	M	Med-gr	T3-T4	4V Med	90	70	4m	LLL Md	0	N	0,6	np	np	*	np	g1	II	0	0	0	S	T3-T4	0	0	0	C	0	0
117	139	F	C-Met	C5-C6	0	88	48	7m	Cerv p	0	N	np	np	*	*	np	0	IV	R LL anesth	C	0	S	C5-C6	i	0	0	C	s	0
118	140	M	Meta-g	C4-C5	P.C.Met	89	32	17d	Cerv p	0	N	np	np	np	*	np	0	III	R BS/C4	0	0	C	C4-C5	w	0	0	C	s	0

Table 2 **Clinical data** (continued)

PN	1>2	g2	M2	R°T	2>3	g3	M3	SDet (postop)	pS	LT p	SPA	U+Sx	SpD2	3>4	g4	M4	F-UP	Recur?
60	*ag*	0	III	0	Imp	g3	II	b h/pd C6-T12	uc	0	0	O	0	Imp	m4	I	18m*	reop/res T
	ag	0	IV	0	Imp	0	III	b h/pd C5-T12	uc	0	*	0	0	uc	0	III	2y	0
61	uc	0	IV	30 Gy	uc	0	IV	b anesth/C3	*ag*	0	0	0	0	uc	0	IV	1y†	mi recur
62	uc	g2	II	0	uc	g3	II	b dcd/T4	uc	0	0	C	TS	uc	m4	II	1y◊	0
63	*ag*	g2	III	0	Imp	g3	II	L hb H°E/C5	*ag*	0	*	0	0	uc	m4	II	4y	0
64	*ag*	0	IV	0	Imp	0	III	R UL anesth	*ag*	R dcp	0	C	0	uc	0	III	1y◊	0
65	*ag*	0	IV	0	Imp	0	III	L anesth /C2	uc	0	0	0	0	Imp	m4	II	27y	0
66	uc	g2	II	0	uc	g3	II	b h/pd T6-T12	uc	0	0	0	0	uc	m4	II	22y†	0
67	*ag*	0	III	0	Imp	g3	II	R dcd/T6	*ag*	R dcp	* *	0	TS	uc	m4	II	6y	0
68	*ag*	0	III	0	uc	0	III	b H°E tam/C2	uc	0	* *	0	0	Imp	m4	II	5y	0
69	*ag*	0	III	0	Imp	g3	II	b H°E tam/T10	*ag*	0	*	d	0	uc	m4	II	6y	0
70	*ag*	0	III	0	Imp	0	III	b anesth/C7	*ag*	*10m	10m-reop	*10m	*10m	reop	*10m	*10m	10m*	reop/res T
	uc	g2	II	0	uc	g3	II	b anesth/C7	uc	0	*	0	TLKS	uc	m4	II	6y	0
71	*ap>H*	g2	II	0	uc	g3	II	L BS/T5	uc	0	*	d+Sx	0	uc	m4	II	7y	MRI recur
72	*ap>H*	g2	II	0	uc	g3	II	b H°E tam/T4	*ag*	0	* *	d	TS	uc	m4	II	25y	0
73	uc	0	IV	0	uc	0	IV	b UL h/pd	uc	0	0	0	0	uc	0	IV	29y	0
74	uc	g2	II	0	uc	g3	II	b H°E tam/T5	uc	0	*	C	0	uc	m4	II	7y	po Trm
75	uc	g2	I	0	uc	g3	I	O	uc	0	0	0	TLK	uc	m4	I	7y	0
76	uc	0	III	0	uc	0	III	L BS/T7	*ag*	Lumb p	* *	d	TLKS	uc	0	III	5y*	rec >> reop
	uc	g2	II	0	uc	g3	II	L BS/T7	uc	Lumb p	* *	d	TLKS	uc	m4	II	29y	0
77	*ag*	0	III	0	Imp	g3	II	R UL H°E tam	uc	0	0	0	CKS	uc	m4	I	3y	0
78	uc	0	IV	0	uc	0	IV	b anesth/C2	uc	†6m	†6m	†6m	†6m	†6m	†6m	†6m	6m†	mi recur
79	uc	g2	II	0	Imp	g3	I	b H°E tam/T12	*ag*	0	0	d	TLKS	uc	m4	I	8y	0
80	*ag*	0	IV	0	uc	0	IV	h/pdT10-T12 b	uc	◊3m	◊3m	◊3m	◊3m	pdv	◊3m	◊3m	3m◊	0
81	*ag*	g2	II	0	uc	g3	II	b UL h/pd	uc	0	* *	0	CKS	uc	m4	II	7y	0
82	*ag*	0	III	0	uc	0	III	b H°E tam/C4	uc	Cerv p	0	C	0	*ag*	0	IV	2y†	0
83	uc	g2	I	0	uc	g3	I	b H°E tam/T5	*ag*	Dors p	*	0	TK	uc	m4	I	6y	MRI recur
84	uc	0	III	45 Gy	Imp	g3	II	L H°E tam/C2	*ag*	Cerv p	0	0	TKS	uc	m4	II	26y	0
85	*ag*	0	III	45 Gy	uc	0	III	b anesth/T6	uc	Dors p	*	0	0	*ag*	0	IV	18m*	reop/res T
	uc	0	III	0	Imp	g3	II	b anesth/T6	uc	Dors p	*	0	0	*ag*	0	II	9y	0
86	*ag*	g2	II	0	uc	g3	II	L h/pd C8-T2	uc	Dors p	0	0	0	Imp	m4	I	12y	0
87	uc	0	III	0	Imp	g3	II	R LL H°E	Imp	R dcp	0	0	0	uc	m4	II	3y	0
88	uc	0	III	0	uc	0	III	b h/pd T5-T9	uc	0	* *	d	TK	uc	0	III	1y◊	2nd op AC
89	uc	0	III	30 Gy	Imp	g3	II	L H°E tam/T10	*ag*	0	0	C	TKS	uc	m4	II	6y	1 pr op AC
90	*ag*	0	III	0	Imp	g3	II	R H°E tam/T4	uc	0	* *	d	0	Imp	m4	I	4y	0
91	*ag*	0	III	0	Imp	g3	II	b H°E tam/C5	*ag*	0	0	0	TLKS	uc	m4	II	4y	0
92	uc	g2	II	0	Imp	g3	I	b H°E tam/T10	*ag*	*5m	5m-reop	*5m	*5m	reop	*5m	*5m	5m*	op 2 st
	ag	0	IV	45 Gy	Imp	0	III	b H°E tam/T10	uc	0	0	0	TK	uc	0	III	23y	0
93	uc	g2	II	45 Gy	uc	g3	II	b H°E tam/T12	*ag*	b dcp	*	d+Sx	0	uc	m4	II	6y	2 pr op AC
94	*ag*	g2	II	0	uc	g3	II	b H°E tam/C2	*ag*	0	* * *	0	TKS	uc	m4	II	18y	0
95	uc	g2	II	0	uc	g3	II	L H°E tam/T11	Imp	0	*	d	0	uc	m4	II	4y	0
96	*ag*	0	III	0	Imp	g3	I	L hand H°E tam	Imp	Cerv p	0	0	CK	uc	m4	I	3y	0
97	*ag*	0	IV	40 Gy	uc	0	IV	b H°E tam/C2 (+)	*ag*	†9m	†9m	†9m	†9m	†9m	†9m	†9m	9m†	0
98	uc	0	IV	0	uc	0	IV	b dcd/C2	uc	†3m	†3m	†3m	†3m	†3m	†3m	†3m	3m†	mi recur
99	uc	0	IV	40 Gy	uc	0	IV	b dcd/T4 (-)	Imp	0	* * *	C	0	uc	0	IV	14m†	mi recur
100	uc	g2	II	0	*ag*	0	III	L LL H°E tam	*ag*	*8m	8m-reop	*8m	*8m	reop	*8m	*8m	8m*	reop/res T
	uc	0	III	0	*ag*	0	IV	b H°E tam/T12	*ag*	0	0	C	TKS	uc	0	IV	1y	mi recur
101	uc	g2	II	40 Gy	*ag*	0	III	b h/pd T6-T12	uc	Cerv p	* * *	0	CK	uc	0	III	2y†	mi recur
102	uc	0	IV	0	reop	*1m	*1m	b anesth/T10	uc	*1m	1m-reop	*1m	*1m	*1m	*1m	*1m	1m*	reop/res T
	uc	0	IV	40 Gy	uc	0	IV	b anesth/T10	uc	b dcp	* * *	C	0	uc	0	IV	16m†	mi recur
103	Imp	g2	II	35 Gy	Imp	g3	I	b H°E tam/T8	Imp	Dors p	0	0	0	uc	m4	I	18m*	rec >> reop
	uc	0	IV	0	uc	0	IV	b anesth/T8	uc	Dors p	0	C	0	uc	0	IV	16m†	mi recur
104	uc	0	IV	40 Gy	uc	0	IV	b dcd/T5	uc	†11m	†11m	†11m	†11m	†11m	†11m	†11m	11m†	mi recur
105	uc	0	IV	40 Gy	uc	0	IV	b anesth/T9	*ag*	†9m	†9m	†9m	†9m	†9m	†9m	†9m	9m†	mi recur
106	*ag*	0	III	0	uc	0	III	L BS/C2	*ag*	Cerv p	* * *	0	0	Imp	m4	II	27y	0
107	†2d	†2d	†2d	†2d	†2d	†2d	†2d	†2d	†	†2d	†2d	†2d	†2d	†2d	†2d	†2d	2d†	0
108	*ag*	0	III	0	reop	*2m	*2m	b H°E tam/C2	uc	*2m	2m-reop	*2m	*2m	*2m	*2m	*2m	2m*	reop/res T
	ag	0	IV	52 Gy	uc	0	IV	b H°E tam/C2	uc	†3m	†3m	†3m	†3m	†3m	†3m	†3m	3m†	mi recur
109	uc	g2	II	60 Gy	Imp	g3	I	L UL dcd	uc	0	0	0	CK	uc	m4	I	5y	0
110	uc	g2	II	60 Gy	uc	g3	II	R hb anesth/C2	*ag*	0	0	C	0	uc	m4	II	1y*	reop/res T
	uc	0	III	0	uc	0	III	R hb anesth/C2	*ag*	0	0	C	0	*ag*	0	IV	1y†	mi recur
111	*ag*	g2	II	0	uc	g3	II	b h/pd T6-T9	uc	RLLrp	0	d	TLKS	uc	m4	II	5y*	mi recur
	uc	g2	II	0	uc	g3	II	b H°E tam/T12	uc	0	0	d	TLKS	uc	m4	II	4y	mi recur
112	uc	g2	I	45 Gy	uc	g3	I	R LL H°E tam	uc	0	0	C	0	uc	m4	I	3y	mi recur
113	uc	C	III	49 Gy	uc	0	III	b H°E tam/T4	uc	b dcp	0	C	TK	uc	0	III	10y†	mi recur
114	*ag*	g2	II	79 Gy	uc	g3	II	b dcd/T11	uc	b dcp	0	d	0	uc	m4	II	4y†	mi recur
115	*ag*	0	IV	65 Gy	uc	0	IV	L UL h/pd	uc	0	0	0	0	uc	0	IV	3y†	mi recur
116	uc	g2	II	0	uc	g3	II	b H°E tam/T3	*ag*	0	0	C	0	*ag*	0	IV	18m†	mi recur
117	uc	0	IV	0	uc	0	IV	R LL anesth	uc	†3m	†3m	†3m	†3m	†3m	†3m	†3m	3m†	0
118	uc	0	III	20 Gy	*ag*	0	IV	R BS/C4	uc	†3m	†3m	†3m	†3m	†3m	†3m	†3m	3m†	mi recur

Table 2 **Clinical data** (continued)

PN°	n/O	S	HISTO	LEVEL	Prev O	YO	Aop	poP	ES	N	F	LP	M°	T°	I	A	g1	M1	SDef (preop)	U	SpD1	R	LAMIN	P	Cy	H	C	s	D
119	141	F	M-Met	T10-T11	Cut Mel	88	46	9m	LL dcp	N	N	0,3	*	*	np	np	g1	I	0	0	0	C	T10-11	0	0	H	0	0	0
	142		M-Met	T10-T11	6m-C	89	47	15d		N	N	np	np	np	*	np	0	III	R H°E tam/T10	C	0	S		0	0	0	0	0	0
120	143	F	Melano	C2-C5	0	88	25	6m	Cerv p	0	N	0,9	*	*	*	np	g1	II	b H°E tam/C5	0	0	C	C2-C5	w	0	0	C	0	0
	144		Melano	C4-C5	2y-C	90	27	1m		0	N	np	np	*	*	np	0	III	b H°E tam/C5	0	0	S		i	0	0	0	0	Ly
121	145	M	Melano	T10-T11	1y AC-B	69	61	6m	Lumb p	0	N	0,6	*	np	np	np	0	III	b anesth/T9	C	0	S	T9-T11	0	0	0	0	0	0
122	146	M	Lymph	C6-C7	0	91	40	20d	LL dcpE	0	N	np	np	*	*	np	0	III	b H°E tam/T12	0	0	S	C6-C7	w	0	0	0	0	0
123	147	F	Lymph	T11-L2	0	67	23	6m	LL Md	0	N	0,3	*	np	np	np	0	IV	b perin anesth	C	0	B	T12-L1	0	0	0	0	0	nlp
124	148	F	Hb	B°-C1	0	88	49	1y	RUL dcpE	0	N	np	np	*	*	*	g1	I	R hand astereo	0	0	P	C1+O	w	1C	0	0	0	Ly
125	149	M	Hb	T8	0	88	72	18m	LLL dcp	0	N	1,3	*	*	*	np	g1	II	L LL dcd	0	0	C	T7-T9	w	0	0	0	0	0
126	150	F	Hb	C3-C4	0	88	27	14y	LL Md	0	N	0,5	*	*	*	*	g1	II	b h/pd C2-T10	0	0	C	C3-C5	w	1C	0	0	0	Ap
127	151	M	Hb	C6	0	89	45	2m	Cerv p	0	N	np	np	*	*	np	g1	I	0	0	0	C	C5-C7	w	0	0	0	0	0
128	152	F	Hb	C7-T12	0	93	47	5y	RT rp	0	N	np	np	*	*	np	g1	II	L LL dcd	0	0	C	C7-T12	w	1C	0	0	0	0
129	153	F	Hb	C4-C7	0	82	29	10y	LUL dcpE	0	N	1,1	*	*	np	*	g1	I	R BS/C7	0	0	C	C1T1+O	w	1C	0	0	0	Ap
130	154	F	Hb	C4-C8	0	83	37	6m	RUL Md	0	N	np	np	*	np	*	g1	II	L H°E tam/C8	0	0	C	C4-C6	w	0	0	0	0	0
	155		Hb	T10-T11	2nd IMT	83	37			0	N	np	np	*	np	np	g1	II	b H°E tam/T10	0	0	C	T10-11	w	0	0	0	0	0
131	156	F	Hb	T8	0	86	56	5m	LL Md	0	N	0,2	*	*	np	np	g1	II	R H°E tam/T5	0	0	C	T7-T9	w	0	0	0	0	0
132	157	M	Hb	C1-C2	0	90	65	7m	Lhb dcpE	0	N	np	np	np	*	np	g1	II	L h/pd C2-C6	0	0	C	C1-2+O	w	1C	0	0	0	Ly
133	158	M	Hb(im)	C4-T4	0	80	53	6y	Tortic N	N	N	1,5	*	*	np	*	g1	I	b H°E tam/C4	0	0	C	C1-T4	w	1C	0	0	0	0
134	159	M	Hb(im)	C4-T11	0	84	23	13m	Tortic	0	N	0,8	*	*	np	*	g1	II	L h/pd C2-T1	0	0	C	T1-T12	w	2C	0	0	0	Ly
135	160	M	Hb(im)	C1-T10	0	77	47	5y	Tripl	0	N	24	*	np	np	*	0	III	b H°E tam/T6	C	0	C	C5-T10	w	2C	H	0	0	Ly
136	161	M	Hb	C5	0	87	23	3m	Rhb sD	0	N	np	np	np	*	np	g1	I	0	0	0	C	C4-C6	w	0	0	0	0	0
137	162	F	Hb	whole sc	0	92	36	10y	LL Md	0	N	np	np	np	*	np	g1	II	R hb H°E/C5	0	0	C	C2-C5	w	2C	0	0	s	0
138	163	M	Hb	B°-T1	0	90	57	5y	RUL Md	0	N	1	np	*	*	*	g1	II	b H°E tam/C2	0	0	C	C1T1+O	w	1C	0	0	0	0
139	164	M	Hb	C2-C3	0	80	33	10y	L dc Sc N	0	N	1,6	*	*	np	*	g1	I	L H°E tam/C5	0	0	C	C1-C4	w	0	0	0	0	0
140	165	M	Hb	B°-C3	0	92	44	1m	Tetrapl	0	N	np	np	np	*	np	0	IV	b dcd/C1	C	0	C	C1-C3	w	0	0	0	0	Ly
141	166	F	Hb	T1-T3	0	66	32	2y	LLL Md	0	N	0,8	*	np	np	np	g1	I	R anesth/T3	0	0	C	T1-T3	w	1C	0	0	0	0
142	167	F	Hb	conus-m	0	90	22	6y	Lumb p	N	N	np	np	np	*	np	g1	I	0	0	0	C	T11-L2	w	1C	0	0	0	0
143	168	F	Lipoma	T6-L2	0	90	36	11y	b dc Sc	N	N	np	np	np	*	np	g1	I	L LL H°E tam	0	0	B	T6-L2	i	0	0	C	0	Ly
	169		*Lipoma*	*C7-T2*	*2nd IMT*	91	37			0	N	*np*	*np*	*np*	*np*	*np*	*g1*	*II*	*L LL H°E tam*	0	0	I	C6-T1	i	0	0	0	0	Ly
	170		Lipoma	T9-L1	18m-B	93	38			N	N	np	np	np	*	np	g1	II	L LL H°E tam	0	0	D		i	0	0	0	0	Ly
144	171	F	Lipoma	T12-L2	0	84	36	2y	Ur d	0	N	0,9	*	np	np	np	g1	I	perin+L LL anest	d	0	S	L1-L3	i	0	0	0	0	0
145	172	M	Lipoma	T5-T6	0	82	73	10m	LL Md	0	N	1,7	*	*	np	np	g1	II	R BS/T7	0	0	B	T5-T6	i	0	0	0	0	Ly
146	173	F	Lipoma	T1-T4	0	86	44	3m	Parapl	0	N	1,4	*	np	*	np	0	IV	b anesth/T4	C	0	S	T1-T4	i	0	0	C	0	0
147	174	F	Lipoma	C7-T4	0	81	34	4y	RLL dcp	0	N	0,3	*	*	np	np	g1	II	R H°E tam/T4	0	0	S	C7-T4	i	1C	0	0	0	0
148	175	F	Lipoma	T1-T10	0	88	20	3y	LL Md	0	N	np	np	np	*	np	g1	I	b h/pd T6-T9	0	0	I	T1-T10	i	0	0	C	0	0
	176		Lipoma	C1-C6	2nd IMT	91	23			0	N	np	np	np	*	np	g1	II	b h/pd T6-T9	0	0	S	C1-C6	i	0	0	0	0	0
149	177	F	Lipoma	B°-C5	0	64	8m	2m	Tetrapl	0	P	10	*	np	np	np	0	IV	b H°E tam/C2	0	0	P	C1-5+O	i	0	0	0	0	nlp
150	178	M	Lipoma	T12	0	84	56	2y	RLL dcp	0	N	0,1	*	*	np	np	g1	I	b LL H°E tam	0	0	C	T11-L1	i	0	0	0	0	0
151	179	F	Lipoma	T8-T10	0	93	4m	4y	/sC Lip	0	N	np	np	np	*	np	g1	I	0	0	0	S	T8-10	0	0	0	0	0	0
152	180	M	Lipoma	T4-T6	0	92	52	16y	Dors p	0	N	np	np	np	*	np	g1	II	b LL H°E tam	0	TS	I	T4-T6	i	0	0	C	0	0
153	181	M	Lipoma	conus-m	0	89	73	6y	Ur d	0	N	np	np	*	*	np	g1	II	0	d	0	I	T11-L2	i	0	0	0	0	0
154	182	M	Schwa	C3-C7	0	93	47	10y	RUL dcpE	0	N	np	np	*	*	np	g1	II	R hb H°E/C5	0	0	C	C3-C7	w	0	0	0	0	0
155	183	F	Schwa	C6-T1	0-NF2	78	34	2d	Parapl	0	N	2,2	*	np	np	np	0	IV	b anesth/T1 b	C	0	P	C6-T1	0	xC	H	0	0	Ly
156	184	M	Mening	C2	0	75	31	1y	Cerv p	0	N	1,5	*	np	np	np	g1	I	L LL HypE	0	0	C	C2-C4	w	0	0	0	0	0
157	185	F	Cavern	C7-T1	0	93	16	15d	RUL rp	0	N	np	np	np	*	*	0	IV	b H°E tam/T2	C	0	C	C6-T1	w	1C	H	0	s	0
158	186	F	*Cavern*	*T6-T9*	0	86	63	*1m*	*Dors p*	0	N	0,2	*	*	*	*np*	*g1*	*II*	*b H°E tam/T10*	*d*	0	C	T6-T9	w	0	H	0	0	0
159	187	M	Cavern	T4-T5	0	76	36	15y	R dc Sc	0	N	0,3	*	np	np	*	g1	I	R dcd/T7	0	0	C	T4-T6	w	1C	H	0	0	0
160	188	M	Cavern	T10	0	91	59	4m	LL Md	0	N	0,2	*	np	*	np	g1	II	b dcd/T9	0	0	C	T9-11	w	1C	H	0	0	0
161	189	M	Cavern	T7-T8	0	69	16	3m	T h/pd	0	N	0,3	*	np	np	*	g1	II	R BS/T7	0	0	C	T7-T8	w	1C	0	0	0	0
162	190	F	Derm-C	T12-L2	0	90	35	8y	b dc Sc N	N	N	0,5	*	*	*	np	g1	I	L LL H°E tam	0	0	S	T10-L2	i	0	0	C	0	0
163	191	F	Derm-C	T12-L2	0	89	37	25y	LL Md	0	N	np	np	np	*	np	g1	II	b dcd/T12	0	0	C	T11-L3	i	0	0	0	0	0
164	192	M	Epid-C	conus-m	0	76	44	6y	L dc Sc	0	N	0,3	*	np	np	np	g1	II	R perin H°E	0	0	S	T11-L2	i	0	0	0	0	0
	193		Epid-C	Conus-m	11y-S	87	55			0	N	np	np	np	*	np	g1	II	R perin anesth	0	0	S		i	0	0	C	0	0
165	194	F	Epid-C	T5-T8	0	93	29	6m	RLL dcpE	0	N	0,6	*	*	*	*	g1	I	L H°E tam/T9	0	0	C	T5-T8	w	1C	0	0	0	0
166	195	F	Ngl-C	conus-m	0	86	29	6y	Lumb p	0	N	np	np	*	*	np	g1	II	R LL H°E tam	0	0	S	T11-L2	i	1C	0	0	0	Ly
167	196	M	Ngl-C	whole sc	0	77	40	3y	T h/pd	0	N	0,8	*	np	np	np	g1	I	b h/pd T5-T8	0	0	S	C6-T9	i	xC	H	0	0	Ly
168	197	F	Sarcoid	C3-C4	0	88	58	3y	LUL dcpE	0	N	np	np	np	*	*	g1	II	b h/pd C5-T1	0	0	S	C3-C4	i	0	0	0	0	0
169	198	M	Sarcoid	C5-C7	0	82	26	1m	LL Md	N	N	1,6	*	np	np	*	g1	II	R hand H°E tam	0	0	B	C3-T1	0	1C	0	0	0	Ly
170	199	M	Sarcoid	C4	0	91	36	10y	4Ls dcpE	0	N	np	np	np	*	np	g1	I	R h/pd C4-T12	0	0	B	C3-C5	0	0	0	0	s	0
171	200	F	?	conus-m	0	91	45	5y	R bt Myo	0	N	np	np	*	*	np	g1	I	0	0	0	D	T11-L2	0	0	0	0	0	0

Table 2 **Clinical data** (continued)

PN°	1>2	g2	M2	R°T	2>3	g3	M3	SDef (postop)	pS	LT p	SPA	U+Sx	SpD2	3>4	g4	M4	F-UP	Recur?
119	ag	g2	II	0	ag	0	III	R H°E tam/T10	ag	°6m	6m-reop	°6m	°6m	reop	°6m	°6m	6m°	>>metast
	uc	?	III	0	ag	0	IV	R H°E tam/T10	uc	†4m	†4m	†4m	†4m	†4m	†4m	†4m	4m†	mi recur
120	ag	0	III	0	uc	0	III	b H°E tam/C5	uc	L dcp	*	0	0	uc	0	III	2y°	>>metast
	uc	0	III	50 Gy	uc	0	III	b H°E tam/C5	uc	L dcp	*	0	0	ag	0	IV	3y†	mi recur
121	ag	0	IV	0	uc	0	IV	b anesth/T9	uc	0	0	C	0	uc	0	IV	1y†	2 pr op AC
122	Imp	g2	II	0	uc	g3	II	b H°E tam/T2(-)	Imp	0	0	0	0	uc	m4	II	1y†	0 (SIDA)
123	uc	0	IV	60 Gy	uc	0	IV	b perin anesth	uc	†7m	†7m	†7m	†7m	†7m	†7m	†7m	7m†	mi recur
124	uc	g2	I	0	uc	g3	I	R hand astereo	ag	Cerv p	* *	0	CK	uc	m4	I	5y	reop/res T
125	uc	g2	II	0	Imp	g3	I	L LL dcd	uc	0	0	0	0	uc	m4	I	6y	0
126	ag>H	0	III	0	Imp	g3	II	b H°E tam/C2	ag	LULrp	* * *	0	0	uc	m4	II	5y	mult loc
127	ag	g2	II	0	uc	g3	I	L LL H°E	ag	0	0	0	0	uc	m4	I	4y	0
128	uc	g2	II	0	uc	g3	II	L LL dcd	uc	0	0	0	0	ag	m4	II	1y	0
129	ag	g2	II	0	Imp	g3	I	b H°E tam/C7	ag	LULrp	0	0	0	uc	m4	I	11y	0
130	uc	g2	II	0	reop	°1m	°1m	L H°E tam/C8	uc	°1m	1m-reop	°1m	°1m	°1m	°1m	°1m	1m°	mult loc
	ag	0	III	0	Imp	g3	II	b H°E tam/T10	uc	0	0	0	0	uc	m4	II	2y†	mult loc
131	ag	0	III	0	uc	0	III	b H°E tam/T5	uc	0	*	C	0	ag	0	IV	18m†	mult loc
132	uc	g2	II	0	Imp	g3	I	L h/pd C2-C6	uc	0	0	0	0	uc	m4	I	4y	0
133	uc	g2	I	0	uc	g3	I	b H°E tam/C4	uc	RULrp	0	0	CK	uc	m4	I	13y	0
134	ag	0	III	0	Imp	g3	II	L h/pd C2-T1	uc	0	* *	0	0	Imp	m4	I	9y	0
135	uc	0	III	0	uc	0	III	b LL anesth	uc	0	0	C	0	ag	0	IV	3y†	0
136	uc	g2	I	0	uc	g3	I	0	uc	RULrp	0	0	ImpC	uc	m4	I	6y	0
137	ag	0	III	0	uc	0	III	R hb H°E/C5	uc	0	0	0	0	uc	m4	III	2y†	mult loc
138	uc	g2	II	0	Imp	g3	I	b H°E tam/C2	uc	0	0	0	0	uc	m4	I	3y	0
139	uc	g2	I	0	uc	g3	I	L H°E tam/C5	uc	0	0	0	0	uc	m4	I	13y	0
140	†66d	†66d	†66d	†66d	†66d	†66d	†66d	†66d	†	†66d	†66d	†66d	†66d	†66d	†66d	†66d	66d†	mult loc
141	ag	0	III	0	Imp	g3	II	R anesth/T3	ag	0	* *	0	0	uc	m4	II	27y	0
142	uc	g2	I	0	uc	g3	I	R LL H°E	ag	0	0	0	0	uc	m4	I	3y	0
143	uc	g2	II	0	uc	g3	II	L LL H°E tam	uc	°3m	3m-reop	°3m	°3m	reop	°3m	°3m	3m°	rec >> reop
	uc	g2	II	0	uc	g3	II	L LL H°E tam	uc	L dcp	0	0	0	uc	m4	II	18m°	2nd lmt
	uc	g2	II	0	uc	g3	II	L LL H°E tam	uc	0	0	0	0	uc	m4	II	1y	0
144	uc	g2	I	0	uc	g3	I	perin+L LL anesth	uc	0	0	C	0	uc	m4	I	9y	0
145	uc	g2	II	0	uc	g3	II	R BS/T7	uc	R dcp	* *	0	TK	uc	m4	II	11y	0
146	uc	0	IV	0	uc	0	IV	b anesth/T4	uc	0	0	C	0	uc	0	IV	7y	0
147	uc	g2	II	0	uc	g3	II	R H°E tam/T4	uc	LLLrp	* *	0	0	uc	m4	II	12y	0
148	ag	0	III	0	Imp	g3	II	b H°E tam/T6	uc	0	*	0	0	uc	m4	II	3y°	mult loc
	uc	g2	II	0	uc	g3	II	L H°E tam/T5	uc	0	*	0	0	uc	m4	II	2y	mult loc
149	uc	0	IV	0	uc	0	IV	b H°E tam/C2	uc	0	0	0	0	uc	0	IV	6y◊	0
150	ag	0	III	0	Imp	g3	II	b LL H°E tam	uc	0	0	C	0	Imp	m4	I	9y	0
151	uc	0	I	0	uc	g3	I	O	uc	0	0	0	0	uc	m4	I	1y	0
152	ag	0	IV	0	Imp	0	III	b H°E tam/T8	uc	0	* *	0	TS	uc	0	III	2y	0
153	uc	g2	II	0	uc	g3	II	O	uc	RULrp	0	d	0	uc	m4	II	4y	0
154	Imp	g2	I	0	uc	g3	I	R hb H°E/C5	uc	0	*	0	0	uc	m4	I	1y	0
155	†18d	†18d	†18d	†18d	†18d	†18d	†18d	†18d	†	†18d	†18d	†18d	†18d	†18d	†18d	†18d	18d†	mi recur
156	uc	g2	I	0	uc	g3	I	O	Imp	L dcp	0	0	CK	uc	m4	I	18y	0
157	Imp	0	III	0	Imp	g3	II	H°E tam/T2b(-)	Imp	0	0	0	0	uc	m4	II	1y	0
158	ag	0	III	0	uc	0	III	b H°E tam/T10	ag	b dcp	*	0	0	uc	0	III	7y	0
159	ag	0	IV	0	uc	0	IV	b anesth/T7	ag	b dcp	* * *	C+Sx	0	uc	0	IV	17y	0
160	uc	g2	II	0	Imp	g3	I	b H°E tam/T8	ag	b dcp	*	d	0	uc	m4	I	2y	0
161	ag	0	III	0	Imp	g3	II	R BS/T7	uc	0	* *	0	0	uc	m4	II	24y	0
162	uc	g2	I	0	uc	g3	I	L LL H°E tam (-)	Imp	L dcp	0	0	0	uc	m4	I	5y	0
163	ag	0	III	0	uc	0	III	b dcd/T12 (-)	Imp	b dcp	0	C	L lor	Imp	m4	II	4y	0
164	uc	g2	II	0	Imp	g3	I	R perin H°E	uc	0	0	C	0	ag	m4	II	11y°	rec >> reop
	ag	0	III	0	Imp	g3	I	R perin anesth	ag	0	0	d	0	uc	m4	I	6y	rec >> reop
165	uc	g2	I	0	uc	g3	I	L H°E tam/T9(-)	Imp	Lumb p	0	0	0	uc	m4	I	1y	0
166	ag	0	III	0	Imp	g3	II	R H°E tam/T12	ag	0	0	0	0	uc	m4	II	7y	0
167	ag	0	III	0	uc	0	III	R hb anesth/T5	ag	†3m	†3m	†3m	†3m	†3m	†3m	†3m	3m†	0
168	uc	?2	II	0	Imp	g3	I	L h/pd C7-C8	Imp	0	*	0	0	uc	m4	I	5y	0
169	ag	0	III	0	uc	0	III	R hand H°E tam	ag	b dcp	* * *	C	0	uc	0	III	11y	0
170	uc	g2	I	0	uc	g3	I	R BS/C4	Imp	0	*	0	0	uc	m4	I	3y	0
171	uc	g2	I	0	uc	g3	I	O	uc	0	0	0	0	uc	m4	I	2y	0

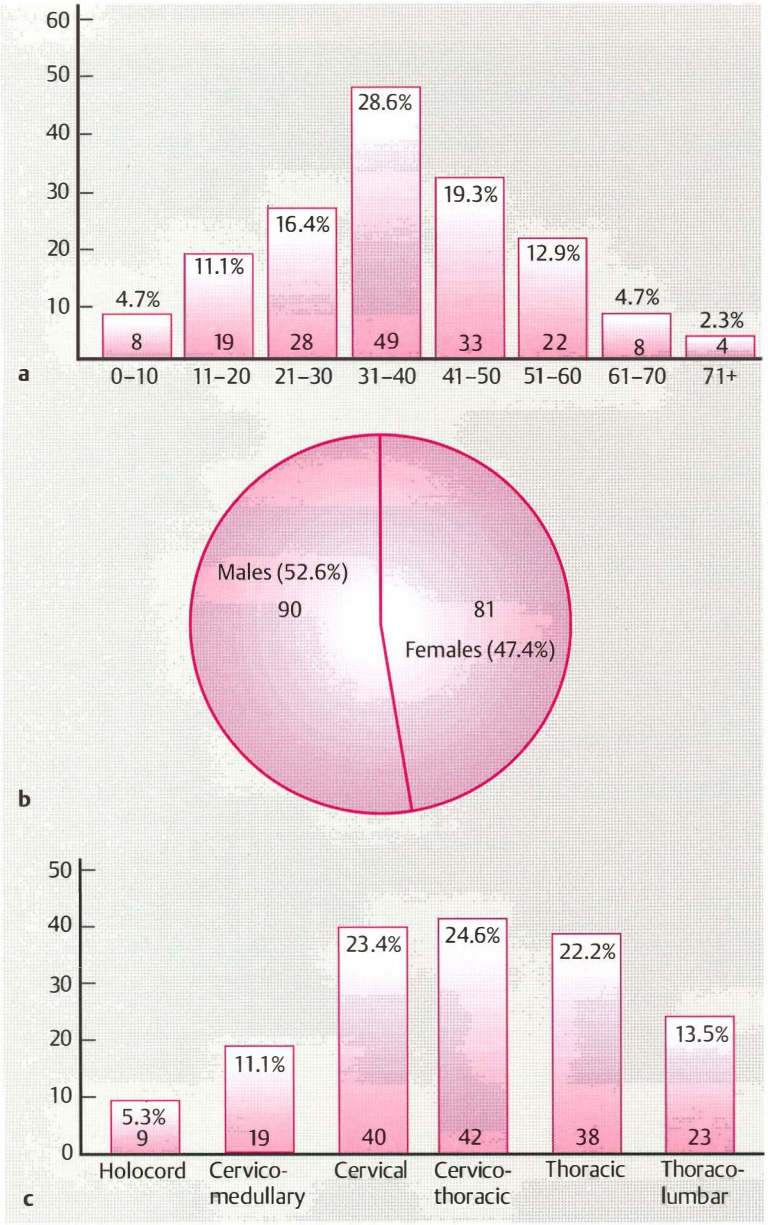

Fig. **14** **Patient data** (171 patients). **a** Age at the time of the first operation, **b** sex, **c** tumor location

Table **3** **The McCormick classification** of clinical functioning in intramedullary spinal cord tumor patients (ref. 169)

I	Neurologically normal, mild focal deficit not significantly affecting the function of the involved limb, mild spasticity or reflex abnormality, normal gait: 57 cases (33.3%)
II	Presence of sensorimotor deficit affecting the function of the involved limb, mild to moderate gait difficulty, and severe pain or dysesthetic syndrome impairing the quality of life, although the patient can still function and walk independently: 76 cases (44.5%)
III	More severe neurological deficit, with the patient requiring a cane or brace to walk, or with significant bilateral upper extremity impairment; the patient may or may not be able to function independently: 19 cases (11.1%)
IV	Severe deficit, with the patient requiring a wheelchair, cane, or brace, with bilateral upper extremity impairment; the patient is usually not independent: 19 cases (11.1%)

Discussion

These clinical observations are consistent with those reported in the literature, and in particular with the observations regarding the duration of preoperative symptoms – two to three years, according to Guidetti et al. (98) – the predominance of pain (35, 98, 165) and the low rate of sphincter dysfunction. The analysis of preoperative symptoms in the literature is disappointing. A number of authors have repeated well-known and previously described symptomatology, without providing any detailed analysis of their own patient series (40, 54, 68, 166). Conversely, unusual manifestations have been given more emphasis: torticollis (259), abdominal pain (225), sciatica related to dorsal column compression (76), arm stiffness (284), synkinesis (29, 30), and isolated arm clonus (225). An association between hydrocephalus and IMT has been inconsistently observed: Rifkinson-Mann et al. (222) reported 25 cases in 171 patients (15%) in a series mainly consisting of children, while their survey of the literature mentions only 36 such cases. Except during the terminal stage, no such association was observed in our 171 patients, who were mostly adults.

1.2 Diagnosis

Neuropathology

A. Jouvet, I. Salmon, M. Tommasi, G. Saint-Pierre, M.-C. Rousselet

Very few publications have dealt with the histological aspects of IMTs in any detail (27). It is our belief, however, that neuropathological correlations are crucial in reaching the correct diagnosis. Histological diagnosis can be made only after two separate microscopic examinations. *Intraoperative histological diagnosis* is essential for the neurosurgeon in selecting the surgical strategy. This examination presents difficulties, some of which are generic to intramedullary spinal cord tumors, but these are usually resolved at the *final histological examination,* which includes routine or special staining and immunolabeling techniques. In some cases, electron microscopy is useful in refining or confirming a diagnosis.

Classification and Histological Grading

The histological data from our Lyons and Brussels sample material were reviewed according to the World Health Organization classification criteria (129, 130). However, there are a few points in this classification that need to be refined with regard to ependymomas and astrocytomas. For all the other intramedullary spinal cord tumors we have observed, our classification and description conform to the WHO criteria.

Ependymoma

We have abandoned the classification of Fokes and Earle (81) that was used in our previous report on intraspinal ependymomas (77).

Various histological subtypes need to be taken into account. The *typical* or *standard* form includes the ependymomas that were termed "cellular" in the previous classification. These are characterized by large numbers of perivascular pseudorosettes (which are produced by the tapering processes of tumor cells surrounding blood vessels), "epithelial" ependymomas, which have ependymal tubes, and mixed ependymomas, i.e., combinations of the two preceding forms. The *cellular form in the WHO classification* includes those ependymomas with a higher cell density, in which perivascular pseudorosettes are rarer. The *clear-cell form* shows pseudo-oligoglial and pseudometastatic appearances. The *papillary form*, which has a poorer prognosis, is extremely rare. The *malignant ependymoma* is the last form described in the WHO classification.

We believe it is useful to add a *pseudoneurinomatous form* of ependymoma, also called *tanycytic ependymoma,* and this is described below (p. 78, Fig. **67**). Subependymomas occur rarely within the spinal cord.

Grading of ependymomas. Opinions differ concerning the grading of ependymomas. All spinal cord ependymomas are grade II in the WHO classification, although most of them could be rated as grade I in view of their good prognosis. Grade III malignant ependymomas located in the spinal cord are very rare. Subependymomas are rated grade I, but we have seen cases with subependymal foci in the periphery of grade II ependymomas.

Due to the adoption of the new WHO classification, nine cases that were rated as grade I in our 1977 report (77) are included in the present report as grade II, although the seventeen intervening years have provided evidence of the benign nature of these tumors *[1, 4, 7, 8, 19, 21, 32, 33, 46].*

Astrocytoma

Astrocytomas can be divided into three categories: ordinary, pilocytic, and dysplastic.

Ordinary astrocytoma (Fig. **56a**). Intramedullary spinal cord astrocytomas are often classified as fibrillary. Their fibrillary appearance results from the proliferation of the tumor cells along white-matter tracts, and this is much more common in the spinal cord than in the brain. This fibrillary appearance was a prominent feature in the peripheral regions of our rare cases of protoplasmic or gemistocytic astrocytomas. For this reason, we have preferred to classify these three forms of diffuse astrocytoma as "ordinary," in accordance with the classification of supratentorial astrocytomas by Daumas-Duport et al. (46). Spinal cord astrocytomas often correspond to grade II of the WHO classification. In our view, however, some rare astrocytomas with a very low cell density and a good prognosis should be rated as grade I. *Malignant anaplastic astrocytomas,* which rarely occur in the spinal cord, correspond to grade III of the WHO classification. Glioblastomas (grade IV of the WHO classification) are even less common.

Pilocytic astrocytoma (Fig. **56b**). In addition to the so-called "ordinary" astrocytomas, a grade I pilocytic astrocytoma has been documented. This is composed of bundles of long slender cells, and has a microcystic component. The rare occurrence of the latter feature in the spinal cord causes diagnostic difficulties.

Dysplastic astrocytoma. We have described a group of astrocytomas as being dysplastic, since they seem to us to be more hamartomatous than tumoral in nature. Their course is similar to that of pilocytic astrocytomas. For these two reasons, they can be rated as grade I astrocytomas.

Material and Methods

Selection criteria and discussion of diagnoses. Our personal experience is based on an analysis by three neuropathologists (A. Jouvet, I. Salmon, M. Tommasi), using light microscopy, of specimens from 214 operations. Fifteen cases were excluded: two because the pathological process was not neoplastic (one demyelination, one ischemia); two because the final histological examination showed no evidence of tumor; and 11 because the tumors were not intramedullary in their location. In a quarter of the cases, the diagnosis was rediscussed, and in 15 cases, the initial diagnosis was modified. On 11 occasions this was due to the results of immunolabeling, and on four occasions it followed the consensus opinion of the three pathologists. In one case, what was thought to be a tumor was not in fact a neoplastic process: a pilocytic astrocytoma was excluded from the series because it was in reality a case of fibrillary gliosis adjacent to a vascular malformation that had bled.

In six cases, we reclassified the type of glioma, as follows: two cellular ependymomas were reclassified as grade II astrocytomas *[92, 94]*, and one cellular ependymoma was reclassified as a grade III astrocytoma *[103]*. Three tumors initially considered to be fibrillary astrocytomas were in fact pseudoneurinomatous ependymomas *[13, 53, 54]*. The diagnoses of six glial tumor subtypes were modified either from grade II to grade I *[68, 70, 74, 75, 109]* or from grade I to grade II *[87]*. Finally, one "meningioma" was reclassified as a hemangiopericytoma *[156]*, and one "epidermoid cyst" was reclassified as a neuroglial cyst *[166]*.

Distribution of histological diagnoses (Table **4**). Of the 171 patients, 141 (including one patient *[171]* who did not undergo histological examination) underwent surgery once, 28 twice, and one three times. Thus, 170 histological diagnoses were made on the basis of 199 examinations in 200 operations.

Methods. Frequently, because of the small size of specimens, the intraoperative examination was limited to the study of touch preps and smears stained with toluidine blue. Whenever possible, we also an-

Table **4** **Histological diagnosis**

	n	*Total*
Primary glial tumors of the spinal cord		110
Ependymoma	62	
Subependymoma	2	
Astrocytoma	41	
Ganglioglioma	4	
Oligodendroglioma	1	
Metastases from CNS tumors		6
Cauda equina ependymoma	4	
Fourth ventricle ependymoma	1	
Medulloblastoma	1	
Malignant nonglial tumors		7
Metastases from visceral cancers (2) or melanoma (1)	3	
Primary melanoma	2	
Primary lymphoma	2	
Benign nonglial tumors		33
Hemangioblastoma	19	
Lipoma	11	
Schwannoma	2	
Meningioma (hemangiopericytoma)	1	
Pseudotumoral processes		14
Cavernoma	5	
Epidermoid (2) or dermoid (2) cysts	4	
Neuroglial cyst	2	
Sarcoid granuloma	3	
Total		170

alyzed frozen sections stained with toluidine blue, complemented by smears stained with hemalum and phloxine. Specimens of all IMTs were also fixed with Bouin's solution or formalin, embedded in paraffin, and stained using standard methods, hemalum – phloxine – saffron (HPS) for the second, definitive examination. In equivocal cases, we carried out special silver staining of reticulin fibers; immunolabeling for the detection of glial fibrillary astrocytic protein (GFAP), myelin basic protein (MBP), epithelial membrane antigen (EMA), and protein S 100 (PS 100). Anti-leu 7 labeling (human natural killer-1 marker, corresponding to cellular distribution 57 surface cell markers, an antibody for the detection of myelin-associated glycoprotein) was found in the oligodendrogliomas and schwannomas.

Electron microscopy is very useful in diagnosing difficult cases. However, it requires the availability of special fixation media at the time of intraoperative examination. It was not used systematically in all the cases in this study.

Diagnostic Pitfalls Common to All IMTs

The difficulties inherent in the histological diagnosis of IMTs result from the small size of biopsy specimens, the presence of cysts underlying or overlying the tumor, bleeding from lesions with large draining veins, the presence of tumors invaginated into the spinal cord, the possibility that the IMT may be exophytic and, finally, the occurrence of nonneoplastic expansive processes in the spinal cord.

Difficulties Relating to the Nature of the Specimen

The **small size of tissue specimens** is often an obstacle to the study of numerous microscopic fields, a practice that may be essential in some cases when only a minute portion of the tumor may reveal the actual nature of the lesion. Small specimen sizes make it particularly difficult to distinguish certain fusiform ependymomas from fibrillary or pilocytic astrocytomas, and to determine their grades. In addition, the small quantity of embedded material is rapidly consumed by serial sections prepared for light microscopy and immunolabeling.

Specimens from the periphery of tumors. Intense perilesional reactive gliosis may be mistaken for a glioma when the actual lesion is a vascular malformation or a hemangioblastoma (Fig. **62**). Similarly, peritumoral changes, such as the presence of macrophages, may suggest ischemic lesions or a pseudotumoral form of multiple sclerosis.

Difficulties Relating to Specimens from a Cyst Wall

When an intramedullary spinal cord cyst is present, determining whether or not its wall is neoplastic is a frequent and significant problem. In some cases, the macroscopic aspect of the lesion will allow the surgeon to distinguish between IMT and gliosis; otherwise, the diagnosis must depend on the intraoperative histological analysis, which in these cases may be unreliable. The intense gliosis that can be induced by a cyst or a syringomyelic or hematomyelic cavity may show the same cell density, Rosenthal fibers, regular and irregular cytonuclear characteristics, as well as similar numbers of macrophages, as seen in cystic pilocytic astrocytoma (18). The differential diagnosis is complicated by the fact that pilocytic astrocytomas with microcystic features occur very rarely in the spinal cord, and astrocytes with a gemistocytic appearance can be observed in gliosis. For these reasons, the diagnosis of astrocytoma (especially pilocytic astrocytoma) or fusiform cell ependymoma may be difficult or even impossible using intraoperative histological examination.

Difficulties Relating to Hemorrhage and IMT Draining Vessels

In cases of hemorrhagic lesions, it is often equally difficult, and sometimes impossible, to distinguish between vascular malformations surrounded by gliosis, on the one hand, and the intense vascularity that can often be seen in the periphery of hemangioblastomas or ependymomas, on the other. In one of our cases, multiple sections of hemorrhagic regions led to the demonstration of a hemangioblastoma *[135]*. Conversely, a hemorrhagic lesion initially thought to be a pilocytic astrocytoma was rediagnosed as gliosis in contact with a vascular malformation, and was therefore excluded from the series.

Differential Diagnosis Between IMT and Tumor Invaginating into the Conus Medullaris

Tumors of the filum terminale, which are by definition not IMTs, sometimes invaginate into the conus medullaris, like a finger entering a glove. When this occurs, intraoperative histological examination is necessary. A myxopapillary appearance is characteristic of cauda equina ependymomas. In contrast, when the appearance is "neurinomatous," immunohistochemical analysis is required to differentiate an extramedullary or, rarely, intramedullary spinal cord neurinoma from a pseudoneurinomatous ependymoma. Precise localization of the lesion by the surgeon is essential.

Histological findings requiring particular attention are reported in the sections of Chapter 2 (pp. 60 – 84) in which IMTs are classified as glial tumors, malignant nonglial tumors, benign nonglial tumors, and pseudotumors.

Neurophysiology

F. Mauguière, V. Ibañez, G. Turano, P. Garassus

Introduction

Because of the relatively rare occurrence of IMTs, there have been only a few series in which patients have been investigated using neurophysiological techniques, such as the study of somatosensory evoked potentials (SEPs) and motor evoked potentials (MEPs) obtained by cortical or spinal stimulation. To date, the most important published study using SEPs included 24 cases (114), all of which are included in the 63 observations of the present report; the other studies describe a few IMT cases in isolated reports, or cases included in series of spinal cord compressive lesions (115, 161, 260). SEPs allow segmental examination of the cervical spinal cord and conus medullaris, which is of particular interest in situations in which central spinal cord involvement may manifest itself a long time before the long tracts are affected.

Experience in the use of MEPs is even more limited, and is insufficient to allow any final conclusions to be drawn regarding the diagnostic efficacy of the method (101). Transcutaneous electric or magnetic stimulation at the spinal level depolarizes the motor roots close to their exit from the spinal cord, so that the central motor conduction time, measured by the difference between the MEPs elicited by cortical and spinal stimulation, assesses the motor pathways from the cortex to the initial segment of motor roots, and not exclusively the spinal segment of the motor pathways. This limitation can be overcome by the simultaneous recording of several muscles corresponding to distinct spinal levels, in order to demonstrate a segmental deficit in response to cortical stimulation, suggesting segmental dysfunction. Our experience in using motor evoked potentials in conjunction with somatosensory evoked potentials in evaluating IMTs is based on our experience in 13 patients, eight of whom were studied only after surgery. The two techniques were equally useful in detecting intramedullary spinal cord conduction abnormalities. Only two patients showed normal central conduction in the motor pathways.

However, the possibility that there may be dissociated abnormalities of central conduction in the motor (MEP) and sensory (SEP) pathways is not negligible (four cases of 13). Whenever possible, therefore, both of these neurophysiological investigations should be carried out.

For the above reasons, the data analyzed in the present report concern only SEPs (preoperative and postoperative recordings, as well as intraoperative monitoring). We shall only mention those intraoperative MEP monitoring techniques that remain to be validated in IMTs and are still experimental in standard spinal cord monitoring (e.g., scoliosis surgery).

Study Material and Results

Our SEP data are reported in Table **5**. As these data correspond to a population that has been studied and treated over the past 25 years and analyzed retrospectively, it is not surprising that all patients did not undergo preoperative and postoperative recordings or perioperative monitoring with stimulation of all four limbs. Thirteen patients were evaluated only preoperatively, and 14 only postoperatively. Five patients did not undergo surgery, but they have been included in the series because the intramedullary spinal cord site of their lesions was confirmed by MRI

Table **5** **Somatosensory evoked potential (SEP) data,** including 172 preoperative or postoperative recordings and 21 cases of intraoperative SEP monitoring. Not all patients were studied both before and after surgery, and upper and lower limb SEPs were not recorded in all cases. Consequently, the numbers given for each class of tumor site are not identical to those given in the text when analyzing SEP data according to the lesion site

		Lesion site			Pre		Post		Intra
	n	C	T	LS	UE	LE	UE	LE	
Ependymoma	32	27	4	1	21	20	28	28	12
Astrocytoma	12	5	6	1	8	6	7	9	3
Hemangioblastoma	4	4	0	0	4	4	4	3	1
Other	15	15	8	5	10	13	3	3	5
Total	63	44	15	4	43	43	42	44	21

C Cervical tumors
Intra Intraoperative
LE Lower extremity SEPs
LS Tumors of the conus (lumbosacral)
Post Postoperative
Pre Preoperative
T Thoracic tumors
UE Upper extremity SEPs

scans. These patients are listed under "Other" in Table **5**.

The table summarizes the SEP recordings collected for this study, consisting of 172 preoperative or postoperative recordings and 21 cases of intraoperative SEP monitoring. Not all patients were studied both before and after surgery. Upper and lower limb SEPs were been recorded in all cases. The numbers given for each class of tumor site are therefore not identical to those given in the text in the analysis of preoperative and postoperative SEP results in relation to the level of the lesion.

SEP Recordings and Normative Data

The SEP recording technique has now been well established for ten years (7, 50, 51, 62, 159). The following points should be emphasized.

The **major benefit associated with SEPs** is their ability to analyze separately segmental responses and spinal cord conduction, in relation to segmental deficits and deficits below the level of the lesion observed before, or resulting from, surgery. It is therefore essential to use a technique that allows one to obtain pure segmental responses uncontaminated by extraspinal cord potentials. This obvious fact necessitates the use of a noncephalic reference point for the recording of segmental responses. While the location of this point is not yet unanimously accepted, we have ample evidence of the superiority of this type of recording in intramedullary spinal cord lesions that may cause posterior horn dysfunction, particularly IMTs (114) and syringomyelia (162, 218). After stimulation of the median, ulnar, and posterior tibial nerves, this analysis of segmental responses is reliable only for the lower cervical cord segments (C6–T1) and segments L5 and S1 of the lumbosacral area. To date, recordings of upper cervical, thoracic, and sacral segmental responses below S1 have not been validated for the diagnosis of IMTs.

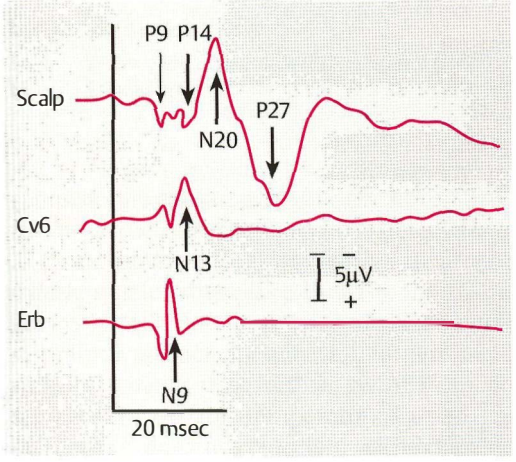

Fig. **15** **Normal median nerve SEPs** (stimulation at the wrist). The N13 potential voltage reflects the postsynaptic response of dorsal horn neurons in the lower cervical cord. The interpeak P9P14 interval reflects the conduction from the brachial plexus trunks up to the cervicomedullary junction via dorsal column fibers

Scalp Scalp axial parietal recording contralateral to stimulation (reference electrode contralateral to stimulation)
Cv6 Recording at the spinous process of the sixth cervical vertebra (supraglottal reference electrode)
Erb Supraclavicular Erb's point recording (reference electrode: shoulder contralateral to stimulation)

The **evaluation of conduction times**, based on the measurement of latency intervals between the peaks of two potentials at two distinct levels of sensory pathways, is subject to two limitations. First, the blockade of afferent volleys in the long tracts of the spinal cord abolishes the potentials produced upstream of the blockade, making this type of parameter unusable. Secondly, temporal dispersion of the ascending volley may reduce the amplitude of the SEPs without abnormally delaying their peak latencies. This observation is valid for propagated potentials (88) and segmental potentials (162), and requires normative data not only for the latencies but also for the amplitudes of spinal cord potentials. We studied the following parameters.

Upper limb SEPs obtained by stimulation of the median or ulnar nerve at the wrist (Fig. **15**). a) Peak latencies of the N9 and P9 potentials obtained from the supraclavicular fossa and the scalp (activity of the brachial plexus trunks); b) peak latencies of the P14 (afferent volleys reaching the cervicomedullary junction) and N20 (first response of the primary sensory cortex) potentials obtained from the scalp; c) P9–P14 (conduction time in the posterior columns of the cervical region) and P14–N20 (conduction time in the lemniscal tract and thalamocortical tract) intervals; d) P9–P14 amplitude ratio (dispersion index of afferent volleys in the posterior columns of the cervical region); e) amplitude and latency of the N13 cervical potential (response of the dorsal horn of the cervical spinal cord).

Lower limb SEPs (stimulation of the tibial or saphenous nerve at the ankle). a) Latency and amplitude of the N22 lumbar potential (response of the dorsal horn at the level of the conus); b) latency and amplitude of the P39 potential (response of the primary sensory cortex); c) N22–P39 interval (conduction time between the conus medullaris and the cerebral cortex).

All the above parameters were analyzed using the normative values from our laboratory (114, 218).

Preoperative SEPs: Diagnostic Value

Cervical tumors. SEPs were recorded in 36 patients in whom imaging examinations (all patients) and surgery (33 patients) had confirmed the presence of

an intramedullary spinal cord tumor involving the cervical segments, whether the solid part of the tumor itself or the associated cyst. In this group we included those tumors whose inferior extent reached the thoracic or even lumbar segments, whenever their cervical extension interfered with the SEPs obtained by upper limb stimulation (median or ulnar nerve stimulated at the wrist). The histological diagnosis was known in 33 cases, and included: 21 cases of ependymoma *[9, 12, 14, 23, 25, 26, 27, 29, 34, 35, 37, 41, 43, 44, 47, 48, 49, 53, 55, 59, 64];* four cases of astrocytoma *[76, 79, 81, 82];* four cases of hemangioblastoma *[124, 126, 129, 134];* one case of lipoma *[148],* one case of lymphoma *[122];* one case of gangliolioma *[107];* and one case of sarcoidosis *[169].*

Overall assessment of SEPs. A single patient *[83]* had normal SEPs on stimulation of upper and lower limbs; the tumor was a grade II astrocytoma, extending from C2 to T9, with decreased touch and temperature sensation from T5 to T7, but without any segmental sensory deficit at a cervical level or sensory changes below the level of the lesion. With a 97% detection rate of abnormalities for all clinical presentations, SEPs are unquestionably an essential diagnostic examination for the assessment of spinal cord function in patients with cervical IMTs.

Abnormalities in the cervical segmental responses (N13 potential). Abnormalities in the N13 segmental response provide an indication of the level of the lesion, although they do not indicate whether the cervical level is that of the cyst or that of the solid tumor itself. A recording of this response was made in 35 of the 36 patients in our series. The N13 potential was absent (Figs. **16**, **17**) or abnormally low in 30 patients (86%). Abnormalities were bilateral in 22 cases, and coexisted with normal responses of the brachial plexus roots in all patients. Amplitude abnormalities of the N13 potential reflect a predominant dysfunction of the postsynaptic neurons of the dorsal horn at the C6–C7 or C8–T1 level, depending on whether they are observed after stimulation of the median or ulnar nerve at the wrist. In 32 patients, sensory abnormalities were clinically evaluated in the week preceding or following the SEP recordings. The N13 potential was abnormal at least on one side in the 17 patients presenting with a suspended sensory deficit at the cervical level; the same findings were observed in 11 of the 15 patients without upper extremity sensory signs. These results confirm the frequency (73%) of subclinical abnormalities of the posterior horn potentials in cervical spinal cord pathology, which we have already reported in a smaller series of patients with IMT (114) and with cervical myelopathy (217).

In IMTs, the causative process of N13 abnormalities may be the tumoral cyst or the tumor itself (114), but any spinal cord lesion that can destroy postsynaptic neurons or desynchronize their re-

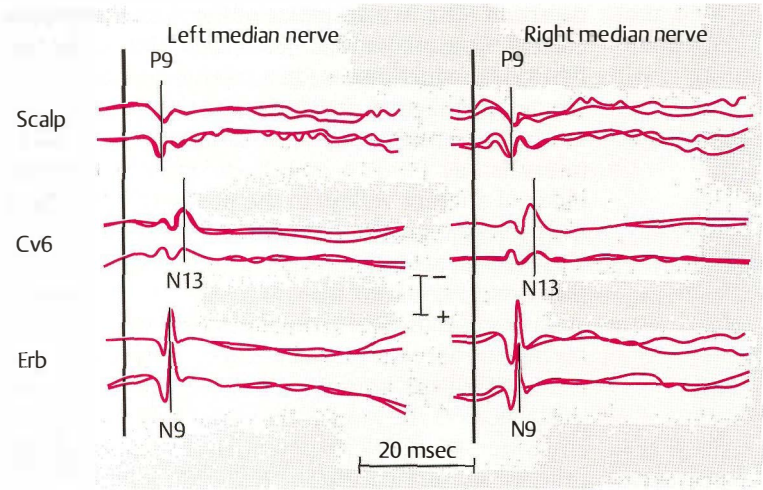

Fig. **16** **Preoperative and postoperative SEP recordings.** Postoperative restoration of the N13 potential with absent P14 and N20 potentials before and after surgery (holocord ependymoma whose solid part was cervical, case *27*). Median nerve SEPs recorded before (lower traces for each derivation) and two months after surgery (upper traces). Before surgery, conduction in the dorsal columns was abnormal, as reflected by the absence of P14 and N20 potentials on both sides. These SEP abnormalities remained unchanged after surgery. The dorsal horn response of the cervical cord (N13) was abnormally reduced before surgery, and returned to normal after removal of the tumor (adapted from Ibáñez et al. 1992, ref. 114)

Scalp Scalp axial parietal recording contralateral to stimulation (reference electrode contralateral to stimulation)
Cv6 Recording at the spinous process of the sixth cervical vertebra (supraglottal reference electrode)
Erb Supraclavicular Erb's point recording (reference electrode: shoulder contralateral to stimulation)

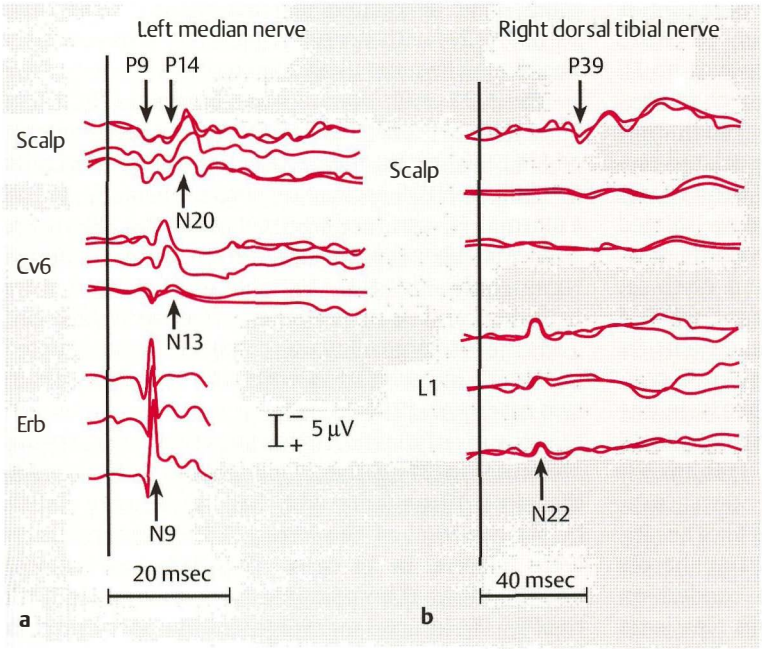

Fig. **17** **Preoperative and postoperative SEP recordings.** Postoperative restoration of N13 and P39 SEPs (cervical ependymoma, case *55*). SEP recordings performed before surgery (lower traces for each derivation), two weeks after surgery (middle traces) and 12 months after surgery (upper traces). Before surgery, the N13 and P39 potentials were not identifiable, and the P9–P14 interval was normal. Two weeks after surgery, the N13 potential had recovered a normal voltage. Twelve months after surgery, the conduction time in the right fasciculus gracilis (N22–P39 interval) had returned to normal (adapted from Ibáñez et al. 1992, ref. 114)

a Right median nerve

Scalp Scalp axial parietal recording contralateral to stimulation (reference electrode contralateral to stimulation)
Cv6 Recording at the spinous process of the sixth cervical vertebra (supraglottal reference electrode)
Erb Supraclavicular Erb's point recording (reference electrode: shoulder contralateral to stimulation)

b Right dorsal tibial nerve

Scalp Vertex parietal electrode (Pz) (reference electrode at the left earlobe)
L1 Spinous process of the L1 vertebra (reference electrode at the left knee)

sponses can cause such abnormalities. This is particularly true of syringomyelic lesions (62, 124, 218, 274) and extrinsic compression, as in cervical spondylotic myelopathy (217). In IMTs, the relationships between N13 potential abnormalities and clinical symptoms are not unequivocal. In particular – contrary to what is observed in syringomyelia (218) – segmental pain and temperature loss in the upper extremities does not correlate with N13 abnormalities. Less surprisingly, touch and joint sensation in the upper limbs is preserved when N13 abnormalities are isolated, i. e., free of any posterior column conduction disorder (normal P9–P14 interval). Only lost or diminished reflexes of the upper extremities correlate significantly with N13 abnormalities (114).

In the five patients with no abnormal N13 response, two presented with lesions entirely located above the C5 level – one astrocytoma *[82]* and one hemangioma located at the cervicomedullary junction *[124]*. Far from being false-negatives, these two cases emphasize the topographical specificity of N13 abnormalities: the SEP profile of these patients was that of a cervicomedullary dissociation, with preserved cervical segmental responses and interrupted or time-dispersed conduction in the fasciculus cuneatus, as evidenced by an abnormal P14 lemniscal potential (160). However, this topographical evidence does not hold true for the remaining three patients, two with a cervical cyst extending from C4 to T1 rostral to an ependymoma *[2, 12]*, and one case of C1–C6 lipoma *[148]*. It is notable, however, that no patient in whom the solid part of the tumor involved segments C6 to T1 showed a normal N13 potential.

Conduction abnormalities in the posterior columns. a) Fasciculus cuneatus (FC). Latency interval measurement (288) and measurement of the P9–P14 amplitude ratio (88) allow reliable evaluation of conduction in the FC fibers, with a small degree of inter-individual variability in normal subjects. In 27 patients (75%), the interval increased or was not

measurable due to the absence of the P14 potential. These abnormalities were bilateral in 16 cases (Fig. **16**). The eight cases in which there was no FC conduction abnormality did not have any characteristic features, but it is notable that four of them presented with a thoracic tumor with an associated cervical cyst *[2, 37, 79, 83]*. Only 17 (40%) of the 43 cases of P14 abnormality in this series showed an isolated increase in the P9–P14 interval. In other words, temporal dispersion of the ascending volley is often associated with disappearance of the far-field P14 potential, or with an isolated abnormality in its amplitude. The impact of cervical IMTs on FC conduction is marked by a significant increase in the P9–P14 mean conduction time: 5.7 ± 1 ms for the 48 measurements carried out in our patients, as against 4.6 ± 0.5 ms for 72 measurements in 36 normal subjects of comparable age (t 7.5, $p < 0.001$). This increased conduction time in the FC contrasts sharply with the P14 – N20 intracranial mean conduction time, which remained identical in patients (5.0 ± 0.7 ms) and in controls (4.9 ± 0.6 ms). *The latency increase of N20 potential in cervical IMTs therefore specifically reflects conduction slowing in the fasciculus cuneatus.*

b) Fasciculus gracilis (FG). It is somewhat irrelevant to speak of conduction in the fasciculus gracilis with regard to potentials evoked by stimulation of the tibial nerve, since some of the responses, both segmental and cortical, are triggered by afferent volleys running from muscle fusorial fibers, which, in the spinal cord, are not conveyed through the FG. It is nevertheless customary to consider that the N22–P39 latency interval reflects FG conduction, even though part of the ascending volley follows the lateral columns of the spinal cord. On the other hand (and this is true both for the stimulation of the tibial nerve and for the saphenous nerve, which contains no fusorial fibers), this interval reflects the quality of conduction from the L5–S1 segments to the cortex, including the intracranial segment of the sensory pathways. Its value is therefore different from that of the P9–P14 interval, which specifically explores conduction up to the cervicomedullary junction.

The *P30 potential,* equivalent to the P14 potential in upper extremity SEPs, allows evaluation of conduction in the spinal segment proper, but it has not been studied sufficiently for routine diagnostic use. Another obstacle is the fact that the N22 segmental response may not be recordable for technical reasons in 15–30% of normal subjects, in our experience. As a consequence, in the 31 cases of cervical tumors with tibial or saphenous nerve recordings, N22 responses were considered to be technically reliable in 25 cases (81%). Only three patients had abnormal N22 responses; in two cases *[122, 126],* tumoral extension or a concurrent peripheral neuropathy might have accounted for this result. In the third patient *[124]* with a cervicomedullary tumor, a false-positive is the most likely explanation.

The *N22–P39 interval* was abnormal (Fig. **17**) in 37 of the 62 recorded SEPs (59.7%) – either augmented (11 SEPs) or not measurable (26 SEPs) – owing to an abolished P39 cortical response. Five patients had a normal FG conduction time while the SEPs were abnormal after median nerve stimulation. In two of these, only the N13 segmental responses were pathological, but in the other three cases *[26, 124, 126],* the afferent volley was dispersed or interrupted in the FC, in association with N13 abnormalities in two cases *[26, 126]*.

In terms of *diagnostic testing,* FG conduction was abnormal in 24 of the 31 patients (77.4%) studied, including 18 patients who had no sensory deficit below the level of the lesion (75%); abnormalities were bilateral in 13 cases. This detection rate for abnormalities is comparable to that obtained with the P9 – P14 interval measurement in upper limbs, so that the hypothesis that FG fibers are more sensitive to compression than FC fibers (a hypothesis that was put forward to suggest the superior performance of lower limb SEP tests in cervical myelopathy) (294)) is not relevant as regards IMTs. It seems likely, in this situation, that neurophysiological abnormalities better reflect the transverse extension of tumoral infiltration than the extrinsic compression of spinal cord fibers-hence the variety of features observed.

Finally, it should be borne in mind that a pure loss of pain and temperature sensation produced by a lesion of the spinothalamic tract is associated with a normal N22–P39 interval.

Thoracic tumors. The neurophysiologist cannot use segmental abnormalities to locate thoracic intramedullary spinal cord tumors, as these are lesions in which the only expected SEP abnormality will be FG conduction. The same is true of lumbar tumors that involve the L1–L3 lumbar segments but do not affect the projecting segments of the tibial or saphenous nerve fibers. For this reason, they do not affect the N22 potential. Nine patients studied prior to surgery presented with a lesion that met these criteria. Sensation was normal in only one case *[162];* five cases showed a suspended sensory loss not consistently associated with a deficit below the level of the dorsal lesion *[47, 67, 102, 112, 160];* in three patients, a deficit below the level of the lesion was isolated *[69, 71, 165]*.

Abnormalities of N22 segmental response. Despite our selection criteria, two patients presented with unilateral abnormalities of the N22 potential. In one of them *[162],* the lesion extended to L2, and it may well have had an impact on the N22 response, either by a mass effect or because the extension down the spinal cord was lower than previously

thought by the surgeon. This explanation was not the case with the second patient *[160]*, who presented with a T10 cavernoma; in this patient, a falsely abnormal N22 potential seems the most likely explanation.

Abnormalities of intraspinal conduction (prolonged N22–P39 interval or absent P39). Intraspinal conduction, evaluated by stimulation of the lower extremities, was abnormal in seven of nine patients *[47, 67, 69, 71, 102, 160, 165]*. In three, the abnormalities were bilateral *[47, 102, 165]*. In ten abnormal SEPs, five recordings showed an increased N22–P39 interval, and in five the P39 potential was absent. None of the three patients with a normal P39 potential had a dorsal column sensory deficit of the lower limbs; one of them *[112]* had sciatica, probably related to dorsal column compression, without signs of permanent deficit. In a single case *[67]*, conduction abnormalities were subclinical, i.e., free of any sensory deficit below the level of the lesion.

SEPs were recorded *after upper extremity stimulation* in five of these patients; the recording was normal in all cases.

Tumors of the conus medullaris. Four patients were included in this category, defined by tumor location affecting the L4, L5, S1, and S2 segments, and with possible changes in the N22 segmental potential, evoked by stimulation of the posterior tibial or saphenous nerve at ankle joint level (Table **5**). The N22 potential was abnormal in three cases, and spinal cord conduction was abnormal in two cases.

Intraoperative SEP Monitoring

All the technical considerations relevant to SEP monitoring have been reported in a recent survey by Nuwer et al. (192). Intraoperative monitoring of central conduction was carried out in 21 patients. This group includes 16 cervical tumors: 12 ependymomas *[9, 14, 23, 29, 34, 35, 37, 41, 43, 49, 59, 64]*; two astrocytomas *[79, 83]*; one hemangioblastoma *[129]*; one case of multiple lipomas *[148]*; two thoracic tumors, one metastatic ependymoma *[112]*, and one astrocytoma *[67]*; and three pseudotumors, one cervical sarcoidosis *[169]* and two thoracic epidermoid *[165]* and dermoid cysts *[162]*. In all cases, SEPs were recorded from scalp leads after stimulation of mixed nerves whose fibers penetrate the spinal cord below the segment corresponding to the inferior limit of the tumor mass (median or ulnar nerves for cervical tumors located above segment C5, posterior tibial nerve for tumors located at lower levels).

With one exception *[35]*, patients in whom P14, N20, or P39 could not be recorded before surgery were not monitored. The advantage of remote monitoring (scalp leads) is that it does not interfere with the surgical procedure; the shortcoming is that it requires signal averaging. Under optimal (but rare) conditions, this requires an acquisition time of two minutes per recording, with 500 stimuli delivered at a rate of five per second, without rejection of responses contaminated by artifacts. Monitoring systems based on epidural or intradural recording of the dorsal columns above the tumor in response to electrical stimulation of a peripheral nerve (121) or caudal spinal cord (134) have yet to show their superiority over surface recordings in intramedullary spinal cord tumor surgery. The same applies to the intraoperative use of transcranial motor evoked potentials (244). In a single patient *[165]*, presenting with a T5–T8 intramedullary epidermoid and associated cyst, we monitored the action potentials recorded directly from the two dorsal columns above the lesion in response to tibial nerve stimulation, because the scalp P39 potential was absent after stimulation of the left tibial nerve and very abnormal after stimulation of the right one before surgery, thus precluding the monitoring of scalp SEPs. Any disappearance, voltage decrease greater than 50%, or increased latency of potentials P14, N20, or P39 greater than 10% of the value measured under anesthesia at the start of surgery, was considered significant. At least one postoperative follow-up recording was performed in all patients but one. Overall, transient or permanent SEP abnormalities occurred during surgery in 15 patients (71%), i.e., in a considerable proportion of patients and a number that was in itself sufficient to justify the use of intraoperative monitoring. These abnormalities were always observed when the dorsal columns were being retracted. The correlations between abnormalities observed intraoperatively and the status of postoperative SEPs suggest that the latter do indeed reflect a conduction abnormality directly related to mechanical deformation (reversible or not) of the dorsal column fibers.

Based on monitoring results, the following correlations were noted.

No change (five cases) **or improvement** (one case) **in intraoperative SEPs**. In the five patients *[9, 34, 35, 83, 129]* whose scalp SEPs remained stable during surgery (Fig. **18**), postoperative central conduction was found to be identical to the value measured before surgery, whether this value was normal or not. Likewise, the data obtained from the postoperative clinical test sensation below the level of the lesion remained identical to those obtained during the preoperative examination. However, surgical tumor removal had an effect on spinal cord function in all of these patients, for two reasons. First, segmental responses can be affected, in spite of the absence of any changes in spinal cord conduction; this was the case in two patients *[34, 35]* whose segmental sensation deteriorated. Secondly, it is clear that the occurrence of conduction abnormalities and signs of sensory deficits can be observed after sur-

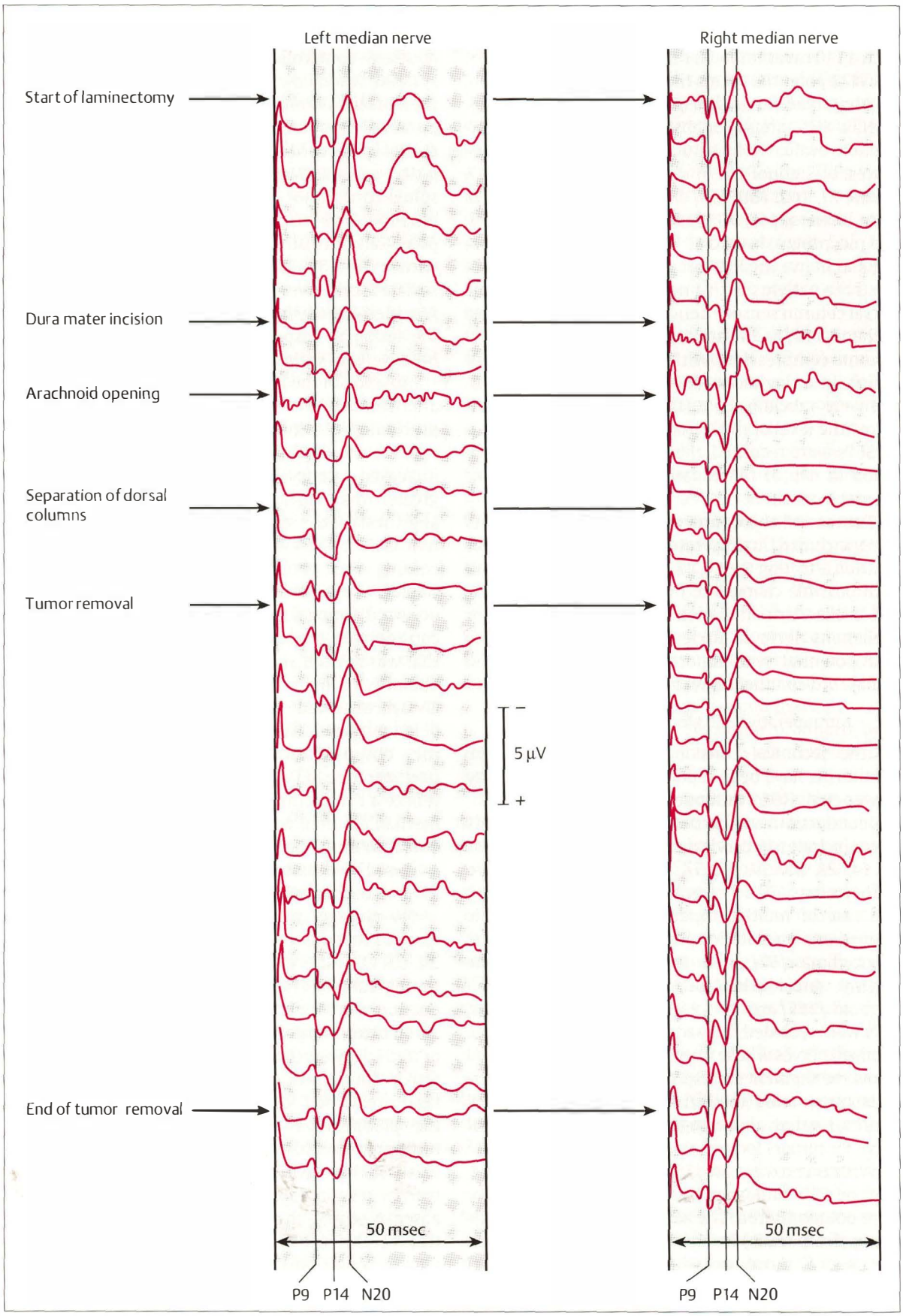
Left median nerve
Right median nerve
Start of laminectomy
Dura mater incision
Arachnoid opening
Separation of dorsal columns
Tumor removal
End of tumor removal
5 µV
50 msec
50 msec
P9 P14 N20
P9 P14 N20

Fig. 18 **Median nerve SEP monitoring during the removal of a cervical ependymoma** (case *34*). Median nerve SEPs were recorded using a noncephalic reference electrode placed at the shoulder opposite to the stimulation. A transient and nonsignificant voltage decrease of the responses was observed. The P9–P14 conduction time remained unchanged throughout the operation. After surgery, this patient had normal touch and joint sensation, and the P9–P14 interval was normal

gery in tracts whose function was not monitored intraoperatively – motor or spinothalamic fibers, or in the absence of monitoring of one of the dorsal columns, as in two patients in this series *[9, 35]*.

Intraoperative SEP improvement remains an exceptional event, which we observed through direct recording of the dorsal columns above the level of the lesion during the removal of a cystic lesion of the thoracic spinal cord *[165];* SEP recording one week after surgery demonstrated the recovery of potential P39 that had been absent before surgery.

Reversible intraoperative SEP abnormalities (seven cases). When SEPs are transiently abnormal during surgery, their return to baseline values at follow-up examination is not commonly observed. We observed it in four of the seven patients in this group *[43, 49, 59, 169],* three of whom presented with a sensory deficit below the level of the lesion aggravated by surgery. In the three other patients *[29, 37, 41],* lasting postoperative SEP abnormalities, associated with worsening of the sensory deficit below the level of the lesion in two, while postoperative SEPs had returned to baseline values at the end of surgery, are puzzling. Although we cannot prove it, we would hypothesize that dorsal column injury, even when transient, may increase the risk of early secondary changes. Evidence of this would require the continuation of monitoring throughout the immediate postoperative period.

Lasting deterioration of intraoperative SEPs (eight cases). Permanent SEP abnormalities mainly affect the N20 and P39 potentials, both of which may disappear during surgery. The sensory deficit below the level of the lesion worsened postoperatively in seven of the eight patients in this group *[14, 23, 64, 67, 79, 112, 148],* while preoperative dorsal column improvements remained unchanged in the eighth patient *[160].* In the five patients with loss of the N20 or P39 responses, partial postoperative SEP recovery was observed only once *[14]* three weeks after surgery. A prognosis of irreversible voltage decrease, without complete abolition of the N20 or P39 potentials, cannot be determined, as the population sample is too small with three cases *[67, 112, 148];* moreover, the only patient *[67]* whose postoperative SEPs could not be evaluated was in this group. In the other two patients, we observed either irreversible loss of N20 *[148]* or a small increase in central conduction time *[112],* both associated with postoperative sensory deficit below the level of the lesion.

Postoperative SEP Follow-Up

The period of time elapsing between surgery and the first postoperative SEP examination varied considerably: some patients were tested within two weeks of surgery, and others several years after tumor removal, i.e. for the purpose of the present retrospective study (maximum time: 24 years). In order to present consistent results and provide easier analysis, we have chosen to report the postoperative SEPs from the 35 patients who were tested at least one year after surgery, since we observed that after one year, SEPs remained stable. This group consisted of 25 patients with cervical tumors and ten with thoracic or lumbosacral tumors. The time-span since the last SEP recording ranged from one to five years in 18 cases, and exceeded five years in 17 cases. The following results are based on data obtained during the latest available recording for each patient.

Cervical tumors (25 cases) (Figs. **16**, **17**). Only five patients *[12, 34, 76, 111, 134]* (20%) had normal bilateral upper extremity SEPs. Of the potentials studied, the N20 was least affected. It was bilaterally normal (upper limbs) in 12 patients (48%), as against seven patients for the N13 potential (28%) and nine patients for the P14 potential (36%). Five patients *[26, 29, 31, 34, 46]* (20%) had normal bilateral lower extremity P39 potentials.

Qualitative analysis. Figure **19** shows the postoperative progression of the N13, P14, and P39 potentials in the 29 patients who had preoperative upper extremity, lower extremity, or both upper and lower extremity SEP recordings. Recordings were judged to have improved if there was at least unilateral: 1) recovery of an abolished potential, even if still abnormal; 2) return to normal voltage or latency; 3) presence of shorter P9–P14 and N22–P39 intervals, i.e., shortened by more than one or two milliseconds, respectively. Conversely, worsening was defined as either the abolition of a potential or the occurrence of voltage or latency abnormalities, or the presence of P9–P14 or N22–P39 intervals increased by one or two milliseconds, respectively. Figure **19** emphasizes three findings: 1) potential P39 is most often affected by surgery (48% of 21 cases), probably because of trauma to the fasciculus gracilis during posterior column retraction; 2) potential P14 is most often improved (38% of 29 cases), due to restored or resynchronized conduction in the cervical posterior columns as a result of surgery; 3) potential N13 most often remains unchanged (50% of 25 cases). Although rare, the possibility of improvement of this

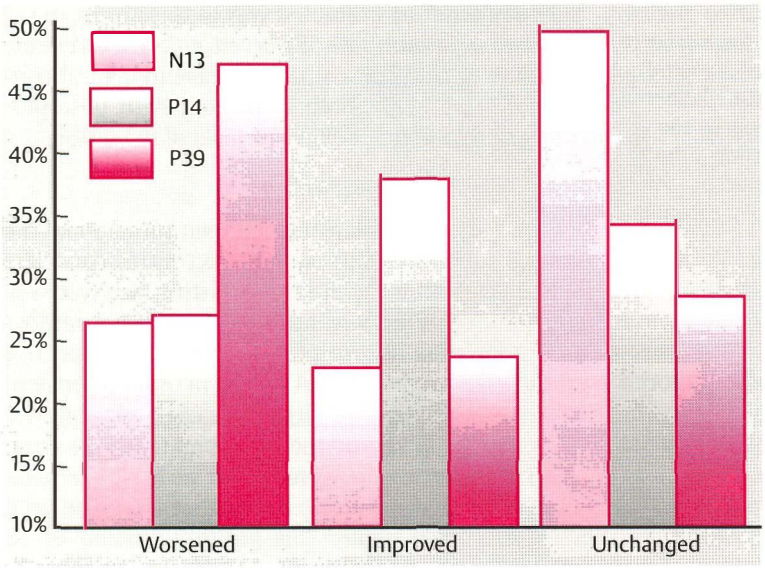

Fig. **19** **Postoperative development of N13, P14, and P39 SEPs**

Table **6** **Central conduction times** before and after surgery. The number (n) refers to the number of nerves (median and/or ulnar, and posterior tibial) for which the latency interval was measurable

	Before surgery	After surgery	p
Cervical tumors (25 cases)			
P9–P14 (n = 22)	5.5 ± 0.1 msec	5.1 ± 0.6 msec	0.076
P14–N20 (n = 28)	5.1 ± 0.6 msec	5.2 ± 0.7 msec	n.s.
N22–P39 (n = 10)	17.3 ± 4.0 msec	18.8 ± 6.8 msec	n.s.
All tumors (35 cases)			
N22–P39 (n = 23)	17.9 ± 3.4 msec	18.6 ± 4.9 msec	n.s.

potential has been reported (114). It most often results from cyst drainage, but was also observed twice after removal of a tumor invading the cervical spinal cord below C4 (Figs. **16**, **17**). Finally, it is notable that in eight patients with cervical tumors in whom an SEP recording was carried out more than ten years after surgery, upper extremity SEPs were normal in two *[76, 134]* and lower extremity SEPs were normal in only one *[46]*.

Qualitative analysis of central conduction changes. We used the paired *t*-test to compare intervals P9–P14, P14–N20 and N22–P39, when they were measurable, before and after surgery (Table **6**). The advantage of this analysis is that it makes use of quantitative data, but the drawback is that it does not take account of voltage changes, or of recordings in which conduction times are not measurable due to the absence of one potential. Overall improvement of dorsal column conduction in the cervical region was confirmed by a postoperative reduced P9–P14 interval, which was just at the level of statistical significance. By contrast, the N22–P39 interval did not vary, despite the above-mentioned frequent impairment of the P39 potential. The large variability of this interval is not the sole explanation for this absence of significant change; moreover, the same comparison performed on the total number of tumors confirms this result, in spite of the increased number of measurements and the reduction of their variability (Table **6**). In fact, in most cases, impaired conduction is responsible for lower limb SEP voltage abnormalities or the disappearance of P39 potentials, precluding quantitative analysis of latencies. The data in Table **6** suggest that when surgery does not cause P39 abolition, it induces no lasting slowing of central conduction, resulting in an increased N22–P39 interval.

Tumors of the conus medullaris and thoracic tumors (ten cases). Nine of the ten patients in this group *[1, 20, 47, 53, 69, 71, 72, 93, 112]* showed abnormal P39 potentials, at least on one side, one year or more after surgery. Preoperative recordings had been performed in five of them *[47, 69, 71, 83, 112];* three presented with an abnormal P39 potential at least unilaterally *[47, 69, 71];* in three cases, the potential deteriorated, according to the above

criteria *[69, 71, 112];* one remained unchanged *[47],* the P39 potential being absent both before and after surgery. The only patient whose potentials were normal after surgery had normal responses before surgery *[83].* This finding confirms the particular sensitivity of the fasciculus gracilis fibers already noted in cervical tumors.

Postoperative Neuroclinical Correlations

Although fairly large, our series does not allow statistical analysis of correlations between postoperative sensory and SEP changes. Only 29 of the 35 patients selected had been studied before surgery, and all the necessary data, i.e. preoperative and postoperative SEP recordings of the four limbs and a complete profile of preoperative and postoperative sensory signs, were available in only 20 of these 29 patients (15 cervical and five thoracic tumors). Consequently, we were unable to study the progression of segmental sensory deficit and sensory deficits below the level of the lesion for each evoked potential separately. However, global analysis clearly shows a parallel trend in clinical and neurophysiological data, since SEPs were impaired in the clinically involved region in eight patients whose sensory signs worsened. In seven patients whose sensory deficits were improved or unchanged after surgery, SEPs improved, or remained stable. Discrepancies between clinical and SEP changes were observed postoperatively in the remaining five cases in this series of 20. In two of them, the discrepancies can be explained by the fact that they showed a worsening of a suspended sensory loss or loss of pain and temperature sensation below the level of the lesion, related to a lesion in the spinothalamic tract that was not accompanied by segmental response changes. In the other three patients, the discrepancy is explained by the occurrence of infraclinical abnormalities of potential P39.

Conclusions

This analysis of SEP recordings made over a 15-year period allows us to conclude that SEPs provide reliable and consistent data both for the diagnosis and the postoperative follow-up of IMTs. SEPs are clearly relevant to any IMT preoperative evaluation, providing invaluable information about the functional status of the spinal cord. They also provide objective evidence of abnormalities of the sensory pathways, and may sometimes reveal abnormalities that are not clinically apparent.

Carrying out intraoperative SEP recording is technically difficult but useful during the operative procedure, as is shown by the Lyons experience reported in this monograph. This study shows that one of the risks associated with surgery is injury to the dorsal columns. The awareness of this risk inevitably raises the question of whether intraoperative monitoring is useful. Every surgeon knows how difficult it is to demonstrate the impact of monitoring on the result of a surgical procedure, since so many factors influence postoperative results. However, it should be remembered that dorsal column injury is currently detected during 70% of operations. Irreversible abnormalities are predictive of postoperative sensory deficits. Conversely, the absence of dorsal column conduction changes is a good indicator. Finally, one of the benefits of SEP recording is the demonstration that surgery can be followed by complete restoration of spinal cord sensory function.

Neuroradiology

J.-C. Froment, D. Balériaux, F. Turjman, Z. Patay, F. Rio

Introduction

It is clear that magnetic resonance imaging (MRI) is the diagnostic modality of choice in the diagnosis of spinal cord tumors. However, the specific type of investigation performed depends on locally available radiological techniques and equipment. Diagnosis using MRI is optimal when the MR images can be correlated with previously obtained clinical and laboratory data (12).

The questions confronting the neuroradiologist involve varying degrees of difficulty. Is there a lesion? If so, is it intramedullary or extramedullary? Is it a tumor? If it is a tumor, what are its characteristics? What is the exact location and extent of the solid portion of the tumor? Is there a cystic component? Is there an intratumoral cyst? Are there satellite cysts at the upper pole or the lower pole, or both? Is there an associated hydrosyringomyelia? Is there a cyst affecting the medulla? Is there any signal enhancement after injection of gadolinium? Has there been acute or chronic hemorrhage into the lesion? Is there imaging evidence of a cleavage plane between the tumor and healthy spinal cord tissue? Is it possible to make a histological diagnosis of the lesion or, at least, to differentiate low-grade from high-grade tumors?

Preoperative MRI has been available only for patients who have undergone surgery since 1984 in the Brussels series, and since 1986 in the Lyons series, i.e., 109 of the total 200 surgical procedures performed.

Radiological Techniques

The routinely available radiological techniques used for the diagnosis of spinal cord pathology are: standard radiographic films, CT scans, water-soluble myelography, spinal arteriography, and MRI. MRI is

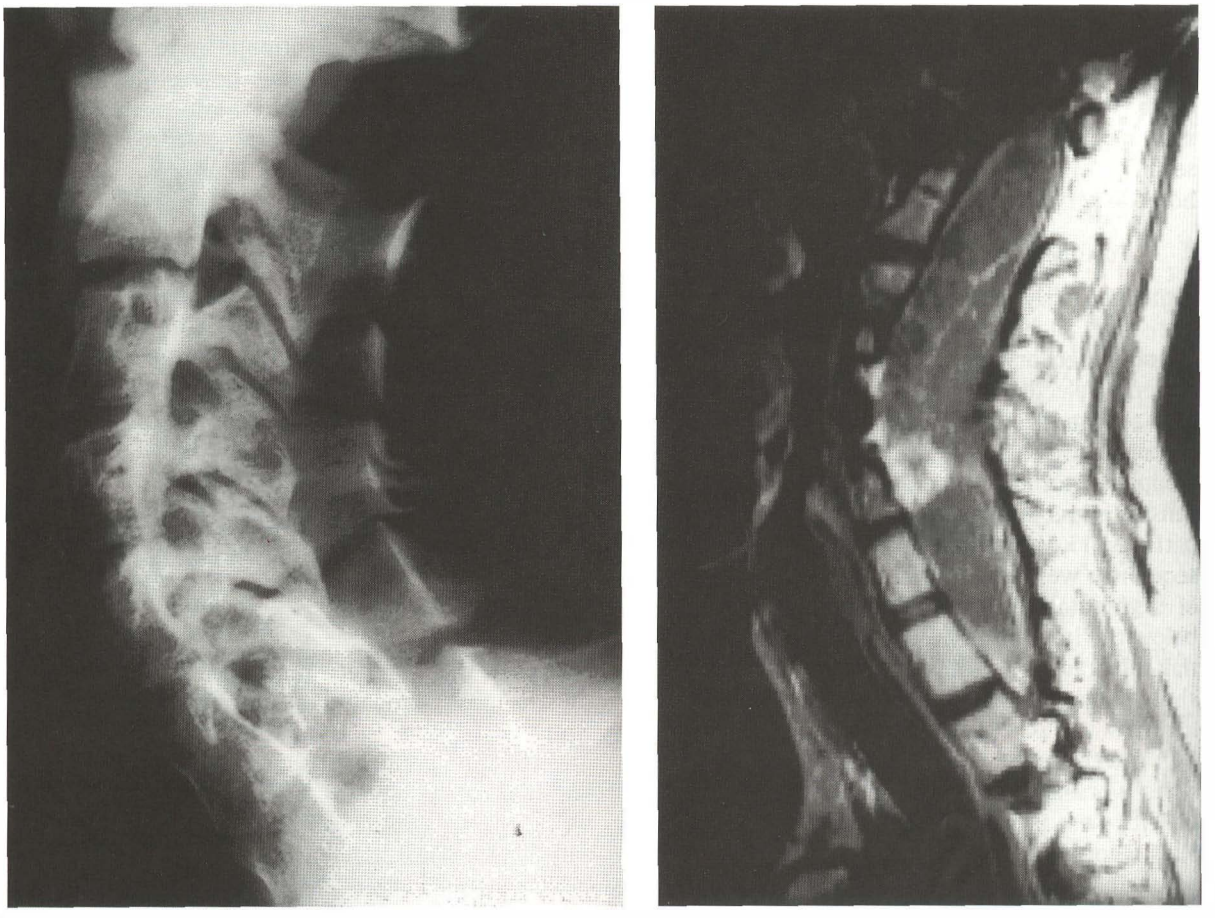

Fig. 20 **Fibrillary astrocytoma grade II in a 16-year-old girl** (case *91*). **a** Plain film of the cervical spine, lateral view: considerable enlargement of the cervical spinal canal, and vertebral scalloping produced by chronic erosion of the vertebral bodies. **b** Sagittal postcontrast T1-weighted image: a large cystic tumor with a small enhancing nodule following contrast administration, located anteriorly at the C6 level

now without question the most relevant and effective imaging procedure. If MRI is not available, myelography complemented by postmyelographic CT scanning can locate the site of the abnormality. However, if this examination strongly suggests a spinal cord tumor, an MRI examination is warranted (24).

Although the value of **standard radiographic films** is limited, this examination is useful for the general purpose of tumor localization and diagnosis-widened spinal canal (Fig. **20**), signs of chronic erosion, signs of osteolysis, etc. Also, in several cases of cervicothoracic IMTs, we observed cervical straightening with disappearance of the physiological lordosis (Figs. **55**, **62**).

Myelography is invasive and provides limited information, since it does not directly image the spinal cord itself and only defines abnormalities of the spinal cord contour (Fig. **21**) (148). It cannot differentiate precisely between cystic and solid components. However, it does show pathological vascular patterns supplying solid nodules, as in the case of hemangioblastomas, for example (Fig. **22**). In the presence of a complete or incomplete myelographic block (77), identification of the level of the upper pole of the lesion may not be possible. and this examination must be supplemented by subarachnoid injection of contrast above the level of the block or by postmyelogram CT scanning (Fig. **23**). As the diagnosis of an intramedullary spinal cord tumor is rarely an emergency (103), it is preferable to carry out MRI instead of a relatively uninformative myelogram, which is not only uncomfortable but also potentially hazardous to the patient. The relatively exceptional cases that present as emergencies with an abrupt worsening of symptoms may be due to intratumoral bleeding (42). Even in these cases, MRI remains the examination of choice to directly visualize the area of hemorrhage.

Plain or contrast-enhanced CT scanning can be carried out as the first examination to identify patho-

Fig. **21** **Grade III astrocytoma** (case *102*). Thoracic myelogram, with nonspecific focal enlargement of the spinal cord. No information is gained about the exact limits of the tumor or its nature

logy of the spinal canal, associated bone abnormalities, or altered density of the spinal contents (fat, blood, etc.) (Fig. **64**) (10, 11, 52, 96, 102, 123, 138, 182, 184, 206, 242, 251, 273). A myelo-CT scan will confirm the diagnosis of an enlarged spinal cord and show the two poles of the tumor more accurately (Fig. **23**). Today, myelo-CT scanning is complementary to MRI examinations in exceptional cases only (176).

Spinal angiography is not indicated as a screening test for spinal cord tumors. It remains the examination of choice for the diagnosis of vascular malformations, and is only exceptionally carried out as a preoperative examination for the purpose of pinpointing the spinal cord or tumor blood supply, or both. It can be useful in cases of hemangioblastoma, as a means of visualizing the feeding arteries (Fig. **22**) and before performing preoperative embolization, if needed (52, 141, 142, 242, 267).

MRI is the indispensable examination for the imaging evaluation of intramedullary spinal cord tumors (13, 14, 31, 155, 238, 240). The examination is dependent on the technical capabilities of each different MRI system, particularly the available coils (surface coils). The purpose of the study is to obtain the best possible spatial resolution and, hence, optimal lesion evaluation and accurate preoperative localization of the extent of the tumor (89). Thin sagittal sections (3–5 mm) are systematically obtained along with axial and coronal sections.

Three-dimensional MRI provides images in all planes, including reconstructed images in complex planes, and very thin slices (1 mm) with sufficient signal (Fig. **24**). At the present time, its systematic use is slow due to secondary data processing. The radiologist may choose among a wide range of imaging sequences and techniques, based on the pathology and time restrictions: T1-weighted (spin echo, gradient echo), T2-weighted, and T2*-weighted sequences (spin echo with multiple echoes, turbo-spin echo with single or multiple echoes, gradient echo, etc.). T1-weighted and T2-weighted images are complementary; both are valuable, and they should be systematically obtained (Fig. **29**) (126).

Contrast injection (gadolinium ethylenediamine tetra-acetic acid, EDTA) is also an essential element of MRI studies (263, 264, 275, 292). The pattern of enhancement provides additional information that may be helpful in making a histological diagnosis (28, 55, 198, 248). MRI is sensitive to flow phenomena. This information can be "extracted" in order to obtain reconstructed images showing the vascular pattern of the region imaged. Magnetic resonance angiography, a technique widely used for the study of the cerebral vasculature, has rarely been used in spinal cord imaging, although preliminary results seem promising (90).

Imaging Diagnosis

MRI is the most effective and sensitive technique for the detection of an intramedullary spinal cord lesion (13, 14, 31, 155, 238, 240). The interpretation of the images involves three steps: 1) identification and location of the intramedullary spinal cord lesion; 2) a thorough and systematic analysis of cystic and solid tumoral components, before and after the administration of contrast; and 3) diagnostic formulation.

Identification and Location of the Intramedullary Spinal Cord Lesion

An intramedullary spinal cord lesion is defined by morphological and spinal cord signal abnormalities, which are nearly always associated with enlargement of the spinal cord. In our experience, any tumoral infiltration produces spinal cord enlargement.

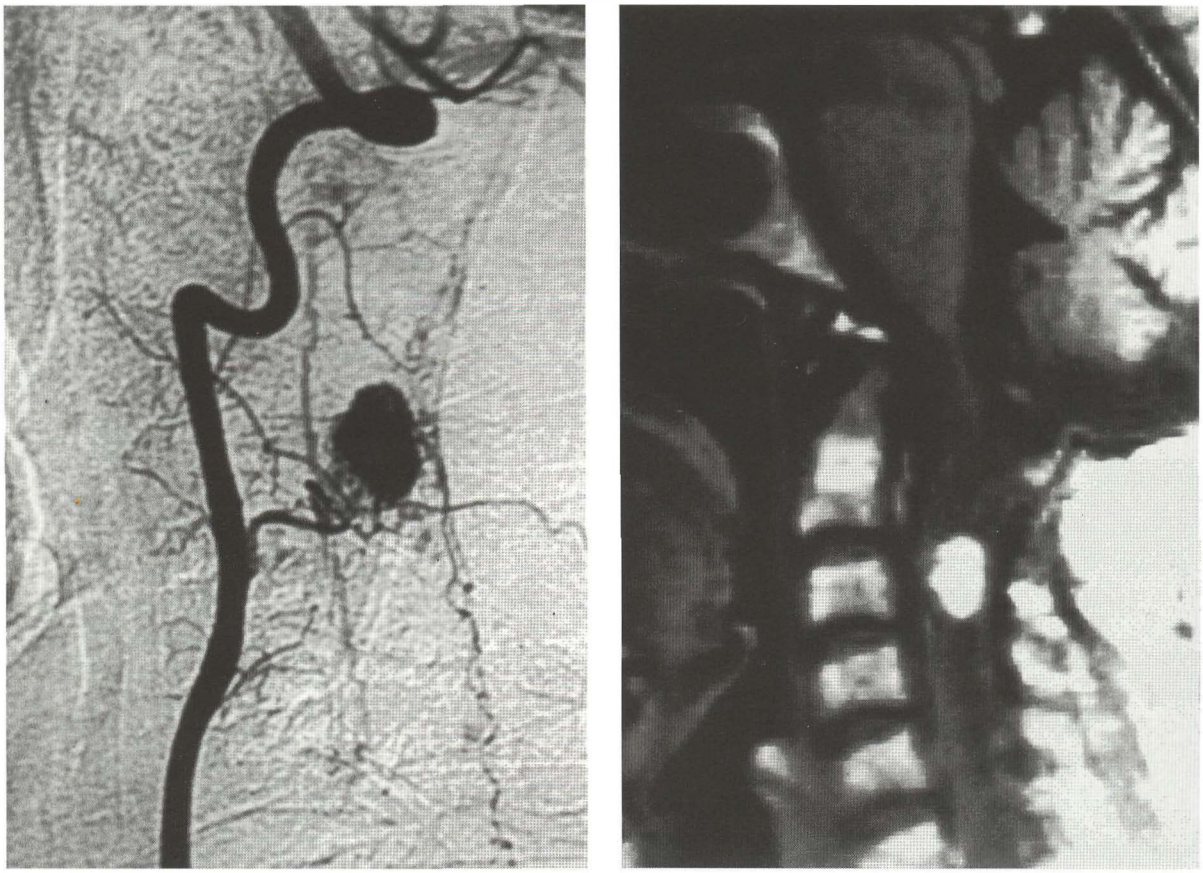

Fig. 22 **Multiple hemangioblastomas in von Hippel–Lindau disease** (case *126*) (courtesy of Prof. J.-F. Bonneville, Centre Hospitalier Universitaire, Besançon). **a** On the vertebral angiogram, a hypervascular nodule can be seen at the level of C3, which enhances on the sagittal T1-weighted postcontrast MR scan (**b**). **c** Lower thoracic myelogram: dilated tortuous feeding arteries and draining pial veins that perfectly match the images seen on the spinal cord angiogram (**d**)

Conversely, however, an enlarged spinal cord may not be caused by a neoplastic process, particularly when enlargement is limited to one or two vertebral segments. As a rule, MRI can be used to determine whether a lesion is intramedullary or extramedullary, provided that multiplanar images are obtained. However, this distinction may be difficult or impossible to establish in IMTs with an exophytic component (69, 97, 100, 109), extramedullary lesions invaginating into the cord (Fig. **31**), and in the very rare cases of intramedullary spinal cord neurinomas (Fig. **68**). If a complete MRI examination (T1, T2, T1 after gadolinium injection) is negative, then imaging evaluation is terminated, and the diagnosis of IMT is considered to be questionable.

Diagnostic Criteria for IMTs

Topography. A comparison with plain films can be useful in order to establish the precise vertebral level of the lesion, in case of vertebral abnormalities. If this is not possible, anatomical structures allowing identification of the level of the lesion must be included in the MRI field. The use of a large imaging field (e.g. with a body coil, using a 512 matrix) allows localization of the two poles of the tumor by counting vertebrae from the odontoid process or the sacroiliac joint. A central location within the spinal cord favors the diagnosis of an ependymoma, and an eccentric location suggests the diagnosis of an astrocytoma, hemangioblastoma, or lipoma. The precise location of the lesion must be evaluated with axial or coronal sections (Figs. **25**, **29**). This finding is mentioned in the literature (70) as a means of distinguishing tumors that tend to arise from an eccentric location from those that originate from the center of the spinal cord. Our experience does not confirm this, as only 62.5% of ependymomas had a central location, and 57% of astrocytomas were paracentral. By contrast, all solid hemangioblastoma nodules were found in the periphery, which confirms their subpial location (Figs. **28**, **62**).

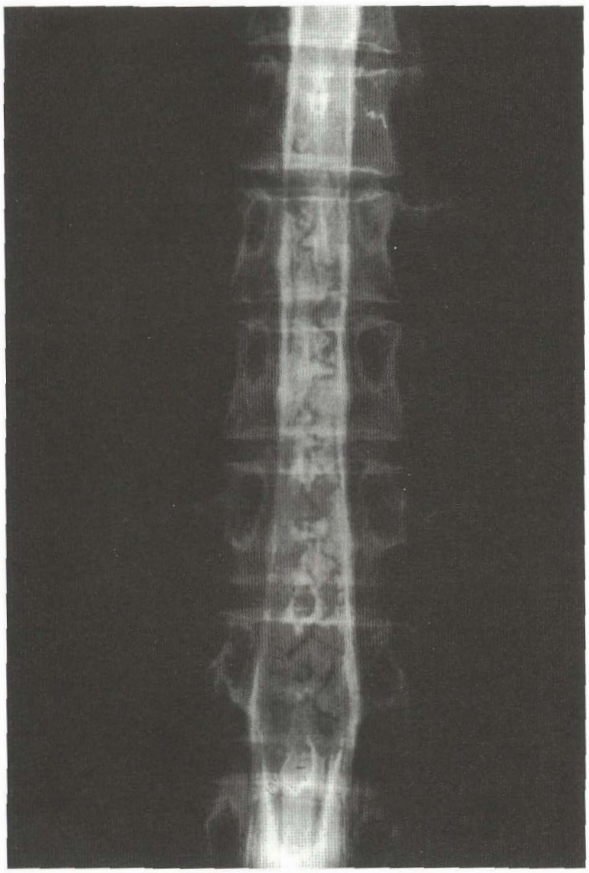

Fig. **22c**

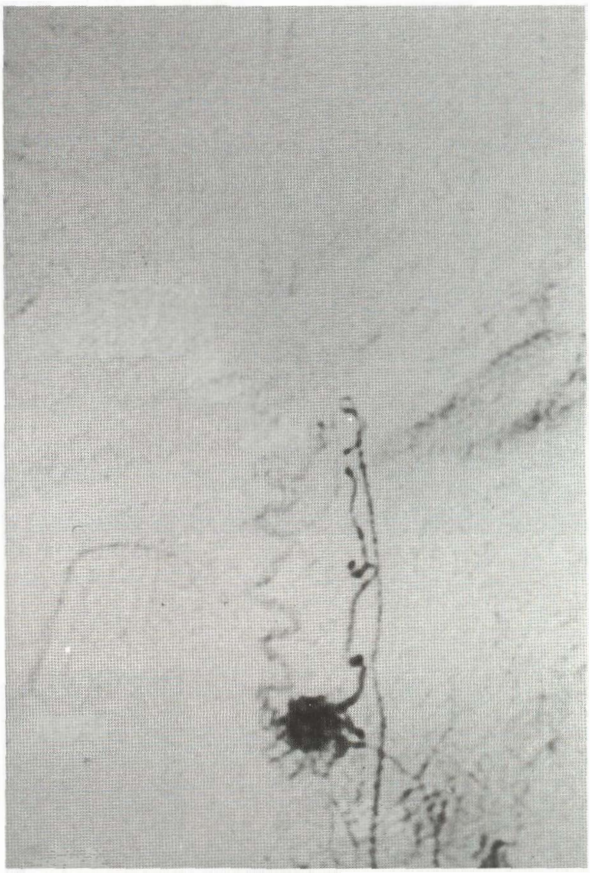

Fig. **22d**

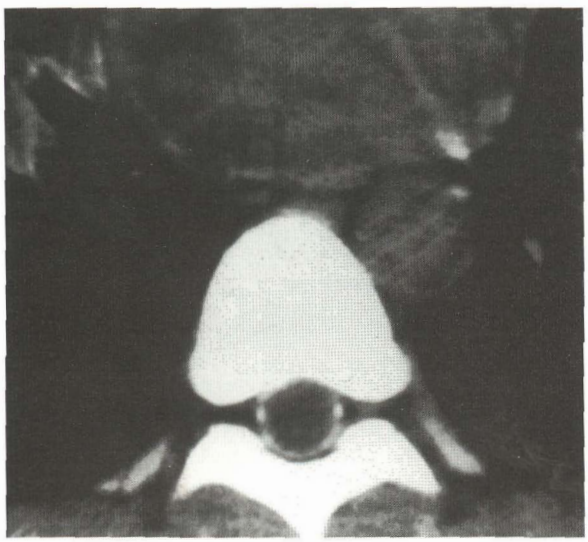

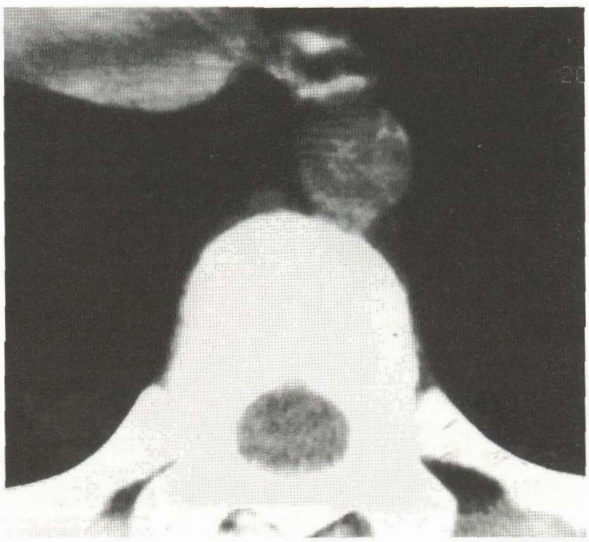

Fig. **23** **Grade II thoracic ependymoma.** Serial axial postmyelogram CT scans at the levels of **a** T7, **b** T11, **c** T12, and **d** L1. Extensive neoplastic enlargement of the thoracic spinal cord (courtesy of Prof. J.-C. Froment)

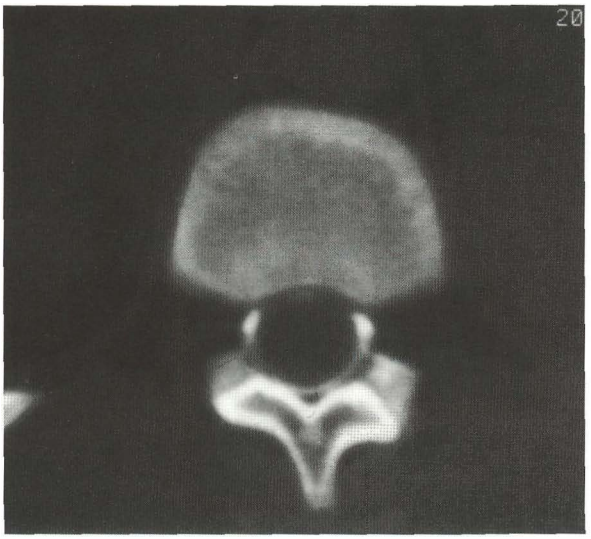

Fig. **23c**

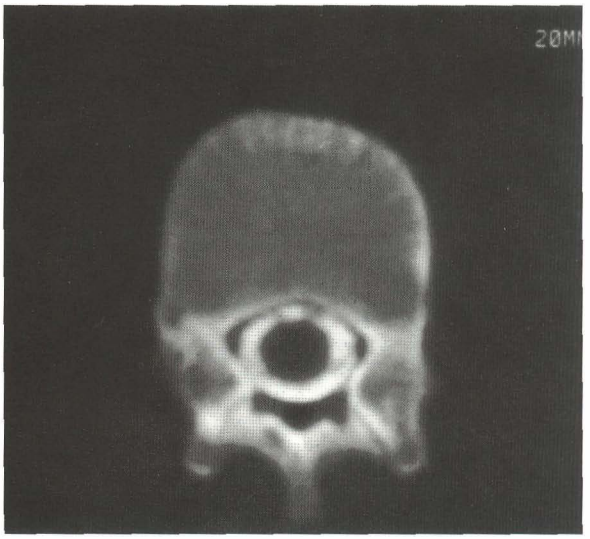

Fig. **23d**

a

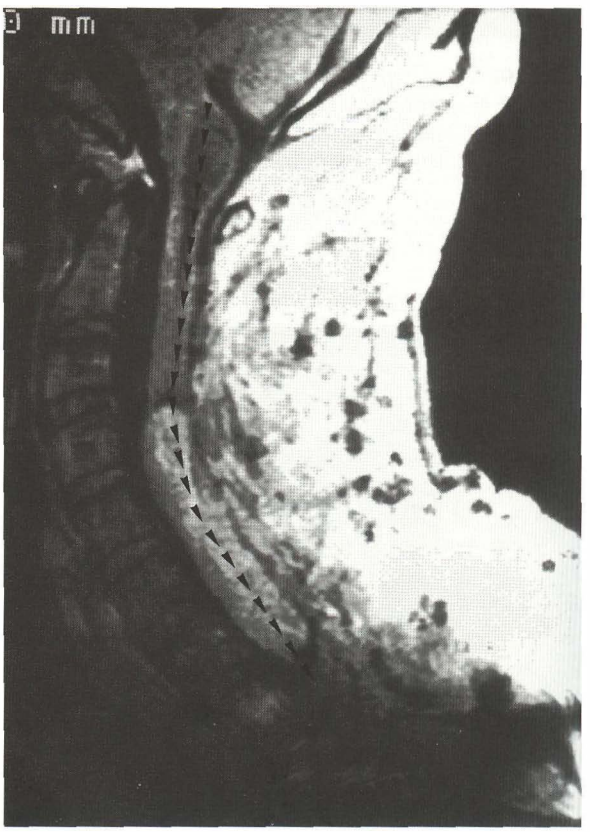

Fig. **24** **Three-dimensional acquisition** (case *60*). Grade II cervicothoracic ependymoma treated with two staged operations. Three-dimensional acquisition provides sagittal images (**a**) at 1-mm intervals, with complex coronal reconstructions (**b**) following the curved plane of the spinal cord (arrowheads)

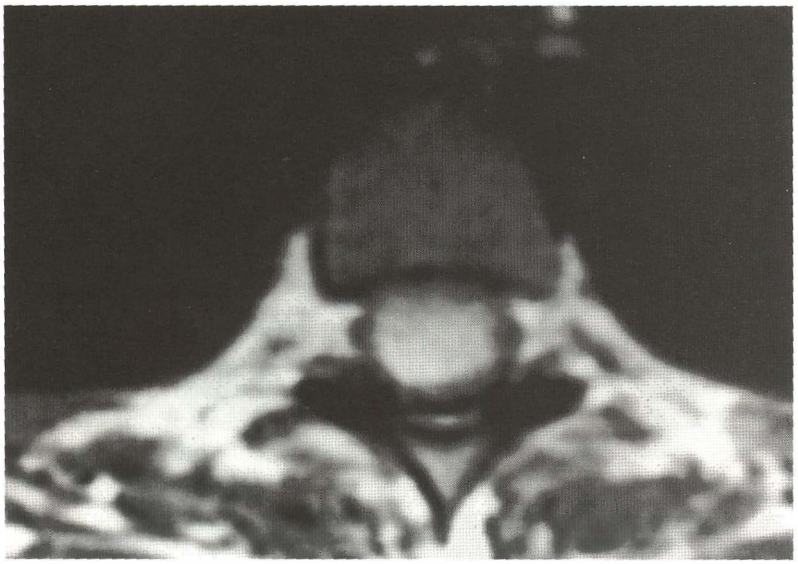

a

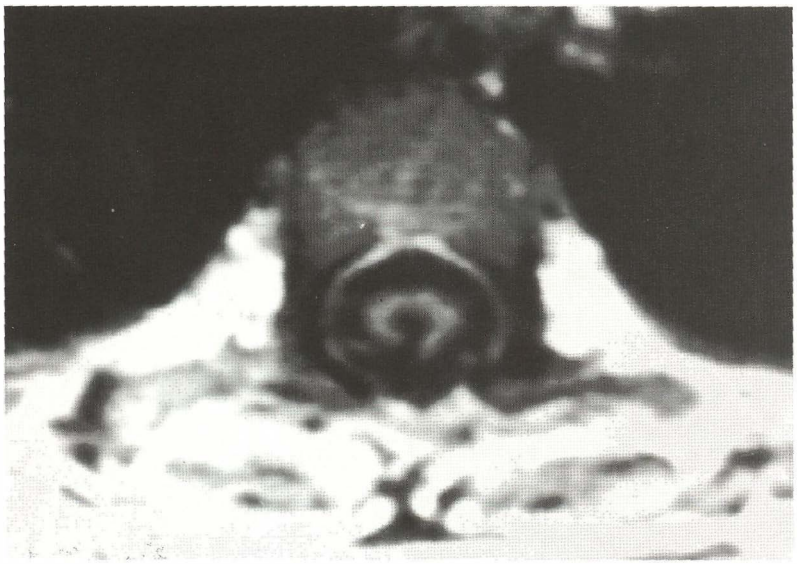

b

Fig. **25** **Topographical aspects of intramedullary tumors:** central versus eccentric position (cases *5*, *95*)
a Grade II cervical ependymoma (case *5*; same case as in Fig. **74**). Axial postcontrast T1-weighted image: homogeneous enhancement and central location of the tumor. The residual cord is hard to identify. **b** Axial T1-weighted image in the same patient after total removal of the mass. The postoperative cavity is clearly centrally located within the spinal cord
c Grade II cervical astrocytoma (case *95*). Axial gadolinium-enhanced T1-weighted image: eccentric position of a partially enhancing mass responsible for an irregular enlargement of the spinal cord. **b** Control examination one year after biopsy of this infiltrative tumor. Increased tumor volume, with a persistent eccentric position of the tumor

Fig. **25c**

Fig. **25d**

Signal characteristics. MRI allows solid and cystic portions of the tumor to be distinguished, and demonstrates the presence or absence of edema and signal changes after contrast injection.

Solid portions. Most IMTs are hypointense or isointense on T1-weighted images, and isointense or hyperintense on T2-weighted images. These signal abnormalities are generally well-defined, and may have either a homogeneous or heterogenous appearance. The presence of a clear hyperintensity on a T1-weighted image suggests the presence of subacute blood (3–5 days and up to one month after bleeding). Thus, MRI can be used to confirm the diagnosis of intramedullary spinal cord hematoma (Fig. **33**). An area of signal loss on T2-weighted images, more apparent on T2*-weighted images, especially with high magnetic fields, and more or less well defined on T1-weighted images, reflects the presence of hemosiderin, characteristic of the presence of chronic blood (several months or years). An absent signal at both poles of the solid part of the tumor presents a "cap-like" appearance (14), and has been correlated histologically and intraoperatively with areas of chronic hemorrhage. Although this finding is not pathognomonic, we observed it in 30% of ependymomas (Fig. **26**) and 12% of hemangioblastomas, but in

no cases of astrocytoma. Small intratumoral hypointense areas on T1-weighted and T2-weighted images might suggest calcifications, but we have never encountered this finding. Intratumoral hypointensity is best interpreted as representing flow void phenomena corresponding to intratumoral vessels.

Cystic portions. Cysts associated with the solid portion of the tumor are a common observation (93, 232, 276, 287). Several types of cysts should be distinguished. Intratumoral cysts have a signal that is usually different from cerebrospinal fluid, since it is rich in protein, or contains blood. They are characterized by a decreased signal on T1-weighted images and an increased signal on T2-weighted images, amplified on successive echoes. Their contours are usually well-defined, and their walls are enhanced after injection of contrast (Fig. **57**).

Polar cysts, also called satellite cysts, may be present at the upper and lower poles, on either side of the solid tumor. The signal intensity is similar to that of cerebrospinal fluid, i.e., decreased signal on T1-weighted images and an increased signal on T2-weighted images. However, it may sometimes vary slightly, with a less marked T1 decreased signal compared with that of the cerebrospinal fluid (Fig. **55**). These cysts appear to be under tension, and are often rounded at both ends, with walls that do not enhance with contrast injection. The ends of hydrosyringomyelic cavities associated with an IMT (8, 83) are often filiform, and may coexist with a satellite cyst with which they do not visibly communicate. They also appear to be under tension, and may sometimes display spectacular haustra (Fig. **27**), whose anatomical substratum is not visible at the opening of the cavity. The walls of these cavities have no

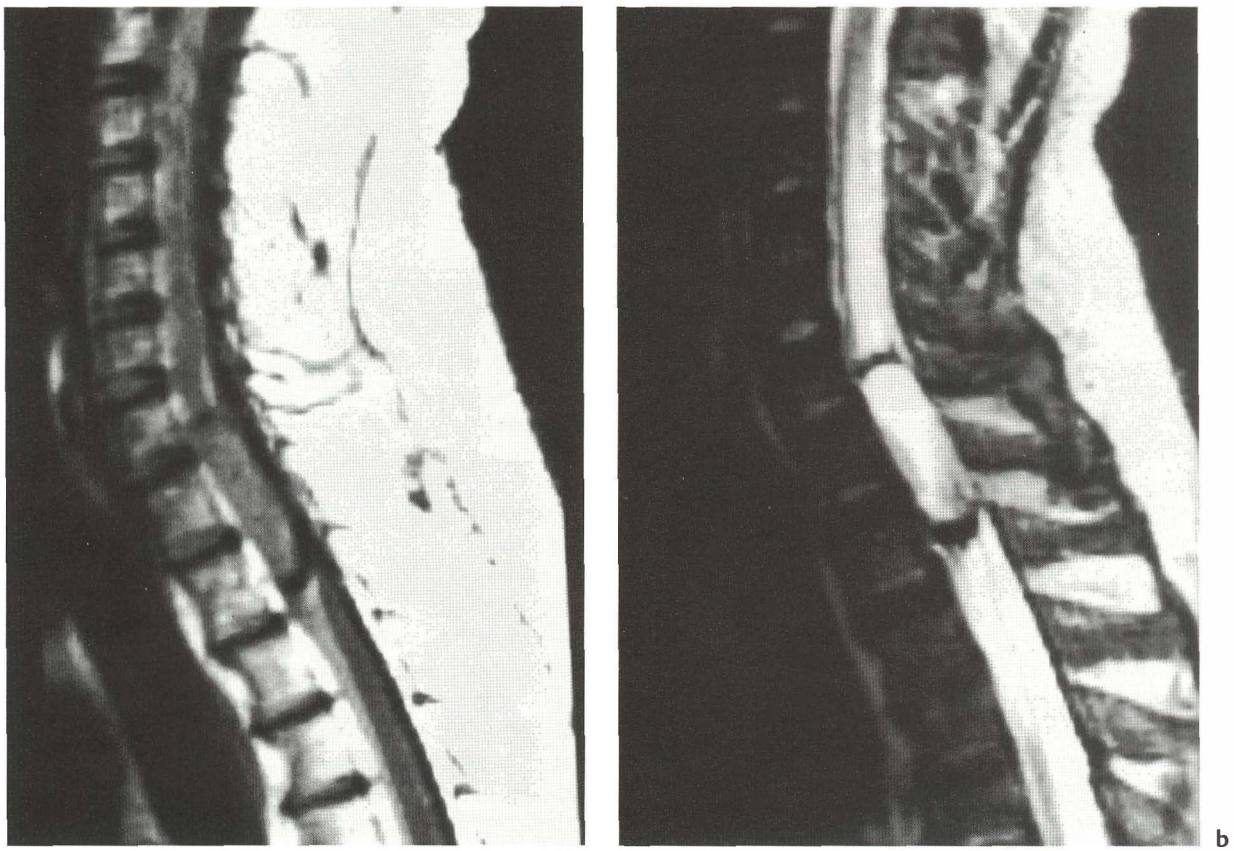

Fig. **26** **Grade II cervical ependymoma:** "cap" sign (case *42*). **a** Sagittal postcontrast T1-weighted image and **b** T2-weighted image: an oval-shaped tumor with a nonenhancing, isointense signal on the T1-weighted image and a homogeneous, hyperintense signal on the T2-weighted image. Peripheral areas of signal loss (on the T1-weighted and T2-weighted images), "capping" both tumor poles. This appearance is characteristic of old hemosiderin deposits due to repetitive hemorrhages. **c** Sagittal T1-weighted image and **d** T2-weighted image after complete removal of the tumor: at the periphery of the resection site, areas of decreased signal are still visible. Note the segmental spinal cord atrophy

Fig. **26c**

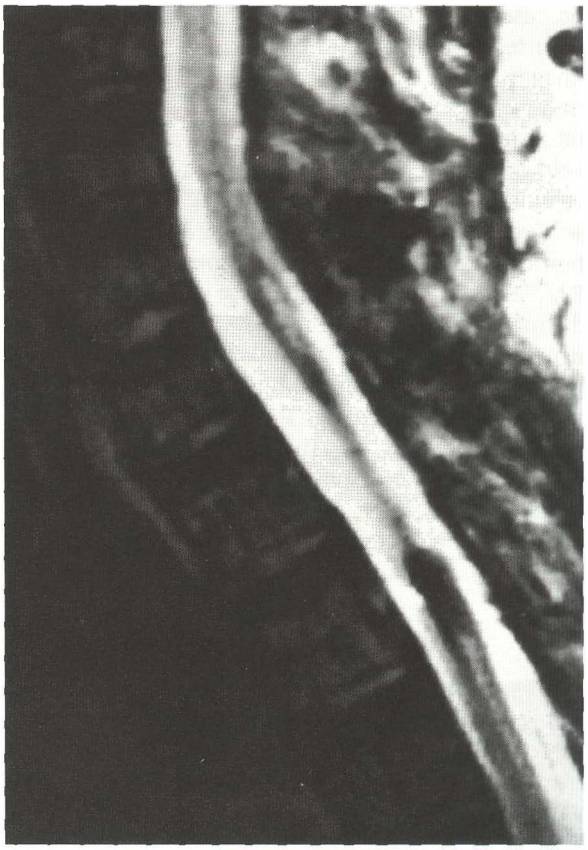

Fig. **26d**

specific characteristics, and display no signal enhancement after gadolinium injection. Such cavities, present in IMTs, may also be associated with space-occupying extramedullary spinal cord lesions.

Finally, well-defined cysts of the medulla also have a tense and convex appearance under the floor of the fourth ventricle, with the same signal as cerebrospinal fluid, and they are quite characteristic (Fig. **27**). They are located at a distance from the tumor, and may (Fig. **55**) or may not (Fig. **27**) communicate with the underlying hydrosyringomyelic cavity. After tumor removal and concurrent opening of the satellite cyst and drainage of the hydrosyringomyelic cavity, these brain stem cysts (which in fact seem to be the most rostral part of the cavitation process) regress progressively and disappear within a few months (Figs. **27**, **55**, **71**).

Peritumoral edema can best be observed on T2-weighted images as an area of hyperintensity (Fig. **75**). Peritumoral edema may be particularly extensive, especially in hemangioblastomas (Fig. **28**), and disappears after tumor removal (256).

Findings after injection of contrast medium. The behavior of lesions after contrast injection is fundamental to the imaging diagnosis. Contrast enhancement of the walls of a cyst indicates the neoplastic nature of the cyst (Fig. **57**). Contrast enhancement of the solid portion of the tumor may (rarely) be absent (Figs. **29**, **78**), moderately intense (frequently), or very intense (particularly in hemangioblastomas). Contrast enhancement can be partial or total, and there is no necessary correlation between the volume of enhancement of the lesion and the actual volume of the tumor itself. In fact, while contrast enhancement does suggest an area of tumor infiltration, the absence of enhancement does not necessarily mean that tumor is not present (Fig. **30**). It is important to note the homogeneity of the contrast enhancement, since enhancement is frequently heterogeneous in astrocytomas (Figs. **25**, **57**) and homogeneous in ependymomas (Figs. **25, 74, 75**). The rate at which contrast is taken up and disappears may provide clues to the histological nature of the tumor, since astrocytomas enhance more slowly and progressively than ependymomas do (198).

Diagnostic Discussion

Because of its diagnostic accuracy, MRI is the examination of choice for all spinal cord disorders, both

glial and nonglial tumors, as well as pseudotumors, some of which are quite characteristic (lipomas, cavernomas, epidermoid cysts, etc.). In other circumstances, the clinical course and laboratory findings will help to establish the relationship between an apparently nonspecific IMT image and its etiology. This is true for metastases, melanoma, lymphoma, and sarcoidosis. However, in most cases, a final diagnosis can only be established on the basis of histological findings.

In general, the *solid and cystic components of IMTs are reliably detected.* Thus, all the factors needed for decision-making and preparation of surgery are available. However, imaging has its limitations, as evidenced by discrepancies between conclusions based on MRI and surgical and histological data. MRI cannot provide a fully reliable assessment of the discrete or infiltrating nature of an IMT, nor can it accurately evaluate the histological nature of an IMT, i.e. ependymoma, astrocytoma, or another glioma.

An enlarged spinal cord or a signal abnormality is not pathognomonic of an IMT. Some extramedullary spinal cord lesions (e.g., enteric cysts, Fig. **31**) are difficult to distinguish from intramedullary spinal cord lesions when they have invaginated into the cord. Their extramedullary nature is usually recognized when MRI is performed using multiple imaging planes. However, distinguishing between intramedullary and extramedullary spinal cord tumors may be difficult in IMTs that are partially exophytic.

Nontumoral intramedullary spinal cord lesions causing spinal cord enlargement may produce diagnostic difficulties, because IMTs are nearly always characterized by an enlarged spinal cord. In practice, several diagnoses can be discussed: hydrosyringomyelia, multiple sclerosis, certain vascular malformations, and postradiation myelopathy.

The differential diagnosis between hydrosyringomyelia and IMT is difficult to establish solely on the basis of the myelographic findings, since both disorders can produce an enlarged spinal cord. CT and myelography performed 24 hours after myelography can demonstrate late opacification of an intramedullary spinal cord cavity due to syringomyelia. By contrast, MRI diagnosis of a fluid-filled intramedullary spinal cord cavity on sagittal and axial slices is quite easy. The presence of a Chiari mal-

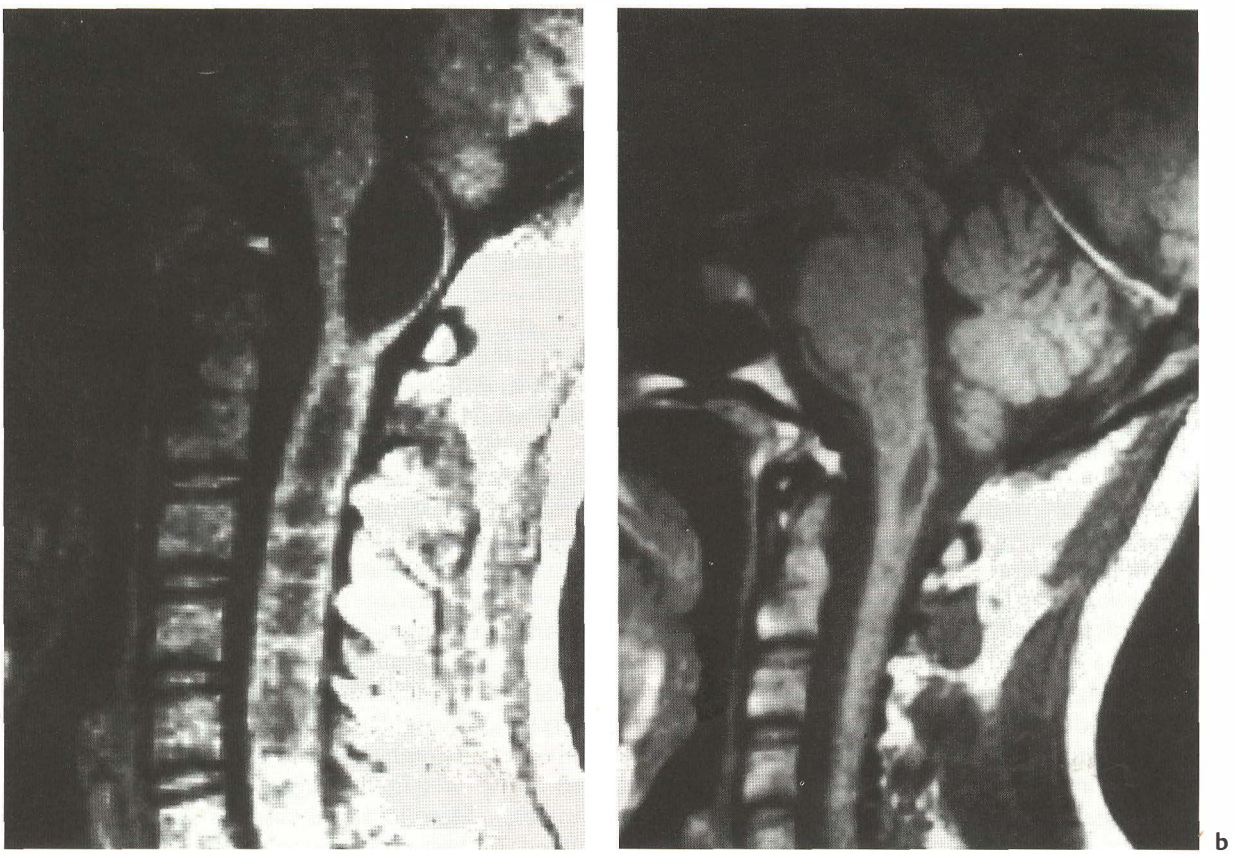

a b

Fig. **27** **Grade I holocord astrocytoma** (case *79*; same case as in Fig. **56b**). **a** Brain stem cyst at the upper end of an extensive hydrosyringomyelic cavity. **b** Postoperative regression of both the brain stem cyst and the syrinx

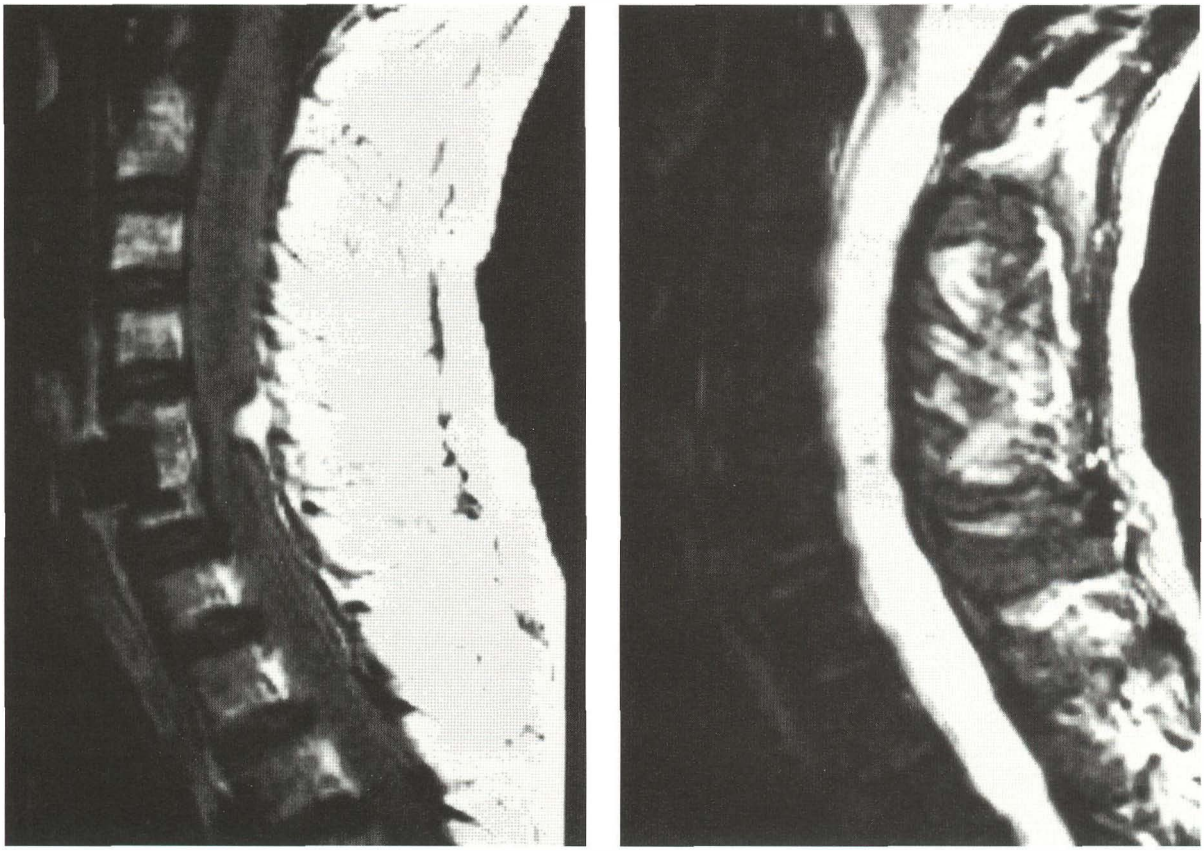

Fig. **28** **Cervical hemangioblastoma of C5** (case *127*). **a** Sagittal postcontrast T1-weighted image: extensive enlargement of a diffusely hypointense cervical spinal cord from C1 to T2, with a small, intensely enhancing nodule located posteriorly. Note the previous surgical procedure at the level of C5–C6 (Cloward). **b** On the T2-weighted image, the enlarged cervical spinal cord is hyperintense from extensive associated edema. **c** The postoperative T1-weighted image shows normal morphology and signal in the cervical cord. **d** T2-weighted image: the edema has disappeared

formation, a flow void in the cavity in a non-refocused T2-weighted image or in specific flow analysis images, and an absence of intramedullary spinal cord contrast enhancement are arguments in favor of nonneoplastic process. Conversely, the absence of a flow void is an argument in favor of a tumoral cyst.

Multiple sclerosis with isolated spinal cord symptomatology may be a difficult problem in differential diagnosis. A multiple sclerosis plaque is characterized by a localized intramedullary spinal cord signal on T2-weighted images, associated in the acute stage with a moderately focal spinal cord enlargement and contrast enhancement after injection (Fig. **32**). The clinical context, and a search for intracranial signs of demyelination on T2-weighted images (in particular an increased periventricular signal), will help to establish the correct diagnosis (140, 151). The disappearance of intramedullary spinal cord contrast enhancement a few weeks after the first MRI examination will help to confirm the diagnosis of the demyelinating disease.

An MRI signal abnormality without spinal cord enlargement is not suggestive of IMT. Images with a vascular appearance are sometimes misleading. As is the case in the brain, it is fairly easy to diagnose an intramedullary spinal cord hematoma, but the presence of hemorrhage does not exclude the possibility of an underlying tumor, and only a repeat MRI examination, at a distance in time from the bleeding episode, will avoid this diagnostic pitfall (Fig. **33**). A long serpiginous vascular structure with a nidus, visualized on myelography and MRI (particularly T2-weighted or T2*-weighted images) suggest a spinal cord angioma. More localized vascular structures can be noted in hemangioblastomas, but the latter are characterized on postcontrast MRI by a homogeneous and intense nodular enhancement.

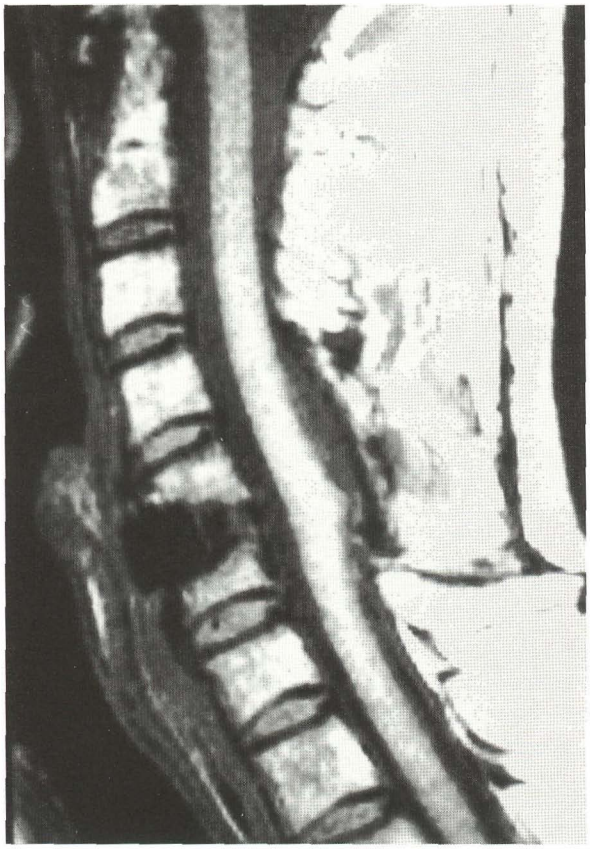

Fig. **28c**

Fig. **28d**

Dural fistulas with perimedullary venous drainage may be associated with extensive areas of T2 hyperintensity in the spinal cord, without marked increase or with moderate increase in spinal cord size. Spinal cord arteriography will confirm the diagnosis. With conventional spinal cord angiography, the diagnosis of vascular malformations is very difficult when there has been thrombosis of the malformation.

Postradiation myelopathies with focal spinal cord enhancement after contrast administration may raise difficult problems of interpretation *[273]*. A patient's history of radiotherapy applied to the suspect area, the time of onset, and the acute mode of occurrence of major neurologic symptoms, along with findings of postradiotherapy bone matrix changes, are useful in making the diagnosis. In this case, the decisive argument in favor of postradiation myelopathy is the absence of a marked increase in spinal cord size, although such an enlargement may occur during the acute phase and subsequently regress. This regression gives way to spinal cord atrophy, as a follow-up MRI examination will demonstrate.

Neuroradiological considerations with regard to the various histological types of tumor are discussed in Chapter 2 (pp. 60–84).

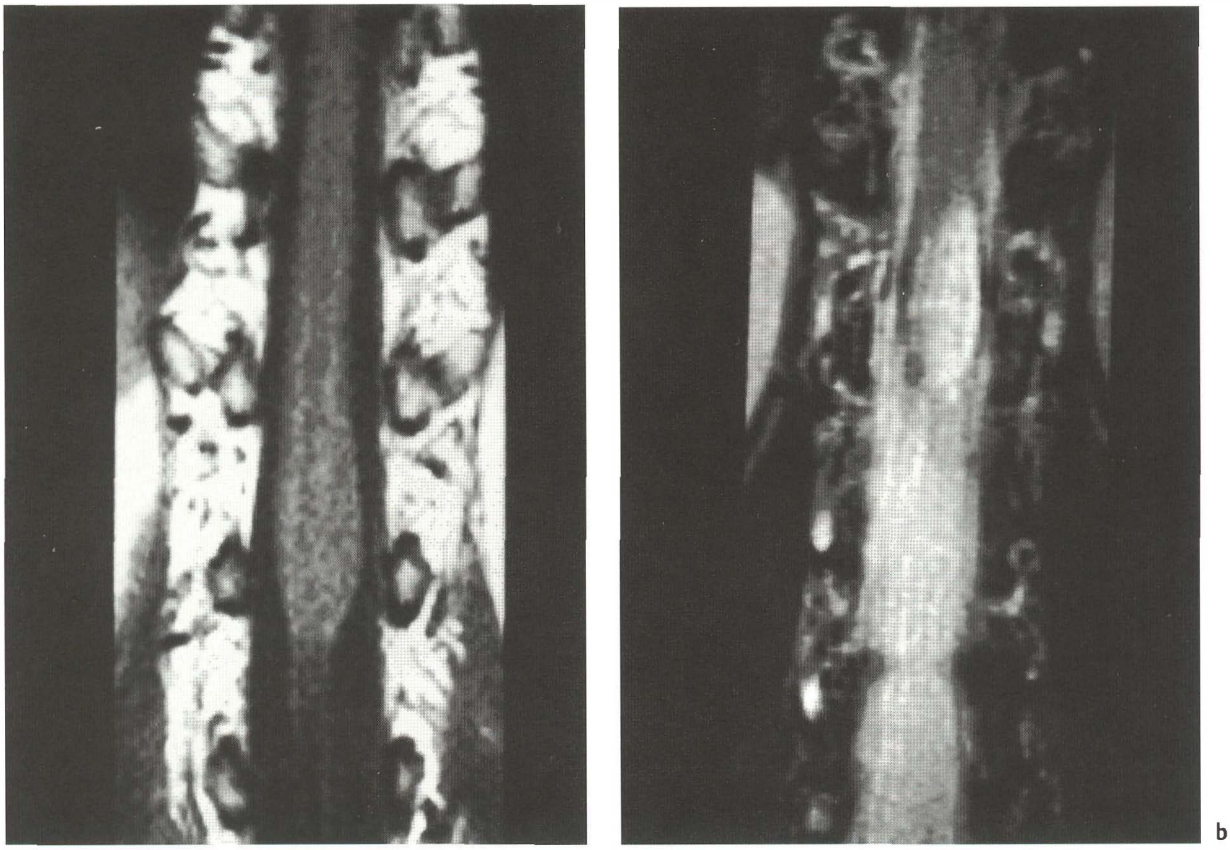

a b

Fig. **29** **Grade III astrocytoma of the conus** (case *100*; same case as in Fig. **79**). Coronal T1-weighted (**a**) and T2-weighted images (**b**). The T1-weighted image shows the morphological changes better, while only the T2-weighted image is able to demonstrate the precise tumor limits of this high-signal lesion, which did not enhance on the postcontrast T1-weighted image. **c** A sagittal T1-weighted image and **d** T2-weighted image are useful cuts that are complementary to the coronal images. **e** Axial T1-weighted image and **f** T2-weighted image. The T2-weighted image provides additional evidence of the eccentric left position of the tumor

Fig. **29c**

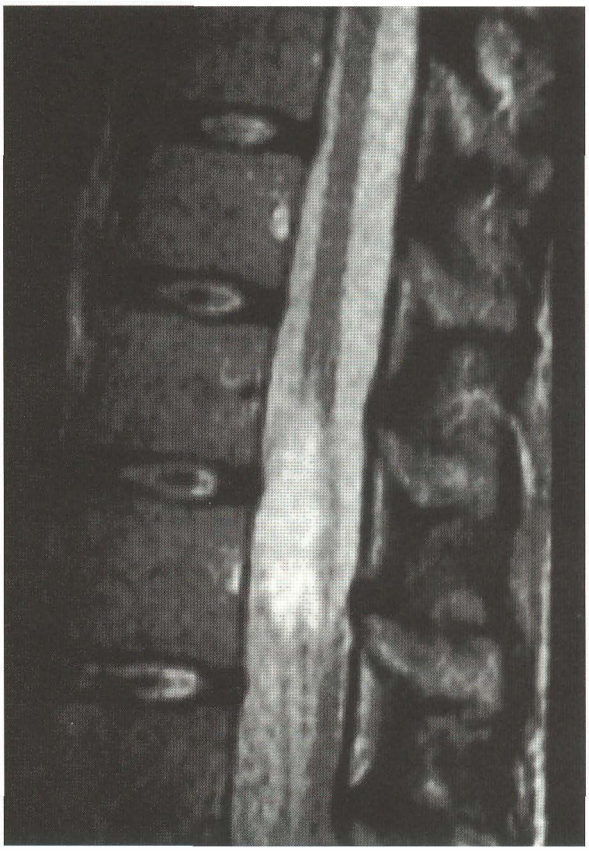

Fig. **29d**

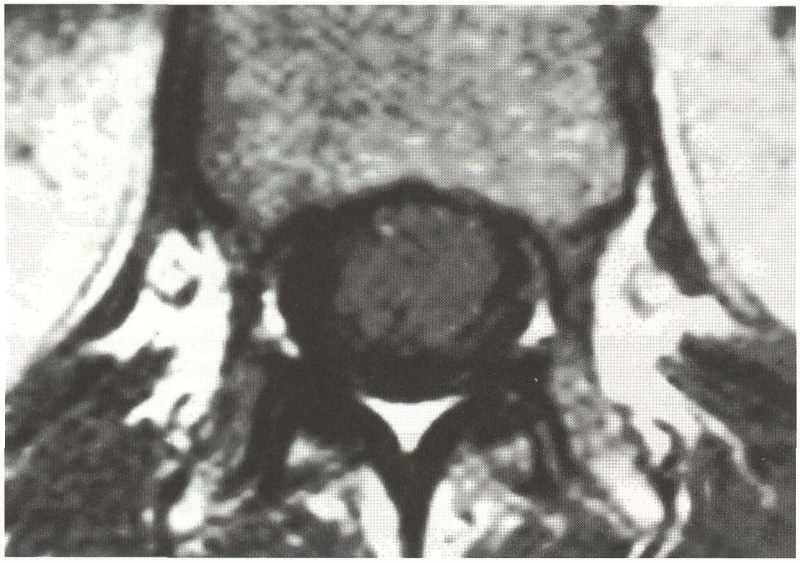

Fig. **29e**

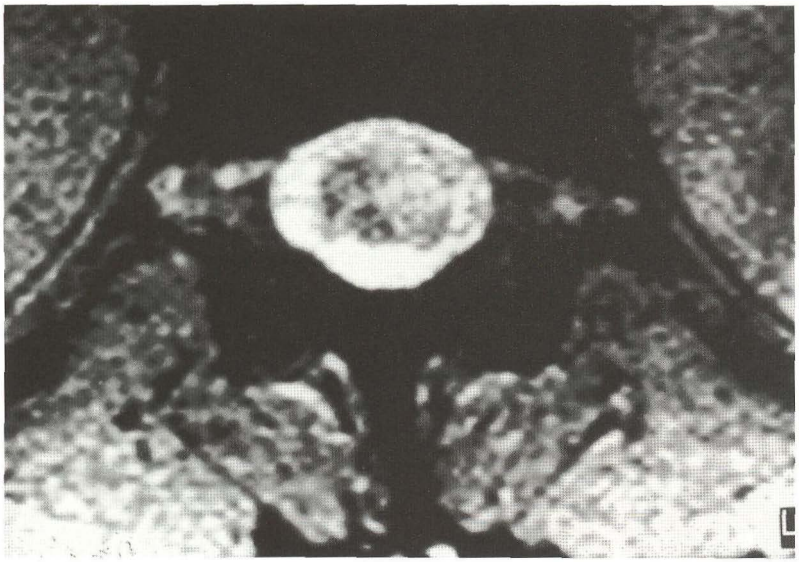

Fig. **29f**

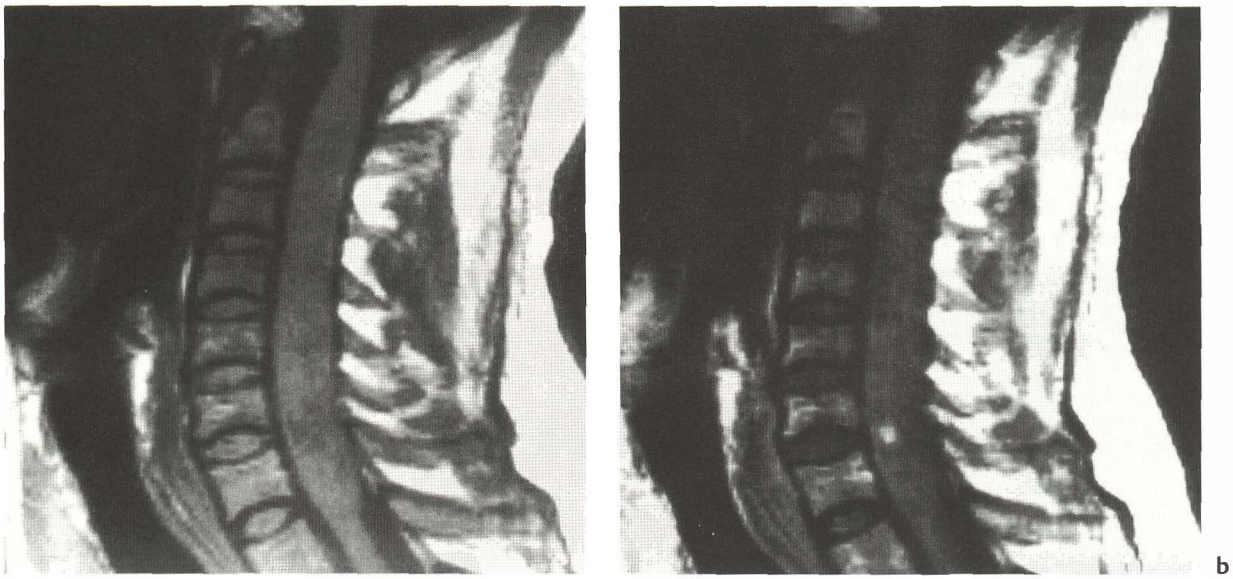

a b

Fig. **30** **Nodular contrast enhancement in a cervical subependymoma** (case *64*).**a** Sagittal T1-weighted image: diffuse widening of the cervical spinal cord. The tumor infiltration has ill-defined borders, and shows a heterogeneously hypointense signal. **b** On the postcontrast sagittal T1-weighted image, only a small nodular enhancement is seen within the lower part of the tumoral mass

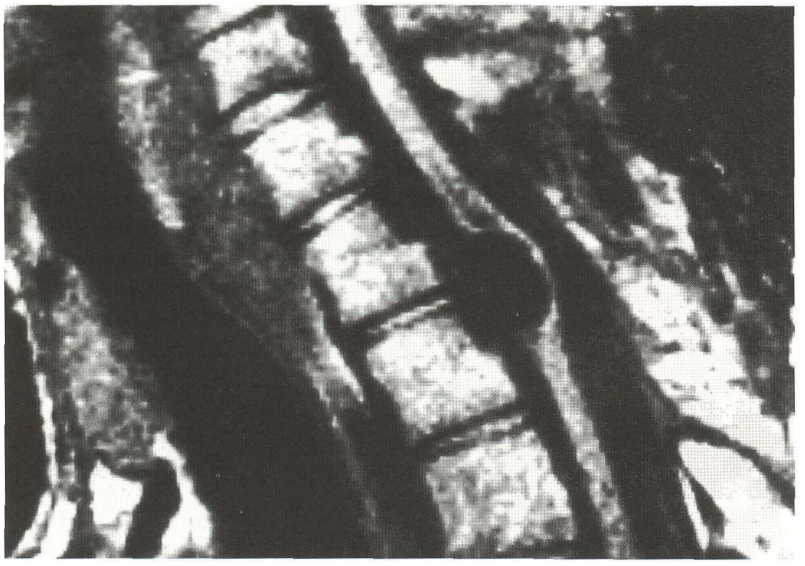

a

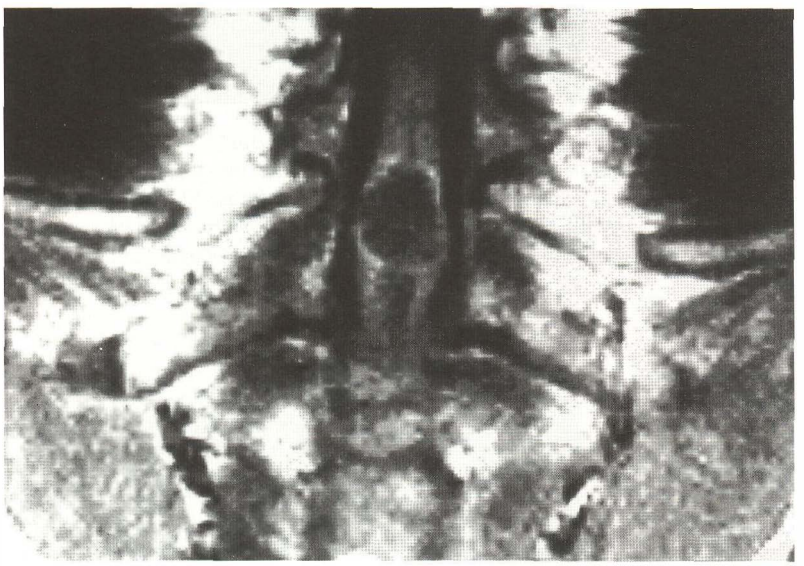

b

Fig. **31** **Enteric cyst. a** The sagittal T1-weighted image and **b** coronal T1-weighted image show a cystic lesion, anteriorly located within the spinal cord at the cervicothoracic level. A small syrinx is seen at the upper pole of the lesion. The extra-axial position of this mass may be suspected because of the border between the anterior aspect of the spinal cord and the upper pole of the lesion (courtesy of Prof. J.-C. Froment)

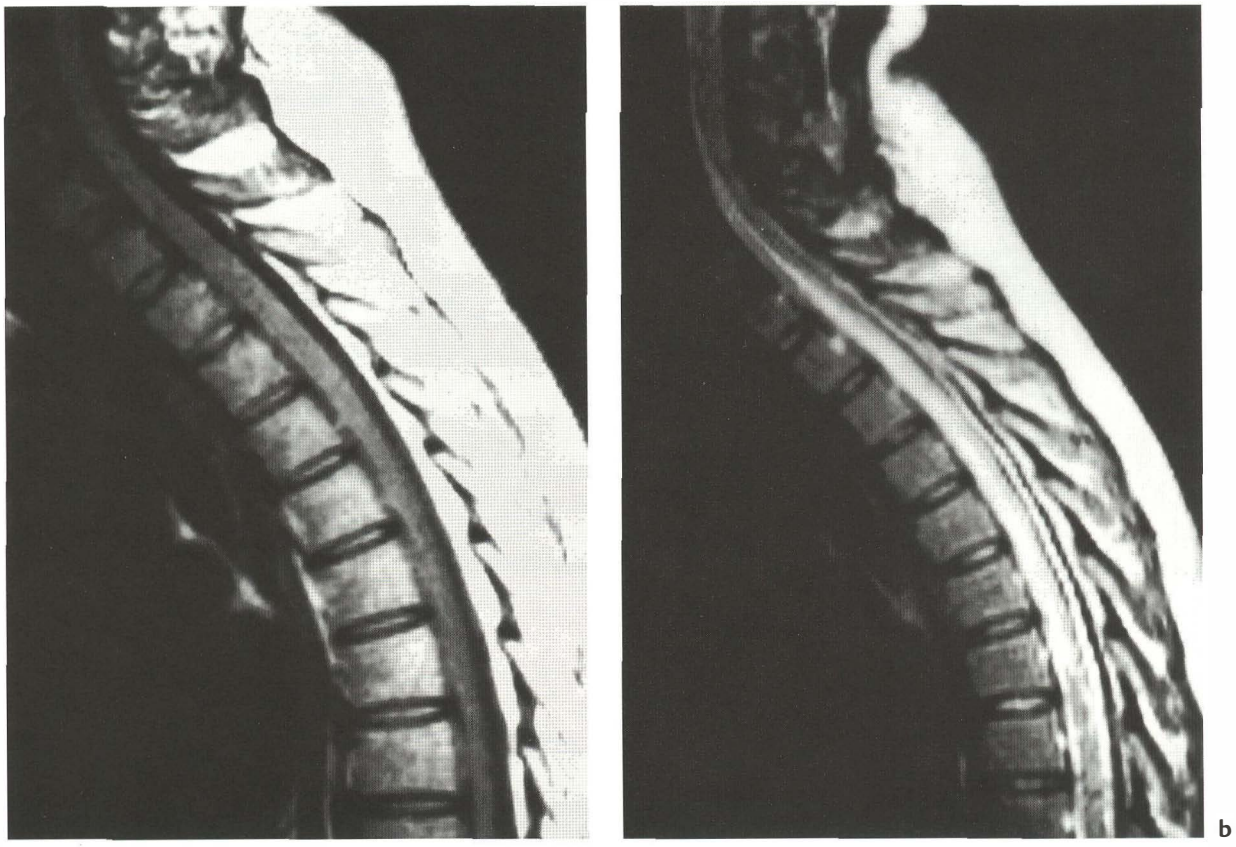

Fig. **32** **Multiple sclerosis. a** Sagittal T1-weighted image, **b** T2-weighted image, and **c** postcontrast T1-weighted image: a very slightly expanded upper thoracic spinal cord. There is an isointense signal on the T1-weighted image, and a hyperintense signal on the T2-weighted image. Well-delineated nodular enhancement is seen on postcontrast T1-weighted image. **d** The eccentric position of the lesion is best demonstrated by the axial postcontrast T1 images. Minimal cord enlargement and absence of cysts are strong arguments in favor of a demyelinating disease. **e** A brain MRI must be carried out to look for cerebral lesions (courtesy of Prof. D. Balériaux)

Fig. **32c**

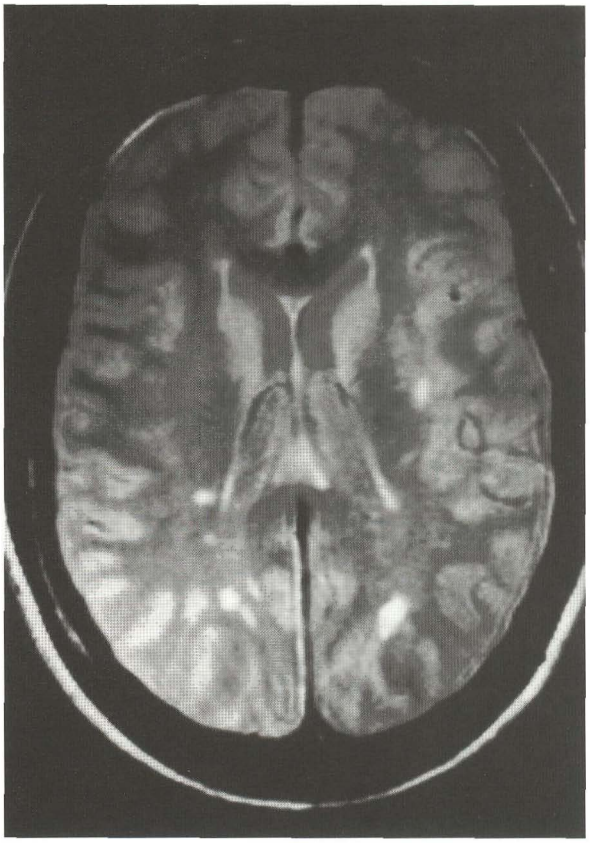

Fig. **32e**

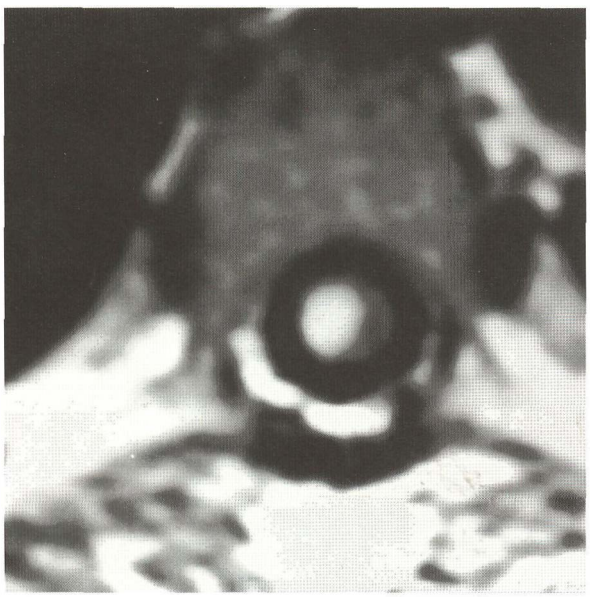

Fig. **32d**

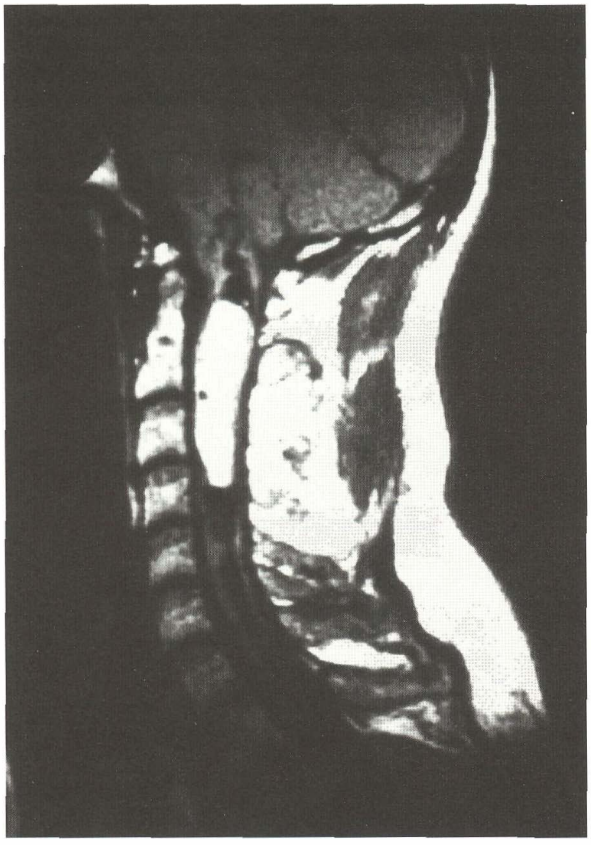

a

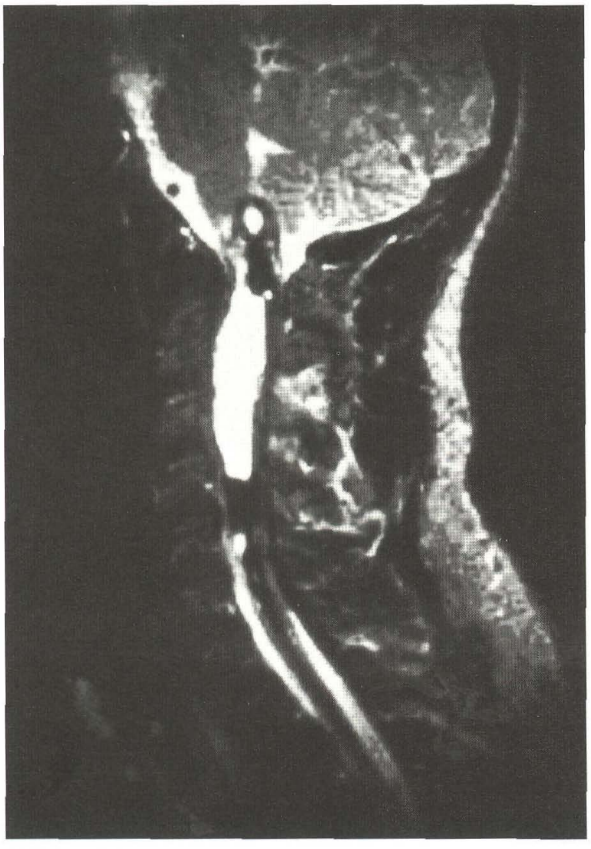

b

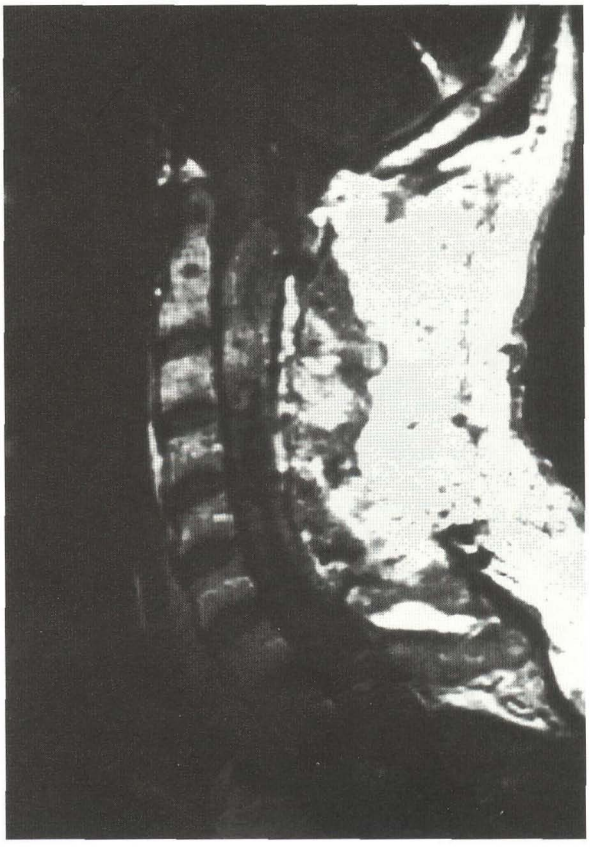

c

Fig. 33 **Intramedullary hemorrhage in an ependymoma** (case *41*). **a** Sagittal T1-weighted image and **b** sagittal T2-weighted image: a well-circumscribed intramedullary mass with a hyperintense signal on both MR sequences. This signal behavior suggests subacute hemorrhage (methemoglobin). In addition, note the hypointense signal loss "caps" at both poles of this mass lesion, suggesting chronic iron deposition (hemosiderin). **c** Postcontrast control MRI performed after surgical drainage of the hematoma: enhancement of the wall of the residual cystic component suggests the presence of a tumor

1.3 Surgery (Figs. 34 – 53)

J. Brotchi, G. Fischer, O. De Witte, J. Noterman, J. Remond, T. Rizk

The aim of the neurosurgeon has always been to achieve complete removal of an IMT without causing damage to the spinal cord. The improvement of diagnostic tests, the development of new operative tools, and technical advances in perioperative monitoring have largely contributed to the improvement of surgical results. The surgical strategy is determined by analyzing the MRI data in three planes. It is essential to define the limits of the tumor's solid portion, as this will determine the extent of the laminectomy. It is also essential to localize the lesion within the spinal cord with regard to its lateralization and depth. Some extensive or multiple lesions may be treated with two separate surgical procedures. This was the case for nine of our patients *[2, 8, 10, 50, 52, 55, 130, 143, 148].* In other circumstances, deliberate or inadvertent partial removal may justify further removal at an early or later date: nine patients in our series *[25, 40, 45, 57, 60, 70, 85, 100, 102].* Finally, a second operation may be warranted by early or late recurrences: nine patients in our series *[24, 32, 76, 92, 103, 108, 110, 119, 120],* including six presenting with a malignant tumor. In addition, four patients with recurrent tumors were referred to us for a second or third operation *[47, 89, 93, 121].*

Operative Position

The patient is placed prone on bolsters, freeing the thorax and abdomen from any pressure. This is the most widely used position for all tumor locations. The sitting position may be used for cervical lesions, provided suitable steps are taken by the anesthesiologist to minimize the known risk of air embolism (231), as described in our previous work (77). In both positions, immobilization can be achieved with a three-point head fixation to prevent inadvertent cervical flexion and to prevent pressure sores on the face. The kneechest position is contraindicated because of the risk of myoglobinuria and rhabdomyolysis during lengthy procedures (153). When SEP monitoring is established, electrode placement should be checked at this stage of the procedure.

Surgical Procedure

A midline incision is made, centered at the level of the lesion but extending above and below it, cutting across the raphe and allowing symmetrical retraction of muscular masses.

Bone removal should provide sufficient access to the solid part of the tumor. As a rule, it is recommended to expose one additional vertebra above and below the tumor. This step is delicate (more so than is usually believed), whether laminectomy or laminotomy is performed. Laminectomy, if carried out gently and patiently with removal of small pieces of bone, avoids any damage to the adjacent spinal cord. It is less hazardous to use a fine straight bone rongeur rather than a laminectomy cutting top rongeur. A small rongeur is necessary for the lateral aspect of the laminectomy, as the lateral masses must be preserved and can only be approached obliquely.

Pediatric surgeons favor laminotomy (64, 212). However, we think the craniotome and the oscillating saw are too dangerous adjacent to the spinal cord and the nerve roots. Along with Raimondi (212) and Di Rocco et al. (54), we prefer to perform cautious drilling, under visual control, using a small (1.5 mm) diamond burr. In infants, one can perform a unilateral incision of the soft tissues, and unilateral laminotomy is possible. The contralateral laminae bend in the fashion seen in greenstick fractures and act as a hinge, allowing the muscle mass to be rotated to the contralateral side.

Hemilaminectomy, proposed for small, mainly extramedullary spinal cord tumors (291), is inappropriate for surgery of intramedullary spinal cord tumors, since midline exposure is required. However, when an extensive laminectomy or laminotomy has to be performed, we recommend the preservation of one posterior arch every five to six vertebrae. It is possible to work underneath it, and it is of great assistance in the fixation of the laminotomy or for the stabilization of the spine.

Hemostasis in the epidural space requires as much care as that in the soft tissues. At this stage, intraoperative ultrasonography is helpful in locating solid and cystic areas, especially when MR imaging has not provided enough information.

Opening of the dura can be performed with or without the microscope, without opening the arachnoid. Dural suspension by simple traction sutures is sufficient, and suspension from muscles allows better access to bone opening.

The arachnoid is opened separately, when possible, with microscissors, particularly when one intends to close it. The SEP electrode is then placed on the dorsal columns and maintained in this position without applying pressure.

The spinal cord is then visualized, enlarged and swollen, smooth and tense, more or less vascularized, and sometimes discolored. Gentle evaluation of its firmness will confirm the location of solid and cystic areas. High-powered microscopic magnification will allow localization of the dorsal median sulcus, which

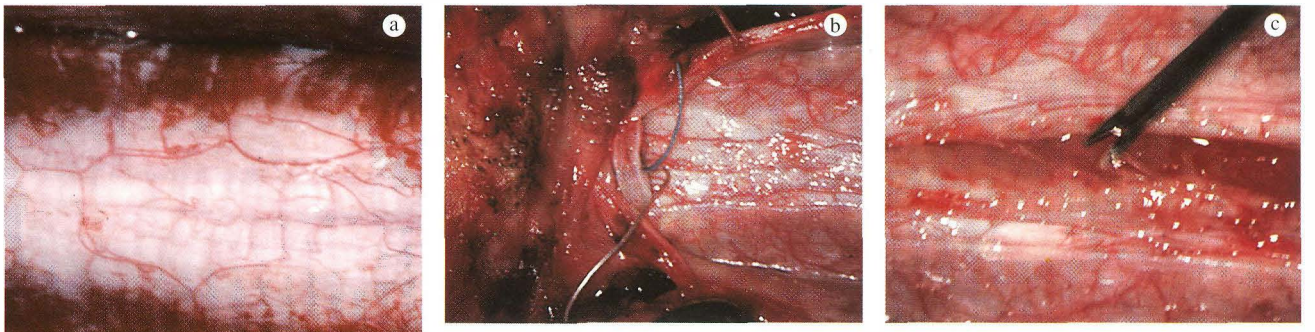

Fig. **34** **C2 – T1 grade II ependymoma** (case *23*). **a** Widened spinal cord. **b** Recording electrode held in position by a cottonoid pledget above the tumor. **c** Tumor biopsy. **d** Debulking with the CUSA, showing a normal spinal cord. **e** Tumor bed. **f** Pial suture

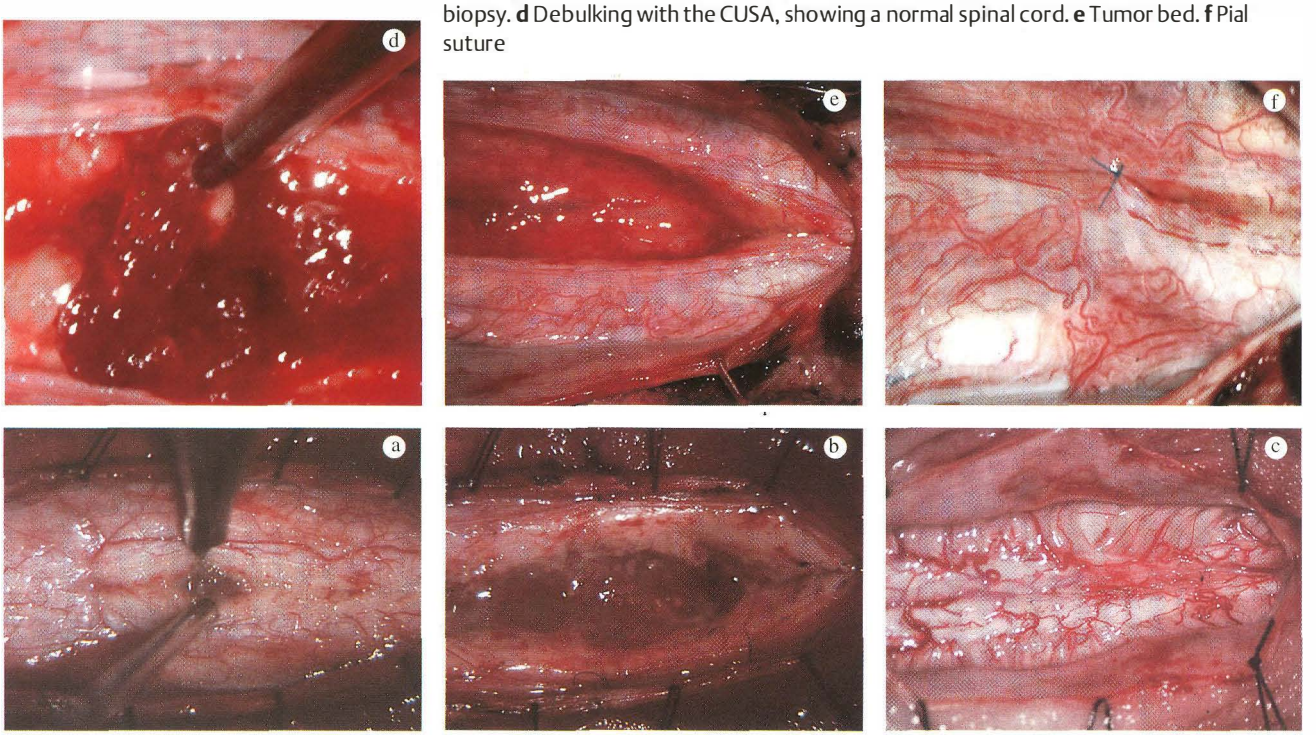

Fig. **35** **C2–T2 grade II ependymoma** (case *28*). **a** Opening of the posterior sulcus. **b** Opened spinal cord and tumor. **c** Closed and sutured spinal cord after tumor removal

appears as a distinct median raphe, over which the very tortuous posterior spinal vein runs. Sometimes, this sulcus is identified only by the convergence of vessels toward the midline. More rarely, the location of the midline has to be evaluated in relation to the posterior roots on either side, but this may prove impossible owing to the asymmetrical distortion of the cord or the adherence of the posterior columns. In such cases, the midline is identified above and below this region, and then the two openings may join.

The term "myelotomy" is inappropriate, as the spinal cord is not incised but opened by spreading the dorsal columns apart. The use of the laser cannot meet this requirement (24), and we disagree with those authors who recommend laser myelotomy (40, 65, 67, 107, 269). In our view, the midline surgical approach is an absolute rule, with one exception: when the lesion is located in one dorsal column and is apparent on the surface without any cortical "mantle." Only the finest surgical instruments suited for neurosurgery are used: microdissectors or spatulas, microforceps, microaspirator, cottonoids moistened with saline at 37 °C.

The vessels of varying size running vertically over the dorsal columns are dissected and mobilized laterally to expose the posterior sulcus, sacrificing the smallest number of vessel branches bridging the two columns and trying to spare all the

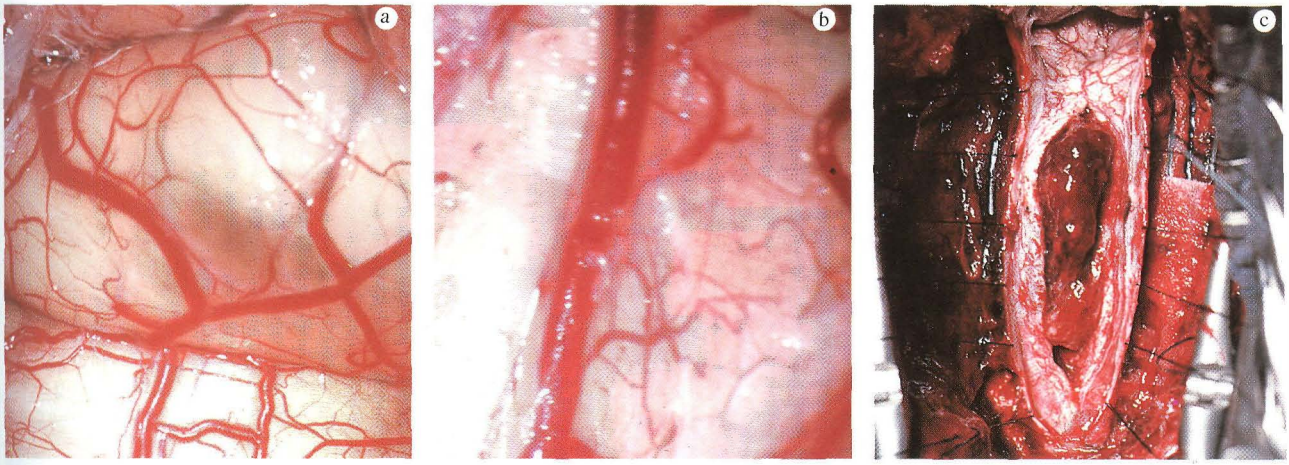

Fig. **36** **C2–C7 grade II ependymoma** (case *3*). **a** Superior satellite cyst. **b** The medial posterior sulcus is clearly identified under high magnification. **c** Removing the tumor

thinnest arterial or venous vessels in the sulcocommissural region. The dorsal columns are carefully retracted and opened gently and progressively over the entire length of the solid portion of the tumor, as if they were pages of a book. This maneuver is continued to expose the rostral and caudal cysts, if present.

The opening of the spinal cord must allow exposure of the poles of the lesion and evaluation of the cyst walls, but should not extend further than this. Depending on the clinical circumstances, analysis of the clear or xanthochromic content of the cyst may be useful, particularly in patients with suspected metastasis.

Pial traction suturing improves the surgical exposure and reduces the severity of repeated trauma due to dissection. At the same time, it exerts a continuous traction effect that alters the monitored evoked potentials. This is not surprising when one uses pial suspension sutures with as much tension as shown in some illustrations in the literature (41, 68, 253). This type of suspension lifts and retracts the spinal cord as much as it does the dura. Concern with the functional state of the dorsal columns is the same when no suspension is achieved using Elsberg's method (61), or when the spinal cord is simply opened, without exerting traction, as was recommended by Malis in 1978 (153). This can be accomplished using a 6–0 suture without tension to hold the median pia mater and the dura mater close together, instead of using suspension with sutures and weights at the ends of the sutures.

The first surgical maneuver consists of exposing a sufficient portion of the tumor to perform a biopsy with forceps and scissors, without coagulation. This is followed by immediate histological examination, while careful hemostasis is carried out before proceeding with surgery. This examination sometimes provides the surgeon with no information at all, e.g., when everything is obvious on visual inspection. More often, however, it provides a great deal of information, e.g., when the limits between the tumor and the spinal cord are not immediately clear. Any information suggesting an infiltrating or malignant tumor, or both, can be crucial in deciding whether tumor removal should be continued or not.

At the same time, it is essential to look for a cleavage plane. Both the surgeon and the histologist can detect this (Fig. **54b**), and its discovery is crucial. Finding the cleavage plane makes tumor removal possible, and if it is not found, the decision on whether to remove the tumor must be deferred. However, in both cases, the surgeon begins by reducing the volume of the tumor using the Cavitron ultrasound aspirator (CUSA*) after setting the suction and vibratory force to a suitably low level, because of the fragility of the location; the pulsed mode provides further safety. Some authors carry out this operation using the laser (40, 67, 107), also using it to vaporize the tumor (63). We have tried this technique, but no longer use it because the laser blackens the tissues, thus changing the color of the tumor and eliminating the basic criterion needed to distinguish between tumor and healthy tissue (24).

Intratumoral resection is performed from inside to outside, and this is sometimes facilitated by the presence of a cyst or an intratumoral hematoma. After strict control of hemostasis, dissection can be started. The danger of arterial injury is located anteriorly, especially in the thoracic region, the vascular territories of which are extremely precarious. Dissec-

* CUSA VALLEYLAB Inc, P.O. Box 9015, Boulder, CO 80301, USA.

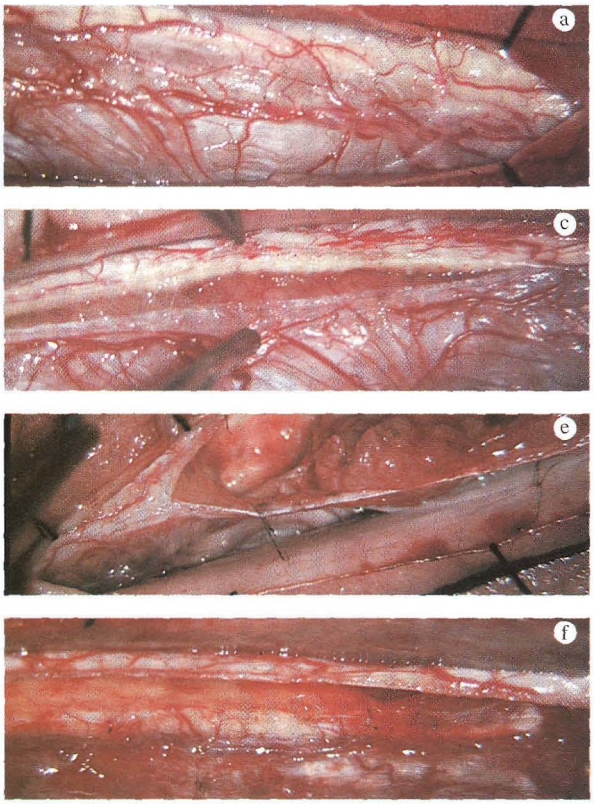

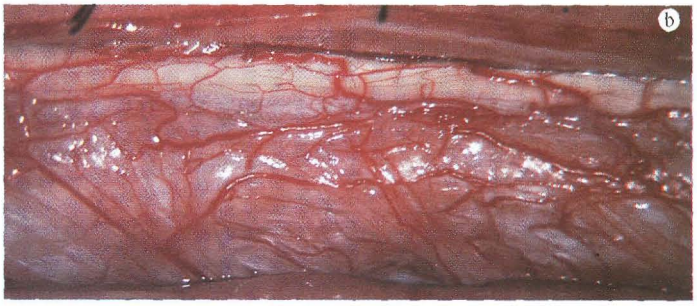

Fig. **37** **C4–T4 grade II ordinary astrocytoma** (case *87*). **a** The tumor involves the left part of the cord. **b** There is a well-defined limit between the tumor and the right normal spinal cord. **c** Discovering a clear-cut cleavage plane. **d** Debulking with the CUSA. **e** Normal spinal cord is seen after gross total removal of the tumor (**f**)

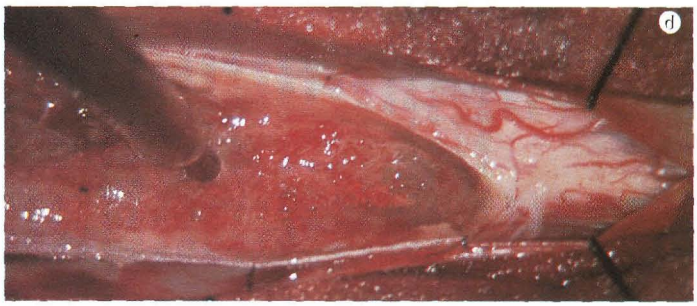

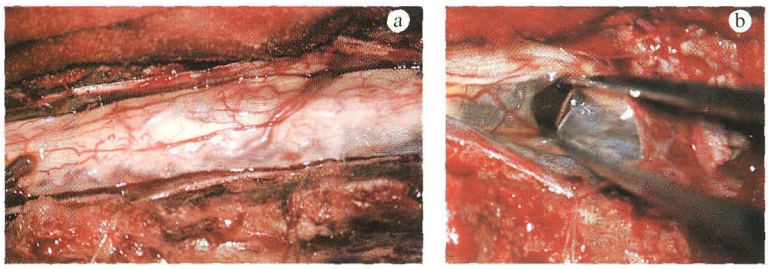

Fig. **38** **Grade I holocord pilocytic astrocytoma** (case *79*). **a** An inferior cyst close to surface of the cord. **b** Opening of the cyst

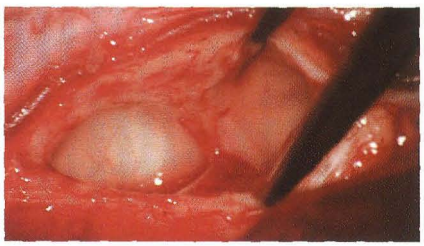

Fig. **39** **Grade II holocord ependymoma** (case *4*). Opening of the inferior cyst with translucent, nontumoral walls

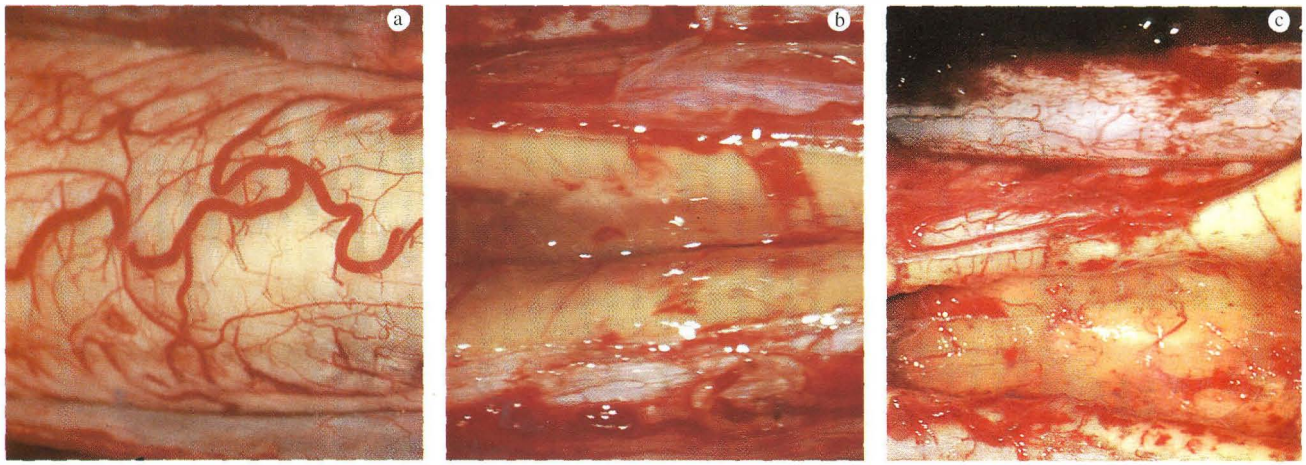

Fig. **40** **Grade II ordinary astrocytoma of the conus:** recurrence after two surgical procedures and radiotherapy (case *93*). **a** Widened spinal cord. **b** A cleavage plane is seen. **c** Gross total removal of the tumor

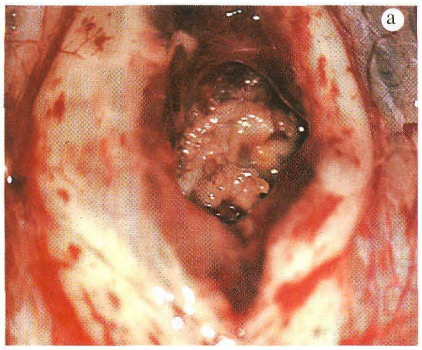

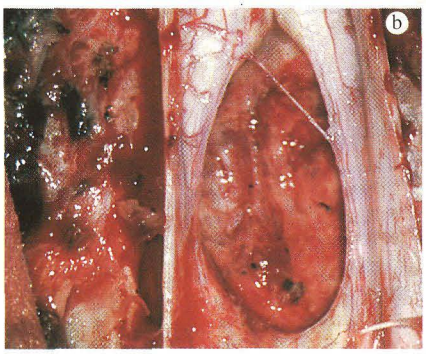

and the histological examination
s. Realizing the difficulties involved
;liosis from glioma, we never again
opsies, and have never had cause to
ɔ. McCormick et al. (169) share our
longer biopsy the cyst walls of
he wall of the cyst is thick, it should
with the tumor and considered as
cyst; intraoperative histological
elp in making this decision.
emoval, the dorsal columns are
al traction and brought together

Fig. **41** **C4 grade II ependymoma** (case *48*). **a** A wide tumor limited to one level. A small bud is still in place. **b** Complete removal. **c** Tumor bed

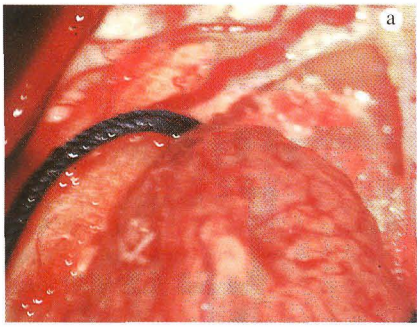

Fig. **42** **C4–T3 grade II ependymoma** (case *44*). **a** Dissection of the superior pole. **b** Tumor feeding branch (arrow) of the anterior spinal artery

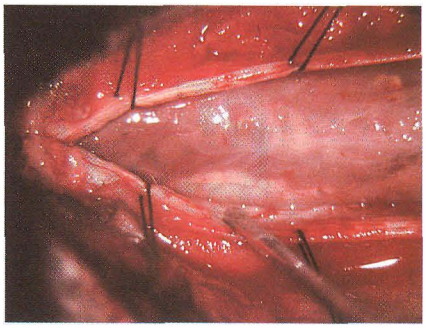

Fig. **43** **Grade II holocord ependymoma** (case *50*). An exophytic tumor lying on the cervical cord

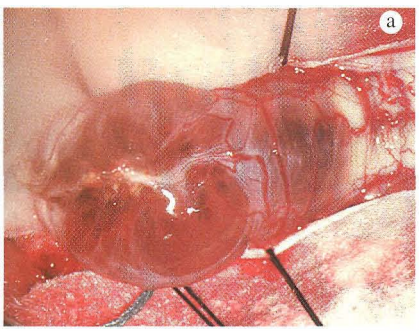

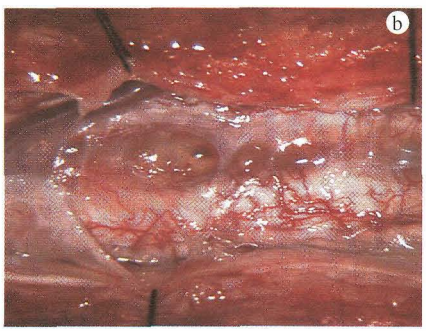

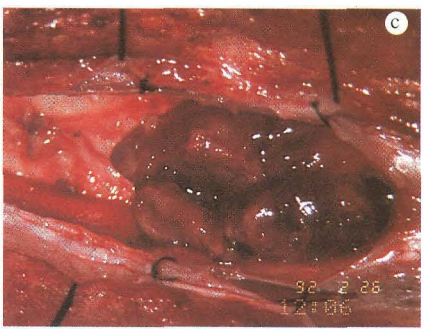

Fig. **44** **T10–L2 grade II ependymoma** (case *40*). **a** Cystic tumor of the conus. **b** Repeat surgery two years after incomplete removal. The midline and the margins of the tumor were difficult to identify. **c** Removal the tumor, which is to be complete

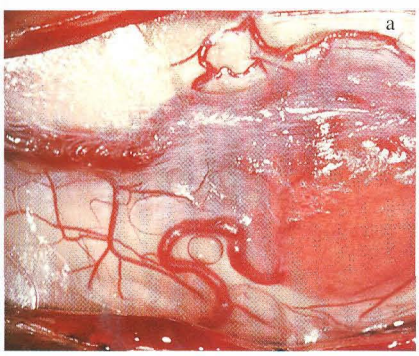

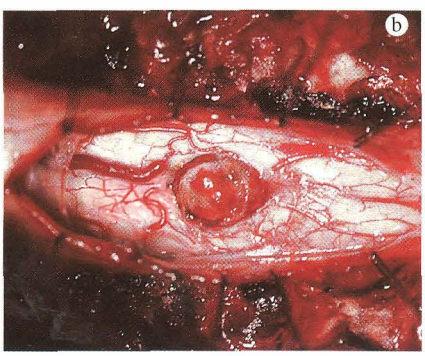

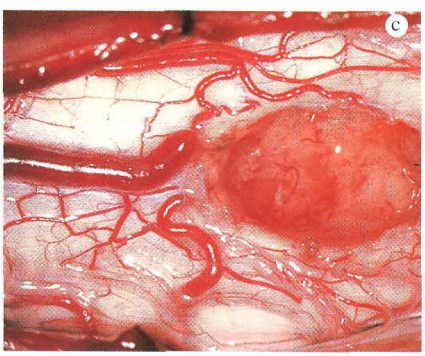

Fig. **45** **C2–C3 hemangioblastoma** (case *139*). **a** Left predominantly intramedullary spinal cord tumor. **b** Disconnected tumor. **c** En bloc removal

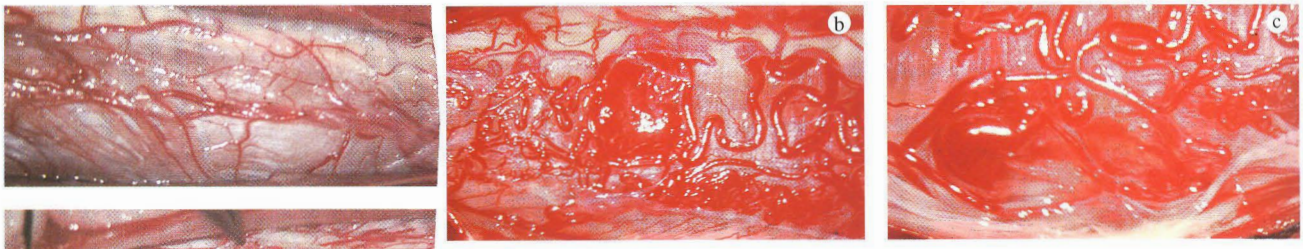

Fig. **46** **C4–C6 hemangioblastoma** (case *130*). **a** A large posterior vascular tumor. **b** Pseudoaneurysmal ectasia. **c** Left tumor limit. **d** Right tumor limit. **e** En bloc removal. **f** Tumor bed

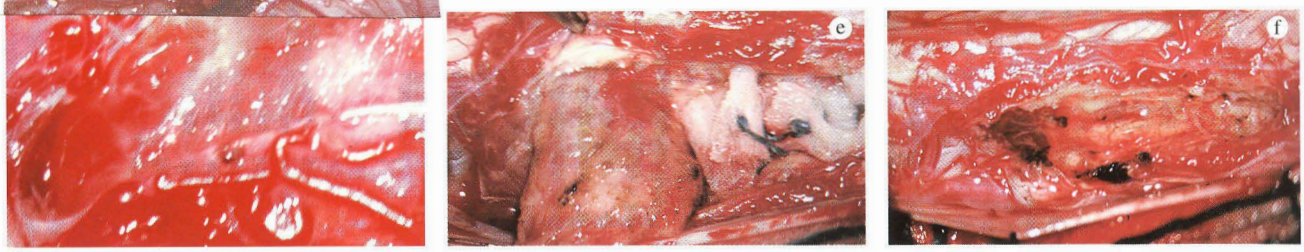

Fig. **47** **C3–C7 extra-axial intra-axial schwannoma** (case *154*). **a** Exophytic part and limit between the extra-axial and intra-axial parts of the tumor. **b** The removed tumor is held near its spinal cord attachment

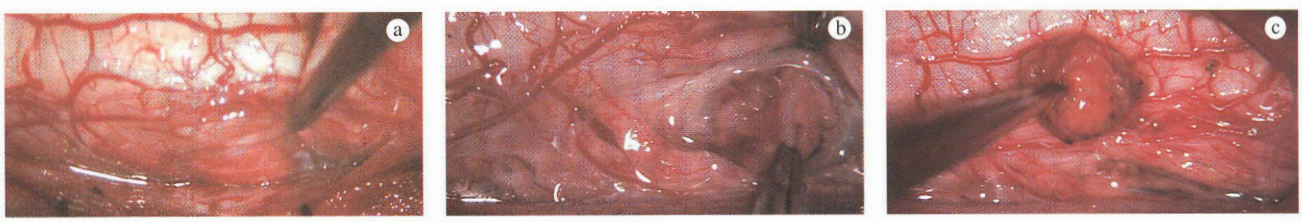

Fig. **48** **T8 hemangioblastoma** (case *125*). **a** A small right lateral intramedullary spinal cord tumor. **b** En bloc removal. **c** Tumor bed

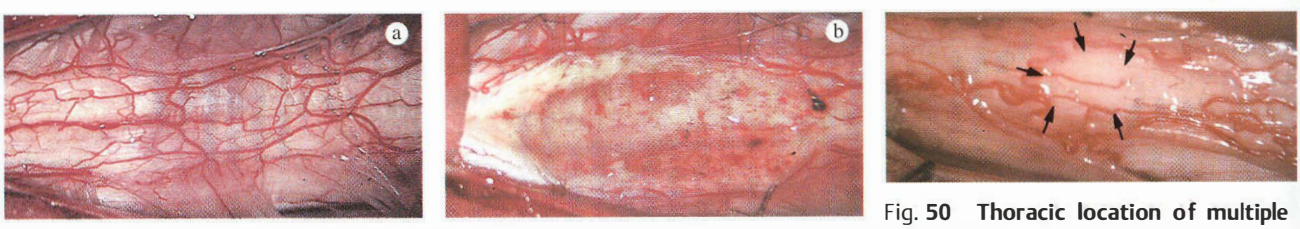

Fig. **49** **C3–C4 intraspinal cord sarcoidosis** (case *168*). **a** Widened spinal cord. **b** Large biopsy of the sarcoid granuloma

Fig. **50** **Thoracic location of multiple sclerosis.** Superficial localized pseudotumor (arrows)

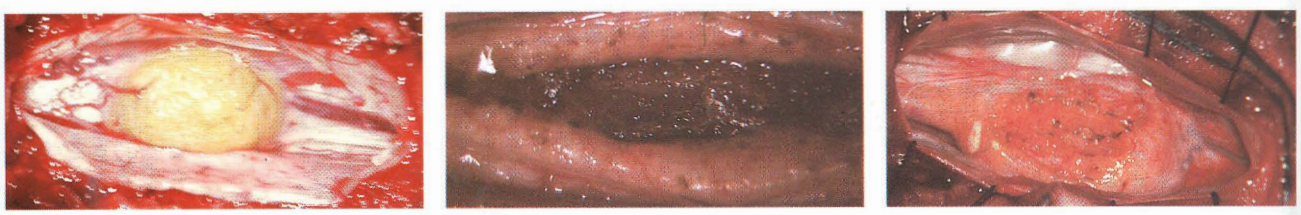

Fig. **51** **T12 extraspinal-intraspinal cord lipoma** (case *150*)

Fig. **52** **C2–C5 intraspinal cord melanoma** (case *120*)

Fig. **53** **Lipoma of the conus,** partial removal (case *153*)

tion is continued laterally, on the side on which resection proves easier. If there is a capsule, or if the tumor is not too friable, it can be grasped, allowing visualization of the correct cleavage plane, which must be respected. Once it has been slightly retracted, the spinal cord separates itself almost spontaneously from the sulcocommissural vessels, the size of which diminishes as one progresses along the dorsal column.

Often, however, this scenario is only theoretical. Patience and common sense are then necessary, as the difficulties are often different on each side of the tumor. Instead of persisting in a particularly difficult area and producing alterations in the SEPs, we prefer to move the microscope either from one pole of the tumor to the other or from one side to the other, and come back with the Cavitron after further reduction of the tumor bulk has been carried out. The absence of a cleavage plane, particularly if the intraoperative appearance is suggestive of an infiltrating tumor, malignant or not, will prompt the surgeon to be cautious and avoid continuing tumor removal at all costs, as this may be both dangerous and useless. On the other hand, if time conditions permit, the objective is total tumor removal.

The last difficulty lies in the vascular pedicle or pedicles that supply the tumor and are connected to the anterior spinal artery. The danger here is real, as some tumors are large enough to separate and even cleave the spinal cord, resulting in a true diastematomyelia and exposing the anterior spinal artery to all sorts of risks. Ignorance of this can lead to catastrophic operative results. Several authors (33, 66, 71, 120, 127, 201, 233) routinely use ultrasonography for intraoperative determination of the size and extent of intramedullary spinal cord tumors, both before and after opening the dura, and for the detection of residual tumor that may have eluded inspection. In fact, when removal is macroscopically complete, there is no more bleeding. In view of the small size of the cord vessels, which stop bleeding spontaneously, it is unusual to have to coagulate an area outside the tumor. When tumor removal is complete, the wall of the cyst or cysts adjacent to the tumor bed is inspected (if this has not already been done). When normal spinal cord tissue can be seen through a transparent cyst wall, surgery can be terminated, as the cyst wall is similar to that seen in syringomyelic cavities and does not contain tumor. We performed biopsy of the wall of such a cyst in only one case *[4]*, and the histological examination only showed gliosis. Realizing the difficulties involved in distinguishing gliosis from glioma, we never again resorted to such biopsies, and have never had cause to regret our decision. McCormick et al. (169) share our opinion, and no longer biopsy the cyst walls of ependymomas. If the wall of the cyst is thick, it should be removed along with the tumor and considered as an intratumoral cyst; intraoperative histological examination can help in making this decision.

After tumor removal, the dorsal columns are released from pial traction and brought together again with caution. Whenever possible, the cord is approximated with 6–0 pial sutures (24, 77, 78), and the arachnoid may also be partially reconstituted if it has been preserved on opening (24, 25). The dura is closed in watertight fashion and without tension; if required, a duraplasty is performed with fascia, which we prefer to lyophilized dura or other foreign material. If laminotomy has been performed, the bone is returned to its place, with caution being taken to avoid compressing the spinal cord, with or without internal fixation and, preferably, with a postoperative orthosis (54, 64, 212, 213). If laminectomy has been performed, the bone gap can be partly filled with a Surgicel lamina. Depending on the situation, a nonsuction drain is inserted into the subfascial or subcutaneous space.

The major postoperative sequelae consist of often distressing pain in the spine and limbs, and temporary aggravation of sensory and motor deficit below the level of the lesion. In addition to symptomatic medical treatment (analgesics, anti-inflammatory drugs, corticosteroids prescribed with caution, etc.), one must emphasize the importance of physiotherapy and early postoperative mobilization in order to achieve a better functional result. In case of sensory and motor deficit, high doses of vasodilators are very effective. The use of hyperbaric oxygenation (110), popular in the Lyons experience, is an adjuvant therapy that is awkward to provide (once or twice daily). It can be used over a period of several days if successive treatments result in some motor or sensory improvement, as was observed in seven of our patients *[2, 20, 26, 71, 72, 126]*. This form of treatment may even be followed by dramatic improvement *[29]*.

Table **2** summarizes the main operative data regarding the tumor, surgical procedure, and technical means used with each patient.

2 Treatment

J. Brotchi, G. Fischer

In this chapter we present our series of 171 patients with IMT who underwent surgery (200 operations), classed according to the histological characteristics of the tumors. The series is summarized in Table **2** (p. 11).

2.1 Tumors of Glial Origin

Ependymoma

Figures **54** and **55** show the most relevant histological and imaging features of intramedullary ependymomas (64 cases in our series).

Intramedullary ependymoma is distinguished from the ependymoma of the filum terminale and cauda equina in that the latter is essentially extramedullary, even when it has invaginated into the conus medullaris. The intramedullary spinal cord ependymoma is, most often, a benign, slowly developing tumor. It may grow to a considerable size, sometimes affecting the entire spinal cord (holocord ependymoma) before it becomes clinically detectable. Our series included 64 patients with ependymomas among 171 IMT patients (37%). There were 29 females and 35 males, age range 18–73 years (mean age: 40.5 ± 12 years), and no children.

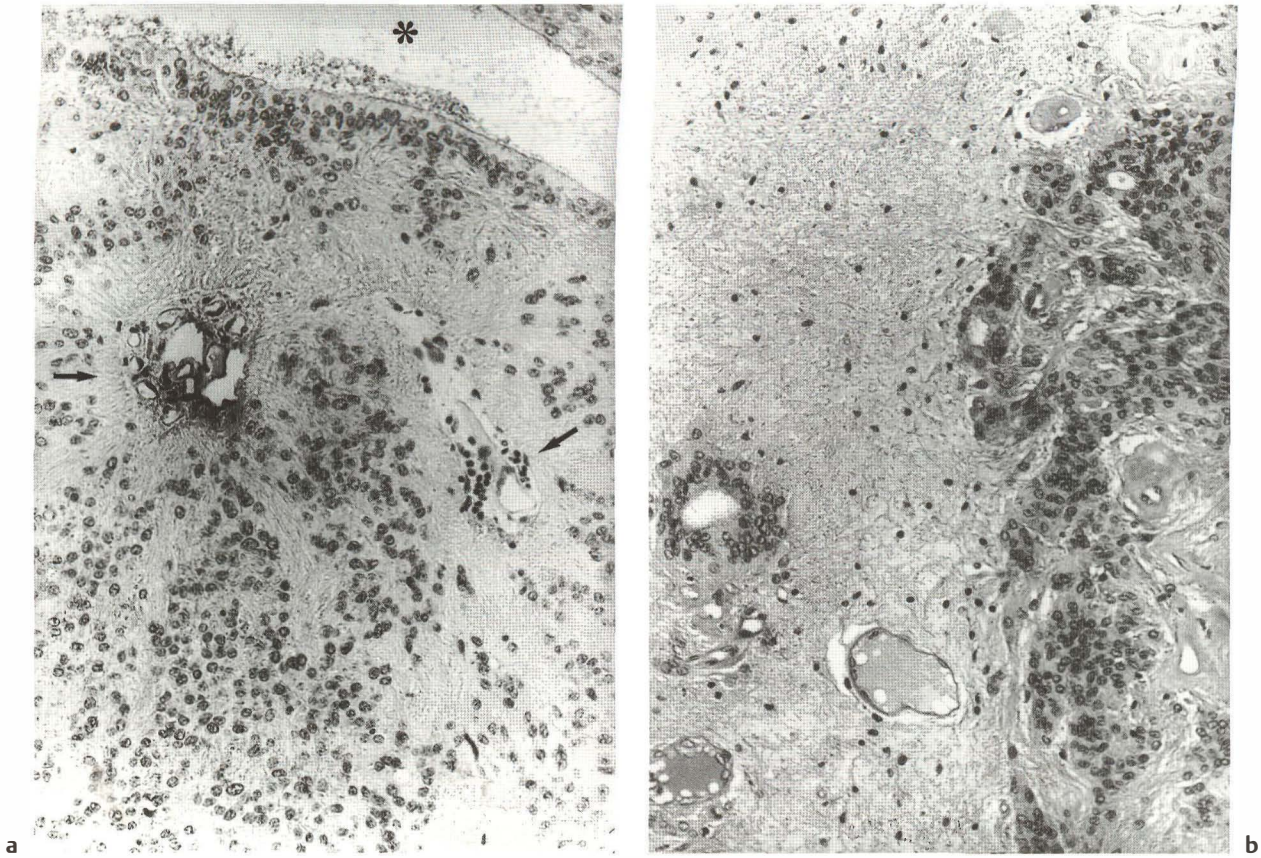

a b

Fig. **54** **a Typical grade II ependymoma** (case *15*). Perivascular (arrows) and tubular (star) structures (HPS × 200). **b Grade II ependymoma** (case *19*), showing a border between neoplastic tissue (right) and neural tissue (left) (HPS × 200)

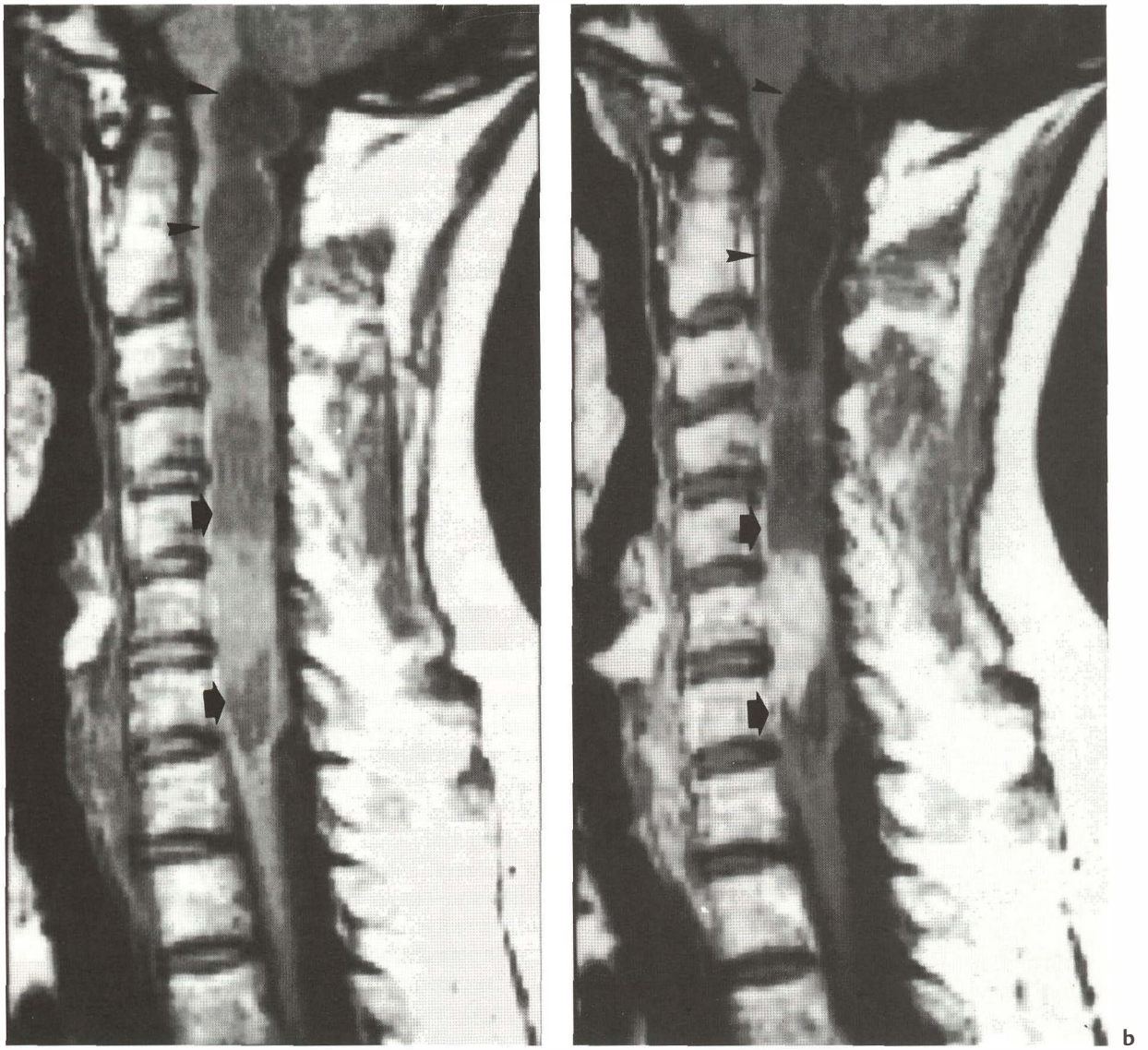

Fig. **55** **Grade II ependymoma** (*case 30*; same case as in Fig. **71**). **a** Sagittal precontrast, **b** postcontrast T1-weighted images, and **c** T2-weighted image. A well-delineated solid mass is seen at C6, which is isointense compared to the cord on both T1-weighted and T2-weighted images. There is intense homogeneous enhancement after contrast administration. Polar cysts (short arrows in **a** and **b**) are found at both ends of the tumor. Their signal behavior is different from that of the cerebrospinal fluid, due to a high level of protein within the cystic fluid. The "cap" sign is seen at the caudal tumor margin (long arrow in **c**). There are brain stem and hydrosyringomyelic cysts (arrowheads in **b**), with signal behavior identical to that of the cerebrospinal fluid. Note the "straight" appearance of the cervical spine

Clinical Symptoms

The clinical symptoms are summarized in Table **2**. Early symptoms consisted of sensory disorders in 39 patients (61%), motor disorders in 24 patients (37.5%), and urinary disturbance in one patient (52). A nocturnal increase in pain, a common feature of ependymoma presentation, was observed in five cases (7.8%). The mean preoperative disease course was 3.9 years (range: 15 days to 15 years).

The patient's functional status at the time of surgery was evaluated according to the functional criteria based on the McCormick classification (169), taking into account both sensory and motor deficits. There were 23 cases without any disabling deficit (grade I); there were 30 with deficits that did not prevent walking (grade II); six patients had deficits that precluded walking (grade III); five patients were totally dependent (grade IV).

Fig. **55c**

MRI Findings
(Fig. **55**)

Ependymomas most commonly affect the cervical spinal cord; 43% of cases studied with MRI were exclusively cervical, 20% extended to the upper thoracic levels, and 3% extended to the medulla. The thoracic site alone was affected in 29% of cases, and 5% were located solely within the conus medullaris.

Seventy-eight percent of ependymomas had one or more cysts. Intratumoral cysts were seen in 22%, unipolar or bipolar cysts in 62%, associated hydrosyringomyelia in 9%, and a lower brain stem cyst was seen in the medulla in 9%.

The solid portion of the tumor was isointense on T1 imaging in 50% of cases, or was heterogeneous, with areas of isointensity and hypointensity, in 50% of cases. A slight T1 hyperintensity occurs rarely, and suggests the presence of intratumoral hemorrhage (4%). On T2 images, ependymomas exhibit hyperintensity (44%) or isointensity (44%). Mixed signal intensity was seen in 12%: 6% with a hyperintense or isointense signal, and 6% with hyperintense, isointense, or hypointense signals. On average, the solid portion extended over the length of 3.6 vertebral bodies (range: 2–13). The tumor was located in the center of the spinal cord in only 62.5% of cases. By contrast, the "cap" sign (a hypointense signal at the poles of the tumor) was observed in 30% of cases.

In our experience, contrast enhancement after the injection of gadolinium was seen in 80% of cases (homogeneous signal in 69%, heterogeneous signal in 31%). Contrast uptake in the solid portion was complete in 87% of cases and partial in 13%. The margins of the lesion were clearly defined in 87% of cases.

A hyperintense signal area on T2-weighted images, consistent with tumor-associated edema, was observed in 60% of cases.

This analysis shows that while we did observe the typical findings reported in the literature, these features are also by no means consistent: in other words, *there are no pathognomonic signs that allow a firm histological diagnosis based on MRI findings.*

Surgery

At surgery, intramedullary spinal cord ependymomas show certain typical features: in most cases, the tumors are well-delineated, with a rounded upper pole and a somewhat more filiform lower pole, and they commonly have a cyst at the pole.

In our experience, we have always found a clear cleavage plane, and usually a tough tumor wall that allows the tumor to be grasped and manipulated. A purple-blue or brown color has helped us to recognize the ependymoma and distinguish it from the normal white spinal cord tissue. The somewhat friable tumor is fairly easily fragmented and removed using the CUSA. In our series, 28 of 64 patients (44%) presented with a cyst at the rostral or caudal pole of the tumor, a percentage that is much lower than that reported in the investigation of the most recent cases. In the absence of a polar cyst, it is not always easy to distinguish between the filiform end of the tumor and the increasingly dense fibrous band into which it merges. The fibrous band should be cut, without exerting excessive traction, where it enters the center of the cord. A final histological examination of the last fragment of resected tissue is recommended.

Our 64 ependymomas were completely removed, except in four patients *[21, 24, 41, 61]*, for one of whom a second procedure was planned *[41]*. In nine

patients *[2, 10, 25, 40, 45, 50, 55, 57, 60]*, complete tumor removal during the initial operation had been considered impossible, due to timidity or caution on the part of the surgeon. In each case, total removal was eventually achieved during a second operation.

Holocord ependymomas can be removed in one or two operative procedures. We saw six such cases; three were removed in one operation *[4, 27, 37]*, and three were resected in two operative procedures *[8, 50, 52]*. In all cases, complete removal was obtained without recurrence, with postoperative follow-up at 20, 6, 3, 22, 9, and 4 years, respectively.

Histology

Classifying the histology of ependymomas is important (Fig. **54**). All ependymomas in our series were grade II (in the WHO classification), except two that were rated as grade III *[61, 62]*.

In 33 cases, the histological structure was classic and typical (Fig. **54**): moderately dense diffuse cellular proliferation, with long or epithelioid cells that sometimes cling to vessels by means of GFAP-positive radiating processes (ependymal pseudorosettes). In one-third of the cases, we observed ependymal rosettes or tubules of cells with a ciliary body at their pole (EMA-positive). Often, the abundance of ependymal rosettes and pseudorosettes makes diagnosis easy, because they can be seen clearly on intraoperative examination of smears and touch preparations.

However, histological variants can make the differential diagnosis difficult when one is working with tiny tissue fragments. This applies to cellular ependymomas (15 cases), in which perivascular rosettes are rare. In one-third of the cases, immunolabeling of smears was necessary to distinguish between an ependymoma (GFAP-positive processes around the vessels, EMA-positive cells in the tubules), an astrocytoma (diffusely GFAP-positive), and an oligodendroglioma (GFAP-positive or negative, MBP-positive or negative). Since immunolabeling is often a poor way to distinguish between these lesions, electron microscopy can be of major value. Ependymomas are rich in microvilli, cilia, and cell junctions.

The presence of clear cells may suggest an oligodendroglioma, or even a metastatic adenocarcinoma (signet-ring cells). In one such case *[21]*, the interpretation of immunolabeling was difficult because of superimposed bleeding and pigmentation; twelve years later, in the absence of recurrence and of any detectable primary tumor, the diagnosis of an ependymoma was upheld.

The pseudoneurinomatous (or tanycytic) form consists of fusiform cells arranged in bundles (ten cases), and resembles neurinoma. In three cases, immunolabeling and special staining were necessary to distinguish between an ependymoma (EMA+, GFAP+) and a neurinoma (PS 100+, Leu7+, GFAP–, EMA–, reticulin network surrounding each cell). This form may also be confused with certain astrocytomas, since immunolabeling is frequently not diagnostic. For these difficult cases, intraoperative examination using cell smears and touch preparations can be very helpful. Ependyma cells separate from tumor fragments and adhere to the glass slide much more readily than schwannoma cells. They can be distinguished from astrocytoma cells by their more regular oval-shaped nucleus, with a large nucleolus and a unipolar fusiform cytoplasm. In such cases, electron microscopy is of considerable value.

Two lesions *[31, 41]* were considered to be cystic ependymomas, although with reservations due to diagnostic difficulties in distinguishing between gliosis and tumor in the cyst wall. Indeed, in cystic ependymomas, tumor infiltration of the cyst wall is often nodular proximally, contrary to the findings in astrocytomas.

Subependymomas *[63, 64]* have unique histological features. As is the case elsewhere in the central nervous system, these consist of small nests of regular nuclei in a rich fibrillary background. Although they are akin to astrocytomas, they are now classified as ependymomas. They would also seem to have a tanycytic origin (9, 111, 236). On MRI, in one of our two cases a localized nodule took up contrast, while the lower pole of the tumor did not enhance (Fig. **30**).

Postoperative Radiotherapy

Postoperative radiotherapy was not given to patients who had undergone surgery for ependymoma with complete removal (57 cases) or subtotal removal (three cases) *[35, 36, 43]*. Among the patients who underwent complete removal, only one *[32]* required a second operation for in-situ recurrent tumor 18 years later.

Two of our patients who underwent incomplete removal *[21]* or partial removal *[24]* were treated with radiotherapy elsewhere, at 60 Gy and 40 Gy, respectively. The first patient *[21]* developed severe cervical kyphosis. The neurological condition of the second patient *[24]* continued to deteriorate; he had to undergo a second operation three months later, and died within ten months.

We have operated on two cases of malignant ependymoma. The first patient *[61]* underwent routine biopsy followed by radiotherapy (35 Gy), and died within three months. The second *[62]* had complete tumor removal, but did not receive radiotherapy because, at the time, the tumor was judged to be grade I – II (78). By our current standards, it would

now be rated grade III. Unfortunately, we do not have long-term follow-up data for this patient.

Discussion

A diagnosis of intramedullary spinal cord ependymoma in the adult patient can be suspected when the major symptomatology consists of subjective peripheral sensory disorders of the limbs or trunk. Epstein et al. (70) observed this in 33 of 38 patients. These symptoms are rarer in the children (68), and are more difficult to elicit. Only MRI can establish the diagnosis of ependymoma. Homogeneous contrast medium uptake is in favor of this diagnosis (68, 163), although it is not absolutely conclusive (12).

The surgical strategy is based on the intraoperative assessment of the feasibility of complete tumor removal. This problem is particularly pertinent in the case of holocord ependymomas (45, 47, 79, 85, 144, 207). A case of two separate intramedullary spinal cord ependymomas was reported by Slooff et al. 30 years ago (249). Today, MRI can demonstrate areas of solid and cystic portions alternating within the same tumor. Exophytic ependymomas are most unusual. Our one case *[50]* was reported in an earlier publication (24). Some cases reported in the literature seem to be more ectopic (extramedullary) than exophytic (arising from intramedullary ependymal cells) (197).

Finally, there is general agreement in the neurosurgical literature that no adjunctive radiotherapy is required after removal of a low-grade intramedullary spinal cord ependymoma (99, 165, 255). We have advocated this approach for several years (22, 23, 24, 77, 78, 79) and will continue to do so.

Astrocytoma

The most characteristic MRI and histological features of intramedullary spinal cord astrocytomas are shown in Figures **56** and **57**. Unlike ependymomas, intramedullary spinal cord astrocytomas occur more frequently in children than in adults. They are more often low-grade tumors. The anatomical and histological variability of the lesion is reflected in the clinical presentation; the onset of symptoms may or may not be insidious, and may develop slowly or rapidly.

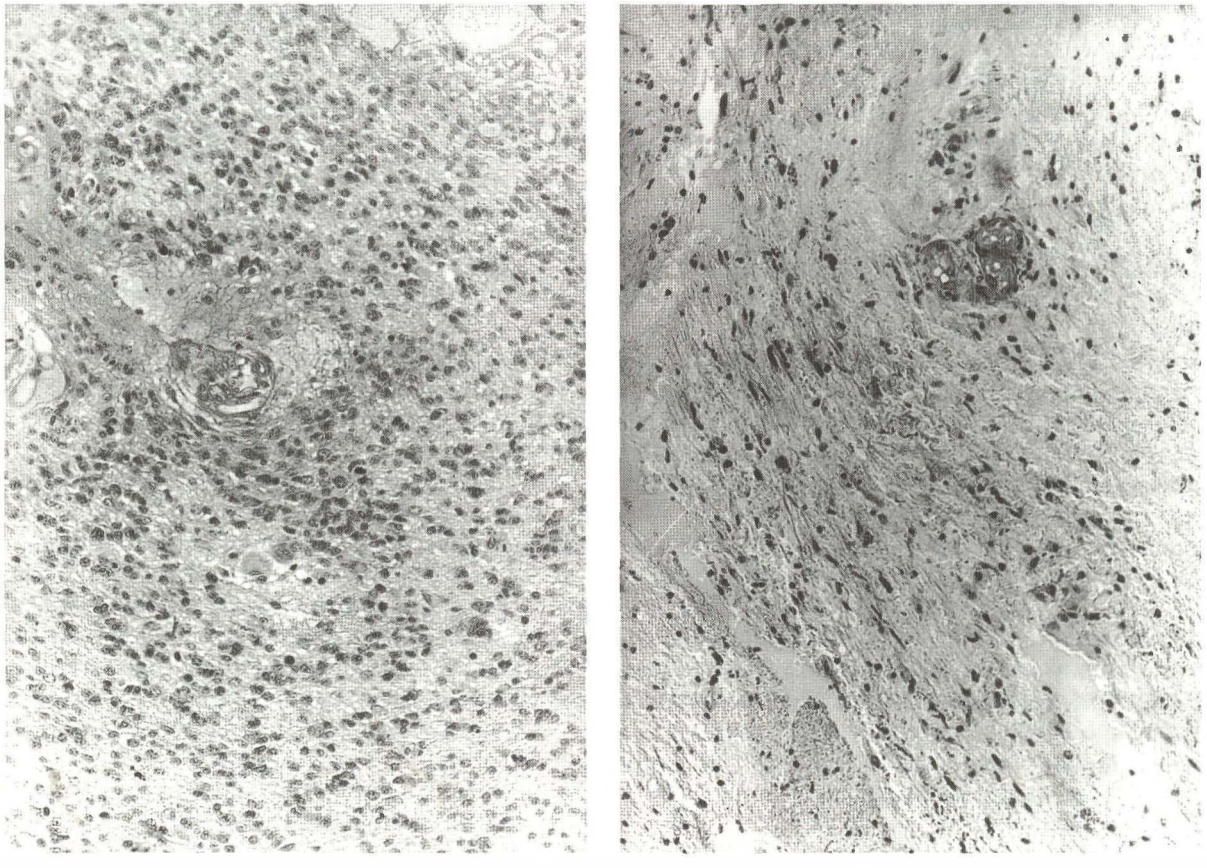

a b

Fig. **56** **a Ordinary grade III astrocytoma** (case *99*) (HPS × 200). **b Relatively hypocellular pilocytic astrocytoma** (case *79*; same case as in Fig. **27**) (AA 39 844, HPS × 200)

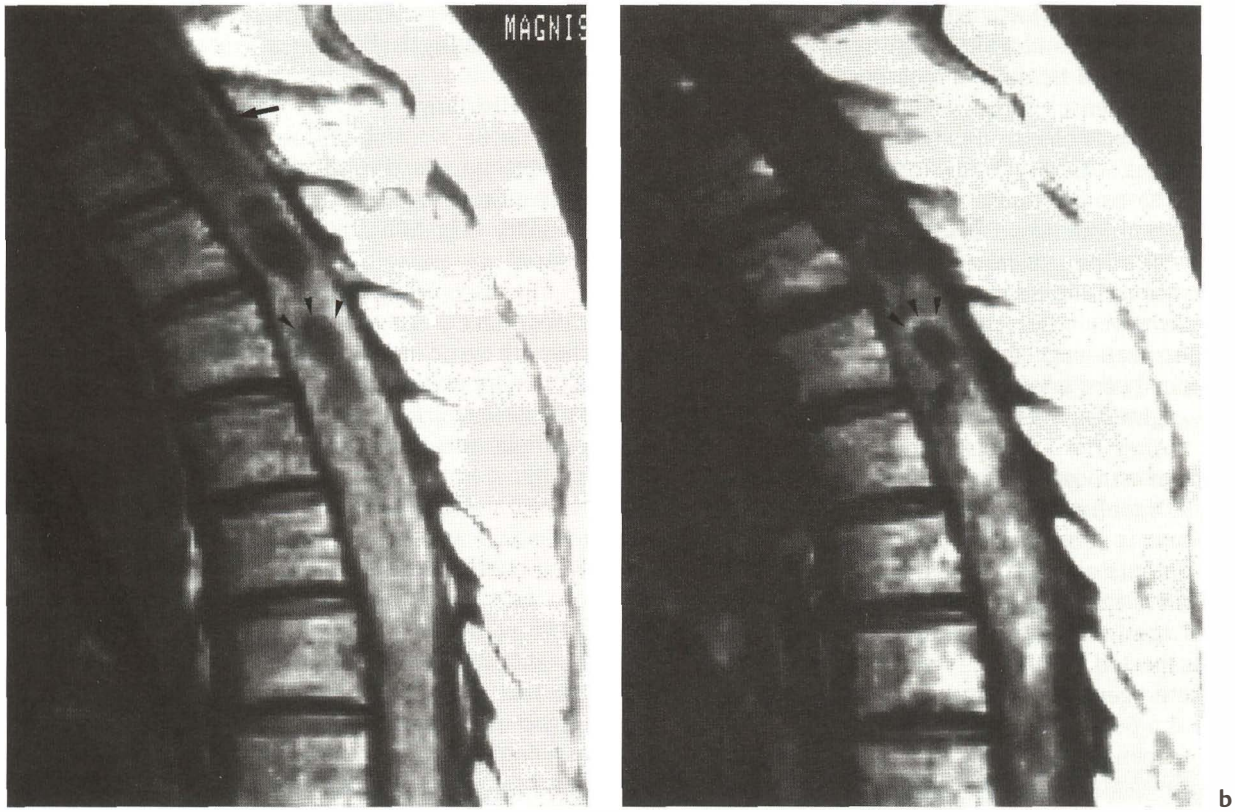

a b

Fig. **57** **Grade II thoracic astrocytoma** (case *83*; same case as in Fig. **76**). **a** Sagittal precontrast T1-weighted image and **b** sagittal contrast-enhanced T1-weighted image, showing partial and heterogeneous contrast enhancement of the tumor. There is an intratumoral cyst with an enhancing wall (arrowheads). Note the associated hydrosyringomyelic cyst (arrow)

Our series includes 41 patients operated on for astrocytoma out of a total of 171 cases of intramedullary spinal cord tumors (24%). The series consisted of 15 females and 26 males, aged 2–67 years (mean 29±15 years); 71% were adults and 29% were children under 15 years of age.

Clinical Symptoms

The clinical symptoms are summarized in Table **2**. The first symptoms in 22 patients (53.6%) were sensory disorders; motor abnormalities were present in 17 patients (41.4%); one patient *[88]* had urinary difficulties, and one *[79]* presented with painless scoliosis. Nocturnal exacerbation of pain, a classic presentation, was noted in two cases (4.8%).

The mean preoperative disease course was 3.6 years (range two months to 24 years).

The patient's neurological function at the time of surgery was evaluated using the McCormick's classification (169), taking account of both sensory and motor deficits. There was an absence of disabling deficit (grade I) in nine cases; a deficit not interfering with gait (grade II) in 17 cases; a deficit preventing walking (grade III) in eight cases; and total dependence (grade IV) in seven cases.

MRI Findings
(Fig. **57**)

Most often, astrocytomas have a thoracic location, either exclusively (42%) or also involving the cervical region (18%) or the conus medullaris (8%). An isolated cervical location was observed in 24% of cases, and in 3% there was extension to the medulla. Isolated involvement of the conus medullaris is relatively rare (5%). Involvement of the whole spinal cord was seen in 3% of cases.

Astrocytomas are often cystic (48% of cases), although less frequently than is the case with ependymomas. The cysts were intratumoral in 42%, polar in 19%, pseudosyringomyelic in 13%, with extension in the medulla oblongata in 3%.

On T1-weighted images, the solid portion of the tumor appears either heterogeneous with a hypointense or isointense signal (41%), or relatively

homogeneous with a hypointense (37.5%) or isointense signal (12.5%). A slightly hyperintense signal was noted in only 3% of our cases. A markedly hyperintense signal, denoting the presence of blood, was observed in 6% of cases. On T2-weighted images, astrocytomas are either hyperintense (64%) or isointense (36%). On average, the solid portion extends over 5.6 vertebral bodies (range: 2–19). The typical eccentric appearance of astrocytomas is found in only 57% of cases. The "cap" sign was never observed. Only 23% of cases had an appearance suggesting the presence of associated spinal cord edema (hyperintense signal area on T2-weighted images).

After the administration of contrast, the signal from astrocytomas is moderately (40%) or markedly (36%) enhanced. Heterogeneity of contrast enhancement is very frequent (83%). After injection, tumor contours appear poorly defined in 50% of cases. In 24% of cases, there is no contrast enhancement at all.

In summary, a diagnosis of astrocytoma should be suspected when the tumor is eccentric, shows heterogeneous contrast medium enhancement, and has a poorly defined border. However, as in the case of ependymomas, there is no pathognomonic appearance.

Surgery

The surgical treatment of intramedullary astrocytomas has certain unique features, due to their infiltrating nature. Traditionally, it has been thought that this tumor cannot be fully removed; however, in our series, surgical removal was believed to be macroscopically complete in 15 cases (37%), subtotal in 11 cases, incomplete in seven cases, partial in two cases, and limited to biopsy in six cases. MRI evaluation does not allow the surgeon to predict whether or not he will find a cleavage plane at the time of operation.

Intraoperatively, the discovery of a necrotic or xanthochromic intratumoral cyst (four cases) has no influence on tumor dissection. However, the presence of a satellite cyst at one of the poles of the tumor, with clear fluid (11 of 41 cases, i.e., 27%), facilitates removal if the tumor can be separated from the adjacent spinal cord (nine cases). However, such cysts may sometimes coexist with an infiltrating tumor *[77, 81]*.

Although the CUSA is useful for "debulking," its use becomes hazardous when a cleavage plane is not present. A point comes at which the surgeon has to work with the utmost care, turn on the pulsed mode and turn off the suction. The risk of creating a false cleavage plane is real, as the distinction in color and firmness between the tumor and the adjacent spinal cord may be deceptive. The principal difficulty is that there is no reliable, histologically confirmable means for the surgeon to distinguish between well-defined and infiltrating astrocytomas.

Histology

The histology of the 41 astrocytomas in our series showed the following main types of astrocytoma: ordinary (Fig. **56a**), pilocytic (Fig. **56b**), and dysplastic.

Macroscopically, ordinary astrocytomas (29 cases) have a grayish, infiltrating appearance, and they are cystic in one-third of cases. Microscopically, 22 tumors were either grade I *[71, 72, 73]* or grade II (19 cases). Thirteen of these were fibrillary, two were protoplasmic, and two were gemistocytic. Two cases could not be graded or characterized (too small fragments) and seven were high-grade tumors. Five were rated as grade III *[99, 100, 101, 102, 103]*, and two were classed as grade IV or glioblastomas *[104, 105]*.

Grade I pilocytic astrocytomas *[74, 75, 76, 77, 78, 79]* are difficult to differentiate from certain types of fibrillary astrocytomas or ependymomas, and from the reactive gliosis found in the walls of adjacent tumor cysts. They may be impossible to diagnose histologically with intraoperative examinations.

We characterized six cases *[65, 66, 67, 68, 69, 70]* as dysplastic astrocytomas (grade I) because of their similarity to gliosis, or to tumors observed in certain phakomatoses. These were often nodular, had low cellularity, sometimes with abnormal nuclei, but without mitotic figures. Like pilocytic astrocytomas, they are better delimited and more easily separated from the adjacent spinal cord than ordinary astrocytomas.

Postoperative Radiotherapy

In low-grade astrocytomas, irrespective of their histological type, we never prescribed adjunctive radiotherapy. We observed no recurrences after complete removal of benign astrocytomas (15 cases, follow-up 3 – 27 years), with the exception of one patient *[83]*, who underwent surgery six years previously, with MRI evidence of recurrence. This patient has been regularly followed up, and has no manifestations of tumor recurrence. The same results have been observed after subtotal removal (seven cases), with a follow-up of five to 25 years.

After incomplete tumor removal (seven cases) or partial tumor removal (one case) *[81]*, two patients died within one year *[97]* and two years *[82]*. Two underwent repeat surgery, after five months *[92]* and one year *[70]*: the first underwent complete removal, and has been followed up for 23 years, and the second had a subtotal removal and has been followed up for five years. In neither case has progressive tumor recurrence been observed. Finally, four pa-

tients are currently receiving an annual MRI follow-up examination, one of whom *[71]* has MRI evidence of tumor recurrence, but without any clinical manifestations.

Among our 41 astrocytoma patients, seven presented with a malignant tumor. Whatever treatment was used, whether repeat surgery *[100, 102, 103]*, radiotherapy *[99, 100, 101, 102, 103, 104, 105]*, or chemotherapy *[100, 103]*, the disease was always fatal within nine months to three years.

Discussion

It seems unrealistic to try to propose a typical clinical picture of intramedullary spinal cord astrocytomas, even though spinal pain may be a predominant symptom both in children and adults (64, 69). In IMTs, the main question is a surgical one – whether or not complete tumor removal is possible. In spite of this, in one-third of our cases, we removed the astrocytoma as if it were an ependymoma, without really knowing, intraoperatively, the real histology of the tumor. Indeed, the surgeon usually receives the result of the intraoperative examination when tumor removal is already under way. Whenever high-powered magnification with the operating microscope showed no cleavage plane and the diagnosis suggested by the neuropathologist was an astrocytoma, we thought it sensible to terminate resection and avoid removing tumor at all costs, knowing that this procedure could prove hazardous as well as unsuccessful.

According to Cooper, histological examination of the border zone between tumor and spinal cord is of considerable diagnostic utility. Cooper considers that, at cellular level, "total" removal of astrocytomas is impossible to perform in adult patients (39). In practice, in adult patients, all authors (39, 69, 165, 255) try to find a way of carrying out total removal, at least macroscopically. Stein (255) reports finding a cleavage plane in 50% of cases. He follows it until it disappears, and reports that this dissection causes no postoperative deficits (165). Epstein (66, 71) emphasizes the value of intraoperative ultrasonography for monitoring complete tumor removal. In his study of a series of 152 totally removed intramedullary spinal cord astrocytomas in children (64), he explains that it is pointless to try and find a cleavage plane, and that the "inside-to-outside" procedure using the CUSA should be applied to remove the tumor as far as the "glia – tumor interface," the remaining fragments being vaporized with the laser. The disagreement between these opinions is more apparent than real, however, when one looks at actual surgical management: all authors agree in recommending the removal of intramedullary spinal cord astrocytomas, whenever possible. This is indeed a sound policy, despite the difficult practical considerations varying from patient to patient that are involved, as surgical management may vary according to the IMT topography.

Our greatest reservation with this strategy concerns patients with astrocytomas of the conus medullaris who present with normal sphincter function. Biopsy is not without risk, and requires the utmost care and caution. By contrast, astrocytomas of the cervicomedullary junction pose do not problems that are any different from those affecting cervical IMTs *[81, 82, 84, 96, 98]*. The medulla can be opened as far as the obex, and cervicomedullary astrocytomas can be completely removed when a cleavage plane is present (72).

Holocord astrocytomas are rarely seen in adults. There was only one case in our series *[69]*. Epstein (64, 65) thinks that holocord astrocytomas account for 60% of intramedullary spinal cord astrocytomas in children. The only unique feature of such tumors, consisting of interspersed solid and cystic portions, is their extent.

Fig. **58** **Grade I ganglioglioma** (case *107*). A slightly hyperintense mass, extending from T1 to T3, with associated cyst formation at both poles. These findings are non-specific for this rare histological type of intramedullary tumor

Exophytic astrocytomas occur very infrequently. Venkataramana et al. (279) reported four patients in whom it was possible to perform complete removal. Our series includes three patients in whom we were able to achieve subtotal *[69]* or incomplete tumor removal *[97, 100]*.

Other Gliomas

What we call "other" gliomas do not constitute, either together or individually, a distinct clinical entity, and they display no characteristic features on imaging studies. When we add our own cases to those reported by the members of the SNCLF, the so-called "other" gliomas account for 33 of 1117 intramedullary tumors, i.e., 3%. Our five cases included one high-grade oligodendroglioma *[110]*, which is an extremely rare spinal cord tumor (82, 206), and four gangliogliomas.

Gangliogliomas are tumors consisting of zones of mature, often dystrophic neuronal cells against a background of glial cells; these neuronal cells are assumed to be nonneoplastic in gangliocytomas, whereas they proliferate in gangliogliomas, and sometimes have a fibrous and inflammatory stroma and calcifications. In our series, two such lesions were grade I *[106, 107]* and two were grade II *[108, 109]*. The glial component of one of the two grade II gangliogliomas recurred as a grade III tumor after two months *[108]*. All these cases were located in the cervical, cervicothoracic *[107]*, or cervicomedullary *[106, 108, 109, 110]* regions, and radical tumor removal could not be carried out. These glioneuronal tumors are rare (one percent in our series). Gangliogliomas accounted for 3.8% of all the central nervous system tumors in the series reported by Miller et al. (174) in which one-third of the patients were children, with a spinal cord location (1.7%) being more frequent than cerebral (1.4%) or cerebellar (0.7%) locations. They have no specific features on MRI (Figs. **58**, **59**). Thus, "other" gliomas are quite rare tumors (41, 186). Their course is a function of their histological grade, and is in every respect comparable to that of astrocytomas (136).

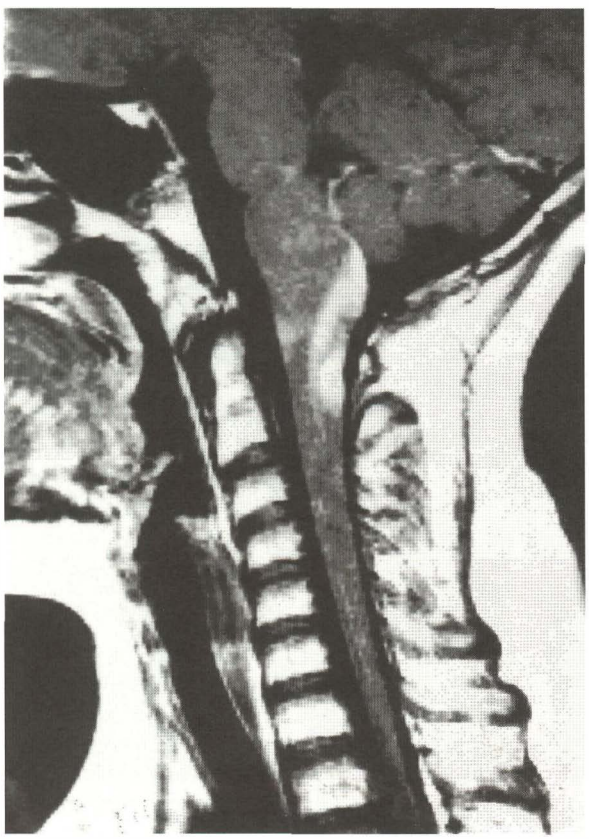

a

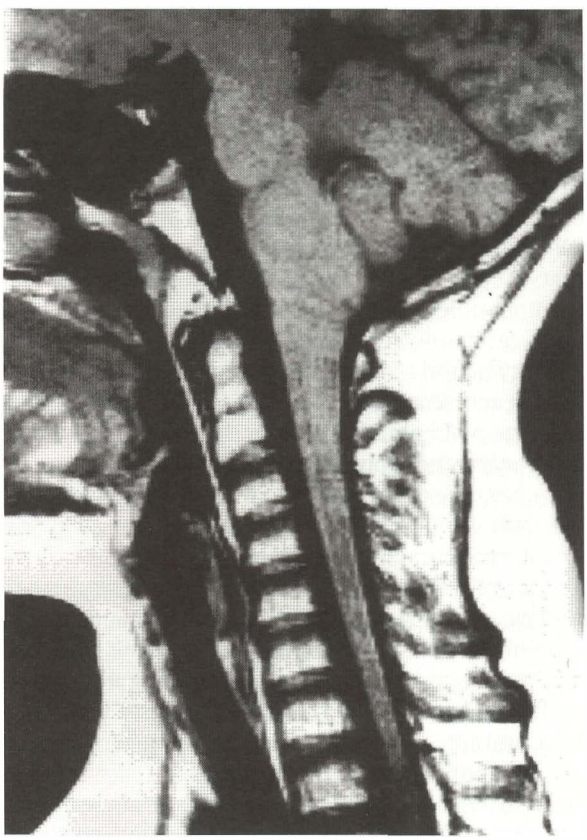

b

Fig. **59** **Grade II ganglioglioma** in a 12-year-old girl (case *109*). **a** Sagittal precontrast T1-weighted image: an ill-defined mass widening the upper cervical spinal cord and medulla. **b** Postcontrast T1-weighted image: there is enhancement in the posterior part of this ill-defined, noncystic mass. MRI is unable to provide any definite histological diagnosis

Intramedullary spinal cord metastases from malignant glial tumors can be considered to be grafts of neoplastic cells disseminated by the cerebrospinal fluid. They may be the first manifestation of the primary lesion (245) or, more frequently, manifest within a few months after surgery for malignant intracranial or cauda equina ependymomas (100) or another neuroepithelial tumor, such as a medulloblastoma of the fourth ventricle (16, 157). Our series included seven such cases in 171 IMTs, while in the SNCLF investigation there were 11 such cases in a total of 946 IMTs. This spreading of neoplastic cells in the cerebrospinal fluid is not limited to glial or primary neuroectodermal tumors, but is also observed in all malignant tumors affecting the nervous system. Possible spinal cord spreading has been reported for brain metastases arising from a visceral cancer (117, 261), but these are not true intramedullary spinal cord metastases.

2.2 Malignant Tumors of Nonglial Origin

Metastases from Visceral Cancers

In the SNCLF study, 4% of operated IMTs were metastases (45 of 1117 cases) secondary to a visceral neoplasm (Fig. **60**). This incidence may appear high compared to our personal series, in which there were only two cases in 171 operated IMTs. The rarity of intramedullary spinal cord metastases from visceral cancers, especially lung cancers, must be acknowledged (251). However, this may be apparent rather than real, since the clinical picture is that of terminal cancer, and spinal cord autopsy is seldom performed in these patients. This rarity is confirmed by autopsy findings (34, 208) and surgical series (15, 75, 117, 118, 173, 204, 261). In their study of a large homogeneous surgical series, Paillas et al. (196) report that the ratio of operated intramedullary spinal cord metastases to operated intracerebral metastases is 2.4% (12 of 489 cases). Finally, an intramedullary spinal cord metastasis as the initial manifestation of cancer deserves special mention. Jacquet et al. (117) reported one case of their own and collected 112 spinal cord metastases in an extensive review of the literature. In 41 of these 112 cases, the metastasis was the presenting manifestation of the systemic neoplasm. The search for the primary lesion is usually guided by histological examination of the IMT. However, the diagnosis of intramedullary spinal cord metastasis should be made with caution, as some ependymomas have a pseudometastatic appearance.

Melanoma

Intraspinal melanomas are rare, usually secondary tumors. A black intramedullary spinal cord tumor is exceptional, and a primary intramedullary spinal cord melanoma, histologically indistinguishable from a melanoma metastasis, is even more unusual (108, 203, 289). There were two such cases in our study *[120, 121]*, with a postoperative survival of 18 months and four years, respectively (Fig. **61**). The prognosis is less grave in primary melanomas (139) than in metastatic melanomas. The latter are more frequently extramedullary (21), and they disseminate as leptomeningeal melanomatosis (86).

Lymphoma

An intramedullary spinal cord lymphoma may occur as part of a multicentric central nervous system lymphoma, or secondary to the meningeal spread of a lymphoma of the brain.

Primary intramedullary spinal cord lymphoma has to be distinguished from systemic lymphomas causing epidural spinal cord compression (104, 250). Parallel to the increased frequency of primary brain lymphomas (in part related to an increased frequency of human immunodeficiency virus infection), it had been thought that the number of primary intramedullary spinal cord lymphomas was bound to increase. This has not been the case, however, at least according to the literature. Indeed, although AIDS-related spinal cord involvement is a frequent occurrence, in most cases the lesion is a vacuolar myelopathy (95). In addition, two cases of "malignant glioma" have been reported in AIDS patients (283).

Primary intramedullary spinal cord lymphoma remains a rare entity: only eight cases have been reported in patients not affected with AIDS (20, 26, 80, 104, 105, 175, 247, 250); it was most often associated (five cases) with cerebral, cerebellar, or brain stem lesions. In our 171 IMTs, we found two cases of intramedullary spinal cord lymphoma. The first *[123]* dates back to 1967. At the time, it was diagnosed as a thoracic spinal cord reticulosarcoma; death occurred at seven months, in spite of postbiopsy radiotherapy (271). The second case *[122]*, observed in 1991 in a patient with AIDS, was treated

a

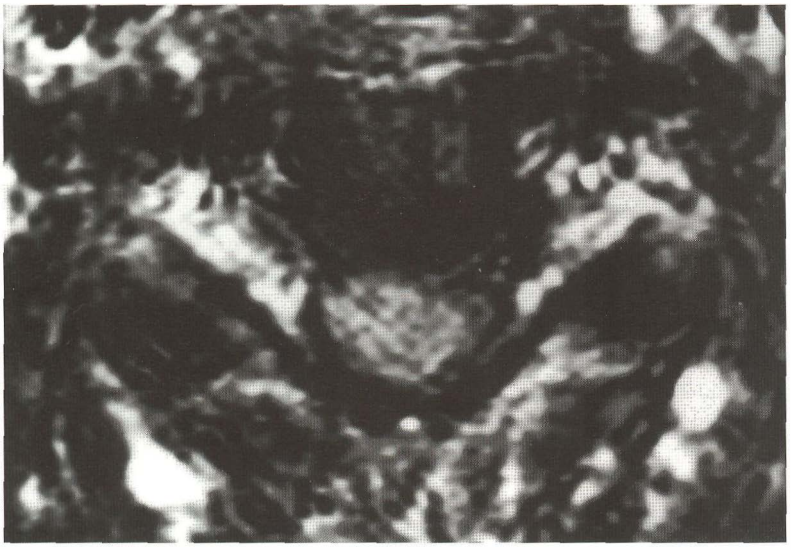

b

Fig. **60** **Intramedullary spinal cord metastasis** (case *118*). **a** Sagittal and **b** axial postcontrast T1-weighted images. There is an intramedullary, centrally located, intensely enhancing mass, without associated cysts

a

b

c

Fig. **61** **Intramedullary spinal cord melanoma** (case *120*). **a** Coronal postcontrast T1-weighted image: an intramedullary cervical mass, strongly enhanced after contrast injection. **b** Sagittal enhanced T1-weighted image, taken two years after total resection (demonstrated by MRI, but not shown here): multifocal recurrence without widening of the spinal cord. **c** Repeat study one year after a second surgical procedure, showing a new recurrence at the C2–C3 level

with subtotal removal of a C6–C7 infiltrating intramedullary spinal cord tumor that was consistent with a non-Hodgkin immunoblastic lymphoma. Death occurred after one year, without recurrence of the intramedullary spinal cord lesion. Thus, a primary intramedullary spinal cord lymphoma may present as an isolated IMT and be surgically treated as such. Once the diagnosis is confirmed, the treatment is the same as for lymphomas in other locations (corticotherapy, radiotherapy, chemotherapy). The prognosis depends on the progression of AIDS, or on the growth potential of the lymphoma within the central nervous system, or both.

2.3 Benign Tumors of Nonglial Origin

With few exceptions, hemangioblastomas, lipomas, schwannomas, and meningiomas are all benign tumors whose location is difficult to classify. Indeed, these tumors are usually not strictly intramedullary, since they essentially lie flush with the surface of the spinal cord (hemangioblastomas, lipomas) or show mixed intramedullary and extramedullary development (neurinomas, meningiomas). In fact, they are IMTs, and exhibit all the clinical, radiological and surgical features of IMTs.

Hemangioblastoma

Hemangioblastomas are vascular tumors that are well delineated, and sometimes multifocal. They often have an associated cyst, and are intimately attached to the leptomeninges.

Eighty cases of hemangioblastomas were reported by members of the SNCLF, representing 7.2% of spinal cord tumors (out of 1117 cases). Our personal series includes 19 patients operated on for hemangioblastoma out of 171 IMT cases (11.1%). There were nine females and ten males, aged 22 to 65 years (mean 40 ± 13 years).

Clinical Symptoms

The clinical symptoms are summarized in Table **2**. The initial symptoms consisted of subjective and objective sensory (12 cases) and motor disorders (seven cases).

Nocturnal enhancement of pain was observed in two cases with lumbar radiculopathy *[142]* and torticollis *[133]*. Symptoms had been present for a mean of 4.2 years prior to the operation (range 1 month to 14 years). The patients' neurological status was rated as follows: absence of disabling deficit (grade I): six cases; deficit not interfering with walking (grade II) 11 cases; deficit interfering with walking (grade III) one case *[135]*; total dependence (grade IV): one case *[140]*.

MRI Findings

(Fig. **62**)

A diagnosis of hemangioblastoma is easy to make in the context of von Hippel Lindau disease (hereditary phacomatosis), especially when there are multiple, cerebellar lesions (40% of our cases with MRI examination). The location of a single hemangioblastoma (60%) is most often thoracic (55%) or cervical (45%). Cysts of the spinal cord are very frequent (87%), with extensive hydrosyringomyelic cysts in 80% of cases, and a localized cyst in 7%.

The solid portion of the hemangioblastoma is nodular and always eccentric. On T1-weighted images, it is isointense (50%), slightly hyperintense (25%), hypointense (12.5%) or hypointense and isointense (12.5%). Because of its small volume, the lesion is not visible on T2-weighted images in 33% of cases. In 50% of cases, it is isointense to the spinal cord, and in 17% it is hypointense.

The "cap" sign is seen in 12% of cases. In a quarter of cases, there is T2 hyperintensity, suggesting the presence of spinal cord edema, which may be extensive and will subside after tumor removal. Injection of contrast is essential: contrast enhancement occurs in all hemangioblastomas. It is very intense, homogeneous, and complete, and will clearly delineate the tumor nodule. In practice, therefore, MRI performed with contrast medium injection and using two imaging planes allows a highly confident diagnosis of hemangioblastoma to be made.

Surgery

The surgical strategy is specific, and depends on the anatomical position of the hemangioblastoma.

Most often, we visualized the hemangioblastoma immediately after opening the dura, on the posterior surface of the spinal cord. When it was covered by the transparent pia, the approach to the tumor was obvious. Opening the spinal cord was never necessary, whether the approach was at the midline

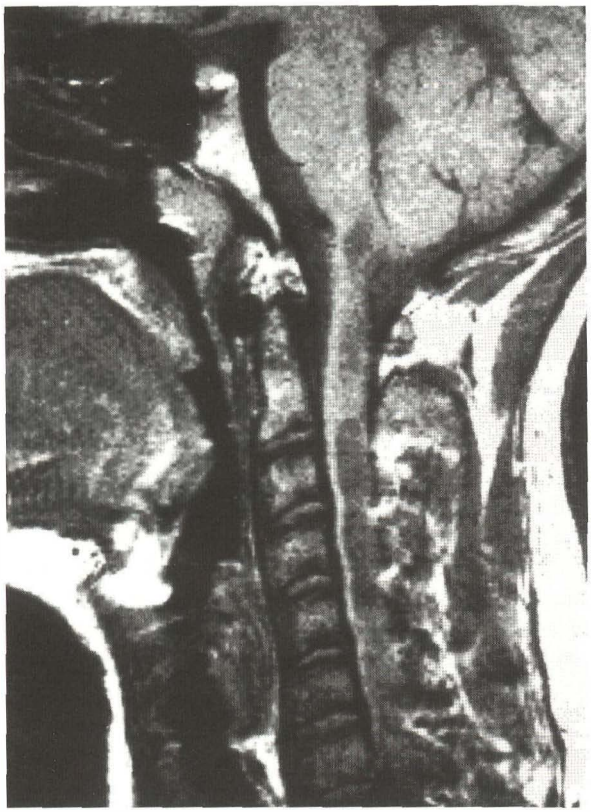

a

b

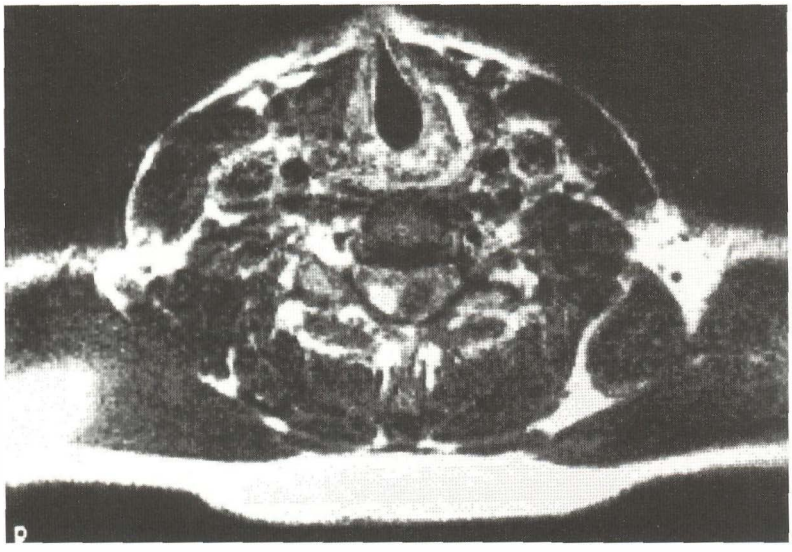

c

Fig. **62** **Hemangioblastoma** (case *137*). **a** Sagittal and **b** right parasagittal postcontrast T1-weighted images. There is cystic involvement of the entire spinal cord, associated with a small, intensely enhancing nodule located at the C6 level (arrow in **b**), eccentrically located on the right, as clearly shown on an axial contrast-enhanced T1-weighted image (**c**). **d** Postoperative MRI, showing disappearance of the cystic component both in this sagittal T1-weighted image and in an axial T1-weighted image (**e**)

Fig. **62d**

Fig. **62e**

between the two dorsal columns (16 cases), or at the lateral aspect of the cord, between the dentate ligament and the posterior root *[136]*.

When the hemangioblastoma was not visible, we opened the posterior sulcus along the midline using the same procedure as for any other IMT. In this fashion, we removed four spinal cord hemangioblastomas, which were completely intramedullary with an enlarged cord but no visible tumor on the surface *[126, 133, 134, 135]*. We never observed a hemangioblastoma of the cord surface anterior to the plane of the dentate ligament.

The surgical technique is also specific. We removed all hemangioblastomas "en bloc," even very large, pseudoangiomatous ones with a solid portion extending over two spinal cord segments *[134]* or three *[129]*. Cautious coagulation on the tumor surface enabled us to obtain slight retraction that helped detach the tumor from the cord and its vascular connections. The smaller the tumor, the easier this maneuver was. The cleavage plane is distinct as long as bleeding does not interfere with the dissection.

In ten of 19 cases, the hemangioblastoma was cystic, with a small, very vascular mural tumor giving rise to a more or less extensive, sometimes holocord cyst *[135, 137]*. In all cases, it was sufficient to open the cyst to remove the mural tumor, without having to perform extensive opening of the spinal cord.

In the case of multiple intramedullary spinal cord hemangioblastomas *[126, 130, 131, 137, 140]*, we operated only on symptomatic lesions. In one particular case *[131]*, we removed two tumors lying close to each other (T3–T4 and T8) during the same procedure. Only one patient *[130]* underwent surgery twice, once for cervical tumor removal (C4–C6), and one year later for thoracic tumor removal (T10–T11).

Histology

The histological features are similar to those of cerebellar hemangioblastomas. The lesions consist of capillaries lying next to each other, separated by foamy cells (Fig. **63a**). The gliosis adjacent to the tumor may be particularly profuse and simulate a glioma (Fig. **63b**).

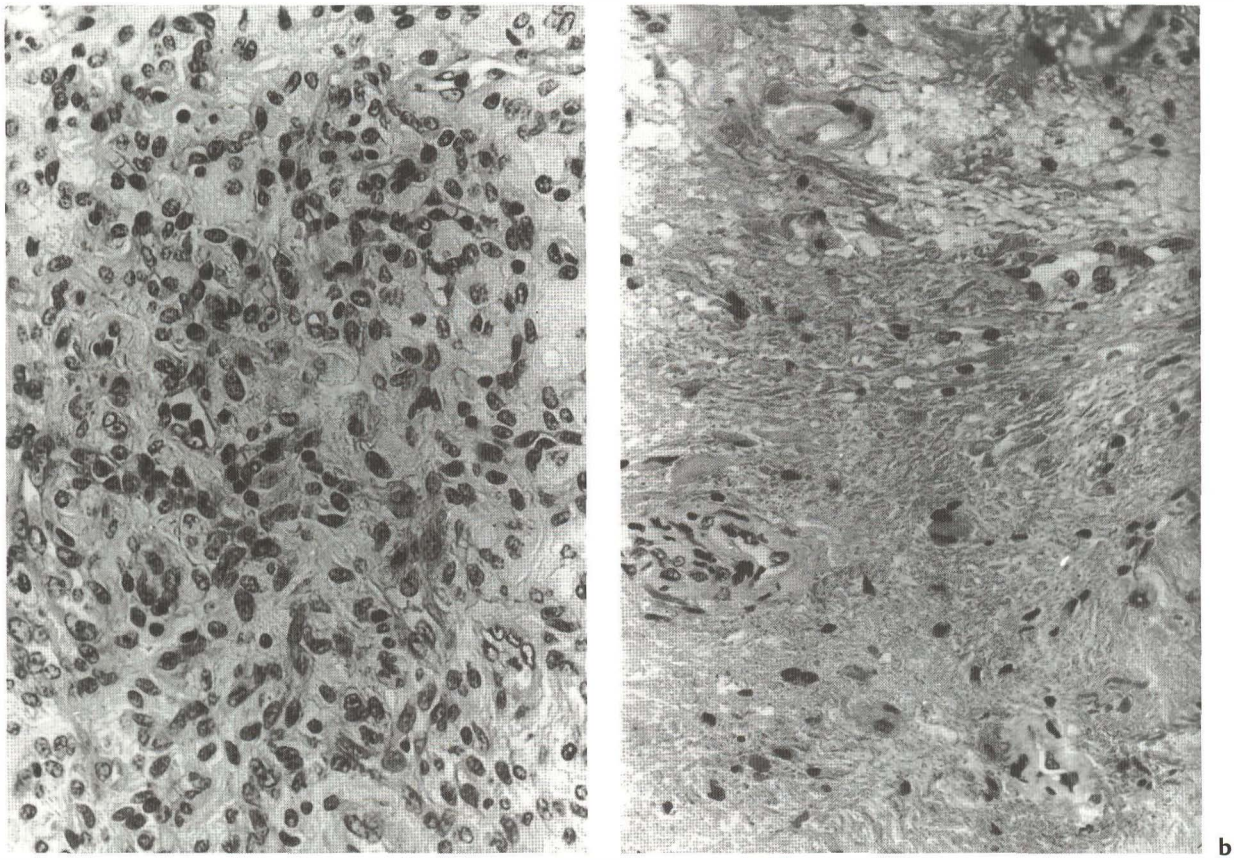

a b

Fig. **63** **Hemangioblastoma** (case *134*). **a** Typical tumoral tissue. **b** Perifocal pseudopilocytic gliosis (HPS × 400)

Discussion

Due to their hypervascular nature, intramedullary spinal cord hemangioblastomas may rarely present with subarachnoid hemorrhage (32, 133, 188, 277). Hemangioblastoma may rarely rupture into the spinal cord, causing abrupt paraplegia (228). Occult bleeding occurs more commonly (228), resulting in hematoma, as in two cases in our series *[135, 141]*, or intratumoral cyst, as in two others *[129, 133]*.

Hemangioblastoma is the only intramedullary spinal cord tumor for which arteriography may be useful when preoperative embolization is possible (84, 267). Although some authors (180) consider this examination mandatory in the evaluation of lower thoracic cord hemangioblastoma, we think this precaution is useful only for large tumors.

In some cases, MRI surprisingly shows a noncystic, enlarged spinal cord, a condition that reverses completely after tumor removal (Fig. **28**). In the two patients presenting with this MR picture, the tumor was very small *[125, 127]*. This unusual situation was reported by Solomon and Stein in 1988 in six patients (252).

Improvements in surgical technique have been developed by Hurth in 1975 (113), Yasargil in 1976 (290) and Resche in 1971 and 1993 (215, 216). The tumor has a cleavage plane that is always present (113, 180, 216, 290). The fundamental principle of intramedullary hemangioblastoma removal is to avoid removing the tumor piecemeal (113, 180, 216) or injuring it during dissection, which means that the CUSA is contraindicated. Intraoperative histological examination is often unnecessary when the diagnosis is obvious. If the diagnosis is not clear, as in tumors involving the center of the cord, one should beware of extensive gliosis in areas bordering vascular lesions, because the biopsy fragments are extremely tiny, and a second biopsy would prove very difficult to perform. At present, the CO_2 laser (107, 243) offers no advantages over bipolar coagulation and, along with Resche (216), we do not recommend its use.

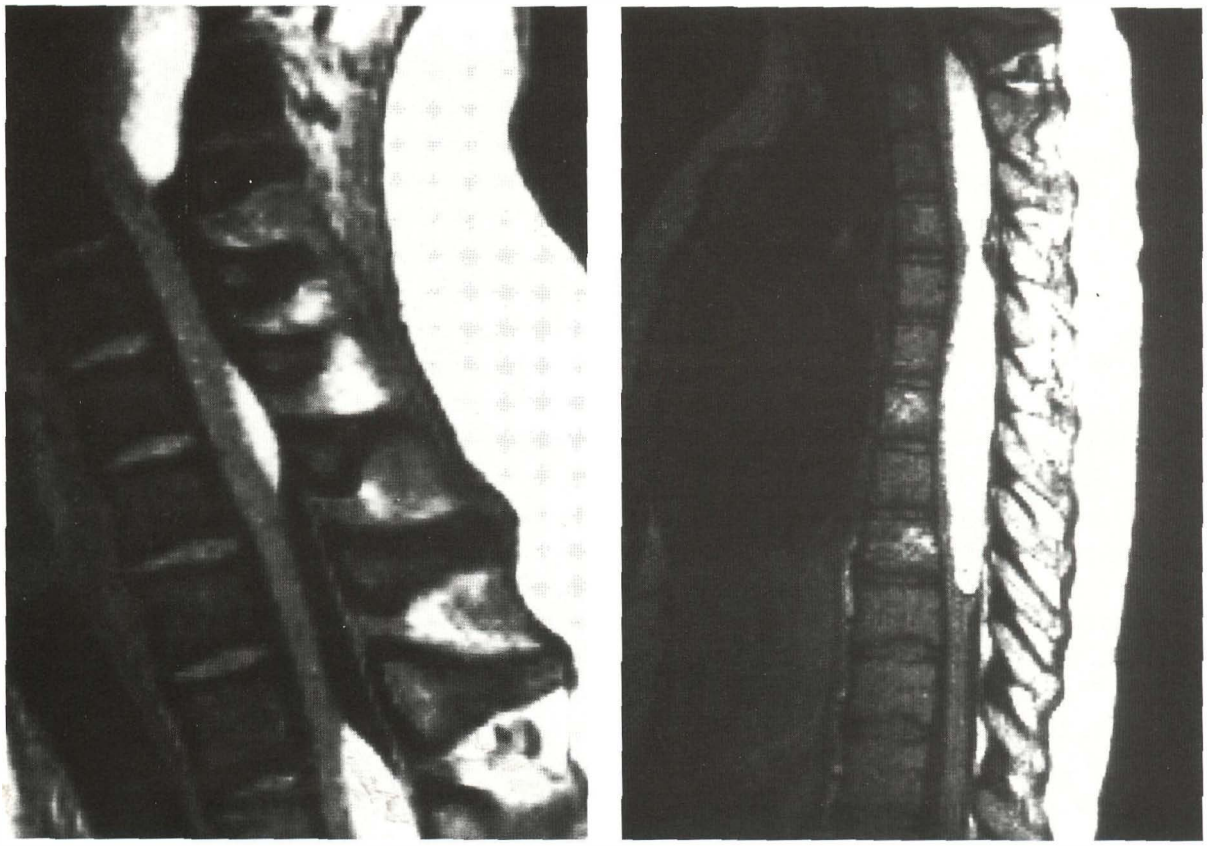

a b

Fig. **64** **Intramedullary spinal cord lipomas** (case *148*). **a–c** Multiple lipomas located posteriorly within the spinal cord, which are well-delineated and strongly hyperintense compared to the spinal cord in these T1-weighted images. **d** The post-myelogram CT scan shows that the masses are hypodense. These findings on both MRI and CT are pathognomonic

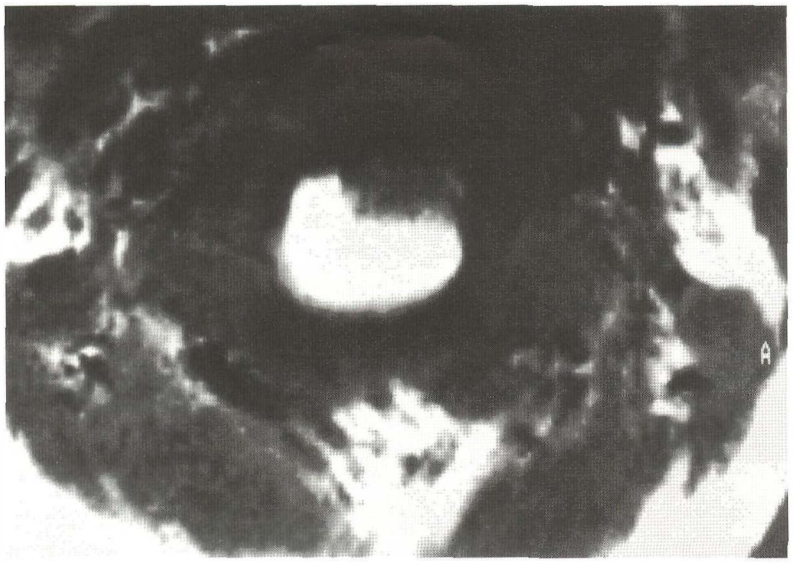

Fig. **64c**

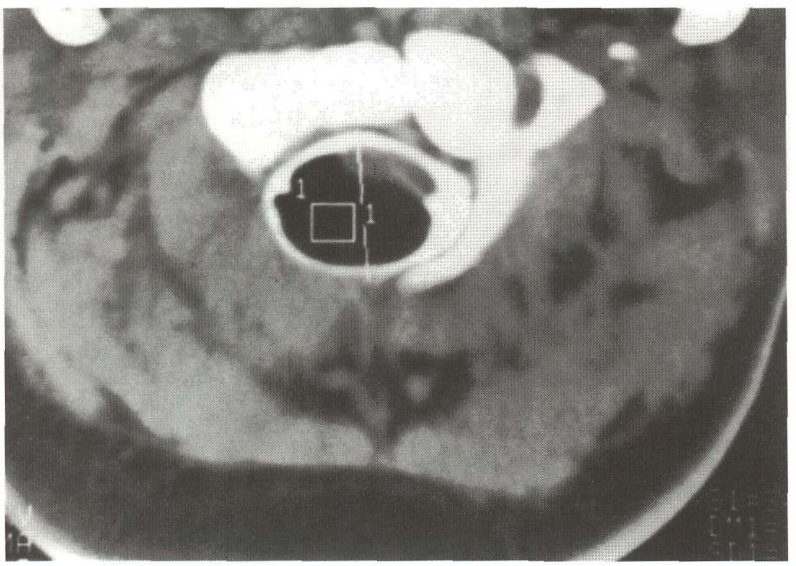

Fig. **64d**

Multifocal forms, which may or may not be associated with other neuraxial or visceral lesions in von Hippel–Lindau disease raise the question of operative indications in the absence of clinical manifestations. It is now generally agreed that only symptomatic lesions should be treated surgically (113, 216).

Lipoma

It is important to distinguish intramedullary spinal cord lipomas from all forms of cauda equina lipoma, which may or may not be associated with dysraphism, and which may involve the conus medullaris. These lesions raise fundamentally different clinical, radiological (Fig. **64**), and surgical problems. Intramedullary lipomas are rare, though not exceptional (11 of 171 in our series, 6.4%), as confirmed by the data from the SNCLF investigation: 82 intramedullary lipomas in 1117 cases, or 7.3%.

Like hemangioblastomas, lipomas present on the surface of the spinal cord, beneath the pia. However, the comparison ends there. Recognizable by their golden yellow color or fibrous texture, lipomas are attached to the arachnoid and embedded in the cord.

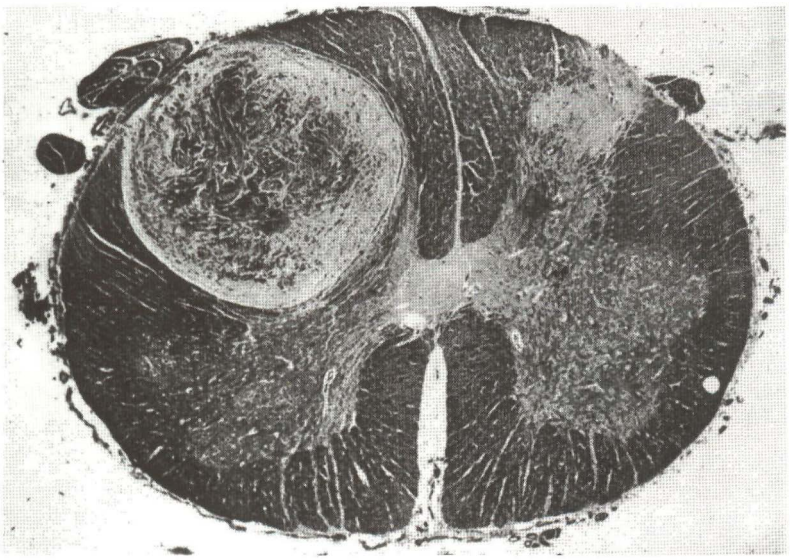

Fig. **65** **Intramedullary spinal cord schwannoma** (from Langford et al., *Tumors of the spinal canal*, ref. 137, p. 389, courtesy of Dekker Inc.)

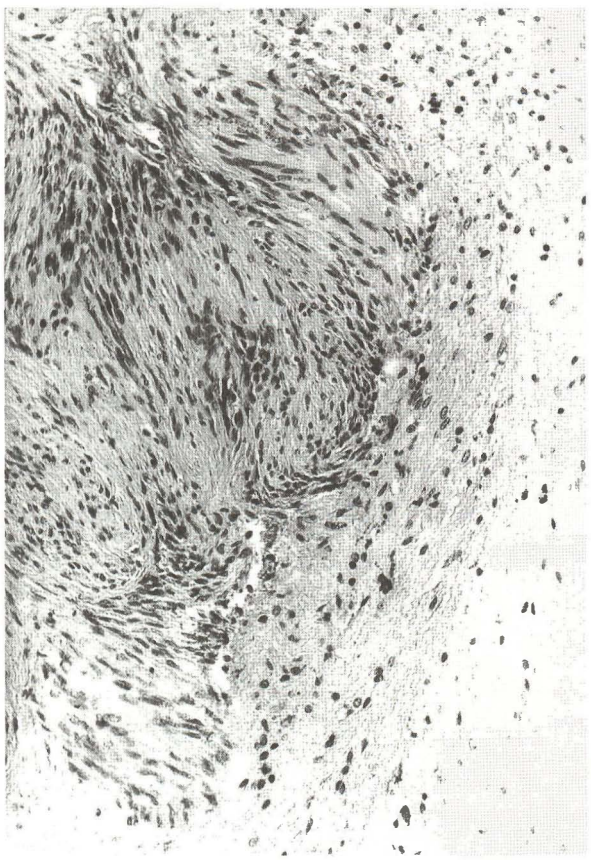

Fig. **66** **Intramedullary spinal cord schwannoma** (case *155*). There is a border between the neoplastic tissue on the left and the gliotic neural tissue on the right (HPS × 200)

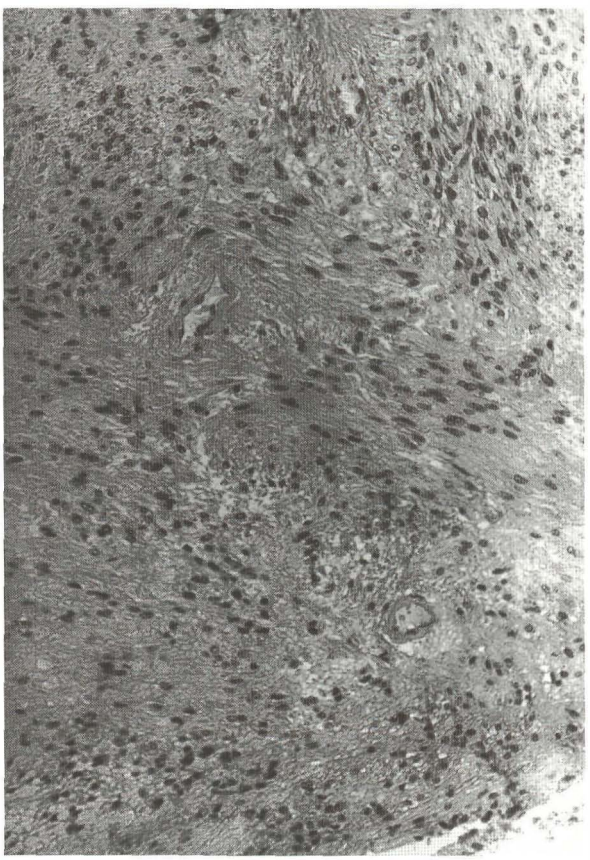

Fig. **67** **Pseudoneurinomatous (tanycytic) ependymoma** (case *12*). Fascicular pattern of the tumoral cells. The immunochemistry showed GFAP and EMA positivity (HPS × 200)

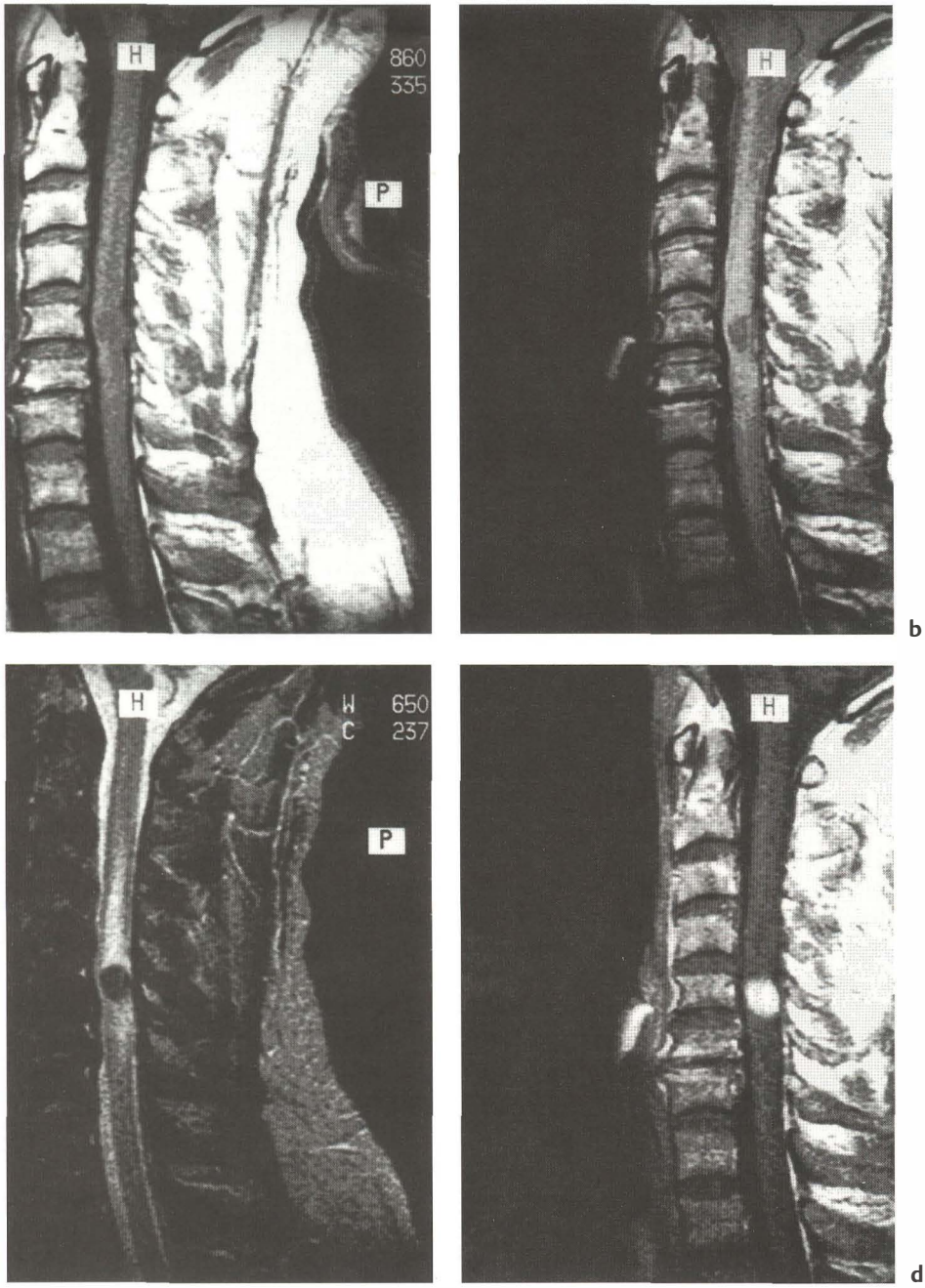

Fig. 68 **Intramedullary spinal cord neurinoma** (case *154*). **a** Sagittal T1-weighted image, **b** proton density weighted image, **c** T2-weighted image, and **d** postcontrast T1-weighted image. There is a hypointense, well-delineated mass with intense enhancement after gadolinium administration. There is also moderate peritumoral edema. Retrospectively, the fact that this lesion was embedded in the cord might have been suspected by examining the posterior aspect of the spinal cord on the sagittal T1-weighted image, which showed small indentations at the border between the tumor and the spinal cord. This case illustrates how difficult it can be to differentiate intramedullary from extramedullary tumors, even when axial cuts are made (**e**). **f** The lesion is also detected on a contrast-enhanced CT scan (courtesy of Dr. P. Parizel, UZA Antwerp, Belgium)

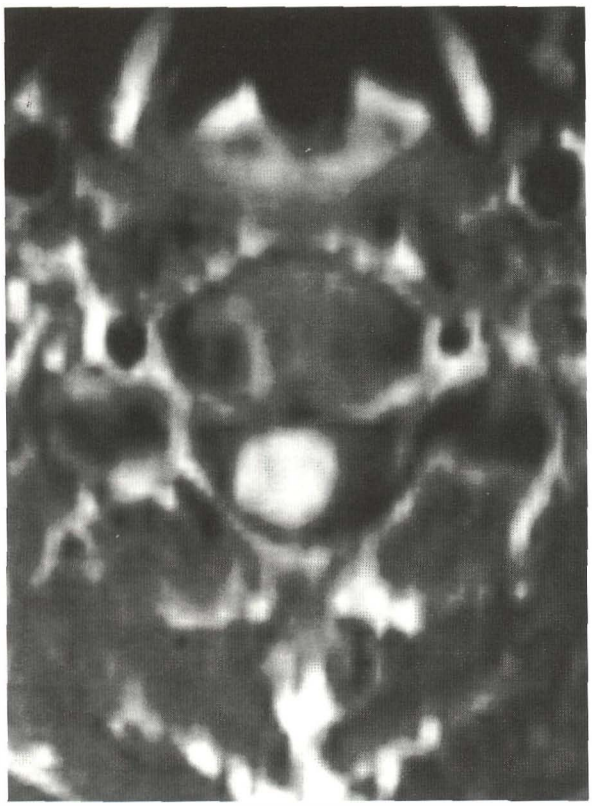

Fig. **68e**

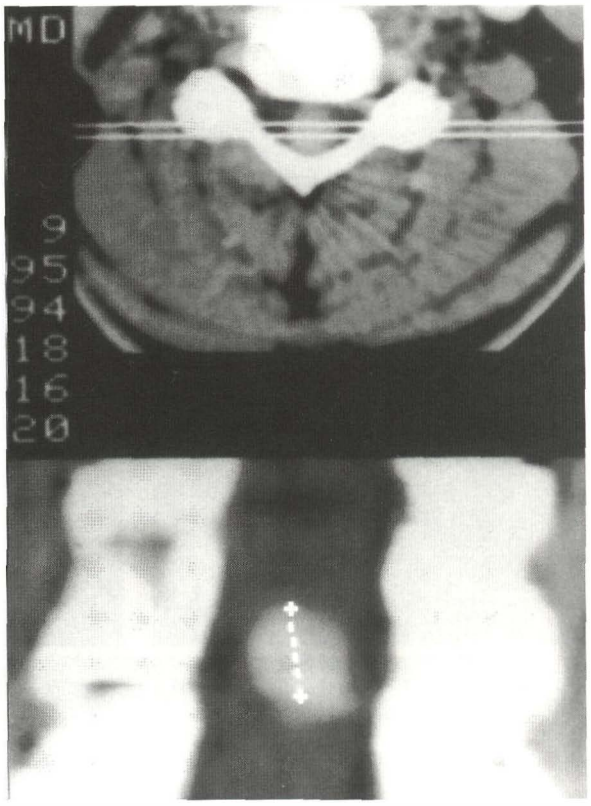

Fig. **68f**

Although the superficial portion of the tumor can be easily removed, the same is not true of the deepest portion of the tumor. Where the lipoma is attached to the spinal cord, it is hard and extremely adherent to the underlying nervous tissue. In our series, only one small lipoma *[150]* was completely removed, without damage to the spinal cord. However, we observed clinical worsening after an attempt to totally remove another T4–T6 lipoma *[152]*. All authors recommend subtotal removal, even when using a CUSA or laser, or both (39, 41, 60, 149, 170, 179). To avoid damaging the cord, a thin rim of tumor should be left (41). The lipoma–spinal cord interface, where the fibrous base of the lipoma is adherent to the spinal cord parenchyma, cannot be visualized, even using high-power magnification with the operating microscope. The lipoma–spinal cord union is comparable to a tightly glued collage: any attempt to separate these tissues is catastrophic.

Angiolipomas and other lipomas with a vascular component are subtypes of extradural spinal cord tumors, which are infrequently intramedullary (209).

Neurinoma

If any proof were needed of the existence of intramedullary spinal cord neurinomas, it would suffice to show the photograph of the specimen published by Langford et al. (137) (Fig. **65**). In fact, although the location is indisputable (i.e., a lesion entirely embedded in the spinal cord and circumscribed by cord tissue), the distinction between intramedullary spinal cord schwannoma (Fig. **66**) and pseudoneurinomatous ependymoma (Fig. **67**) remains difficult using intraoperative histological examination as well as the usual techniques.

Various hypotheses, involving pathogenic malformation, etc., have been advanced and published in the literature (1, 106, 116, 145, 226, 230, 234). In fact, these tumors always arise from the Schwann cells located in the dorsal root entry zone. This explains why a schwannoma, usually and classically extraspinal, exerts pressure on the cord, may in some cases appear both intramedullary and extramedullary (92) and – even rarer – still completely intramedullary (106, 116, 226). This unifying conception is, in our opinion, both simple and logical. According to this hypothesis, the various locations are simply topographic variants of the same radicular

schwannoma. In the series compiled from the SNCLF investigation, there were 19 schwannomas in 1117 cases (1.5%). In our personal series, there were two cases of extramedullary and intramedullary schwannomas, one of which *[154]* was a benign tumor (Fig. **68**) and the other an infiltrating tumor in a patient with end-stage neurofibromatosis type 2 *[155]*.

The diagnosis of intramedullary spinal cord schwannoma is difficult to establish with imaging techniques, and its presence is not always confirmed by its operative appearance. The surgeon may be misled by a blackish appearance, in the case of melanotic schwannomas (158). Only the final histological examination allows definitive identification.

Meningioma

Intramedullary meningiomas are extremely rare. There were only five cases of meningeal tumors in the SNCLF study, including our own case *[156]*, which was actually an extramedullary and intramedullary hemangiopericytoma and was removed without particular difficulty. Salvati et al. (235) reported one case and three from the literature, each with different histological features. The case reported by Barth et al. (17) was an intramedullary meningeal melanocytoma which, despite its benign features, became disseminated in the cerebrospinal fluid after incomplete removal.

2.4 Pseudotumors

We apply this term to the most common lesions that have the appearance of IMTs and present the same surgical problems. We have excluded intramedullary bacterial abscesses (132, 270), fungal infections (281), parasites (2, 278), tuberculomas (221), gummas, and, as a rule, all pseudotumoral lesions observed in infectious, inflammatory, and demyelinating diseases. We have also excluded all diffuse intramedullary spinal cord lesions associated with histiocytosis-X (3), Leigh's disease (119), neuromyelitis optica (Devic's disease) or acute necrotizing myelopathy (224), and, as a rule, all nontumoral diffuse infiltrating glioses and lesions responsible for an enlarged spinal cord. Lastly, we should point out that the intramedullary spinal cord signal, occasionally observed in myelopathies (73), may initially suggest the presence of an IMT.

Cavernoma

Intramedullary spinal cord cavernomas are vascular malformations that may remain asymptomatic for a long time, or cause acute or progressive spinal cord dysfunction. They are frequently undetectable on all imaging studies, with the exception of MRI. Cavernomas usually have a characteristic appearance on T1-weighted MRI and, more especially, T2-weighted and T2*-weighted images (T2*-weighted images are more effective in demonstrating heterogeneous areas containing hemosiderin). The characteristic appearance is that of heterogeneous intramedullary spinal cord lesions with hypointense areas on T2-weighted or T2*-weighted images, and frequently hyperintense areas on T1-weighted images. Spinal cord arteriography is normal. A personal or family history of cavernous hemangiomas, and MRI findings of an intracranial cavernoma, when present, are important in the diagnosis. In the SNCLF investigation, there were 27 cases in 1117 intramedullary spinal cord lesions (2.4%). There were five cases in our series. All had bled: four hematomas *[157, 159, 160, 161]* and one case of hematomyelia with unilateral spinal cord injury *[158]*.

The surgical strategy is the same as for hemangioblastomas: direct removal of the lesion if it is on the surface of the spinal cord, and a midline approach if it is not visible. The technique of removal is the same as for all IMTs. However, en bloc tumor removal seems preferable to us, although some authors prefer to fragment the lesion with the CUSA or laser, or both (168). Opinion is unanimous in recommending complete tumor removal in all patients with clinical signs (6, 43, 164, 171, 193). In the absence of disabling deficit, McCormick and Stein (168) recommend observation, while others, such as Anson and Spetzler (6), favor surgery. We will operate on cavernomas that are causing hematomyelia and those producing symptoms, but we have been quite conservative in recommending surgical removal of incidental cavernomas.

Dermoid and Epidermoid Cysts

Dermoid and epidermoid intramedullary spinal cord cysts behave very much like true IMTs. These lesions are congenital and not iatrogenic, as lesions sometimes are when they are seen in an extramedullary location. The clinical symptomatology is not pathognomonic. CT scanning and MRI allow a definitive diagnosis of such lesions (Fig. **69**).

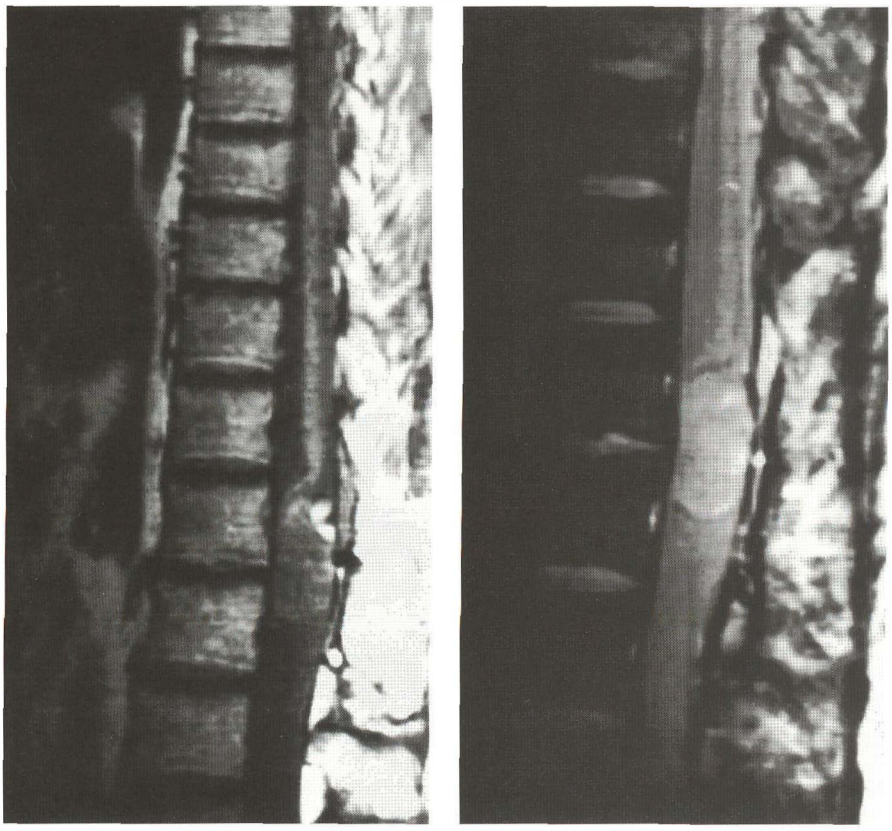

Fig. **69** **Epidermoid cyst** (case *164*). **a** Sagittal T1-weighted image and **b** proton density T2-weighted image. There is an oval-shaped mass at the level of the conus medullaris that is isointense to hypointense on the T1-weighted image and hyperintense on the proton density T2-weighted image. Epidermoid cysts may be hard to detect, as they appear to be isointense to cerebrospinal fluid on T1-weighted and T2-weighted images. Proton density T2-weighted imaging is therefore optimal

There were 32 cases out of 1117 (2.9%) in the SNCLF investigation, an incidence consistent with that reported in the literature (19, 42, 87, 94, 150, 205).

The apparent ease of surgical removal of these lesions is misleading. The pearly contents are indeed easily removed by suction, as is also the case when such lesions are found intracranially, but complete removal of the capsule is more problematic. In our four cases – two epidermoid cysts *[164, 165]* and two dermoid cysts *[162, 163]* – the fibrous attachment of the lesion to the spinal cord had to be left in place. Recurrence was observed 17 years later in one case *[164];* this patient underwent repeat surgery, and a good functional result was again obtained.

Pseudotumoral Cysts

By the term "pseudotumoral intramedullary spinal cord cysts," we mean cystic lesions that behave like true tumors, but which are of neuroglial rather than neoplastic origin on histological examination. We exclude meningeal (181), arachnoidal (191), and enterogenous cysts (241), which are not intramedullary spinal cord lesions. Only the "intramedullary spinal cord pseudocyst" described by Chuang et al. (36) fits the definition of pseudotumoral cysts. In the SNCLF series, the number of pseudotumoral cysts was 27 out of 1117 (2.4%). We also excluded intramedullary spinal cord neuroenteric cysts (177, 223), bronchogenic cysts (59) and teratomatous cysts (195), endometrium ectopic inclusions (229) and, generally speaking, all cysts with anhistic walls of the syringomyelic type (5, 210), with the exception of tumor-associated cysts of IMTs.

Our series included two very unique and quite different cases *[166, 167].* The first was a cystic IMT of the conus medullaris associated with dysraphism. The histological diagnosis was difficult to establish, and we called it a glioependymal cyst. The second case was a patient who underwent surgery three years after the onset of symptoms. The patient had a "holocord IMT" that was completely cystic, and which appeared to be absolutely consistent with a tumor. The histological examination proved negative. Despite a good neurological result, the outcome was marred by intra-abdominal and gastrointestinal complications, which were eventually fatal. Autopsy of the entire spinal cord showed an absence of any neoplastic tissue that might have been responsible for the cyst, which had a thick wall composed of reactive gliotic tissue. Our final diagnosis was a neuroglial cyst. These cases illustrate the diagnostic dif-

a

b

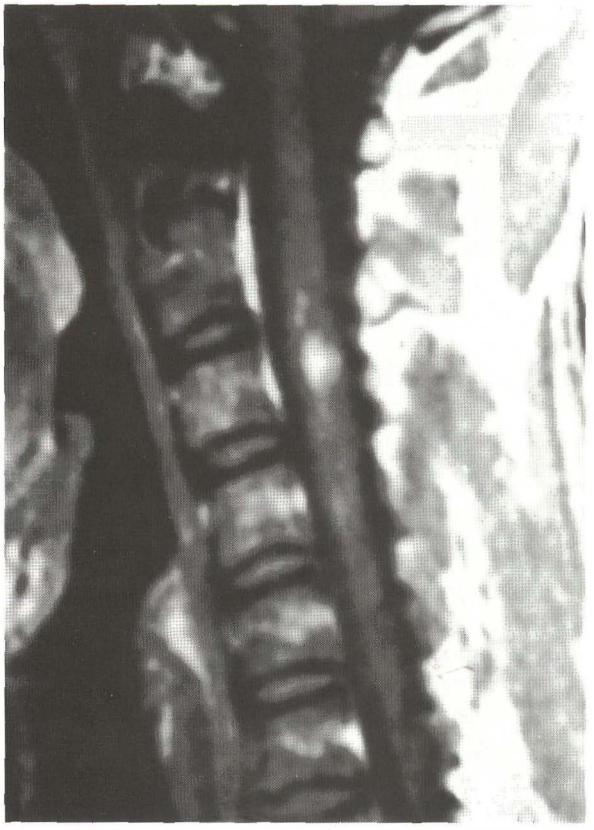

c

Fig. **70** **Cervical intramedullary spinal cord sarcoidosis** (case *170*) (refs. 146, 147). **a** Sagittal precontrast T1-weighted image. There is an isointense mild cord widening from C2 to C4. **b** The T2-weighted image reveals a hyperintense lesion. Postcontrast T1-weighted imaging shows nodular enhancement at the C3 level posteriorly (**c**) and laterally on the right (**d**). On the basis of these MR images alone, the differential diagnosis should include neoplasm, multiple sclerosis, and granuloma

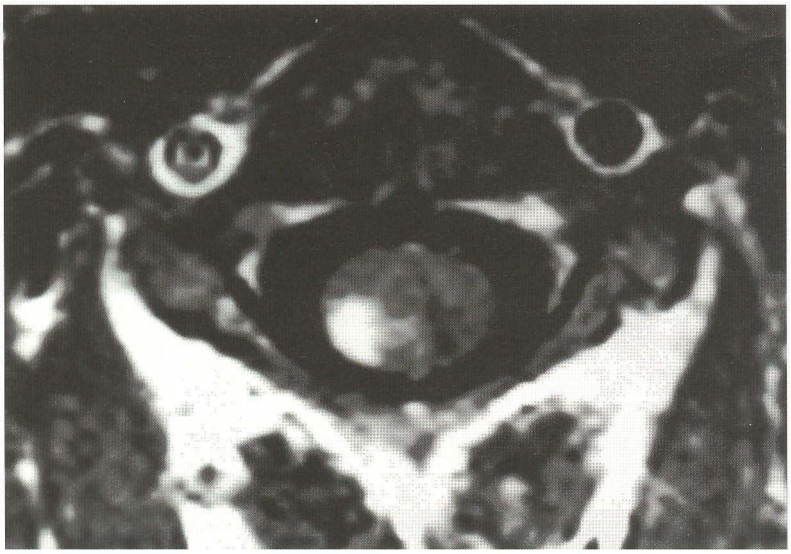

Fig. **70d**

ficulties encountered during surgery when the intraoperative histological examination fails to produce evidence of the tumoral nature of the lesion.

Sarcoidosis

Intramedullary sarcoidosis is rare. The SNCLF study reports five cases out of 1117, including our own three cases. Diagnosis poses few problems in patients with known sarcoidosis, as in one *[169]* of our three cases previously published (38, 280). This is not the case, however, when sarcoidosis presents as an IMT without other systemic manifestations (Fig. **70**), as in the two other cases *[168, 170]*, also previously published (146, 147). MRI is helpful (239), but not pathognomonic (146). The danger here is that one may be tempted to make a diagnosis of an infiltrating astrocytoma, and begin radiotherapy without biopsy. Intraoperatively, one finds a grossly infiltrating and unresectable lesion. Any attempt at removing a sarcoid granuloma is hazardous, pointless, and to no avail. It is much safer to carry out a biopsy and histological examination, particularly as medical treatment (corticosteroids and immunosuppressive agents) can improve the neurological condition of these patients (122). Sometimes, the MR appearance may even return to normal (146). However, intramedullary spinal cord sarcoidosis secondary to advanced ganglionic and pulmonary sarcoidosis responds poorly to medical treatment, which, in the long term, cannot control the neurological deterioration *[169]*.

3 Results

G. Fischer, J. Brotchi

The analysis of our results is based on 171 patients who underwent 200 operations performed over a fairly long period of time – up to 25 years, in the earliest cases. This must be borne in mind when evaluating the overall mortality rate.

3.1 Mortality and Complications

The operative mortality was 2.9%. Five patients died. One, a 66-year-old patient who underwent surgery for a cervicothoracic ganglioglioma *[107]* died two days postoperatively due to a pulmonary embolism. Two succumbed ten days after surgery *[24, 155];* the first, a 31-year-old man, underwent a second operation for a malignant cervicomedullary extension of a thoracic ependymoma that had initially been treated surgically three months earlier *[24],* and the second, a 34-year-old woman with end-stage neurofibromatosis type 2, underwent surgery for an infiltrating cervicothoracic extramedullary and intramedullary neurinoma *[155].* A 40-year-old woman who underwent surgery for a cervicomedullary ependymoma *[6]* died of respiratory distress 22 days postoperatively; and finally, a 44-year-old man who had undergone removal of hemangioblastomas in the cerebellum and medulla, and was dependent on a respirator, died 66 days postoperatively of brain stem dysfunction *[140].*

The early mortality (within the first postoperative year) was as follows: 15 patients died, 12 of whom had undergone surgery for malignant tumors *[61, 78, 104, 105, 108, 110, 117, 118, 119, 121, 122, 123].* Of the three others, one was a 21-year-old man *[97]* who underwent radiotherapy without biopsy before surgery for a cervical grade II astrocytoma. Postoperatively, his condition was unchanged, and he remained bedridden until his death nine months later. The second patient, a 49-year-old man *[98],* only underwent a biopsy for an infiltrating cervicomedullary astrocytoma; the third, a 40-year-old man *[167],* presented with a holocord lesion which was not completely removed, and he died 72 days postoperatively after a series of gastrointestinal complications requiring several operations.

The intermediate mortality (1–5 years) and long-term mortality (more than five years) was also evaluated. Eighteen deaths occurred between one and 22 years after surgery. In 14 patients, tumor growth was the immediate cause *[21, 66, 82, 85, 99, 101, 102, 103, 113, 114, 115, 116, 120, 130].* Three died of complications related to their neurological condition *[36, 131, 135].* Finally, a single patient died of intercurrent disease five years after surgery *[25].*

Surgical complications had no effect on the mortality rate, and included the following: hematoma *[128, 137],* sepsis *[67, 93, 98],* meningocele *[143],* cerebrospinal fluid fistula *[40],* pulmonary embolism *[134],* and a perforated gastric ulcer *[106].*

3.2 Functional Results

The evaluation of IMT surgical results requires separate analysis of specific preoperative and postoperative symptoms (Table **2**). The determination of mortality was based on the total number of patients (171), but the analysis of functional results is based on the total number of operations performed (200), as some patients underwent two operations several years apart. It appears that the patient's functional state is a much more realistic basis for evaluation than a detailed analysis of symptoms. This evaluation must take into account both motor and sensory function, as proposed by McCormick (169) and described below in the section dealing with motor deficit (pp. 87–88).

Patients who have undergone surgery for IMT invariably experience discomfort on awakening in the recovery room. They are in pain, frequently complain of discomfort, and are quite anxious, often more so than patients who have undergone surgery for other conditions. They feel pain everywhere, and have diffuse hyperesthesia and paresthesias. They cannot, or dare not, move. Position sense in the extremities is poorly perceived. Muscle and spinal pain complete this picture of discomfort, which lasts for

several days and is quite unresponsive to the usual analgesic drugs. The disorganization of the sensory pathways shows itself in disturbing and disruptive ways, but is transient and lasts about a week. The severity of this postoperative picture depends on the extent of the surgery; it does not lend itself to objective neurological evaluation, as it is variable and changes from day to day.

Prior to the patient's discharge from the hospital, a basic functional evaluation is made to document motor and sensory function. An increase in postoperative deficit, of varying severity, is seen in nearly all patients. Although this early evaluation provides important information, it does not allow any prognosis to be made, even for the medium term.

It is not until the third postoperative month that an accurate idea of the patient's neurological function can be obtained. The intermediate assessment made at this time is the first assessment of fixed deficits. It is mainly an evaluation of the sensory deficits. The deficits observed, at three months and later, are the permanent sensory deficits, i.e. heat/pain, two-point discrimination, touch and vibration sense. At this time (three months after surgery), motor and sphincter deficits are not yet fixed and may still improve or worsen, or become associated with spasticity or intractable pain, or both.

Long-term evaluation is more difficult to establish. In our opinion, long-term evaluation really begins five years after surgery. However, the columns in Table **2** reporting our long-term results include all patients who were actually followed up for more than one year after surgery, i.e., with the exception of those who were lost to follow-up or who died before the end of the first postoperative year. The information therefore represents an evaluation of sequelae, based on the most recent examination, at least one year after surgery and up to 29 years for the patient with the longest follow-up. The actual long-term evaluation, i.e., for patients with at least five years' follow-up, is discussed below (pp. 99–104).

Table **7** **Preoperative and postoperative sensory deficits**

		Pre-operative	Post-operative
No sensory disorders		24	9
Unchanged	7		
Worsening	17		
Anesthesia below the level of the lesion		22	39
Improved	3		
Unchanged	14		
Worsening	5		
Deficit below the level of the lesion		101	107
Improved	13		
Unchanged	64		
Worsening	24		
Brown–Sequard syndrome		13	16
Improved	1		
Unchanged	7		
Worsening	5		
Segmental pain/temperature postoperative deficit		40	29
Improved	2		
Unchanged	24		
Worsening	14		
Total operations		200	200

Sensory Deficits

Is it possible for a patient presenting with an expansive intramedullary spinal cord lesion to show no abnormalities on sensory examination? It is extremely unlikely, and even less likely after myelotomy and tumor removal.

In fact, very few patients in our series were free of any objective sensory deficit before surgery, and even fewer after surgery (200 operations). The sensory examination was essentially normal before surgery in 24 patients (12%), and after surgery in nine *[13, 28, 55, 76, 136, 151, 153, 156, 171]* (4.5%). In this small group, there were only two patients *[55, 156]* (1%) whose preoperative objective sensory deficit completely resolved after surgery.

Before surgery, only one patient *[83]*, of the 43 (Table **5**) who underwent preoperative SEP evaluation, had normal responses after upper and lower limb stimulation and no changes in the responses in the T5–T7 segments, where she had decreased pain and temperature perception.

After surgery (Table **5**), the value of SEPs as the most sensitive means of evaluating the sensory pathways was confirmed in the 44 cases studied. Thus, in the ten patients with postoperative exacerbation of sensory deficits, eight continued to have significant lasting SEP abnormalities; moreover, all ten patients, whose sensory deficit improved to some extent, also retained SEP abnormalities. Preexisting sensory deficits were unchanged after surgery in 117 cases (58.5%) and were worse in 63 cases (31.5%). Of the patients whose sensory deficits worsened, they were markedly worse in four cases *[19, 61, 97, 159]* and slightly worse in 59 cases. Sensory deficits improved in only 20 cases (10%), including two patients whose deficits completely resolved *[55, 156]*.

Intermediate and long-term results after 200 surgical procedures are shown in Table **7**. Sensory deficits changed little after the third postoperative month.

Motor Deficits

Unlike sensory deficits, motor deficits are not at all fixed at the end of the third postoperative month. The evaluation made at that time shows the stages of functional recovery.

The only clinical classification available for evaluating the functional condition of IMT surgical patients is the four-grade system proposed by McCormick (Table **3**, p. 20), which is simple and can be applied to a large series of patients. It is based on the practical concepts of independent gait and autonomy in everyday activities that are the best indicators of outcome in patients who have undergone surgery for IMT. We therefore used this classification with each of the 171 patients of our series to compare function before surgery, in the early postoperative period (discharge evaluation), at three months after surgery, at one year after surgery, and during the long-term follow-up. Detailed data are shown in Table **2** and summarized in Table **8**.

When early postoperative function (discharge evaluation) was compared with preoperative

Table **8** **Follow-up** of the 200 procedures for intramedullary spinal cord tumors, according to the McCormick classification (Table 3, ref. 169). The postoperative course (improved, status quo, worsening, early reoperation) has been detailed for each category of patients during the first year after surgery, beyond which the neurological status is mostly unchanged

McCormick classification	Preop.	Postop.	3 months	1 year	Latest evaluation
Grade I	59	26	53	61	57
Improved	–	–	–		
Unchanged	26	24	50		
Worsening	33		3		
Reoperation	–	2	–		
Grade II	89	69	69	60	48
Improved	1	24	8		
Unchanged	42	41	57		
Worsening	46	3	4		
Reoperation	–	1	–		
Grade III	30	67	38	22	14
Improved	4	31	10		
Unchanged	19	30	23		
Worsening	7	3	5		
Reoperation	–	3	–		
Grade IV	22	33	22	20	6
Improved	1	9	22		
Unchanged	21	22	–		
Worsening	–	–	–		
Reoperation	–	2	–		
Reoperations (n = 29)			8**	7*	14*
Improved			3	–	2
Unchanged			4	4	11
Worsening			1	3	1
Postoperative follow-up	200	195	190	170	139
Deaths (n = 38)		5	5	10	18
Lost to follow-up (n = 8)				2	6
Patient follow-up	171	166	161	149	125

* Second operation.
** Two-stage operation.

function, there were 86 patients whose condition worsened, 108 in whom it was unchanged, and six who improved. In fact, the condition of each patient was at least slightly worse for a few days. However, an evaluation of postoperative neurological function just prior to hospital discharge showed an early improvement in a good number of patients.

A comparison of neurological function, evaluated at the most recent postoperative examination (but at least one year after surgery), with preoperative function was possible in 163 patients: 61 of 163 patients were rated grade I, 60 grade II, 22 grade III and 20 grade IV, at the end of the first postoperative year. During the same period, seven patients underwent repeat surgery.

The postoperative evaluation at three months indicates the intermediate results between the patients' early postoperative function and their function at one year: 64 patients had improved at the end of the third month after surgery, and 18 additional patients had improved after one year; 117 had an unchanged condition at the end of the third month; six were worse at the third month, and 12 were worse after one year, related to tumor growth or recurrence.

Even in the best of circumstances, therefore, the patient's long-term neurological condition will be the same as the condition he or she presented with prior to surgery. With rare exceptions, patients do not recover from severe preoperative neurological deficits, and those patients who do not have disabling deficits after surgery are those who exhibited few or no deficits prior to operation. Finally, after surgery, motor function improves over a longer period of time than sensory disorders, at least until the end of the first postoperative year. After that time, any increases in motor deficit, and any decreases in the patient's functional capacity, suggest tumor recurrence, usually due to regrowth of a malignant tumor.

Postoperative Spinal Deformity

Spinal deformity may be one of the earliest symptoms leading to the discovery of an IMT, particularly in children. The danger in preoperative assessment lies in treating an apparently idiopathic kyphoscoliosis with metal internal fixation devices, which then have to be removed in order to diagnose and treat the IMT, as in one of our cases *[79]*.

With postoperative spinal deformities, the sometimes extensive laminectomies required for the surgical treatment of IMTs may be responsible for impressive, though fortunately rare (57, 58), disorders of spinal stability observed in the long-term follow-up of patients with benign tumors.

Minor postoperative spinal deformations, such as increased lordosis *[40, 57, 136]* or scoliosis *[1, 10, 148, 152]* or, most often, kyphosis or kyphoscoliosis (20 cases) of varying degrees of severity, were observed in 27 of the 171 patients (15.8%). In eight patients, these deformities were present prior to surgery, and were not exacerbated by surgery.

Severe postoperative spinal deformity was observed in ten of the 171 patients (5.8%). Of these ten patients, six had presented with a marked deformity prior to surgery *[8, 76, 81, 94, 101, 133]*, two had had a cervical deformity *[30, 109]*, and two others had had a normal cervical spine before surgery *[21, 28]*. The severe deformity stabilized spontaneously in seven patients; in three others, the deformity progressed, requiring anterior *[30]* or posterior *[101, 109]* surgical stabilization. These ten cases are summarized in Table **9**.

Four factors are responsible for these severe postoperative deformities: young age (four children aged 2–12 years, six adults); the presence of preoperative spinal deformity (eight cases); cervical laminectomy including C2 (nine of the ten cases), laminectomy involving at least six vertebrae (eight of the ten cases); and malignant neoplasm or adjunctive radiotherapy, or both (three cases). Two or more of these factors were present in eight of the ten patients. The risk of postlaminectomy spinal deformity is well known, especially in children (125, 172, 258, 293). In our series, which includes only 11 children, four (36%) had a significant postoperative spinal deformity. Awareness of the risk factors can enable the surgeon to prevent such deformities by avoiding injury to intervertebral joints, by using osteoplastic laminotomy in children (64, 68, 199, 212, 213) followed by at least four months' immobilization of the spine, by orthopedic and radiological monitoring until the end of the child's growth period, and by not giving radiotherapy to patients with benign IMTs. However, osteoplastic laminotomy may result in a very effective fusion, with a solid block of bone forming the posterior border of the spinal canal. We therefore do not recommend the use of this technique in patients with benign tumors that have been incompletely resected, if repeat surgery is contemplated at a later date *[41]*.

Apart from the cases described above, most postoperative spinal deformities in our series eventually stabilized. Any secondary recurrence of spine deformation should arouse suspicion of tumor recurrence and, regardless of the spinal level, requires radiologic follow-up for several years.

Table 9 **Major postoperative spinal deformities**

n	Histology	Age	Preoperative deformity	Lamin-ectomy	Radio-therapy	Major postoperative deformity
8	Grade II ependymoma	27	Thoracolumbar kyphoscoliosis	C1–T11	0	Thoracolumbar kyphoscoliosis
21	Grade II ependymoma	48	Normal on radiograph	C3–C7	60 Gy	C5–C6 kyphosis
28	Grade II ependymoma	36	Normal on radiograph	C2–T2	0	Cervical kyphosis
30	Grade II ependymoma	58	Deformation of cervical curvature	C1–T1 + occ. craniectomy	0	Cervical kyphosis (postoperative osteosynthesis)
76	Grade I pilocytic astro-cytoma	2	Thoracic scoliosis	T7–L2	0	Thoracic scoliosis
81	Grade II ordinary astro-cytoma	24	Kyphoscoliosis	C1–C6	0	Cervicothoracic kyphoscoliosis
94	Grade II ordinary astro-cytoma	9	Cervical kyphosis	C1–T1	0	Cervical kyphosis + thoracic scoliosis
101	Grade III ordinary astro-cytoma	10	Cervical kyphosis	C2–T1	40 Gy	C2–C3 kyphosis (postoperative spinal fusion)
109	Grade II ganglioglioma	12	Deformation of cervical curvature	C1–C2 + occ. craniectomy	60 Gy	Cervical kyphosis (postoperative osteosynthesis)
133	Hemangio-blastoma	53	Cervical kyphosis	C1–T4	0	Cervical kyphosis

Pain

The severity of dysesthesia and pain of various origins (and the difficulty of relieving it) is a well-known phenomenon in the early postoperative management of IMTs. The radicular and spinal cord sensory pathways adjacent to the area of surgery will manifest a temporary dysfunction that is both diffuse and difficult to classify.

Invariably, at some time after surgery, there will be an appearance or exacerbation of acute, chronic, and intractable pain of variable severity. One may also see diffuse and permanent paresthesias that reduce the patient's quality of life, and for which pharmacological treatment is not very effective. Fortunately, these phenomena are often less severe, and are merely an annoyance which patients are eventually able to adapt to.

In 144 patients with more than one year of postoperative follow-up, only 31 (21.5%) have no complaints of pain, while the other 113 (78.5%) have one or more types of pain. Fifty-seven patients (40%) have spinal pain. In 34, the pain is localized to the cervical or interscapular region, or both; in 15, the pain is thoracic; and in eight, it is localized to the lumbar region. Pain is a result of the laminectomy, impaired vertebral stability, and, in elderly patients, vertebral osteoarthritis. Fifty-four patients (37.5%) have pain or paresthesias, or both, in a radicular distribution. In 19, it involves the upper limbs, in ten the lower limbs, and in 15 the thoracic region. Fifty-one patients (35%) complain bitterly of paresthesias below the level of the lesion, either confined to the extremities (40 cases) or diffuse (11 cases). A few patients are suffering from intractable pain despite chronic treatment. No patient underwent surgical treatment for pain. Dorsal column stimulation was performed in two patients *[159, 162]*, and intrathecal morphine was administered to one patient *[58]*.

Spasticity

Myelotomy and excision of IMTs impairs the presynaptic or postsynaptic descending inhibitory pathways to radicular afferents, to variable extents. Injury to intersegmental neurons and interneurons connecting the anterior and posterior horns causes impairment of the mechanisms that control tone, and seems to be responsible for extensor spasticity. Initially, lower limb spasticity, closely linked to the motor deficit it often aggravates, struck us as being a particularly severe and frequent sequela in patients who had undergone surgery for IMT (77).

However, when the series was reviewed, the postoperative spasticity (Table **2**) proved to be slightly less frequent (44% of cases) and – most importantly – less severe than we had originally thought. In 144 patients with more than one year of follow-up, 11 currently have severe spasticity impairing their quality of life, 31 have less serious spasticity, not interfering with walking or normal upper limb function, 21 are slightly spastic on clinical examination, and 81 patients (56%) are not spastic. It was our intention to try to prevent this complication by closing the spinal cord upon completion of the procedure, using a very fine interrupted pial suture, a technique used for a number of years now. When possible, the arachnoid was also sutured. We were able to do this in 24 patients undergoing surgery either for the first time (22 cases) or for the second time (two cases) *[2, 60]*.

The factors causing postoperative spasticity are too numerous for a correlation to be established between suturing of the pia mater at the end of the operation and the presence or absence of spasticity; however, the restoration of normal spinal cord morphology is unlikely to have any adverse effect.

Sphincter Dysfunction

Sphincter dysfunction (principally urinary difficulties) and sexual difficulties cannot be dissociated from the paraplegic or tetraplegic picture with which they are associated, particularly in the early postoperative period. In the long run, these disorders may emerge from a background of fixed deficit to become the most important part of the clinical picture, warranting specialized management and care.

We took pains to document the urinary disorders experienced by all our patients (Table **2**), especially those persisting after the first postoperative year. In 144 patients with one year of follow-up, 27 (19%) still needed an indwelling catheter or intermittent urinary catheterization; 25 (17%) had or still have urinary disorders, such as dysuria of variable severity, delayed micturition, urinary incontinence, or episodes of urinary infection; 92 (64%) have no urinary difficulties. Along with this, seven patients *[10, 53, 58, 100, 116, 131, 158]* had severe persistent constipation or fecal incontinence, and five males *[11, 29, 71, 93, 159]* complained of sexual disorders (impotence, disorders of erection or ejaculation).

3.3 Postoperative Outcome and Follow-Up

Neuroradiological Follow-Up

D. Balériaux, J.-C. Froment, C. Matos, P. Tournut, P. David

MRI is the examination of choice for postoperative follow-up of IMT patients. The examination must be complete, i.e., it should include T1-weighted, T2-weighted, and post contrast T1-weighted sequences, and at least two perpendicular planes (sagittal and axial scans). In this context, three-dimensional imaging is essential, as it allows fine resolution of the spinal cord and reconstruction in different complex planes, which may be particularly important in patients with vertebral instability (Fig. **71**).

Plain radiographs provide excellent information on the effects of laminectomy on the spine. Abnormalities that can be seen with plain films include abnormal curvature, spinal deformity, impaired spinal stability, and kyphosis or scoliosis, or both. These findings may be present prior to surgery, or may occur as a result of laminectomy. After extensive laminectomy in children, these abnormalities are especially common. These postoperative changes may not be apparent on plain films after laminotomy (Fig. **72**).

Postoperative MRI examination: Timing

Postoperative imaging and the interpretation of MRIs must be meticulously correlated with the operative report, and must take the histological nature of the lesion into account. Early MRI is useful only if it is carried out in the very first postoperative days (Fig. **73**). Later, an examination at six months is recommended. Long-term follow-up depends on the histological nature of the tumor and the type of surgery performed. In the case of benign tumors, the frequency and timing of the follow-up examination depends on the progression of symptoms; for malignant tumors, examinations should be carried out

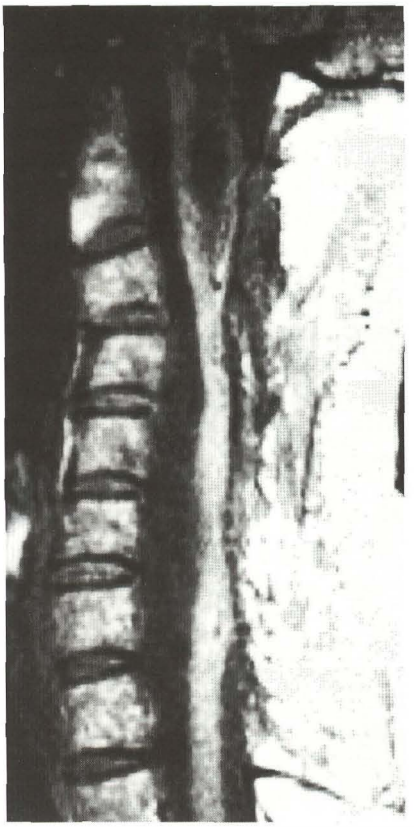

a

b

Fig. **71** **Kyphoscoliosis after extensive laminectomy for a cervical grade II ependymoma** (case *30*; same case as in Fig. **55**). **a** At the first postoperative study, performed three months after total resection of the mass, the previously observed cavities are reduced in size. No contrast enhancement is seen. The spine still has a "straight" appearance. **b** In the postoperative MRI, six months after surgery, kyphoscoliosis involving the entire cervical spine is seen. **c** One year after surgery. The information provided by this three-dimensional 5-mm slice should be compared with the three-dimensional 0.8-mm sagittal gradient echo acquisition image (**d**), allowing reconstruction of complex coronal images (**e**) along the plane of the spinal cord (indicated by the arrowheads in **d**). The remaining small cysts are definitely better shown on these thin slices

c

d

Fig. **71 e**

every six months for a period of two years, followed by annual examinations for five years, or more frequently if the course of the disease is especially rapid (Fig. **57**).

Morphological Analysis

The purpose of MRI examination is to study the condition of the spinal cord, its size and contours, the condition of the parenchyma, with evaluation of its signal, the disappearance of edema, and contrast enhancement by residual or recurrent tumor. MRI can also be used to follow up the size of intramedullary cysts, visualize the subarachnoid space and its relationship to the spinal cord and dura, and provide a general idea of vertebral alignment. MRI also allows assessment of postoperative adhesions between the spinal cord and the dura, and the patency of the posterior subarachnoid space observed when the spinal cord has been closed using pial sutures at the end of the procedure.

Postoperative Changes

Postoperative evaluation is carried out in widely varying circumstances, depending on whether tumor removal was macroscopically total or subtotal, partial or incomplete, or if only a biopsy was performed.

Macroscopically Complete Removal of a Solid Tumor

Reduced spinal cord size is observed (Fig. **74**). The cord appears atrophic at the site of tumor removal. The extent of the atrophy is a function of the initial size of the tumor. At the site of tumor removal, a residual cavity, which usually regresses over time, may be observed (Fig. **62**). However, the size of the spinal cord seldom returns to normal, except in patients with small noncystic tumors (Fig. **28**).

Preoperative spinal cord edema, when present, will completely disappear. Whatever the histological nature of the primary tumor, progressive collapse of cystic cavities usually occurs within a few months (Fig. **27**), and is even more rapid in the case of hemangioblastomas (Fig. **28**) (256).

The cord may be free or, on the contrary, adherent to the dura mater due to scarring, and is well documented with MRI (167). The severity of the adhesions correlates with the way in which the spinal cord was or was not closed after surgery.

Early punctiform or linear contrast enhancement, or both, at the edge of the area of resection, or even within the resection cavity, can sometimes be observed. These enhancements may be transient and, therefore, retrospectively attributable to surgery (transient inflammatory vascular congestion). Subsequent MRI examination should be performed to make certain that these changes disappear. Prior to contrast medium injection, it will, of course, be necessary to carry out T1-weighted MRI without injection in order to identify areas with increased signal, which may either be due to blood in the early stage, or small artifacts (usually thought to be microscopic metal particles) (Fig. **75**).

When tumor removal has been macroscopically complete, with a normal initial MRI examination, subsequent examinations are still necessary to make certain that there has been no recurrence. These examinations should be frequent when histology has shown a potentially rapidly growing lesion (particularly a high-grade astrocytoma or a melanoma). The appearance or reappearance of contrast enhancement suggests tumor recurrence or resumed progression of tumor growth (Fig. **76**). In the particular case of a patient who has received prior radiation to the area of tumor, it may be particularly difficult to distinguish residual tumor (93) from radiation necrosis, or "nontumoral fibrosis" (Fig. **77**).

Incomplete Tumor Removal and Tumor Biopsy

Early MRI examination is of particular value when trying to demonstrate the presence of residual tumo-

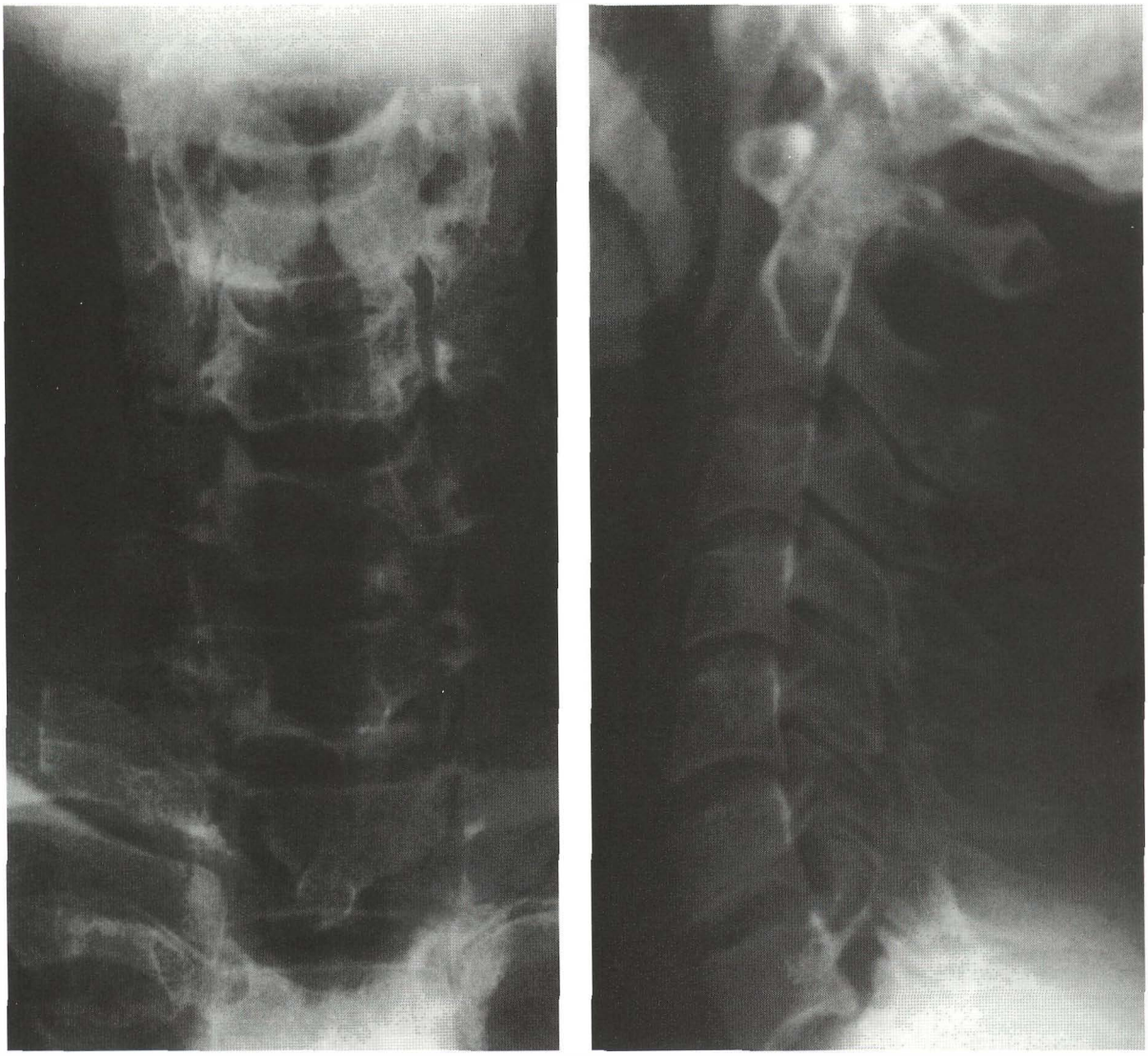

Fig. **72** **Grade II cervical ependymoma** (case *23*). Plain radiographs, lateral view, 20 days after a C2–T1 laminotomy for the ependymoma in a 44-year-old woman

ral tissue. Diagnosis of residual tumor is easy when the lesion was found to enhance after contrast injection prior to surgery. If there was no medium enhancement preoperatively, the diagnosis is more difficult, and is mainly based on the presence of residual increased signal on T2-weighted images (Fig. **78**).

In the case of incomplete tumor removal or biopsy, the examination will accurately evaluate the residual tumor and serve as a baseline for assessing subsequent progression of the lesion. In high-grade lesions, subsequent examinations will demonstrate the rapid progression of the tumor. In some cases, MRI will provide evidence of intramedullary spinal cord or subarachnoid metastases, or both (Fig. **79**), or even brain metastases *[100, 102]* via the cerebrospinal fluid – as also happens, in the reverse direction, with malignant tumors of the posterior fossa *[115]*.

Postoperative Complications

Early complications are rare: hematoma at the operative site or epidural hematoma can be seen as an increased signal on MRI. Phenomena such as arachnoiditis are also exceptional, and may lead to the formation of postoperative arachnoid cysts that compress the cord.

Relevance of Radiotherapy

Radiotherapy has been used in the treatment of IMTs, but its efficacy has not been conclusively demonstrated. No randomized prospective study has ever been conducted with regard to the use of radiotherapy to treat astrocytomas or ependymomas (186).

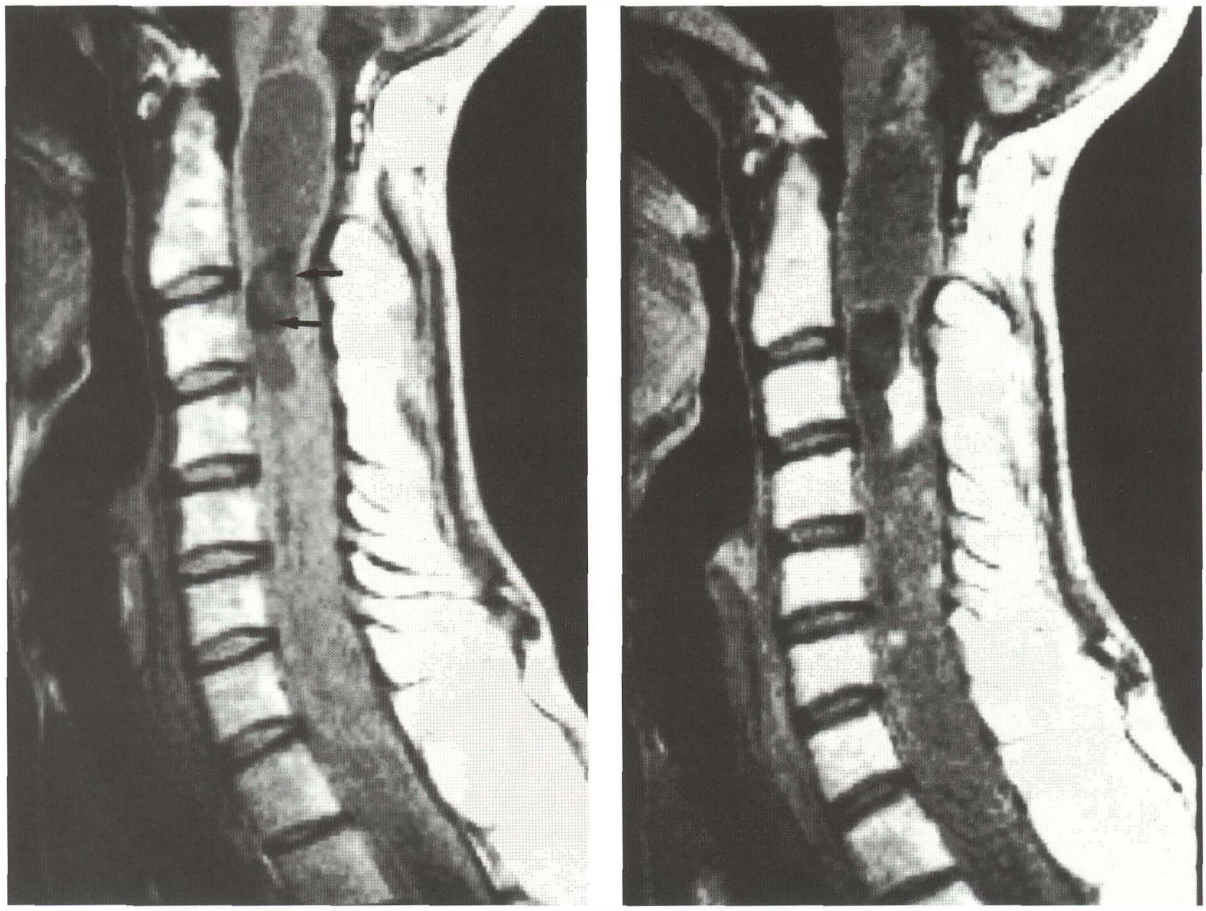

Fig. **73** **Hemangioblastoma: early postoperative MRI** (case *137*). **a** Sagittal precontrast T1-weighted image and **b** postcontrast T1-weighted image. Multiple intensely enhancing tumor nodules can be seen after contrast administration. A larger nodule is seen at the C3 level. Areas of decreased signal intensity are seen corresponding to old hemorrhagic foci (arrows). **c, d** The corresponding MR images, 24 hours after surgery. Recent hemorrhage is not seen. There has been an immediate decrease in the size of the spinal cord, and the cystic components are reduced in size. Complete removal of the nodule at C3 has been achieved, and the small remaining nodules are now better seen due to spinal cord decompression. Note the multiple small cutaneous artifacts due to suture material

Stein (165, 253, 254) does not recommend radiotherapy in patients undergoing surgery for benign intramedullary spinal cord tumors, even after subtotal or incomplete removal. He prefers to follow his patients up and carry out repeat surgery if necessary, and mentions that there is no proof of the efficacy of radiotherapy in malignant tumors. As early as 1977, one of the present authors (77) took a stand against any form of radiotherapy after complete or incomplete removal of benign intramedullary spinal cord ependymoma. Seventeen years later, the relevance of this opinion has been confirmed, as we have observed only one recurrence among 60 patients with benign ependymoma, the patient undergoing a second, macroscopically complete removal 18 years after surgery *[32]*. It does not seem more logical to use "low-dose radiotherapy" (less than 40 Gy), as authors who have had experience with it report have reported that it has no effect on the outcome (74).

We have come to the same conclusions with regard to low-grade astrocytomas. We are aware of the postoperative course of nearly all our 41 cases, with follow-up periods of up to 25 years for two of them. As recommended by Stein (253, 254), we did not treat any of our patients with radiotherapy, and we have no reason to regret our decision. In his numerous contributions on the microsurgical treatment of IMTs, Malis (153, 154) does not appear to favor radiotherapy, and in fact hardly mentions it. Cooper (39, 41), in marked contrast, advocates systematic radiotherapy for all infiltrating glial tumors, regardless of their initial grade and regardless of how

Fig. **73c**

Fig. **73d**

much has been removed. Epstein et al. (69) report that they noted no significant difference in the postoperative outcome in adult patients in relation to whether or not the patients had undergone adjunctive radiotherapy.

The efficacy of radiotherapy cannot be dissociated from the concept of dosimetry. The effective dose, i. e. 40 Gy or more, is hazardous to the spinal cord. In children, myelopathy has been reported to occur with doses of 30 Gy (262). The deleterious effects of radiotherapy on the vertebral column growth are well known to orthopedic specialists (255). In adult patients, doses exceeding 40 Gy cause subclinical functional abnormalities in the spinal cord, manifested by alterations in the motor and somatosensory evoked responses (49). In spite of this, some authors have continued to use these high doses (39, 41). In 1991, Whitaker et al. (286) recommended fractionated radiotherapy up to a total 50 Gy for both children and adults, irrespective of the tumor localization, extent of removal (complete or not), and histological grade, benign or malignant. The authors observed no spinal cord damage related to radiotherapy, and stated that "although the exact role of radiotherapy is ill-defined, low morbidity and long-term survival of patients with a tumoral residue are arguments in favor of radiotherapy."

The work of Kopelson et al. (131) has often been cited in the literature as an additional argument in favor of radiotherapy (41, 69, 186, 286). Their experience is based on a series of 12 ependymomas and 11 astrocytomas of all grades; 18 patients received either adjunctive radiotherapy (nine cases, including eight ependymomas) or postbiopsy radiotherapy (nine cases, including eight astrocytomas). Nine patients died of intercurrent disease between three months and 15 years. Despite eight failures (four ependymomas and four astrocytomas) in his series, he recommends radiotherapy at doses ranging from 40 to 50 Gy even after complete tumor removal, regardless of the histology and grade of the tumor.

Huddart et al. (112) treated 27 astrocytomas of all grades with radiotherapy (50 Gy) over a period of ten years. Seventeen patients were treated after biopsy, seven after partial resection, and three after subtotal resection. Sixteen patients had a recurrence of the

a

b

c

Fig. **74** **Total resection of a grade II lower cervical ependymoma** (case *5*; same case as in Fig. **25**). **a** Sagittal preoperative precontrast T1-weighted image and **b** postcontrast T1-weighted image. There is a well-circumscribed intramedullary mass, with associated cysts above and below the lesion. **c** Sagittal T1-weighted image after total removal of the lesion. There is focal atrophy of the cord, with a central cavity corresponding to the surgical site. No posterior adherence between the cord and the dura

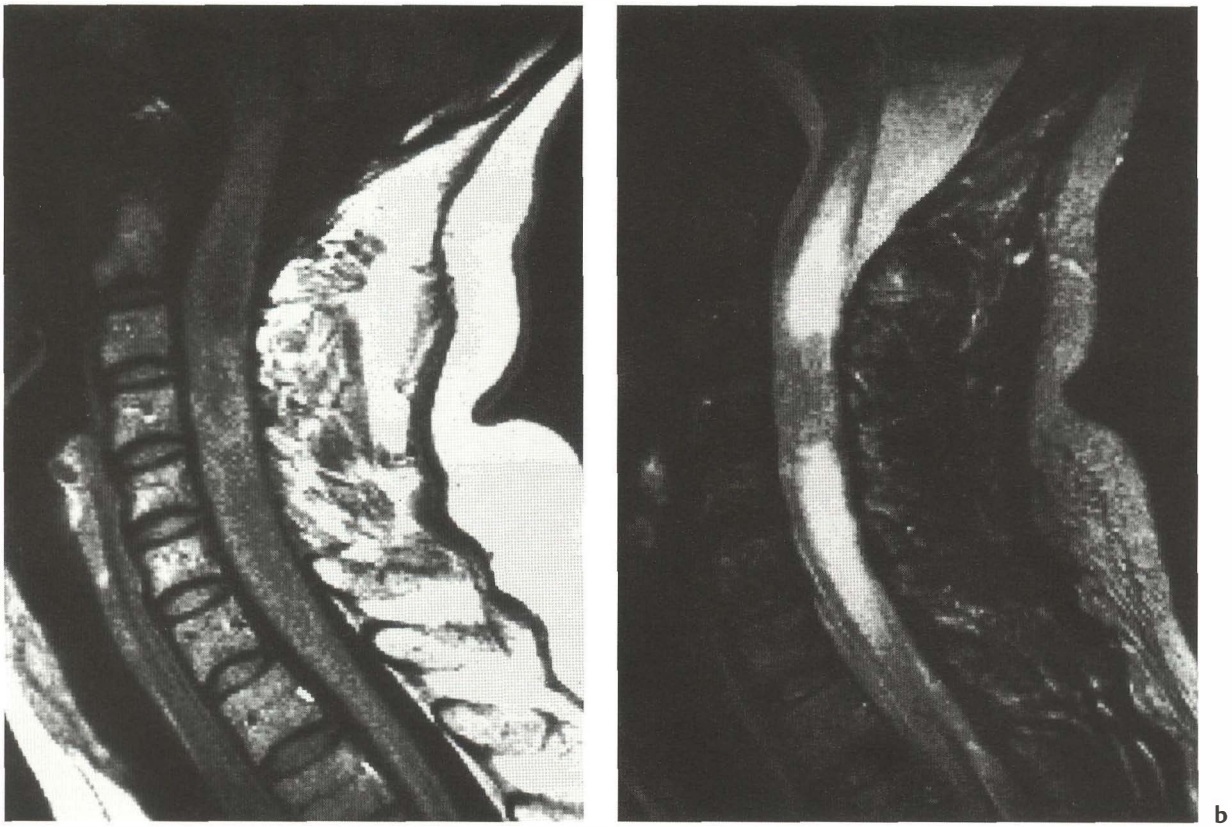

Fig. **75** **Grade II cervical ependymoma** (case *48*). **a** Sagittal T1-weighted image, showing an enlarged spinal cord from C2 to C7. The cord has a heterogeneous low signal intensity, with a slightly hyperintense component at C4. **b** On the T2-weighted image, the tumor is isointense with the spinal cord. Above and below the lesion, there are ill-defined hyperintense areas corresponding to edema. **c** The postcontrast T1-weighted image shows intense, homogeneous enhancement of the solid mass. **d** The postoperative control image shows localized spinal cord atrophy at the C4 level, with adhesion between the spinal cord and dura posteriorly. There is a small metal artifact within the cord (arrowhead). The edema (seen as an extensive low signal intensity area on the preoperative T1-weighted image has disappeared

tumor, 11 at the site of the original tumor and five at locations remote from the primary lesion. On the grounds that 53% of low-grade and 33% of high-grade astrocytomas were controlled three years after surgery, they concluded without reservation that radiotherapy of spinal cord astrocytomas is advisable, as is the case for cerebral gliomas. In 1987, Hardison et al. (103), expressed pessimism with regard to the outcome in children with IMTs, despite their use of radiotherapy after biopsy (17 cases), partial removal (five cases), subtotal removal (three cases) and complete removal (one case). In 1990, Rossitch (227) reported four recurrences after 45 Gy radiation administered to 12 children with low-grade astrocytomas.

There is no convincing evidence in the literature that radiotherapy is of any benefit in preventing tumor recurrence. Indeed, Sandler et al. (237) reported that seven of 15 low-grade IMT patients treated with surgery and radiotherapy (50 Gy on average) presented with a tumor recurrence within the irradiated area. The concept of "prophylactic radiotherapy" cannot be confirmed, in our experience. Its efficacy and harmlessness have not been demonstrated. A careful study (77, 255) of reports that purport to demonstrate a favorable role for this type of adjunctive therapy reveals that they rely, for the most part, on clinical follow-up over a short period of time, during which the beneficial effect of surgical decompression and the natural progression of these IMTs are not taken into account.

Finally, radical removal of a benign IMT is not technically impossible after radiotherapy (69, 165). Focal changes at the cord – tumor interface after radiotherapy will not interfere with surgical dissection (24, 257), because the surgeon can find a "new cleavage plane" (93). However, Stein appropriately emphasizes the deleterious effects of radiotherapy

Fig. **75c**

Fig. **75d**

on the spinal cord tissue adjacent to the tumor site, which can be seen at the time of reoperation (253, 255). Functional results are marred by these effects and, at the repeat surgery, the surgeon is bound to regret that the tumor was not radically removed during the first operation (80, 85, 93, 97).

In conclusion, our opinion regarding adjunctive radiotherapy is based on the above findings and the following caveats:

1. Why should one prescribe radiotherapy to patients whose benign IMT was macroscopically fully removed, and when long-term follow-up has shown that recurrence is not to be feared?
2. Why submit patients with incomplete removal of a benign IMT to radiotherapy when effective radiation doses are more deleterious to the cord than the tumor (not to mention spinal column damage), and low radiation doses are known to be ineffective?
3. Why should one recommend radiotherapy for recurrence or progression of benign tumors when the first effect of such therapy is to compromise the possibility of undertaking repeat surgery?
4. Our attitude regarding patients with malignant IMTs is less categorical: despite the poor results obtained with radiotherapy, 24 of our patients who underwent surgery for IMT received adjunctive radiotherapy, and we do in fact refer those with malignant IMT to radiotherapists and oncologists in the immediate postoperative period. However, having done so, we are aware that the indication for this palliative therapy is based more on compassion than on any proof of its efficacy.
5. Recommending radiotherapy without prior biopsy is indefensible.
6. We will not discuss chemotherapy of intramedullary spinal cord tumors here, as our experience is limited to a small number of patients (six cases). The lack of specific or recent publications on the subject confirms the fact that this is still at the experimental stage for the treatment of both intramedullary spinal cord ependymomas and astrocytomas (186). However, the use of chemotherapy is almost certainly inappropriate for benign IMTs, for the same reasons that make radiotherapy unsuitable, both in children and adults.

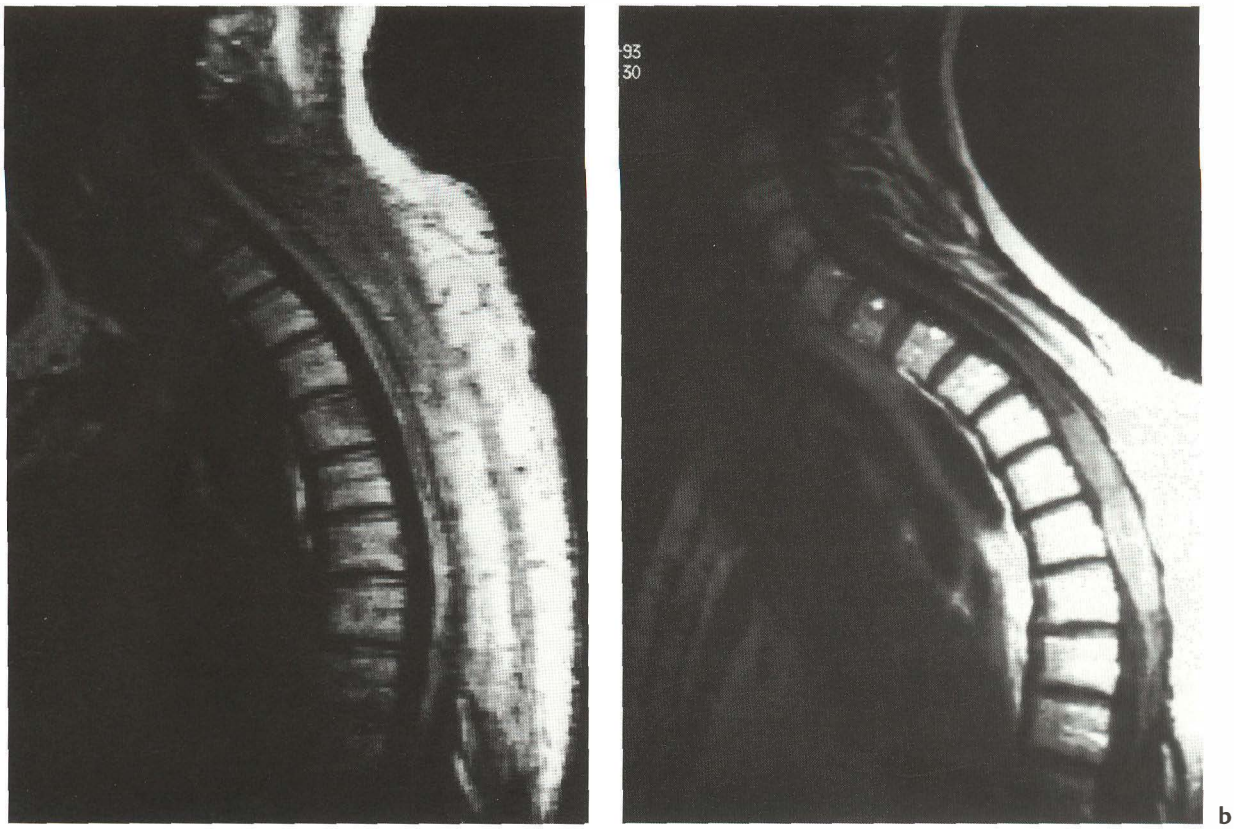

a b

Fig. **76** **Late recurrence of a thoracic grade II astrocytoma** (case *83;* same case as in Fig. **57**). **a** The first postoperative study. A postcontrast T1-weighted image demonstrates total removal of the tumor mass and disappearance of the tumor-related cystic components. **b** The follow-up image, taken five years later, in a patient with no symptoms: tumor recurrence is seen within the old surgical site

Long-Term Follow-Up and Recurrences

When examining the long-term results after IMT surgery, one may speculate on the indications for treatment. Apart from surgery itself, which is not an issue, the two aspects of treatment that need to be examined are the extent of radical tumor removal and the usefulness of adjunctive radiotherapy. With regard to the long-term outcome for patients with IMT, it is apparent that the literature does not provide any clarity, or at least any consensus, on the subject. Several articles discuss the long-term outcome in large series, but "long-term" may be taken to mean one year (99), three years (74), or five years (150, 231) after surgery. Using accepted oncological standards, five years would surely seem to be the most appropriate time-span for an initial assessment of the long-term follow-up, with additional assessments every five years.

In terms of survival and recurrence, the results in the long-term follow-up of low-grade ependymomas and astrocytomas reported in the literature most often remain uncertain (282).

In our experience, as well as in the literature (40, 99, 231, 255, 282), and despite all our efforts, the survival of patients with malignant IMT is less than five years. The longest survival we observed was 34 months in one patient who underwent surgery twice for a grade III thoracic astrocytoma *[103].* Such patients cannot, therefore, be included in the present discussion.

Ninety of the 171 patients in our series were clinically followed up for more than five years, including 70 with MRI follow-up. The follow-up was 5–10 years in 49 patients, 10–15 years in 17, 15–20 years in six patients, 20–25 years in ten patients, and over 25 years in eight.

Our longest follow-up has been with a patient with a grade I thoracic astrocytoma, who underwent surgery 34 years ago *[76],* when she was only two years old, with a second operation 29 years ago, with preservation of autonomic function and independent

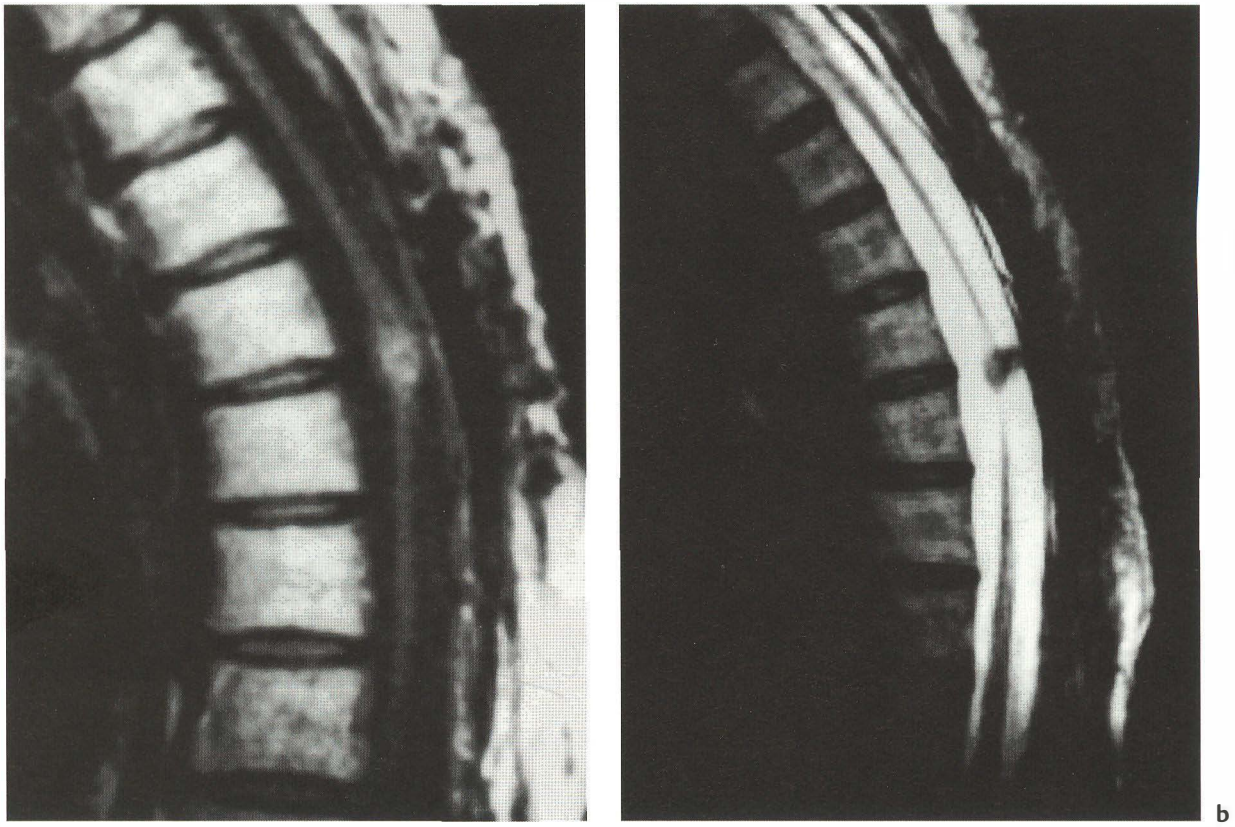

Fig. **77** **Repeat postoperative control MRI in a thoracic low grade II astrocytoma** (case *85*). **a** Sagittal T1-weighted image, **b** sagittal T2-weighted image, and **c** sagittal contrast-enhanced T1-weighted images obtained three years after subtotal removal of a previously biopsied tumor treated with radiotherapy. The thoracic cord is atrophic. A central nodule is shown within the resection site. It is isointense with the spinal cord on the T1-weighted and T2-weighted images, and enhances intensely after gadolinium injection. This nodule corresponds precisely to the site of the former biopsy and previous radiotherapy. Note the hyperintense signal of the irradiated vertebral bodies on T1-weighted images. **d** A postcontrast sagittal study performed seven years after resection of the tumor. The unchanged appearance of this lesion over an extended period of time suggests that it is a benign one, such as scar tissue. This case illustrates the complexity of such postoperative findings: the enhancing nodule can represent either tumor recurrence, scar tissue, or postradiotherapy sequelae

gait. She is now a professor of literature. In these 90 patients with a follow-up of more than five years, 40 presented with ependymomas, 22 with astrocytomas, nine with hemangioblastomas, seven with lipomas, and 12 with other types of tumor.

The therapeutic management of intramedullary spinal cord ependymomas always appeared relatively simple to us (77, 78). These are discrete benign tumors, and gross total removal can be accomplished even in holocord tumors (45, 79, 85, 144, 207). It remained to be seen that patients treated with surgery, but who did not receive radiotherapy, were tumor-free with satisfactory functional results compared with their preoperative function. Forty patients had a follow-up of more than five years: 5–10 years in 20, 10–15 years in nine, 15–20 years in three, 20–25 years in seven, and 27 years in one.

When the clinical results detailed in Table **2**, using McCormick's classification (Table **3**), are assessed, it can be seen that 23 of the 40 patients show a long-term functional outcome identical to the preoperative condition. A single woman *[21]* died at age 63, 22 years after surgery, only a few months after an MRI had revealed no change in the size of her tumor. This patient, whose tumor had been incompletely removed, had undergone adjunctive radiation therapy (60 Gy) at another institution. Although she was functionally grade II in the McCormick classification, she then developed a severe kyphoscoliosis, which could not be managed with the orthopedic techniques available at the time.

Functional improvement was observed in 11 patients. In this group, only one woman *[8]*, who had undergone surgery for a holocord ependymoma 22

Fig. **77c**

Fig. **77d**

years ago (79), has remained paraplegic. She became quadriplegic during childbirth, and was operated on a few days later. Her condition improved after surgery, and she regained partial use of her upper limbs. Her MRI shows an atrophic spinal cord. In this group, one patient whose McCormick rating improved from grade III to grade II died of intercurrent disease five years after surgery *[25]*.

Finally, in the long-term follow-up, six patients are worse compared with their preoperative function. Two patients *[9, 34]* with grade I function deteriorated to grade II; however, these two women were able to resume their prior jobs. Two patients lost the use of their legs: one *[4]* had a 20-year follow-up without tumor recurrence after removal of holocord ependymoma (79), and the other *[3]*, who underwent surgery for a cervical ependymoma, had a good functional result for ten years, but presented with neurofibromatosis 2, and had severe complications after undergoing multiple operations for bilateral acoustic neurinomas and an operation on the conus medullaris with a nondiagnostic biopsy. Finally, two patients presented with severe deterioration following surgery, and did not recover: one *[17]* has lost the use of both upper extremities secondary to a posterior column dysfunction, and the other *[53]* is paraplegic.

The most important point is that, of our 40 patients with more than five years of follow-up, 39 had a gross total or subtotal tumor removal. Only one patient *[32]* had a recurrent ependymoma 18 years after a gross total tumor removal. She underwent repeat surgery five years ago, and she is now functionally McCormick grade I. Similarly, the condition of the 22 patients in the series with less than five years of follow-up has proved satisfactory, with the exception of two patients with incomplete tumor removal: one is about to undergo a second operation *[41]*, and the other *[24]* died in spite of two operations within three months, with a malignant course with tumor invasion of the entire spinal cord and brain stem, although two histological examinations had confirmed the diagnosis of a grade II ependymoma.

In our two cases of grade III malignant ependymoma, one patient *[61]* died one year after surgery, and the other *[62]* was lost to follow-up after one year.

As mentioned earlier, the therapeutic management of intramedullary spinal cord astrocytomas is

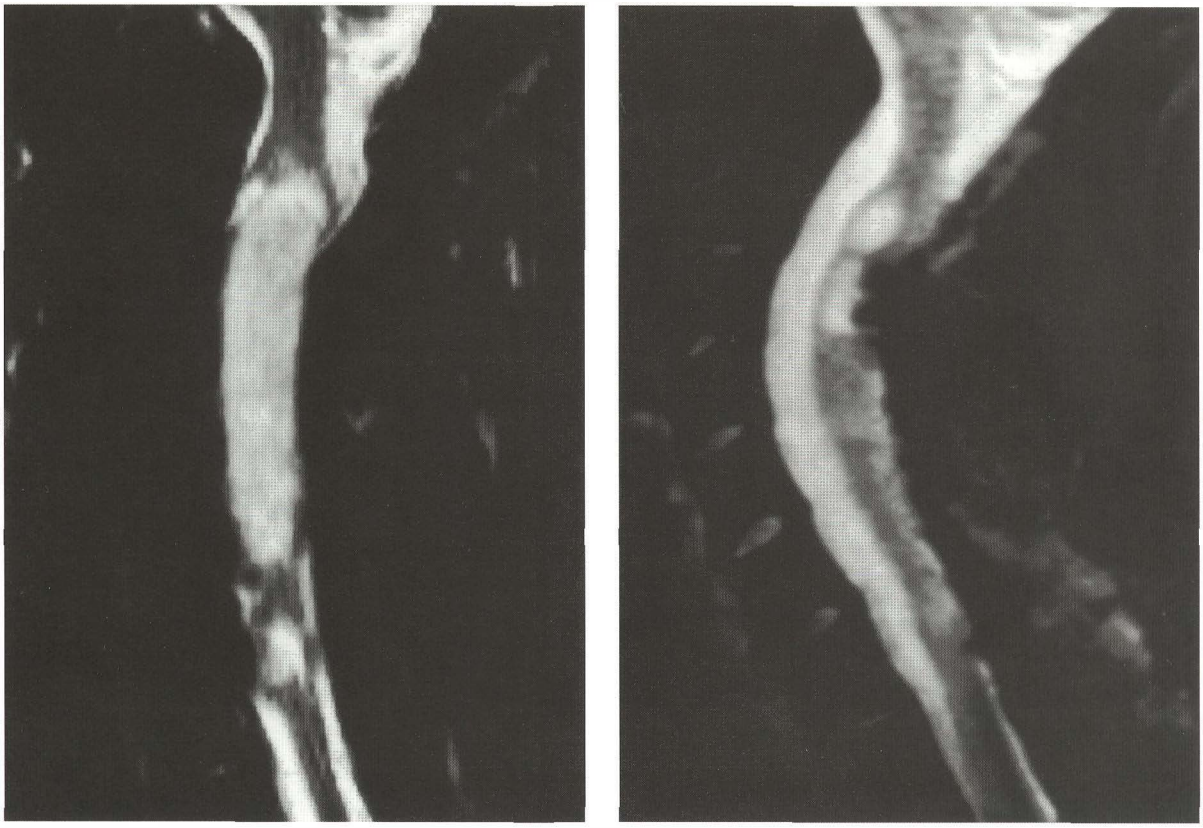

Fig. **78** **Cervical subependymoma** (case *63*). A diagnostic problem encountered on postoperative control MRI in the case of a nonenhancing tumor that was well visualized on a T2-weighted image. **a** Sagittal preoperative T2-weighted image. There is neoplastic widening of the cervical spinal cord from C2 to C7. **b** Postoperative follow-up. The cervical spinal cord shows normal signal intensity, except in the upper part, where a persistent area of increased signal is seen. It is impossible to determine whether this corresponds to residual tumor, and an additional follow-up MRI will be necessary. Note the extensive adhesions between the posterior surface of the cord and the dura

much more controversial (39, 40, 98, 99, 249, 255, 282), particularly in children (67, 103, 214, 227). These tumors are less discrete than ependymomas, and the ability to obtain gross total removal is uncertain, even controversial.

Twenty-two of our patients with intramedullary spinal cord astrocytomas have at least five years of postoperative follow-up: 5–10 years in 13 patients, 10–15 years in one patient, 15–20 years in one patient, 20–25 years in two patients, and 25–29 years in five patients. As with ependymomas, the long-term functional outcome in over 50% of the patients (12 of 22) is identical to their preoperative condition. No patient showed clinical or MRI evidence, or both, of recurrence or tumor progression, with the exception of one female patient *[83]* who underwent surgery six years ago; an MRI carried out for the present study suggested tumor recurrence in the absence of any clinically detectable evidence of tumor growth. Repeat surgery has not been suggested to this patient, who remains at grade I in the McCormick's classification. In the same group, one patient who underwent surgery at the age of 6 *[66]*, with a good functional result (McCormick grade II) for many years, died 22

Fig. **79** **Deteriorating course in a high-grade astrocytoma** (case *100*; same case as in Fig. **29**). **a** Sagittal postcontrast T1-weighted image. Partial removal of an ill-defined mass not completely enhancing after contrast injection (there was no contrast enhancement on the preoperative MRI). **b** The coronal cut shows lateral adhesion between the cord and the dura. **c** A postcontrast sagittal T1-weighted image after a second surgical procedure. The tumor is larger, and the signal behavior changes to an irregular pattern on the T1-weighted image and the T2-weighted image (**d**). **e** A sagittal thoracic T2-weighted image, showing multiple leptomeningeal metastases. Intracerebral lesions were also detected ▶

Fig. **79a**

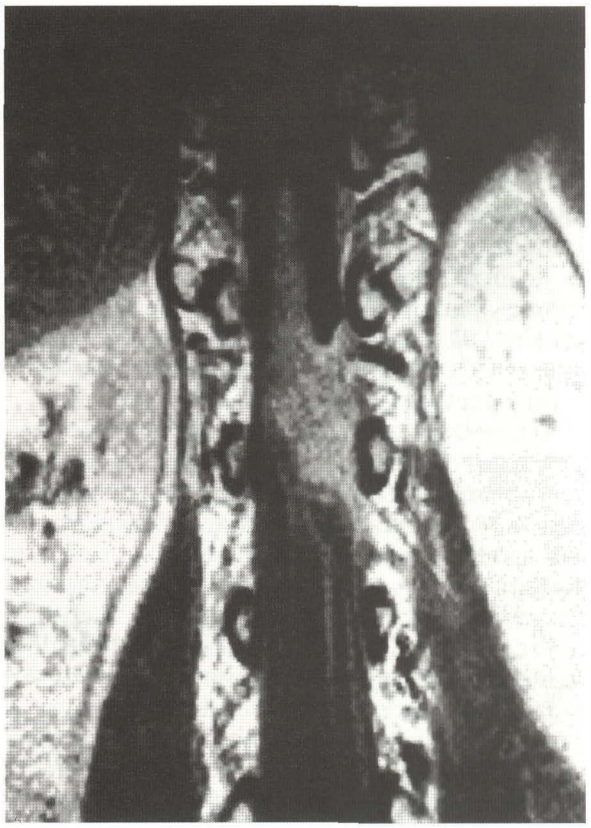

Fig. **79b**

Fig. **79c**

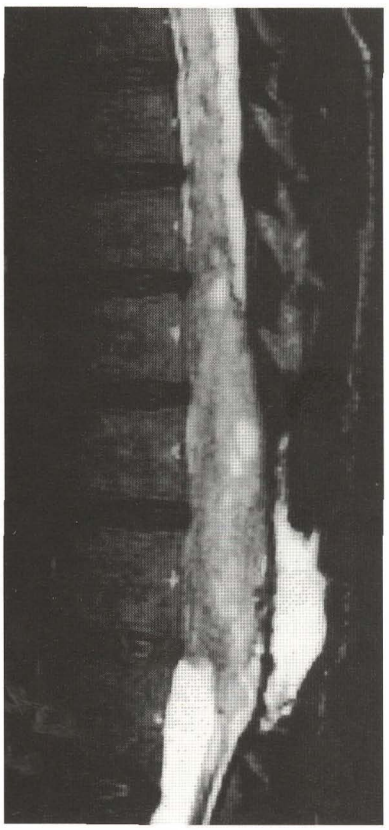

Fig. **79d**

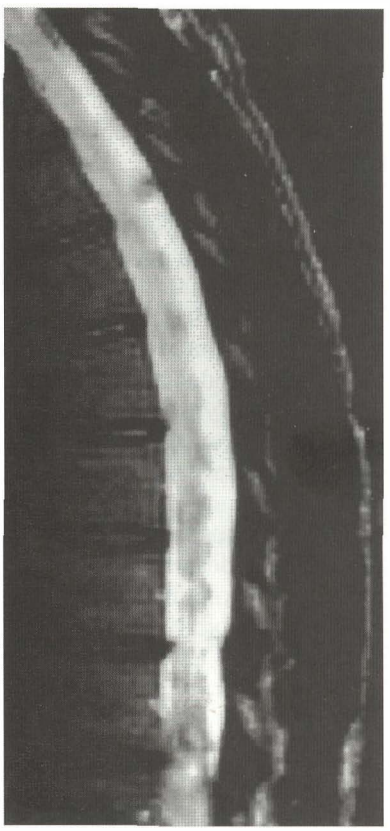

Fig. **79e**

years after surgery in unknown circumstances, probably from progressive tumor recurrence. Another patient in this group *[93]*, who had undergone two prior operations with adjunctive radiotherapy (45 Gy) at other institutions, underwent a gross total tumor removal of a grade II conus medullaris astrocytoma. His postoperative clinical condition (McCormick grade II) has been stable for the past six years, and is identical to his preoperative condition.

An improved functional outcome was seen in three patients who either maintained *[79]* or recovered *[84, 89]* an ability to walk independently after surgery (follow-up eight years, 26 years, and six years, respectively).

Long-term deterioration of function was observed in seven patients. One became paraplegic *[92]*, and has lived for 23 years without a recurrence; a second patient *[85]* remained in the same paraplegic condition as before surgery until his death nine years later. None of the five other patients lost their previous functional independence, although their functional level deteriorated from McCormick grade I to grade II. In this group, one patient *[71]* was thought to have tumor recurrence after incomplete removal of a grade I thoracic astrocytoma, not clinically corroborated (and therefore not submitted to reoperation), and there was one case *[94]* of secondary progressive alteration of initially excellent functional results obtained in a nine-year-old girl who underwent surgery for cervical astrocytoma 18 years ago. An underlying syrinx was responsible for this impairment, and after insertion of a cyst–peritoneal shunt, her patient's clinical condition improved slightly. MRI now shows an atrophic spinal cord free of any residual cyst.

The evaluation of 19 patients with less than five years of follow-up yields a more pessimistic picture, as ten died within 1–34 months of surgery, due to tumor growth. In this group, we recorded seven patients with high-grade (III or IV) astrocytomas, in whom the bad outcome is not surprising: so far, six of them have died. Three patients *[82, 96, 97]* with grade II astrocytomas died from malignant tumor development; one of them *[96]* had received radiotherapy without a previous biopsy at another hospital.

Finally, a quadriplegic, respirator-dependent patient *[78]* underwent surgery and survived for six months after removal of a grade I cervical astrocytoma that had produced spinal cord necrosis from C3 to C5. Our last eight patients, with grade I *[77]* or grade II astrocytomas (seven cases), initially improved.

After the histological findings, surgery is the second factor that has a significant influence on the prognosis. In the 22 patients with a follow-up of over five years, the tumor removal was complete in ten cases and subtotal in seven. However, the benefit of surgical decompression should not be underestimated, since in five of our patients surgery was incomplete *[71, 81]* or limited to biopsy *[73, 75, 84]*, and these five patients are still alive, with follow-up ranging from seven to 29 years. Only one of these patients *[84]* underwent adjunctive radiotherapy (45 Gy).

We observed 31 recurrences in our series of IMTs, manifested by clinical deterioration. In ten patients, recurrence was due to progressive growth of a malignant tumor, which was not surprising. In 16 patients, recurrence was due to a tumor that was not removed after biopsy, or a tumor remnant after partial removal. In five patients, there was a "true recurrence" after gross total removal of a benign *[32, 76]* or malignant tumor *[103, 119, 120]*.

From the 33 patients who underwent repeat surgery, we have excluded eight patients whose operation was staged and performed on two separate occasions *[2, 10, 25, 50, 52, 55, 57, 102]* and the four patients who had two distinct lesions *[111, 130, 143, 148]*. Because of clinical worsening, a second operation was performed in 16 patients; a malignant tumor was present in four cases *[24, 100, 108, 110]* and a benign tumor in eight others *[40, 45, 60, 70, 85, 92, 143, 164]*. Two further patients have not yet undergone the second operation; one has an unresected ependymoma *[41]*, and the other *[124]* has a partially resected hemangioblastoma (the unremoved thrombosed portion has recanalized). Finally, two female patients, one presenting with a lipoma *[144]* and the other *[114]* with a metastatic spinal cord ependymoma, have undergone repeat surgery at another hospital.

If the clinical picture is not consistent with tumor recurrence, we are very reluctant to reoperate on lesions on the basis of an MRI suggesting tumor recurrence. The difficulties of repeat surgery are well known; it is difficult to suggest a second operation in the absence of clinical complaints, as was the case in four of our patients *[45, 71, 81, 85]*. Although, in a few cases, the imaging appearance may require confirmation, we prefer confirmation to be provided by the clinical findings rather than by the intraoperative findings. The observation of two patients in whom reoperation resulted in a negative biopsy *[10]* and dural plasty *[143]*, respectively, has prompted us to act with extreme caution in these circumstances.

Summary and Conclusions

Our experience, based on 171 cases and 200 surgical operations for intramedullary spinal cord tumors, has led us to reach the following conclusions.

1. Although there is no pathognomonic clinical picture for IMT, back or neck pain, radicular pain, or diffuse paresthesia, is always the first sign of an IMT. SEPs are a useful part of preoperative evaluation of IMTs, since they provide information on the functional state of the spinal cord, demonstrate impairment of the sensory pathways, and sometimes reveal abnormalities that are not clinically obvious.
2. MRI is the imaging study of choice, provided that it includes very complete scans and slices and the injection of contrast material. Apart from hemangioblastomas, lipomas, dermoid cysts, and epidermoid cysts, there is no tumor-specific MR image – but there are some important clues, such as the "capping" seen in some ependymomas.
3. IMTs are glial tumors in two-thirds of cases. Histological diagnosis is sometimes difficult, and the distinction between ependymoma and astrocytoma may require the use of additional staining or immunolabeling techniques. Under these conditions, it is understandable that neuropathologists present the results of intraoperative histological examinations with legitimate reservations.
4. The operative approach to IMTs is guided by the anatomy, and is based on the posterior spinal cord midline approach, as a rule; the posterior columns are separated along the midline sulcus, the only exception being superficial tumors, which are approached directly. Under these conditions, one of the major risks of IMT removal is impairment of posterior column function, which can be detected in 70% of cases by intraoperative SEP monitoring. One of the benefits of SEP monitoring is that it demonstrates that surgery can be followed by complete restoration of sensitive spinal cord function.
5. We are not in favor of the laser. We consider that ultrasonography may be a valuable adjunct, but the CUSA, particularly when used in the pulsed mode, is today the most reliable surgical tool for performing safe and effective tumor reduction before finding the optimal cleavage plane.
6. Complete removal of the lesion is the first goal of IMT surgery. This should be performed whenever possible, i.e., when it is possible to visualize a clear cleavage plane between the tumor and healthy spinal cord. If no such plane is found, an attempt at complete tumor removal is impossible, hazardous, and pointless.
7. The presence of an astrocytoma does not necessarily mean that the lesion is an unresectable, infiltrating tumor. The resection of 15 of our 34 low-grade astrocytomas (grades I and II) was macroscopically complete, and to date none of these patients has required a second operation.
8. Any MR image suggesting an IMT should be surgically explored. A tumor cannot be described as "unresectable" if removal has not been attempted. Total removal of benign tumors has been successfully performed in patients who have been referred to us with diagnoses of infiltrating tumors. We have therefore treated a number of these tumors or pseudotumors (ependymomas, schwannomas, or sarcoidosis), with the patients benefiting accordingly.
9. At present, we do not believe there is any place for radiotherapy apart from the treatment of malignant tumors of the spinal cord, which are fortunately rare except in children. Even in these circumstances, the efficacy and harmlessness of radiotherapy have yet to be demonstrated.
10. The low mortality, morbidity, and recurrence rates allow us to recommend surgery as the sole effective treatment for IMTs.